



2023 COASTAL MASTER PLAN

# 50-YEAR FWOA MODEL OUTPUT, REGIONAL SUMMARIES – ICM

ATTACHMENT C2

REPORT: VERSION 03

DATE: FEBRUARY 2024

PREPARED BY: ERIC D. WHITE, MARTIJN BREGMAN, P. SOUPY DALYANDER,  
MADELINE R. FOSTER-MARTINEZ, IOANNIS GEORGIU, KEVIN HANEGAN, DAVID  
LINDQUIST, MIKE MINER, DENISE J. REED, JENNEKE M. VISSER, YUSHI WANG,  
ZHANXIAN WANG



COASTAL PROTECTION AND  
RESTORATION AUTHORITY  
150 TERRACE AVENUE  
BATON ROUGE, LA 70802  
[WWW.COASTAL.LA.GOV](http://WWW.COASTAL.LA.GOV)

# COASTAL PROTECTION AND RESTORATION AUTHORITY

This document was developed in support of the 2023 Coastal Master Plan being prepared by the Coastal Protection and Restoration Authority (CPRA). CPRA was established by the Louisiana Legislature in response to Hurricanes Katrina and Rita through Act 8 of the First Extraordinary Session of 2005. Act 8 of the First Extraordinary Session of 2005 expanded the membership, duties, and responsibilities of CPRA and charged the new authority to develop and implement a comprehensive coastal protection plan, consisting of a master plan (revised every six years) and annual plans. CPRA's mandate is to develop, implement, and enforce a comprehensive coastal protection and restoration master plan.

## CITATION

White, E. D., Bregman, M., Dalyander, S., Foster-Martinez, M. R., Georgiou, I., Hanegan, K., Lindquist, D., Miner, M., Reed, D. J., Visser, J. M., Wang, & Y., & Wang, Z. (2023). 2023 Coastal Master Plan: Attachment C2: 50-Year FWOA Model Output, Regional Summaries - ICM. Version 3. (p. 194). Baton Rouge, Louisiana: Coastal Protection and Restoration Authority.

# ACKNOWLEDGEMENTS

This document was developed as part of a broader Model Improvement Plan in support of the 2023 Coastal Master Plan under the guidance of the Modeling Decision Team:

- Coastal Protection and Restoration Authority (CPRA) of Louisiana – Stuart Brown, Ashley Cobb, Madeline LeBlanc Hatfield, Valencia Henderson, Krista Jankowski, David Lindquist, Sam Martin, and Eric White
- University of New Orleans – Denise Reed

This document was prepared by the following team members:

- Eric D. White – CPRA
- Martijn Bregman – The Water Institute of the Gulf
- P. Soupy Dalyander – The Water Institute of the Gulf
- Madeline Foster-Martinez – University of New Orleans
- Ioannis Georgiou – The Water Institute of the Gulf
- Kevin Hanegan – Moffat & Nichol
- David Lindquist – CPRA
- Mike Miner – The Water Institute of the Gulf
- Denise J. Reed – University of New Orleans
- Jenneke M. Visser – University of Louisiana Lafayette
- Yushi Wang – The Water Institute of the Gulf
- Zhanxian Wang – Moffat & Nichol

Computational resources for the 2023 Coastal Master Plan were supported by a National Science Foundation (NSF) Extreme Science and Engineering Discovery Environment (XSEDE) grant; NSF grant number ACI-1548562.

# EXECUTIVE SUMMARY

Analysis for the 2023 Coastal Master Plan focused on a regional approach to understanding the dynamics of a changing coastal Louisiana landscape. This report examines representative datasets from the Integrated Compartment Model (ICM) simulations of a future without action (FWOA), under two scenarios of possible future environmental conditions. Across all five coastal regions, model outputs are shown to provide a thorough understanding of how, and why the future landscape will look different from what it looks like today. Rather than simply reporting the same datasets at fixed locations in a repetitive format, this report instead is structured such that the data will tell a compelling narrative of one, or a few, narratives for each coastal region and how that region may experience change in the future.

This report is specifically focused on the 2023 Coastal Master Plan FWOA under the lower and higher project selection environmental scenarios. These are outputs from the FWOA simulations that were directly used to assess a candidate project's robust performance under both scenarios. These simulations represent two possible outcomes for coastal Louisiana if we were to put our shovels (and dredges) down after we finish building all of the projects that we currently have funding (and permits) to construct. While we know that these two scenarios are not exact forecasts of the next 50 years, they are based upon real potential future climates, and were developed from the latest available data provided by international climate change modeling efforts.

The five regions examined are: Chenier Plain, the Central Coast, Terrebonne Basin, Barataria Basin, and the Pontchartrain/Breton. This report will discuss all five subroutines of the ICM that interact to update the coastal landscape: the hydrology model (**ICM-Hydro**), the wetland vegetation model (**ICM-LAVegMod**), the wetland morphology model (**ICM-Morph**), the barrier island and tidal inlet models (**ICM-BI and ICM-BITI**). The sixth, and final, ICM subroutine does not provide feedback to the landscape, but instead uses environmental and landscape outputs to calculate habitat suitability indices for a variety of important fish, fowl, and wildlife species in coastal Louisiana (**ICM-HSI**).

# TABLE OF CONTENTS

COASTAL PROTECTION AND RESTORATION AUTHORITY .....	2
CITATION .....	2
ACKNOWLEDGEMENTS.....	3
EXECUTIVE SUMMARY .....	4
TABLE OF CONTENTS.....	5
LIST OF TABLES .....	7
LIST OF FIGURES .....	7
LIST OF ABBREVIATIONS .....	16
1.0 INTRODUCTION.....	17
2.0 PONTCHARTRAIN & BRETON .....	22
2.1 Introduction.....	22
2.2 FWOA Stage .....	23
2.3 FWOA Tidal Range .....	23
2.4 FWOA Salinity .....	24
2.5 FWOA Total Suspended Solids (TSS).....	24
2.6 FWOA Water Temperature.....	25
2.7 FWOA Vegetation .....	27
2.8 FWOA Wetland Morphology.....	39
2.9 FWOA Barrier Island Morphology .....	46
2.10 FWOA Habitat Suitability Indices .....	52
2.11 Discussion .....	57
3.0 BARATARIA.....	64
3.1 Introduction.....	64
3.2 FWOA Stage .....	66
3.3 FWOA Tidal Range .....	66
3.4 FWOA Salinity .....	67
3.5 FWOA Total Suspended Solids (TSS).....	68
3.6 FWOA Water Temperature.....	70
3.7 FWOA Vegetation .....	71
3.8 FWOA Wetland Morphology.....	77
3.9 FWOA Barrier Island Morphology .....	83
3.10 FWOA Habitat Suitability Indices .....	88

3.11 Discussion .....	94
<b>4.0 TERREBONNE .....</b>	<b>100</b>
4.1 Introduction.....	100
4.2 FWOA Stage .....	100
4.3 FWOA Tidal Range .....	101
4.4 FWOA Salinity .....	102
4.5 FWOA Total Suspended Solids (TSS).....	103
4.6 FWOA Water Temperature.....	104
4.7 FWOA Vegetation .....	105
4.8 FWOA Wetland Morphology.....	111
4.9 FWOA Barrier Island Morphology .....	119
4.10 FWOA Habitat Suitability Indices .....	124
4.11 Discussion .....	130
<b>5.0 CENTRAL COAST.....</b>	<b>136</b>
5.1 Introduction.....	136
5.2 FWOA Stage .....	136
5.3 FWOA Tidal Range .....	137
5.4 FWOA Salinity .....	138
5.5 FWOA Total Suspended Solids (TSS).....	139
5.6 FWOA Water Temperature.....	139
5.7 FWOA Vegetation .....	140
5.8 FWOA Wetland Morphology.....	147
5.9 FWOA Habitat Suitability Indices .....	155
5.10 Discussion .....	160
<b>6.0 CHENIER PLAIN .....</b>	<b>164</b>
6.1 Introduction.....	164
6.2 FWOA Stage .....	164
6.3 FWOA Tidal Range .....	166
6.4 FWOA Salinity .....	169
6.5 FWOA Total Suspended Solids (TSS).....	170
6.6 FWOA Water Temperature.....	171
6.7 FWOA Vegetation .....	173
6.8 FWOA Wetland Morphology.....	180
6.9 FWOA Habitat Suitability Indices .....	187
6.10 Discussion .....	192

7.0 REFERENCES..... 194

## LIST OF TABLES

Table 1. Ecoregion abbreviations and the region in which they are located ..... 20  
 Table 2. Symbol codes used in ICM-LAVegMod to represent each modeled species . 21  
 Table 3. Summary of total sediment volume placed ( $10^6$  m<sup>3</sup>) over FWOA simulation in scenarios S07 and S08 for the Pontchartrain/Breton region of the coast ..... 50  
 Table 4. Summary of total sediment volume placed ( $10^6$  m<sup>3</sup>) over FWOA simulation in scenarios S07 and S08 for the Barataria region of the coast..... 87  
 Table 5. Summary of total sediment volume placed ( $10^6$  m<sup>3</sup>) over FWOA simulation in scenarios S07 and S08 for the Terrebonne region of the coast..... 122

## LIST OF FIGURES

Figure 1. Spatial resolution for ICM subroutines in the area around Marsh Island in Vermilion Bay. .... 18  
 Figure 2. Master plan regions of coastal Louisiana. .... 19  
 Figure 3. Ecoregions used in modeling analyses for the 2023 Coastal Master Plan. . 20  
 Figure 4. Water temperature, under S07, in Lake Maurepas (compartment 33); this demonstrates the warmer winter minimums in areas less connected to Mississippi River. .... 25  
 Figure 5. Water temperature, under S07, in the Bird’s Foot Delta at Fort St. Philip (compartment 135); this demonstrates the colder winter minimums in areas with direct connection to the Mississippi River..... 26  
 Figure 6. Water temperature, under S08, in Lake Maurepas (compartment 33); this demonstrates the warmer winter minimums in areas less connected to Mississippi River. .... 26  
 Figure 7. Wetland type (Forested, Fresh, Intermediate, Brackish, or Saline [FFIBS] score) distribution of the Pontchartrain and Breton basins under scenario S07 in Year 25. .... 28  
 Figure 8. Wetland type (FFIBS score) distribution of the Pontchartrain and Breton basins under scenario S07 in Year 50. .... 29  
 Figure 10. Wetland type (FFIBS score) distribution of the Bird’s Foot Delta under scenario S07 in Year 25. .... 31  
 Figure 11. Wetland type (FFIBS score) distribution of the Bird’s Foot Delta under scenario S07 in Year 50. .... 32  
 Figure 12. Change in vegetation cover under S07 is shown at representative points within the Bird’s Foot Delta..... 33  
 Figure 13. Wetland type (FFIBS score) distribution of the Pontchartrain and Breton basins under scenario S08 in Year 25. .... 34

Figure 14. Wetland type (FFIBS score) distribution of the Pontchartrain and Breton basins under scenario S08 in Year 50. ....	35
Figure 15. Change in vegetation cover under S08 is shown at representative points for different locations throughout the Pontchartrain and Breton basins. ....	36
Figure 16. Wetland type (FFIBS score) distribution of the Bird’s Foot Delta under scenario S08 in Year 25. ....	37
Figure 17. Wetland type (FFIBS score) distribution of the Bird’s Foot Delta under scenario S08 in Year 50. ....	38
Figure 18. Change in vegetation cover under S08 is shown at representative points within the Bird’s Foot Delta.....	39
Figure 19. Inundation dynamics at QAQC1693 under S07.....	40
Figure 20. Inundation dynamics at CRMS0117 under S07.....	41
Figure 21. Inundation dynamics at QAQC0329 under S07.....	41
Figure 22. Cumulative land change by Year 45 (left) and Year 50 (right) for the Orleans Landbridge and Pearl River areas under S08. ....	42
Figure 23. Cumulative land change by Year 30 (left) and Year 40 (right) for the marshes north of MRGO under S08. ....	43
Figure 24. Accretion and inundation dynamics at TRNS1301, adjacent to the Mid-Breton Sediment Diversion outfall, under S08.....	44
Figure 25. Accretion and inundation dynamics at QAQC0398, further afield from the Mid-Breton Sediment Diversion outfall, under S08.....	45
Figure 26. Barrier islands located within the Pontchartrain region of the coast. ....	47
Figure 27. Elevation in MHW for the initial condition in the southern portion of the Pontchartrain region along with Year 50 results for S07 and S08. ....	48
Figure 28. Elevation in MHW for the initial condition in the northern portion of the Pontchartrain region along with Year 50 results for S07 and S08. ....	49
Figure 29. Summary of sediment volume placed in scenarios S07 and S08 for the Pontchartrain region of the coast.....	50
Figure 30. Tidal inlet cross-sectional area changes over time in Pontchartain/Breton, under S07. ....	51
Figure 31. Tidal inlet cross-sectional area changes over time in Pontchartrain/Breton, under S08. ....	52
Figure 32. Oyster HSI scores compared to salinity simulated for the Bay Boudreau area over the first 20 years of the S07 environmental scenario. ....	53
Figure 33. Small juvenile brown shrimp HSI scores across the Lake Borgne and Biloxi Marsh areas for Year 1 (left) and Year 50 (right) of the S07 environmental scenario.. ....	54
Figure 34. Total HSI score for alligator and seaside sparrow in the Upper Breton ecoregion over the 50-year S07 environmental scenario simulation. ....	54
Figure 35. Total HSI score for juvenile blue crab and mottled duck in the Upper Breton ecoregion over the 50-year S08 environmental scenario simulation.....	55
Figure 36. Small juvenile brown shrimp HSI scores across the Lake Borgne and Biloxi Marsh areas for Year 1 and Year 50 of the S08 environmental scenario.....	56
Figure 37. Total HSI score for oysters in the Chandeleur Sound ecoregion over the 50-year S08 environmental scenario simulation.. ....	56

Figure 38. Comparison of vegetation cover change in the upper ecoregions of the Pontchartrain Basin between the two scenarios. ....	58
Figure 39. Comparison of vegetation cover change in the lower ecoregions of Pontchartrain and Breton basins between the two scenarios. ....	59
Figure 40. Comparison of conditions under S07 and S08 at QAQC1598 on the Orleans Landbridge. ....	60
Figure 41. Comparison of conditions under S07 and S08 at TRNS1401 near the Bohemia Spillway. ....	61
Figure 42. Tidal inlet cross-sectional area changes over time in Pontchartrain/Breton, under S07 and S08. ....	62
Figure 43. Tidal range for ICM-Hydro compartments contributing tidal prism to Barataria Basin tidal inlets. ....	63
Figure 44. Land change, under S07, after 50 years in the outfall of the Mid-Barataria Sediment Diversion, as compared to a future without the diversion on. ....	65
Figure 45. Salinity, under S07, in Lac des Allemandes (compartment 171); this demonstrates the slow increase in salinity intrusion in the upper basin, even though this area maintains a fresh condition. ....	67
Figure 46. Salinity, under S07, in Wilkinson Canal (compartment 227); this demonstrates the mitigating impact on salinity intrusion due to the Mid-Barataria Sediment Diversion, which decreases over time due to sea level rise. ....	67
Figure 47. Salinity, under S07, in northern Barataria Bay (compartment 249); this demonstrates the seasonal fluctuations of Gulf-dominated waters, without a clear increase over time (likely due to mitigating effects of the Mid-Barataria Sediment Diversion). ....	68
Figure 48. Salinity, under S08, in Wilkinson Canal (compartment 227); this demonstrates the mitigating impact on salinity intrusion due to the Mid-Barataria Sediment Diversion. ....	68
Figure 49. TSS, under S07, in Lac des Allemandes (compartment 171); this demonstrates the lower sediment concentrations in the areas of Barataria without river influences. ....	69
Figure 50. TSS, under S07, in Wilkinson Canal (compartment 227); this demonstrates the highest sediment concentrations in the immediate outfall area near the Mid-Barataria Sediment Diversion. ....	69
Figure 51. TSS, under S07, in northern Barataria Bay (compartment 249); this demonstrates the elevated TSS levels due the diversion, but a decrease in magnitude longitudinally from the Mid-Barataria Sediment Diversion outfall. ....	69
Figure 52. Water temperature, under S07, in Wilkinson Canal (compartment 227); this demonstrates the cooler winter minimums in areas connected to the Mississippi River; here as a result of the Mid-Barataria Sediment Diversion. ....	70
Figure 53. Water temperature, under S07, west of Caminada Bay (compartment 217); this demonstrates the warmer winter minimums in areas without direct connection to the Mississippi River. ....	70
Figure 54. Water temperature, under S08, in Wilkinson Canal (compartment 227); this demonstrates the cooler winter minimums in areas connected to the Mississippi River, here as a result of the Mid-Barataria Sediment Diversion. ....	71

Figure 55. Wetland type (FFIBS score) distribution of the Barataria Basin under scenario S07 in Year 25. ....	72
Figure 56. Wetland type (FFIBS score) distribution of the Barataria Basin under scenario S07 in Year 50. ....	73
Figure 57. Change in vegetation cover under S07 is shown at representative points for different locations throughout Barataria Basin.....	74
Figure 58. Wetland type (FFIBS score) distribution of the Barataria Basin under scenario S08 in Year 25. ....	75
Figure 59. Wetland type (FFIBS score) distribution of the Barataria Basin under scenario S08 in Year 50. ....	76
Figure 60. Change in vegetation cover under S07 is shown at representative points for different locations throughout Barataria Basin.....	77
Figure 61. Inundation dynamics at QAQC1300 under S07.....	78
Figure 62. Vegetation coverage in grid cell 70704 (includes QAQC1300) under S07. ....	79
Figure 63. Cumulative land change by Year 40 (left) and Year 50 (right) for the upper Barataria Basin under S08.....	80
Figure 64. Cumulative land change by Year 35 (top left), Year 40 (top right) and Year 50 (bottom) for the lower Barataria Basin under S08.....	81
Figure 65. Organic accretion and inundation dynamics at CRSM4529 under S08.....	82
Figure 66. Organic and mineral accretion and inundation dynamics at QAQC1313 under S08. ....	82
Figure 67. ICM-BI barrier islands and headlands within the Barataria region of the coast. Background imagery from Google Earth.....	83
Figure 68. Elevation, relative to mean high water, for the initial condition in the eastern portion of the Barataria region along with Year 50 results for S07 and S08.	84
Figure 69. Elevation, relative to mean high water, for the initial condition in the western portion of the Barataria region along with Year 50 results for S07 and S08..	85
Figure 70. Sediment placement volumes for barrier islands within the Barataria region of the coast. ....	86
Figure 71. Tidal inlet cross-sectional area changes over time in Barataria, under S07. ....	87
Figure 72. Tidal inlet cross-sectional area changes over time in Barataria, under S08. ....	88
Figure 73. Oyster HSI scores compared to salinity simulated for northeast Barataria Bay over the first 20 years of the S07 environmental scenario. ....	90
Figure 74. Small juvenile brown shrimp HSI scores across the lower Barataria region for Year 1 (left) and Year 50 (right) of the S07 environmental scenario.....	90
Figure 75. Gadwall HSI scores across the middle Barataria region for Year 1 (left) and Year 50 (right) of the S07 environmental scenario..	91
Figure 76. Water depths simulated for a model cell west of Lake Salvador for Year 1 and Year 50 of the S07 environmental scenario. ....	91
Figure 77. Total HSI score for juvenile blue crab and eastern oyster in the Lower Barataria - northeast ecoregion over the 50-year S08 environmental scenario simulation..	92

Figure 78. Small juvenile brown shrimp HSI scores across the lower Barataria region for Year 1 (left) and Year 50 (right) of the S08 environmental scenario.....	93
Figure 79. Total HSI score for juvenile blue crab and small juvenile brown shrimp in the Lower Barataria - northwest ecoregion over the 50-year S08 environmental scenario simulation.....	93
Figure 80. Comparison of vegetation cover change in the upper ecoregions of Barataria Basin between the two scenarios. ....	94
Figure 81. Comparison of vegetation cover change in the lower ecoregions of Barataria Basin between the two scenarios. ....	95
Figure 82. Comparison of S07 and S08 conditions at CRMS0225 in LBAne. ....	96
Figure 83. Comparison of S07 and S08 conditions at QAQC1435 in LBAsw.....	97
Figure 84. Tidal range for ICM-Hydro compartments contributing tidal prism to Barataria Basin tidal inlets. ....	98
Figure 85. Tidal inlet cross-sectional area changes over time in Barataria, under S07 and S08. ....	99
Figure 86. Stage in compartment 609, under S07, representative of the Terrebonne region directly influenced by the Atchafalaya River where seasonal discharge trends are evident.....	101
Figure 87. Tidal range in compartment 484, under S07, showing the long-term increase in tidal range in Terrebonne Bay with sea level rise.....	102
Figure 88. Tidal range in compartment 649, under S08, showing the slight long-term decreases in tidal ranges.....	102
Figure 89. Salinity in compartment 666, under S07, showing the seasonal patterns resulting from Atchafalaya River discharge. ....	103
Figure 90. TSS in compartment 666, under S07, showing the slight long-term reductions in peak seasonal TSS values. ....	104
Figure 91. TSS in compartment 744, under S08, showing the reductions in peak values in the last decade of simulation.....	104
Figure 92. Wetland type (FFIBS score) distribution of the Terrebonne region under scenario S07 in Year 25. ....	106
Figure 93. Wetland type (FFIBS score) distribution of the Terrebonne region under scenario S07 in Year 50. ....	107
Figure 94. Change in vegetation cover under S07 is shown at representative points in the Terrebonne region. ....	108
Figure 95. Wetland type (FFIBS score) distribution of the Terrebonne region under scenario S08 in Year 25. ....	109
Figure 96. Wetland type (FFIBS score) distribution of the Terrebonne region under scenario S08 in Year 50. ....	110
Figure 97. Change in vegetation cover under S08 is shown at representative points in the Terrebonne region. ....	111
Figure 98. Salinity and inundation dynamics at CRMS0365 under S07.....	112
Figure 99. Salinity and inundation dynamics at QAQC0738 under S07.....	113
Figure 100. Salinity and inundation dynamics at QAQC1012 under S07.....	113
Figure 101. Salinity and inundation dynamics at TRNS0801 under S07. ....	114
Figure 102. Vegetation change in grid cell 27880 (includes QAQC1012) under S07. ....	114

Figure 103. Vegetation change in grid cell 27822 (includes TRNS0801) under S07.	115
Figure 104. Sediment dynamics at CRMS0338 under S08.	116
Figure 105. Maximum 2-week salinity and mean annual stage compartment 658 under S08.	117
Figure 106. Sediment dynamics at CRMS0290 under S08.	118
Figure 107. Sediment dynamics at CRMS0301 under S08.	119
Figure 108. ICM-BI barrier islands located within the Terrebonne region of the coast.	120
Figure 109. Elevation, relative to mean high water, for the initial condition in the Terrebonne region along with Year 50 results for S07 and S08.	121
Figure 110. Sediment placement volumes for barrier islands within the Terrebonne region of the coast.	122
Figure 111. Terrebonne tidal inlet cross-sectional area changes over time, under S07.	123
Figure 112. Terrebonne tidal inlet cross-sectional area changes over time, under S08.	124
Figure 113. Small juvenile brown shrimp HSI scores across the Terrebonne region for Year 1 (left) and Year 50 (right) of the S07 environmental scenario.	125
Figure 114. Water depths simulated for a model cell in the western Penchant ecoregion for Year 1 and Year 50 of the S07 environmental scenario.	126
Figure 115. Gadwall HSI scores across the Penchant ecoregion for Year 1 (left) and Year 50 (right) of the S07 environmental scenario.	126
Figure 116. Total HSI score for crayfish in the Verret ecoregion over the 50-year S07 environmental scenario simulation.	127
Figure 117. Total HSI score for juvenile blue crab and juvenile spotted seatrout in the Eastern Terrebonne ecoregion over the 50-year S08 environmental scenario simulation.	128
Figure 118. Small juvenile brown shrimp HSI scores across the Terrebonne region for Year 1 (left) and Year 50 (right) of the S08 environmental scenario.	129
Figure 119. Total HSI score for juvenile spotted seatrout and mottled duck in the Penchant ecoregion over the 50-year S08 environmental scenario simulation.	129
Figure 120. Comparison of vegetation cover change in the Terrebonne region between the two scenarios, by ecoregion.	131
Figure 121. Comparison of S07 and S08 conditions for QAQC1091 in ETB.	132
Figure 122. Comparison of S07 and S08 conditions for CRMS0322 in WTB.	132
Figure 123. Comparison of S07 and S08 for QAQC0721 in PEN.	133
Figure 124. Tidal range for ICM-Hydro compartments contributing tidal prism to Terrebonne Basin tidal inlets.	134
Figure 125. Stage, under S07, in compartment 599, representative of the Central Coast region directly influenced by the Atchafalaya River and Wax Lake Outlet where seasonal discharge trends are evident.	136
Figure 126. Tidal Range, under S08, in compartment 934, showing the decrease in tidal range in later years.	137
Figure 127. Salinity, under S07, in compartment 934, showing the seasonal patterns resulting from Atchafalaya River discharge.	138

Figure 128. Salinity, under S08, in compartment 791, showing the slight saline intrusion in later years that is driven by this scenario’s higher rate of sea level rise. ....	138
Figure 129. TSS, under S08, in compartment 762, showing the reductions in peak values in the last decade of simulation. ....	139
Figure 130. Wetland type (FFIBS score) distribution of the Central Coast region under scenario S07 in Year 25. ....	141
Figure 131. Wetland type (FFIBS score) distribution of the Central Coast region under scenario S07 in Year 50. ....	142
Figure 132. Changes in species composition and corresponding changes in FFIBS score for TRNS0403, west of the Wax Lake Outlet (Point D in previous maps). ....	142
Figure 133. Change in vegetation cover under S07 is shown at representative points in the Central Coast region. ....	143
Figure 134. Wetland type (FFIBS score) distribution of the Central Coast region under scenario S08 in Year 25. ....	144
Figure 135. Wetland type (FFIBS score) distribution of the Central Coast region under scenario S08 in Year 50. ....	145
Figure 136. Change in vegetation cover under S08 is shown at representative points in the Central Coast region. ....	146
Figure 137. Elevation dynamics at CRMS0544 under S07. ....	147
Figure 138. Changes in pixel elevation over time for points along Transect03 - location of points shown in top figure. ....	148
Figure 139. Progressive increase in vegetated cover at grid cell 48422 under S07. ....	149
Figure 140. Elevation dynamics at QAQC2204 under S07. ....	150
Figure 141. Cumulative land loss for part of the Central Region for Years 25 (top left), 30 (top right), and 35 (bottom) under S08. ....	151
Figure 142. Cumulative land loss for S08 by Year 30 (top left) and Year 32 (top right) for an area near the Atchafalaya River in ATD, with inundation-induced loss conditions at TRNS0602 (lower panel). ....	152
Figure 143. Cumulative land loss by Year 40 for S08 in eastern TVB and western ATD (A); land elevation (B); organic accretion (C); mean annual inundation depth (D) for CRMS0542, CRMS0513 and TRNS0403 under S08. ....	154
Figure 144. Total HSI score for crayfish in the Atchafalaya Basin ecoregion over the 50-year S07 environmental scenario simulation. ....	155
Figure 145. Small juvenile brown shrimp HSI scores across the Teche/Vermilion/Bays ecoregion for Year 1 and Year 50 of the S07 environmental scenario. ....	156
Figure 146. Total HSI score for gadwall and mottled duck in the Teche/Vermilion/Bays ecoregion over the 50-year S07 environmental scenario simulation. ....	157
Figure 147. Total HSI score for alligator and seaside sparrow in the Teche/Vermilion/Bays ecoregion over the 50-year S07 environmental scenario simulation. ....	158
Figure 148. Total HSI score for gadwall and mottled duck in the Atchafalaya Delta ecoregion over the 50-year S08 environmental scenario simulation. ....	159
Figure 149. Small juvenile brown shrimp HSI scores across the Teche/Vermilion/Bays ecoregion for Year 1 and Year 50 of the S08 environmental scenario. ....	160

Figure 150. Comparison of vegetation cover change in the Central Coast region between the two scenarios, by ecoregion. ....	161
Figure 151. Comparison of conditions for S07 and S08 for CRMS0479. ....	162
Figure 152. Comparison of conditions for S07 and S08 for QAQC2200. ....	163
Figure 153. Stage, under S07, in Grand Lake on the interior of the Mermentau system of locks (compartment 1223). ....	165
Figure 154. Stage, under S07, in West Cove of Calcasieu Lake – directly connected to the Gulf (compartment 1278). ....	165
Figure 155. Stage, under S08, in Grand Lake on the interior of the Mermentau system of locks (compartment 1223). ....	166
Figure 156. Stage, under S08, in West Cove of Calcasieu Lake – directly connected to the Gulf (compartment 1278). ....	166
Figure 157. Tidal range, under S07, in the Mermentau River, immediately upstream of the outlet at the Gulf (compartment 1212). ....	167
Figure 158. Tidal range, under S07, in the Mermentau River, between the Gulf outlet and the Catfish Point structure at Grand Lake (compartment 1232). ....	167
Figure 159. Tidal range, under S07, in Grand Lake on the interior of the Mermentau system of locks (compartment 1223). ....	167
Figure 160. Tidal range, under S08, in southwestern Sabine Lake (compartment 1322). ....	168
Figure 161. Tidal range, under S08, in Johnson Bayou – adjacent to Sabine Lake (compartment 1313). ....	168
Figure 162. Tidal range, under S08, in the interior of southern Sabine Basin, north of Hamilton Lake and south of Starks South Canal (compartment 1311). ....	168
Figure 163. Salinity, under S07, in the Mermentau River, immediately upstream of the outlet at the Gulf (compartment 1212). ....	169
Figure 164. Salinity, under S07, in the Mermentau River, between the Gulf outlet and the Catfish Point structure at Grand Lake (compartment 1232). ....	169
Figure 165. Salinity, under S07, in Grand Lake on the interior of the Mermentau system of locks (compartment 1223). ....	169
Figure 166. TSS, under S07, in largely disconnected marsh south of White Lake (compartment 1185). ....	170
Figure 167. TSS, under S08, in largely disconnected marsh south of White Lake (compartment 1185). ....	171
Figure 168. Temperature, under S07, in largely disconnected marsh south of White Lake (compartment 1185). ....	172
Figure 169. Temperature, under S08, in largely disconnected marsh south of White Lake (compartment 1185). ....	172
Figure 170. Wetland type (FFIBS score) distribution of the Chenier Plain region under scenario S07 in Year 25. ....	174
Figure 171. Wetland type (FFIBS score) distribution of the Chenier Plain region under scenario S07 in Year 50. ....	175
Figure 172. Change in vegetation cover under S07 is shown at CRMS0619, a representative point in the Chenier Plain region. ....	176
Figure 173. Wetland type (FFIBS score) distribution of the Chenier Plain region under scenario S08 in Year 25. ....	177

Figure 174. Wetland type (FFIBS score) distribution of the Chenier Plain region under scenario S08 in Year 50. ....	178
Figure 175. Change in vegetation cover under S08 is shown at representative points in the Chenier Plain region. ....	179
Figure 176. Salinity and inundation dynamics at CRMS0677 under S07. ....	180
Figure 177. Salinity and inundation dynamics at QAQC2072 under S07. ....	181
Figure 178. Sediment dynamics at QAQC2058 under S08. ....	182
Figure 179. Inundation dynamics at CRSM0581 under S08. ....	183
Figure 180. Sediment dynamics at CRSM1738 under S08. ....	184
Figure 181. Salinity, elevation, and inundation dynamics at CRSM0570 under S08. ....	185
Figure 182. Land change and dynamics for parts of the Sabine ecoregion under S08: cumulative land change by Year 45 (top left) and by Year 50 (top right). ....	186
Figure 183. Existing conditions elevation (left) – darker brown shows higher marsh elevation; and areas of wetland loss at Year 50 under S08 (right). ....	187
Figure 184. Adult spotted seatrout HSI scores compared to salinity simulated for the marshes along the lower Mermentau River over the first 20 years of the S07 environmental scenario simulation. ....	188
Figure 185. Adult spotted seatrout HSI scores across the Mermentau/Lakes and Chenier Ridges ecoregions for Year 1 (left) and Year 50 (right) of the S07 environmental scenario. ....	189
Figure 186. Alligator HSI scores across the Mermentau/Lakes and Chenier Ridges ecoregions for Year 1 (left) and Year 50 (right) of the S07 environmental scenario. ....	189
Figure 187. Total HSI score for alligator and mottled duck in the Mermentau/Lakes ecoregion over the 50-year S07 environmental scenario simulation. ....	190
Figure 188. Total HSI score for juvenile blue crab and juvenile gulf menhaden in the Chenier Ridges ecoregion over the 50-year S08 environmental scenario simulation. ....	191
Figure 189. Adult spotted seatrout HSI scores across the Mermentau/Lakes and Chenier Ridges ecoregions for Year 1 and Year 50 of the S08 environmental scenario. ....	191
Figure 190. Comparison of S07 and S08 conditions for QAQC0989 in MEL. ....	192
Figure 191. Comparison of S07 and S08 conditions for QAQC2023 in CHR. ....	193

# LIST OF ABBREVIATIONS

1D.....	ONE DIMENSIONAL
CPRA .....	COASTAL PROTECTION AND RESTORATION AUTHORITY
CRMS .....	COASTWIDE REFERENCE MONITORING SYSTEM
DEM .....	[TOPOBATHYMETRIC] DIGITAL ELEVATION MODEL
FFIBS .....	FORESTED, FRESH, INTERMEDIATE, BRACKISH, SALINE
FWOA .....	FUTURE WITHOUT ACTION
FWOCFP.....	FUTURE WITHOUT CURRENTLY FUNDED PROJECTS
GIWW .....	GULF INTRACOASTAL WATERWAY
HNC .....	HOUMA NAVIGATIONAL CANAL
HSDRRS.....	HURRICANE & STORM DAMAGE RISK REDUCTION SYSTEM
HSI .....	HABITAT SUITABILITY INDEX
HYDRO .....	ICM-HYDROLOGY MODEL
ICM .....	INTEGRATED COMPARTMENT MODEL
LAVEGMOD.....	LOUISIANA VEGETATION MODEL
LULC .....	LAND USE/LAND COVER
MORPH .....	MORPHOLOGY MODEL
MRGO .....	MISSISSIPPI RIVER GULF OUTLET
NAVD88 .....	NORTH AMERICAN VERTICAL DATUM OF 1988
NSF .....	NATIONAL SCIENCE FOUNDATION
OMAR .....	ORGANIC MATTER ACCUMULATION RATE
PPT .....	PARTS PER TRILLION
QAQC .....	QUALITY ASSURANCE AND QUALITY CONTROL
SEA LEVEL RISE .....	EUSTATIC SEA LEVEL RISE
TSS .....	TOTAL SUSPENDED SOLIDS
ABBREVIATIONS FOR MODEL ECOREGIONS PROVIDED IN: ..... TABLE 1	
ABBREVIATIONS FOR VEGETATION SPECIES CODES PROVIDED IN: ..... TABLE 2	

# 1.0 INTRODUCTION

Analysis for the 2023 Coastal Master Plan focused on a regional approach to understanding the dynamics of a changing coastal Louisiana landscape. This report examines representative datasets from the Integrated Compartment Model (ICM) simulations of a future without action (FWOA), under two scenarios of possible future environmental conditions. Across all five coastal regions, model outputs are shown to provide a thorough understanding of how, and why the future landscape will look different from what it looks like today. Rather than simply reporting the same datasets at fixed locations in a repetitive format, this report instead is structured such that the data will tell a compelling narrative of one, or a few, of each coastal region and how that region may experience change in the future.

This report is specifically focused on the 2023 Coastal Master Plan FWOA under the lower and higher project selection environmental scenarios. These are outputs from the FWOA simulations that were directly used to assess a candidate project's robust performance under both scenarios. These simulations represent two possible outcomes for coastal Louisiana if we were to put our shovels (and dredges) down after we finish building all of the projects that we currently have funding (and permits) to construct. While we know that these two scenarios are not exact forecasts of the next 50 years, they are based upon real potential future climates, and were developed from the latest available data provided by international climate change modeling efforts.

The five regions examined are: Chenier Plain, the Central Coast, Terrebonne Basin, Barataria Basin, and the Pontchartrain/Breton. This report will discuss all five subroutines of the ICM that interact to update the coastal landscape: the hydrology model (**ICM-Hydro**), the wetland vegetation model (**ICM-LAVegMod**), the wetland morphology model (**ICM-Morph**), the barrier island and tidal inlet models (**ICM-BI and ICM-BITI**). The sixth, and final, ICM subroutine does not provide feedback to the landscape, but instead uses environmental and landscape outputs to calculate habitat suitability indices for a variety of important fish, fowl, and wildlife species in coastal Louisiana (**ICM-HSI**).

## SPATIAL UNITS AND TERMINOLOGY

To understand interactions among ICM subroutines, it is important to recognize that the different subroutines act on separate, overlapping grids with different resolutions (Figure 1). ICM-Hydro **compartments** are the largest (i.e., the lowest resolution) and are irregularly shaped to account for landscape features. These compartments were refined for 2023 Coastal Master Plan to more closely align with expected flows due to known hydrologic features (e.g., natural ridges, control structures, etc.). ICM-Morph **pixels** are the smallest (i.e., highest resolution) at 30 m x 30 m and make up a regular grid. Elevation and land cover type is calculated and tracked, with the existing conditions digital elevation model (DEM) as the starting point, at this finer scale and then aggregated up as needed to inform calculations for other subroutines. ICM-LAVegMod **grid cells** are sized in between at

480 m x 480 m and are aligned with the ICM-Morph pixels such that 256 are captured in each ICM-LAVegMod grid cell. The ICM-HSI subroutine uses the same grid cells as ICM-LAVegMod.

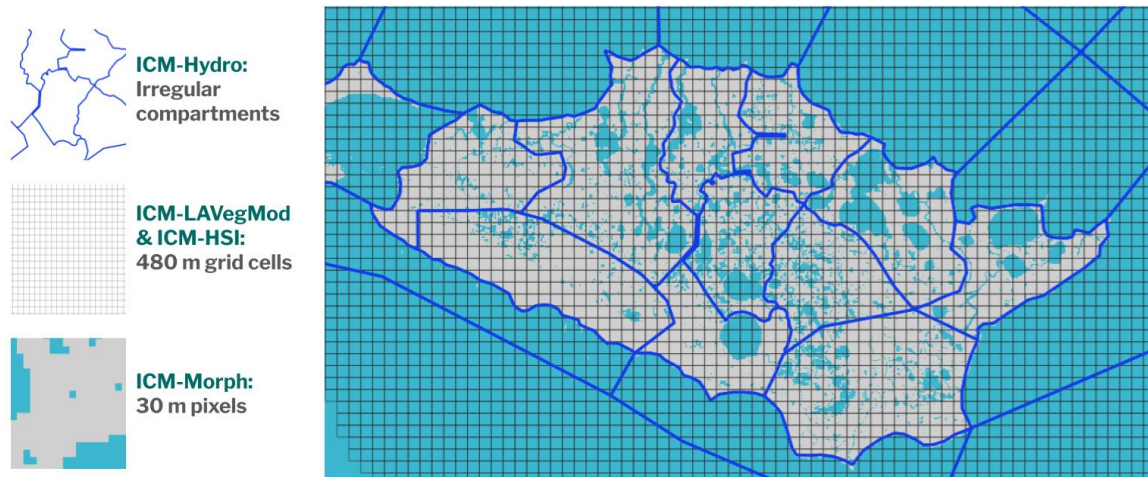


Figure 1. Spatial resolution for ICM subroutines in the area around Marsh Island in Vermilion Bay.

Throughout this report, model output will often be referred to via the model resolution that was used to derive the data. For instance, if discussing water levels, the report may reference the water level in a specific *compartment/ICM-Hydro compartment*. Similarly, vegetation coverages will be discussed at for a specific *grid cell/grid/ICM-LAVegMod grid*.

Prior to starting simulations for the 2023 Coastal Master Plan, a number of locations were identified as ‘model save points’. These would be locations at which all model data, down to a specific pixel, would be saved in order to conduct quality assurance and quality control (QAQC) on model processes and simulations. These **QAQC save points** were located following three different criteria:

- **CRMS locations** – every observation station within the Coastwide Reference Monitoring System (CRMS) was selected as a save point. These are labeled following the CRMS convention and will appear in this report as a four digit integer appended to “CRMS”, i.e., **CRMS1234**
- **Transects** – several transects were deliberately placed at a variety of locations around the coastal domain. These included areas such as in the outfall locations of planned sediment diversion projects, across the interior of the Cameron-Creole Watershed, and other similar points of interest across the coast. These are labeled by appending a four digit integer to “TRNS”, i.e., **TRNS0701**. The first two digits indicate the transect ID, and the last two digits identify the location along the transect. Therefore TRNS0701 is the first point in transect 7, TRNS0702 is the next location, followed by TRNS0703, etc.
- **QAQC points** - the third category of save points was randomly placed. A random placement geospatial algorithm was used to place 100 locations within each

ecoregion. These randomly placed locations were also numbered with a four digit integer, i.e., **QAQC1234**.

Following the method above, there are 2,941 QAQC save points with archived annual data from every ICM simulation. These data timeseries are used throughout the report and will be labeled as coming from a location with a name such as CRMS1234, TRNS1234, or QAQC1234.

## ECOREGION AND REGIONAL BOUNDARIES

The 2023 Coastal Master Plan analysis, stakeholder engagement, and document layout are structured around the five primary regions of coastal Louisiana: the Chenier Plain, the Central Coast, Terrebonne Basin, Barataria Basin, and the Pontchartrain/Breton basins (Figure 2). Model data for each of these regions is further subdivided into ecoregions (Figure 3), which are an amalgamation of ICM-Hydro compartments that are conterminous and all located with a specifically unique portion of the coast. The number of ecoregions varies per region, but they were delineated following physical barriers (such as landbridges), flowpaths (such as a bayou or river), natural demarcations such as ridges, or even human-made delineators (such as shipping lanes). Throughout this report, the model outputs will be summarized by region, with discussion often referring to these finer scale ecoregion boundaries. The ecoregions in this report will be referenced using an abbreviation, as listed in Table 1.

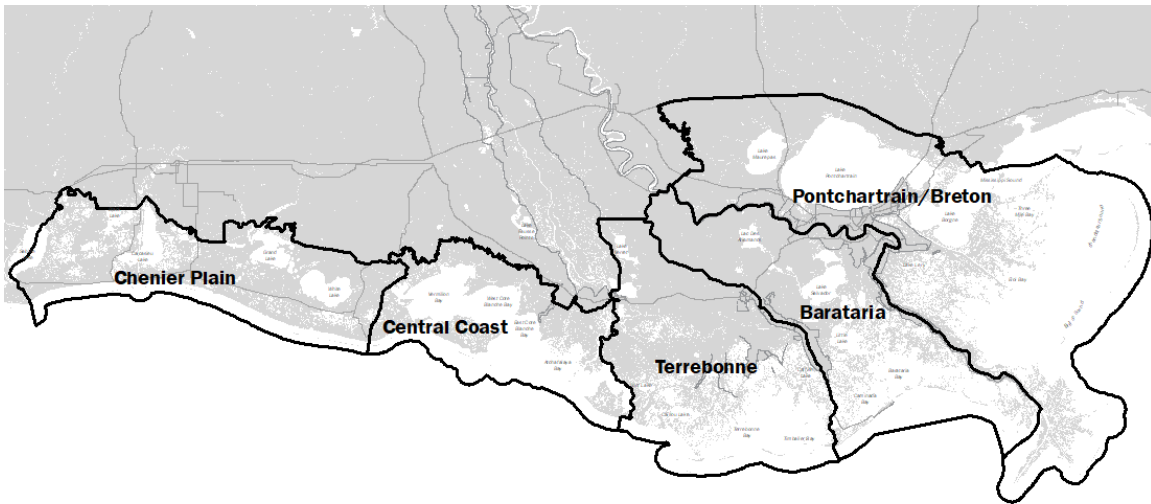


Figure 2. Master plan regions of coastal Louisiana.

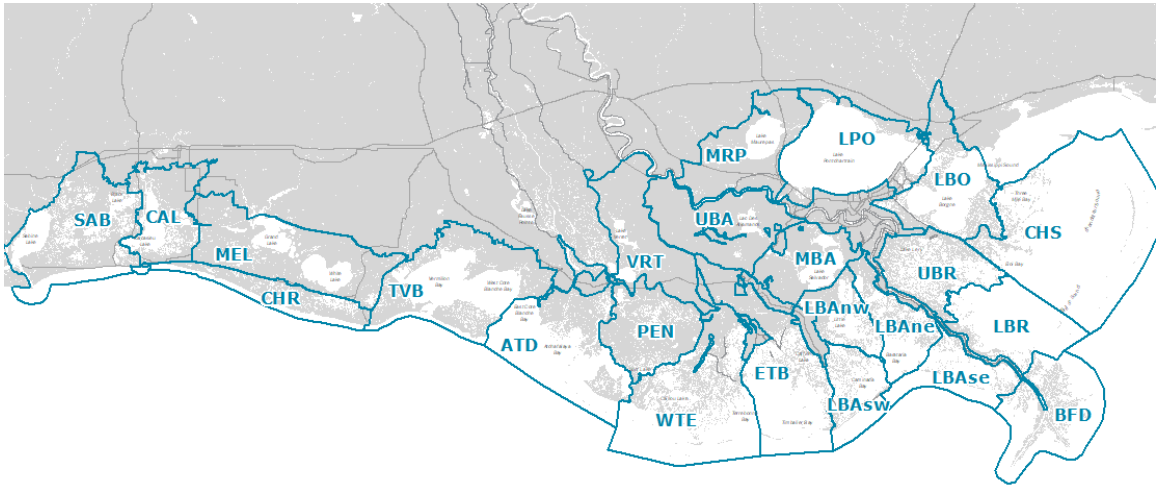


Figure 3. Ecoregions used in modeling analyses for the 2023 Coastal Master Plan.

Table 1. Ecoregion abbreviations and the region in which they are located

<b>Abbreviation</b>	<b>Ecoregion</b>	<b>Region</b>
ATD	Atchafalaya Delta	Central Coast
BFD	Bird's Foot Delta	Pontchartrain/Breton
CAL	Calcasieu	Chenier Plain
CHR	Chenier Ridges	Chenier Plain
CHS	Chandeleur Sound	Pontchartrain/Breton
ETB	Eastern Terrebonne	Terrebonne
LBAne	Lower Barataria (NE)	Barataria
LBAw	Lower Barataria (NW)	Barataria
LBAse	Lower Barataria (SE)	Barataria
LBAsw	Lower Barataria (SW)	Barataria
LBO	Lake Borgne	Pontchartrain/Breton
LBR	Lower Breton	Pontchartrain/Breton
LPO	Lake Pontchartrain	Pontchartrain/Breton
MBA	Mid Barataria	Barataria
MEL	Mermentau/Lakes	Chenier Plain
MRP	Maurepas	Pontchartrain/Breton
PEN	Penchant	Terrebonne
SAB	Sabine	Chenier Plain
TVB	Teche/Vermilion/Bays	Central Coast
UBA	Upper Barataria	Barataria
UBR	Upper Breton	Pontchartrain/Breton

VRT	Verret Basin	Terrebonne
WTE	Western Terrebonne	Terrebonne

## VEGETATION SPECIES ABBREVIATIONS

Throughout this report, the vegetation model (ICM-LAVegMod) results will be discussed both as the overall species mixture/assembly, as well as the relative cover of the individual plant species included in the model. When referring to individual species, the results are reported in the text using a shorthand code as listed in Table 2.

Table 2. Symbol codes used in ICM-LAVegMod to represent each modeled species

Code	Vegetation species	Code	Vegetation species
AVGE	<i>Avicennia germinans</i>	QUNI	<i>Quercus nigra</i>
BAHABI	<i>Baccharis halimifolia</i>	QUTE	<i>Quercus texana</i>
CLMA10	<i>Cladium mariscus</i>	QUVI	<i>Quercus virginiana</i>
COES	<i>Colocasia esculenta</i>	SALA	<i>Sagittaria lancifolia</i>
DISP	<i>Distichlis spicata</i>	SALA2	<i>Sagittaria latifolia</i>
DISPBI	<i>Distichlis spicata</i>	SANI	<i>Salix nigra</i>
ELBA2_Flt	<i>Eleocharis baldwinii</i>	SCAM6	<i>Schoenoplectus americanus</i>
ELCE	<i>Eleocharis cellulose</i>	SCCA11	<i>Schoenoplectus californicus</i>
IVFR	<i>Iva frutescens</i>	SCRO5	<i>Schoenoplectus robustus</i>
JURO	<i>Juncus roemerianus</i>	SOSE	<i>Solidago sempervirens</i>
MOCE2	<i>Morella cerifera</i>	SPAL	<i>Spartina alterniflora</i>
NOTMOD	Not Modeled	SPCY	<i>Spartina cynosuroides</i>
NYAQ2	<i>Nyssa aquatica</i>	SPPA	<i>Spartina patens</i>
PAAM2	<i>Panicum amarum</i>	SPPABI	<i>Spartina patens</i>
PAHE2	<i>Panicum hemitomon</i>	SPVI3	<i>Sporobolus virginicus</i>
PAHE2_Flt	<i>Panicum hemitomon</i>	STHE9	<i>Strophostyles helvola</i>
PAVA	<i>Paspalum vaginatum</i>	TADI2	<i>Taxodium distichum</i>
PHAU7	<i>Phragmites australis</i>	TYDO	<i>Typha domingensis</i>
POPU5	<i>Polygonum punctatum</i>	ULAM	<i>Ulmus americana</i>
QULA3	<i>Quercus laurifolia</i>	UNPA	<i>Uniola paniculate</i>
QULE	<i>Quercus lyrate</i>	ZIMI	<i>Zizaniopsis miliacea</i>

# 2.0 PONTCHARTRAIN & BRETON

## 2.1 INTRODUCTION

The Pontchartrain/Breton region reaches from the east bank of the Mississippi River to the Mississippi state line and includes New Orleans, Mandeville, and Slidell. The region also includes Lakes Pontchartrain and Borgne as well as the Bird's Foot Delta of the Mississippi River. The region is surrounded by the Breton and Chandeleur sounds, which are separated from the Gulf by a string of barrier islands.

The Pontchartrain/Breton region is bordered on the south by the Mississippi River levee and the river itself below East Point a la Hache. It encompasses Breton Island, the Chandeleur Islands, and the lower part of the Pearl River floodplain.

The ecosystems in this region are very diverse. Managed lands include Joyce Wildlife Management Area, St. Tammany Wildlife Refuge, the Big Branch Marsh, Bayou Sauvage, Delta and Breton National Wildlife Refuges. To the east, the Breton Wildlife Refuge provides important wintering habitat for the federally threatened piping plover. The Chandeleur Islands are the only place in Louisiana where true seagrasses are found. At the other end of the region, the Maurepas Swamp includes more than 100,000 acres of cypress tupelo swamp, bottomland hardwood forest, and fresh and intermediate marshes. Between these is a productive estuary, including Lake Pontchartrain, Lake Borgne, Breton Sound, and Chandeleur Sound and includes extensive areas of marsh on the Orleans Landbridge and Biloxi Marsh. These areas support vibrant recreational and commercial fisheries. For example, in 2020, the region accounted for 37% of the state wide crab landings.

The wetlands of the Pontchartrain/Breton region have been degrading like the rest of the coast. A number of innovative restoration projects have already been implemented. For example, the Caernarvon Freshwater Diversion was constructed in 1991. It was designed to manage salinity levels in the Breton Sound area to be suitable for oysters in the public seed grounds. It has since shown that it can build and sustain land and is now operated to better support ecosystem restoration. The West Bay Sediment Diversion, completed in 2003, is an uncontrolled diversion of Mississippi River freshwater and sediments on the west bank above Head of Passes in the Bird's Foot Delta. The success of these projects supports the currently planned diversion projects in the region, including the River Reintroduction to Maurepas Swamp and the Mid-Breton Sediment Diversion; both of which are active in the 50 year FWOA simulations.

## 2.2 FWOA STAGE

### LOWER PROJECT SELECTION SCENARIO (S07)

Under a FWOA, there is a clear cross-basin gradient in water level dynamics across the Pontchartrain/Breton basins. This gradient is less pronounced for the open-water areas of the Pontchartrain Basin (Lakes Borgne, Pontchartrain, and Maurepas), however, a pronounced increase of stage is found for lake-adjacent marshes and interior/upland areas. Timeseries plots show that lower parts of the basin mostly follow the astronomic tide, whereas upper portions are mostly influenced by signals from river distributary channels and diversion outfalls.

The stage in areas near diversion outfalls is impacted by diversion operation, as can be seen in timeseries plots indicating high stages around springtime driven by higher Mississippi River discharge rates. However, even under several decades of sea level rise under S07, the spatial distribution of river-flood dominated versus astronomic tide dominated signals remains evident across the Pontchartrain/Breton region.

### HIGHER PROJECT SELECTION SCENARIO (S08)

The trends and gradients of water levels under S08 in the Pontchartrain/Breton region are consistent with those seen under S07; however the magnitude of increases in water levels during later decades is greater due to the higher rates of sea level rise.

## 2.3 FWOA TIDAL RANGE

### LOWER PROJECT SELECTION SCENARIO (S07)

The tidal range follows an expected pattern with the largest ranges in the offshore, with a gradual decline of in tidal range towards the upper portions of the basins. The outfall areas of the Mid-Breton sediment diversions show much lower tidal range compared to other interior areas; this is in line with expectations given the more static water level that will be set by the outfall levels, not tidal water levels. The same applies to the Bird's Foot Delta area, albeit to a lesser degree due to its higher exposure to offshore. There is hardly any gradient in tidal range across Lake Pontchartrain and Lake Maurepas. The described patterns remain applicable throughout the 50-year simulation period; however, there is a slight increase of tidal ranges over time with rising sea levels.

### HIGHER PROJECT SELECTION SCENARIO (S08)

The trend in tidal ranges in Pontchartrain/Breton under S08 are consistent with those seen under S07. One area of difference is in that the slight increase in tidal range in later decades is more

pronounced under S08 than it was under S07.

## 2.4 FWOA SALINITY

### LOWER PROJECT SELECTION SCENARIO (S07)

The overall pattern in the Pontchartrain/Breton region follows a clear estuarine-gradient pattern; with near-zero salinity concentrations in the uppermost parts of the Pontchartrain and Breton basins, and gradually increasing salinities towards the offshore with brackish and saline waters in the lower portions of the basins.

The effect of operation of the Mid-Breton sediment diversions can be recognized in compartments near the outfalls. Parts of the basins that are more distant from the outfalls also appear to be affected, showing a freshening signature, albeit to a lesser degree than areas immediately adjacent to the outfall. Salinity concentrations increase over time in the upper Pontchartrain and north Chandeleur Sound, which would indicate an increase of salinity intrusion over time as a result of sea level rise.

### HIGHER PROJECT SELECTION SCENARIO (S08)

Salinity concentrations appear to increase over time in the upper Pontchartrain and north Chandeleur Sound, which would indicate an increase of salinity intrusion over time. Simultaneously, a decrease of salinity concentrations over time can be observed in the area ranging from the south Chandeleur Sound to the lower Breton Sound and the west of the BFD, especially in the last decade. This is due to a sea level rise-driven elevation of the downstream water level boundary for the one dimensional (1D) Mississippi River, resulting in increased flow rates through the distributaries and decreased flow rates through the most downstream boundary (Southwest Pass). With the increasing rates of fresh water discharging into the Breton Sound, the salinity level of that region is reduced. This effect is the most impactful in the last decade and more severe under S08 than was seen in S07.

## 2.5 FWOA TOTAL SUSPENDED SOLIDS (TSS)

### LOWER PROJECT SELECTION SCENARIO (S07)

Under S07, low TSS concentrations are found in upper portions of the Pontchartrain/Breton region that are distant from river distributaries or diversion outfalls of any type. Higher TSS can be seen in areas around diversion outfalls, river distributaries, and the BFD. No substantial differences can be observed when comparing across decades. However, within diversion outfall areas, seasonal and interannual changes in TSS can be seen as a function of diversion operations; which in turn are

impacted by the interannual variability of the Mississippi River flow hydrograph.

## HIGHER PROJECT SELECTION SCENARIO (S08)

Trends in TSS across the basin, and over time, are consistent in the Pontchartrain/Breton region between S08 and S07. Impacts of access to riverine sediments is a driving factor in defining TSS dynamics throughout the basin.

## 2.6 FWOA WATER TEMPERATURE

### LOWER PROJECT SELECTION SCENARIO (S07)

There is a clear and persistent increase in temperature over the 50 year FWOA simulation, under S07. This long-term increase is on the order of approximately 1 degree Celsius, and is evident in both the wintertime lows and summertime highs. This increase while evident, is relatively minor in magnitude when compared against the seasonal range in temperatures seen in coastal waters of Louisiana, which range from a wintertime minimum of approximately 10 degrees Celsius in estuarine (non-river dominated) areas (Figure 4). This minimum decreases to approximately 6 degrees Celsius when a region is more heavily impacted by colder waters coming from the snowmelt-impacted Mississippi River (Figure 5).

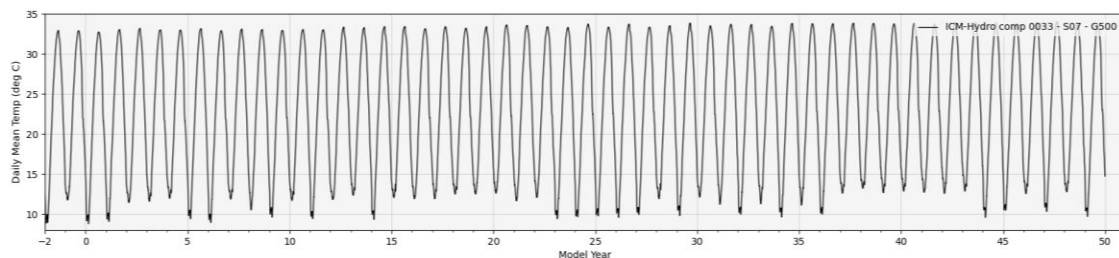


Figure 4. Water temperature, under S07, in Lake Maurepas (compartment 33); this demonstrates the warmer winter minimums in areas less connected to Mississippi River.

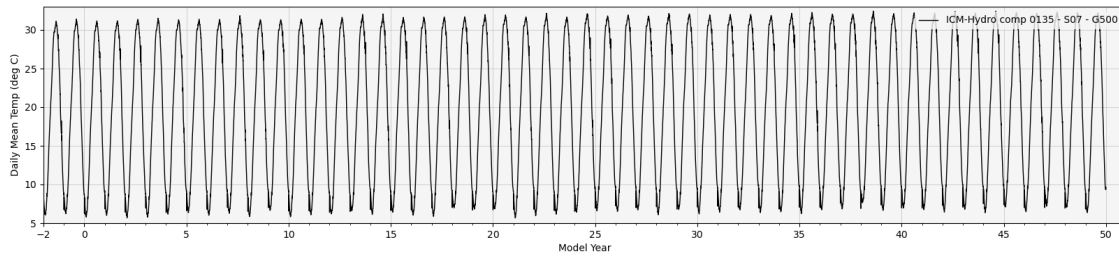


Figure 5. Water temperature, under S07, in the Bird's Foot Delta at Fort St. Philip (compartment 135); this demonstrates the colder winter minimums in areas with direct connection to the Mississippi River.

## HIGHER PROJECT SELECTION SCENARIO (S08)

The results for the Pontchartrain/Breton region under S08 are similar to S07; in particular with respect to interannual variability in temperature; all years are relatively similar with only gradual, and persistent increases over time), however, it is clearly noticeable that S08 has a higher degree of warming than S07. The year-to-year variation in temperatures in the offshore and interior portions of Pontchartrain/Breton region is very similar between S07 and S08.

However, the overall magnitude of increase is greater in S08, given the higher rates of temperature increases in the underlying climate change-derived scenario values. The higher degree of warming of S08 compared to S07 becomes more and more obvious over time. When comparing S08 to S07, consistently higher summertime highs and wintertime lows can be observed in the Breton region. The temperature in the Pontchartrain area is controlled more by the more stable estuarine water temperature boundary and is less impacted by the fluctuating Mississippi River temperatures than other more river-dominated areas (Figure 6).

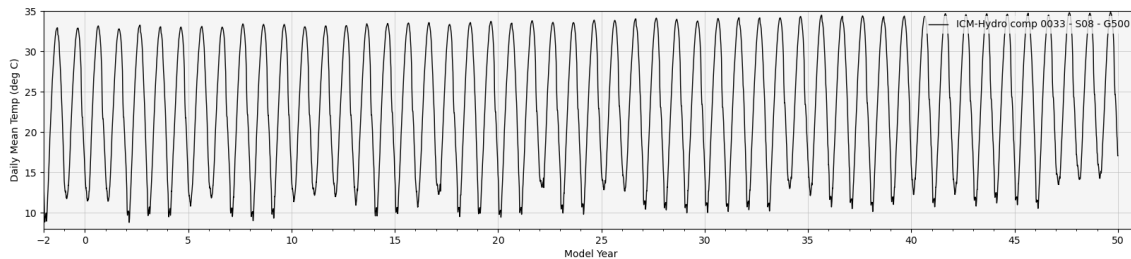


Figure 6. Water temperature, under S08, in Lake Maurepas (compartment 33); this demonstrates the warmer winter minimums in areas less connected to Mississippi River.

## 2.7 FWOA VEGETATION

### LOWER PROJECT SELECTION SCENARIO (S07)

Land and vegetation cover in the MRP ecoregion is stable under S07 (Figure 7 and Figure 8). CRMS5414 illustrates the vegetation cover stability of the Maurepas Swamp (Point A in Figure 9). In LPO, there is some swamp conversion to intermediate marsh and expansion of brackish marsh especially along the north shore of Lake Pontchartrain. This is illustrated with CRMS0006 (Point B in Figure 9), which for the first 40 years was dominated by TYDO and PHAU7, and then converted to SCAM6 in the last decade. In the LBO ecoregion, most of the vegetation changes are in the Pearl River Basin. In the Pearl River Basin, bottomland hardwood is replaced with swamp, and intermediate marsh is replaced with brackish marsh (Figure 7 and Figure 8). The conversion of intermediate to brackish marsh is illustrated with CRMS4110 (Point C in Figure 9), which was dominated by PHAU7 (Years 1 to 37) and converted to SCAM6 (Years 38 to 50). In UBR, the operation of the Mid-Breton Diversion leads to gains in fresh and intermediate marsh. The formation of a small delta by the Mid-Breton Diversion is demonstrated with CRMS0014 (Point D in Figure 9). CRMS0014 experiences delta expansion around Year 30 and keeps gaining land until Year 49. The LBR ecoregion is dominated by intermediate marsh and is relatively stable (Figure 7 and Figure 8). This is demonstrated with CRMS0119, which is dominated by PHAU7 throughout the simulation (Point E in Figure 9). In the CHS ecoregion, saline marsh is slowly lost, as demonstrated by CRMS1024 (Point F in Figure 9).

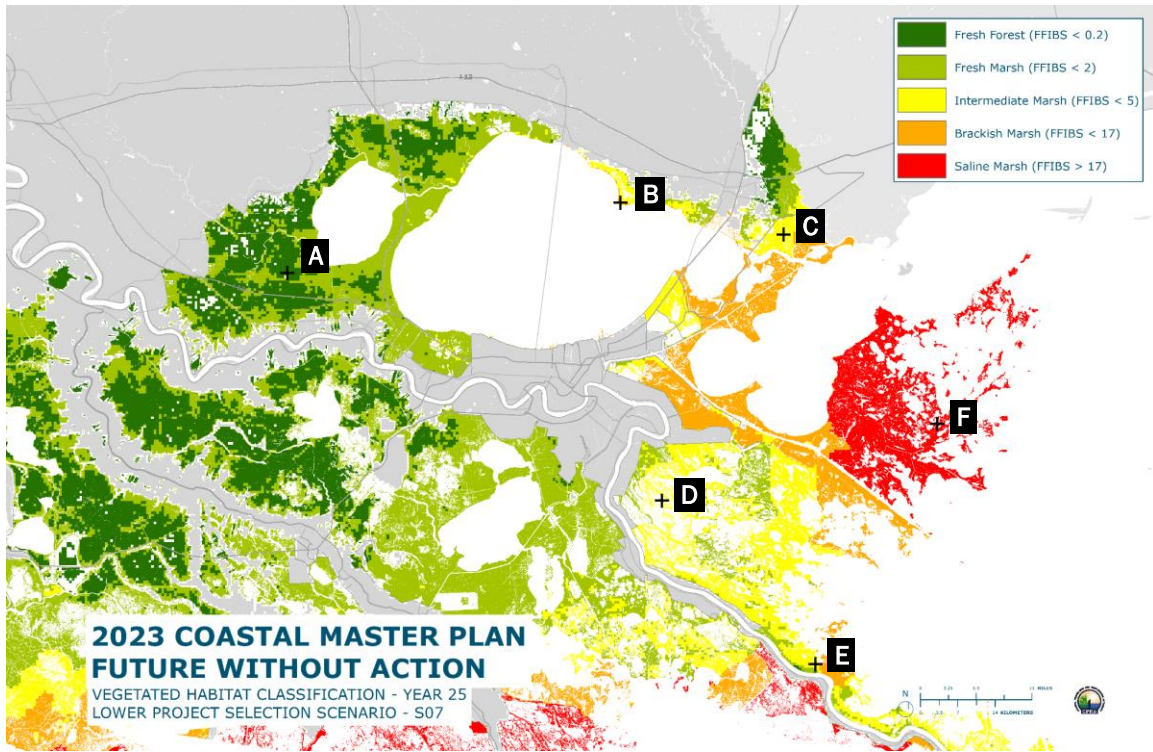


Figure 7. Wetland type (Forested, Fresh, Intermediate, Brackish, or Saline [FFIBS] score) distribution of the Pontchartrain and Breton basins under scenario S07 in Year 25.

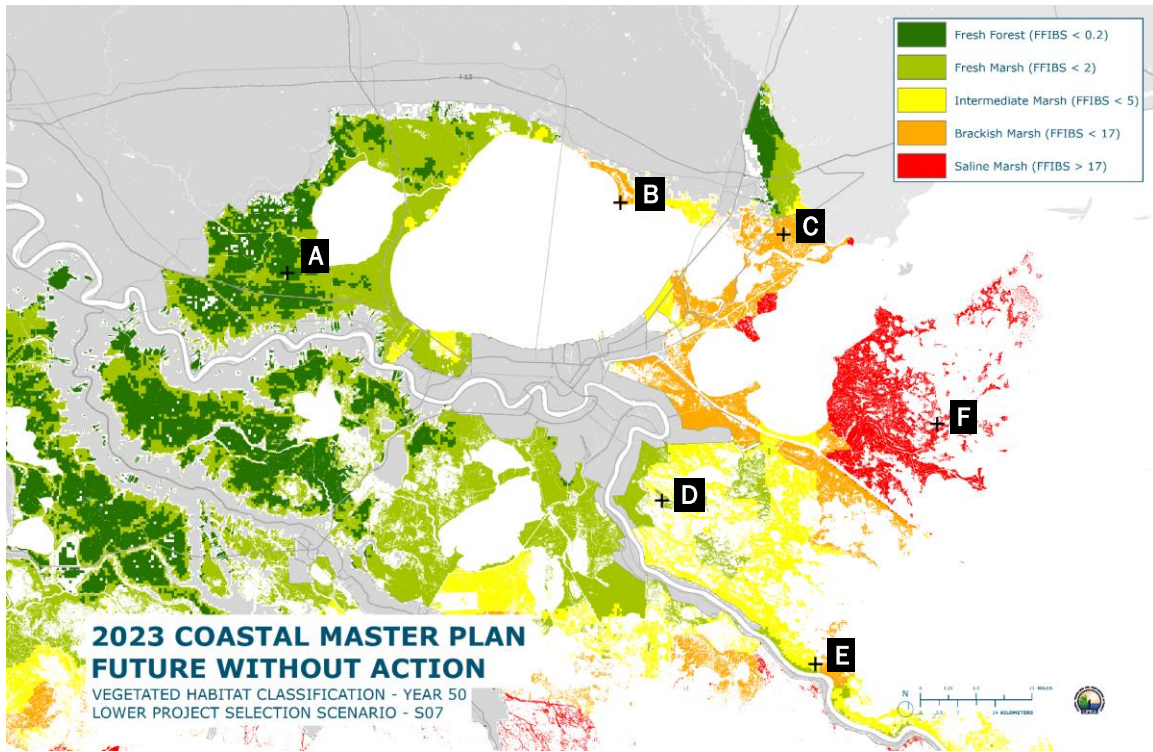


Figure 8. Wetland type (FFIBS score) distribution of the Pontchartrain and Breton basins under scenario S07 in Year 50.

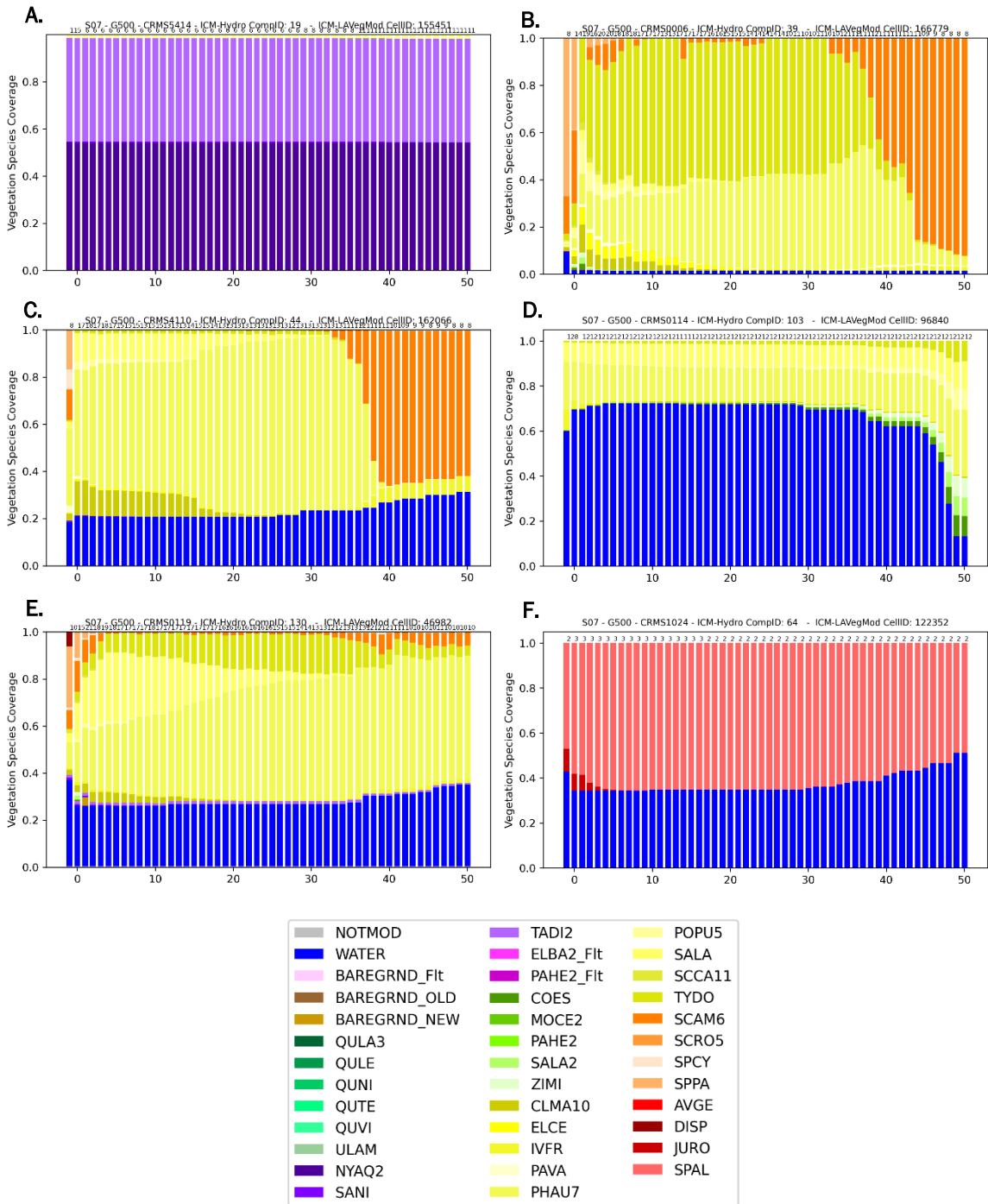


Figure 9. Change in vegetation cover under S07 is shown at representative points for different locations throughout the Pontchartrain and Breton basins. Point locations are shown in previous Pontchartrain/Breton region map figures.

Under S07, there is steady land loss in both brackish and intermediate marshes in the BFD. However, loss on the west side is more rapid than on the east side of the BFD (Figure 10 and Figure 11). This is illustrated with QAQC2415 on the west and CRMS2634 on the east (Points A and B, respectively, in Figure 12). At CRMS2634, there is a steady loss of PHAU7 dominated intermediate marsh. At QAQC2415, brackish marsh dominated by SCAM6 shows similar loss rates to CRMS2634 in the first two decades as more salt tolerant species dominated by JURO start invading in Year 8. In the third decade, brackish marsh is rapidly lost and only a small area of JURO dominated saline marsh remains by Year 50.

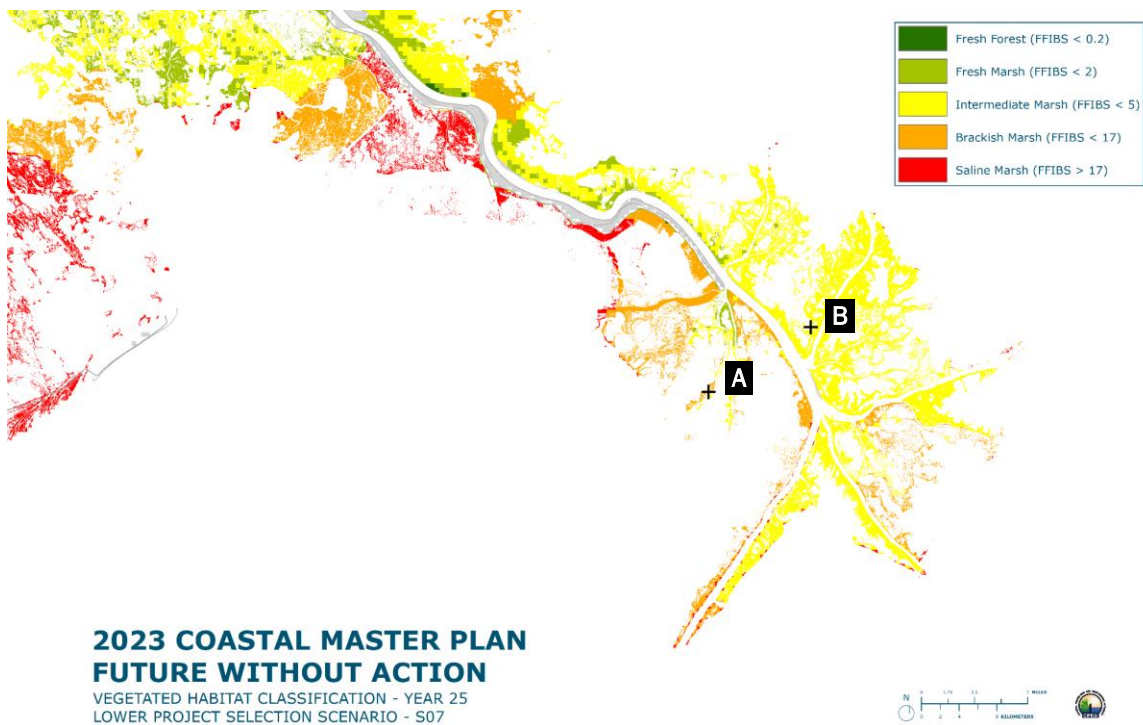


Figure 10. Wetland type (FFIBS score) distribution of the Bird's Foot Delta under scenario S07 in Year 25.

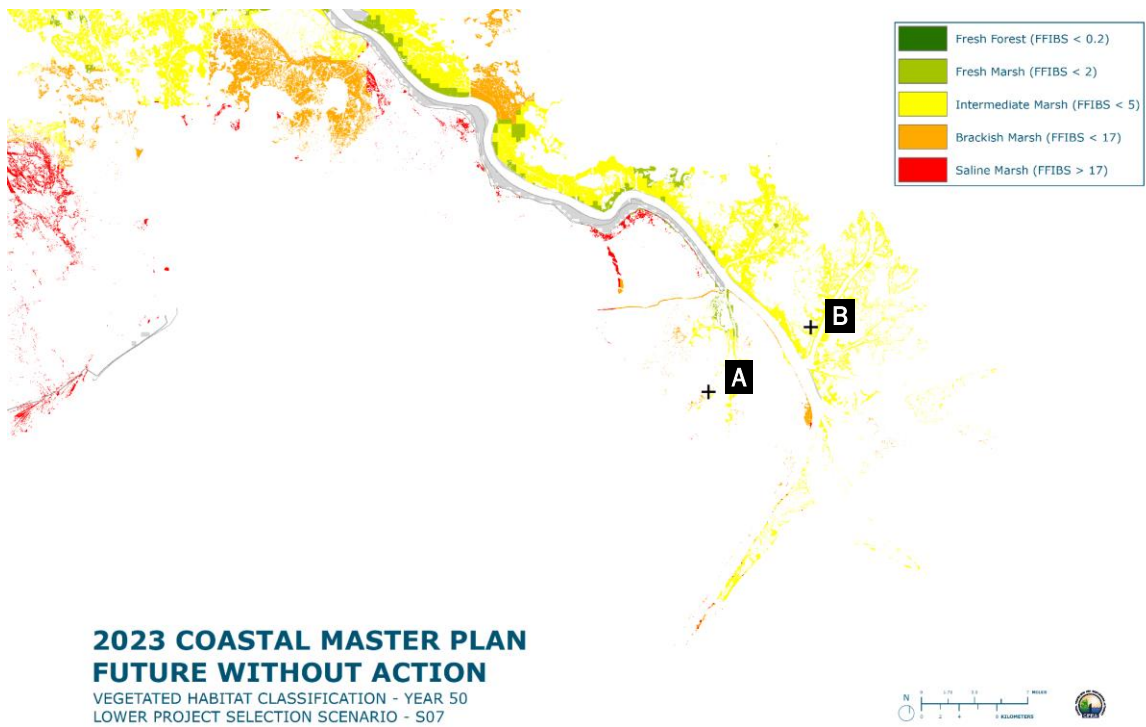


Figure 11. Wetland type (FFIBS score) distribution of the Bird’s Foot Delta under scenario S07 in Year 50.

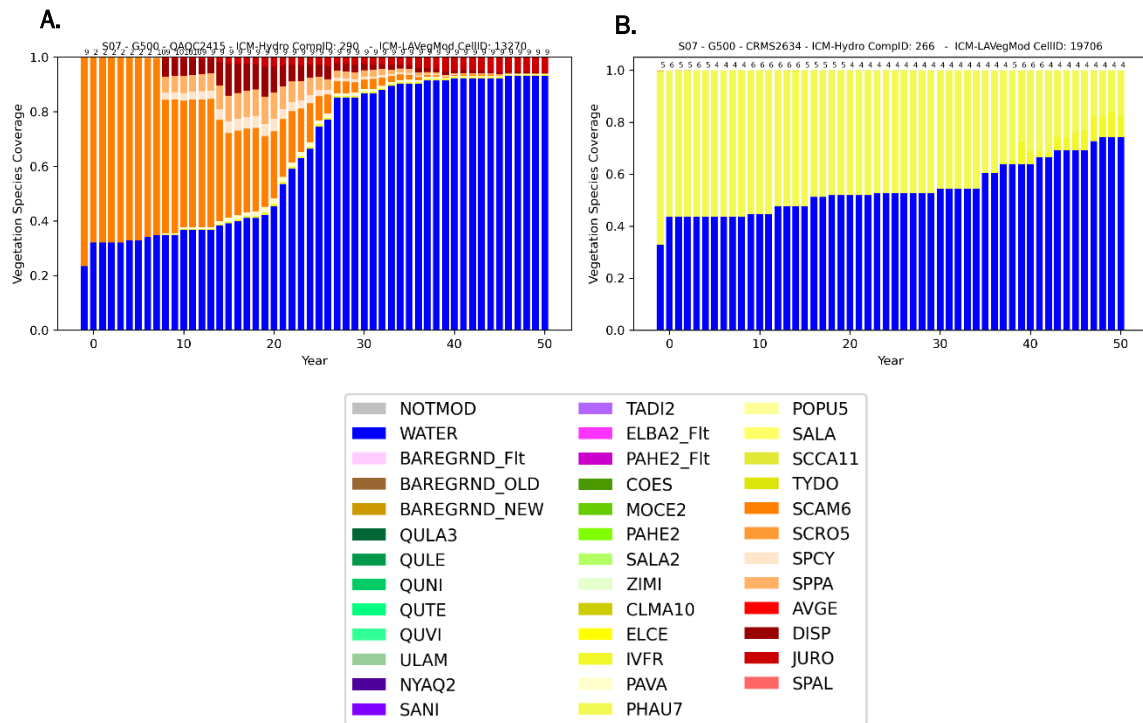


Figure 12. Change in vegetation cover under S07 is shown at representative points within the Bird’s Foot Delta. Point locations are shown in previous Bird’s Foot Delta map figures.

## HIGHER PROJECT SELECTION SCENARIO (S08)

Land and vegetation cover in the MRP ecoregion was stable under S08 (Figure 13 and Figure 14). CRMS5414 illustrates the vegetation cover stability of the Maurepas Swamp (Point A in Figure 15). On the Maurepas landbridge, some fresh marsh transitioned to intermediate marsh. In LPO, there was expansion of brackish marsh especially along the north shore of Lake Pontchartrain. This is illustrated with CRMS0006 (Point B in Figure 15), which is dominated by TYDO and PHAU7, and has increasing SCAM6 and decreasing TYDO starting in Year 30. In the LBO ecoregion, most of the vegetation changes are in the Pearl River Basin. In the Pearl River Basin, bottomland hardwood is replaced with swamp and intermediate marsh is replaced with brackish marsh. This conversion of intermediate to brackish marsh is illustrated with CRMS4110, which was dominated by PHAU7 (Years 1 to 30) and converted to SCAM6 (Years 31 to 50) as marsh was lost (Point C in Figure 15). In UBR, the operation of the Mid-Breton Diversion maintains fresh and intermediate marsh. The maintenance of intermediate marsh by the Mid-Breton Diversion is demonstrated with CRMS0014 (Point D in Figure 15). CRMS0014 maintains its intermediate marsh and even gains some land in Year 46. In the LBR ecoregion, intermediate marsh was relatively stable up to Year 35 and then started losing land. This is demonstrated with CRMS0119 (Point E in Figure 15), which was dominated by PHAU7 throughout the simulation, but started losing land around Year 26. In the CHS ecoregion saline marsh is rapidly lost

starting around Year 25, as demonstrated by CRMS1024 (Point F in Figure 15).

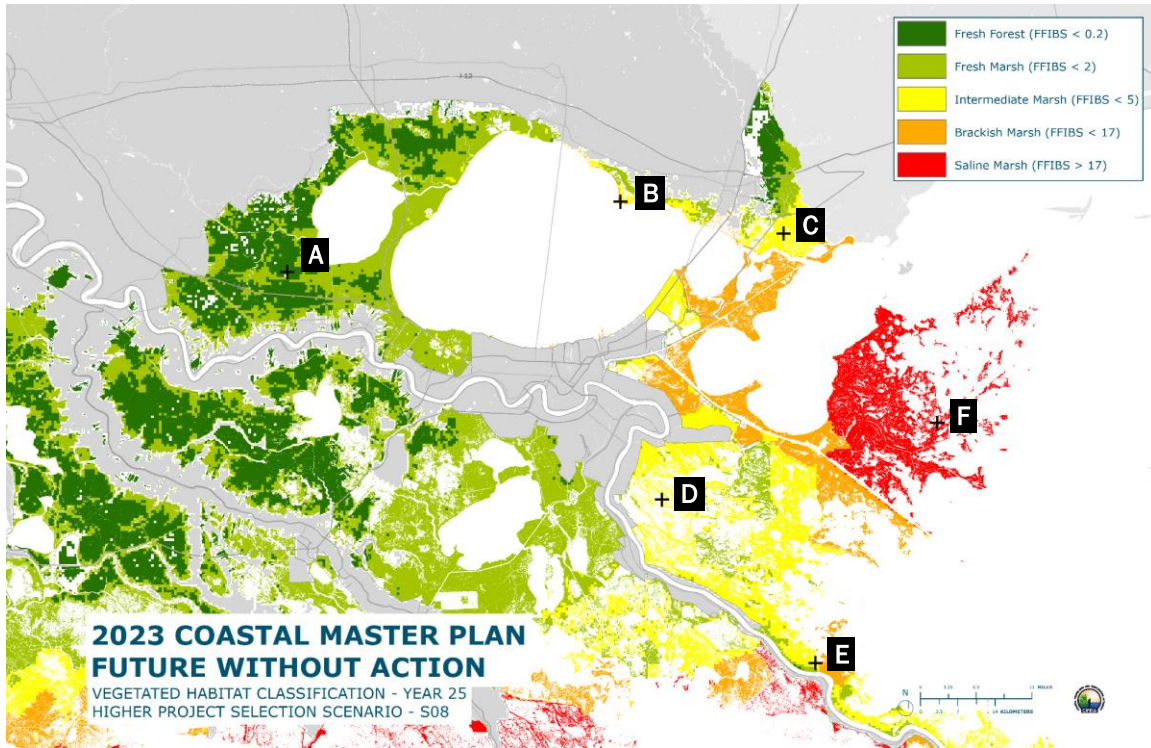


Figure 13. Wetland type (FFIBS score) distribution of the Pontchartrain and Breton basins under scenario S08 in Year 25.

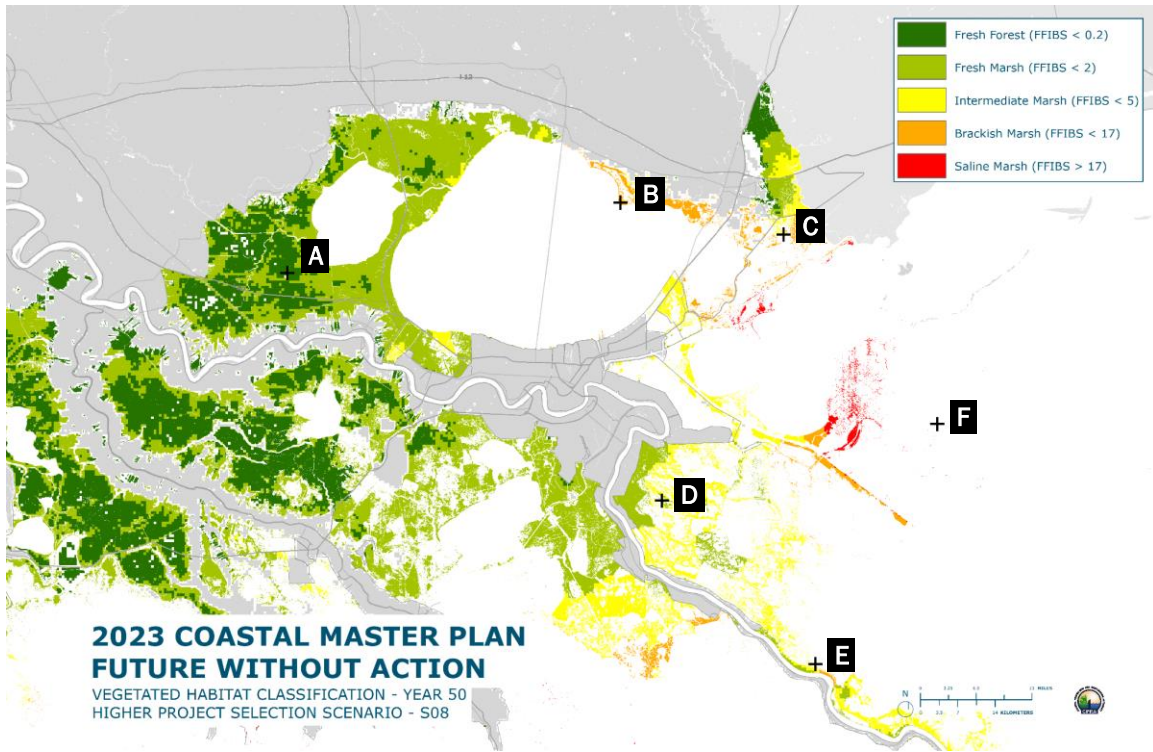


Figure 14. Wetland type (FFIBS score) distribution of the Pontchartrain and Breton basins under scenario S08 in Year 50.

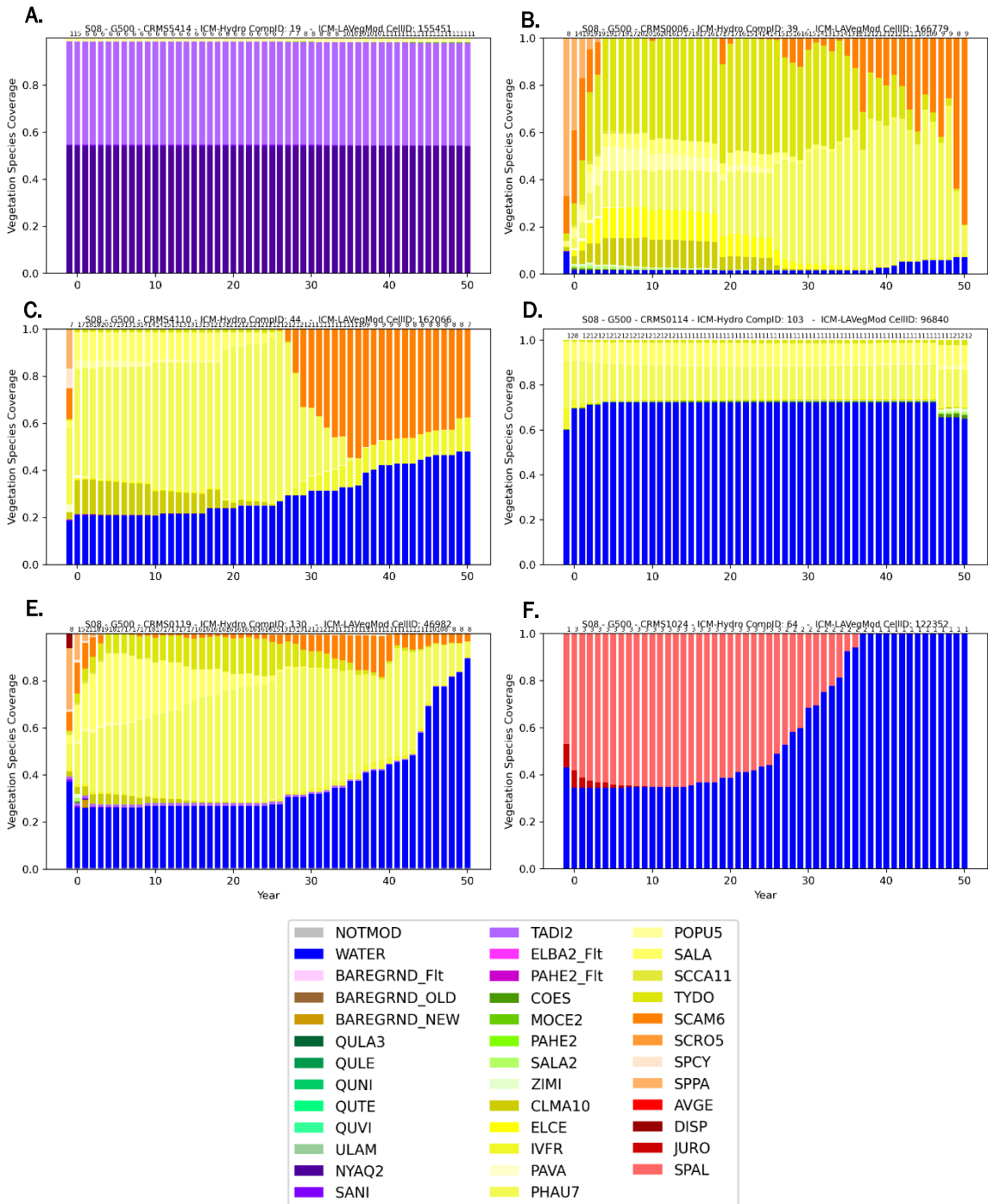


Figure 15. Change in vegetation cover under S08 is shown at representative points for different locations throughout the Pontchartrain and Breton basins. Point locations are shown in previous Pontchartrain/Breton region map figures.

Under S08, there is rapid land loss in both brackish and intermediate marshes in the BFD (Figure 16 and Figure 17). However, loss on the west side is more rapid than on the east side of the BFD. This is illustrated with QAQC2415 on the west and CRMS2634 on the east (Points A and B, respectively, in Figure 18). At CRMS2634 there is a loss of PHAU7 that starts relatively slow in the first two decades and then accelerates until only a few patches remain by Year 38 which survive to the end of the run. At QAQC2415, brackish marsh dominated by SCAM6 shows similar loss rates to CRMS2634 in the first 15 years as more salt tolerant species dominated by JURO start invading in Year 8. From Year 15 to 20 most of the brackish marsh is rapidly lost and only a small area of JURO dominated saline marsh remains over the last two decades.

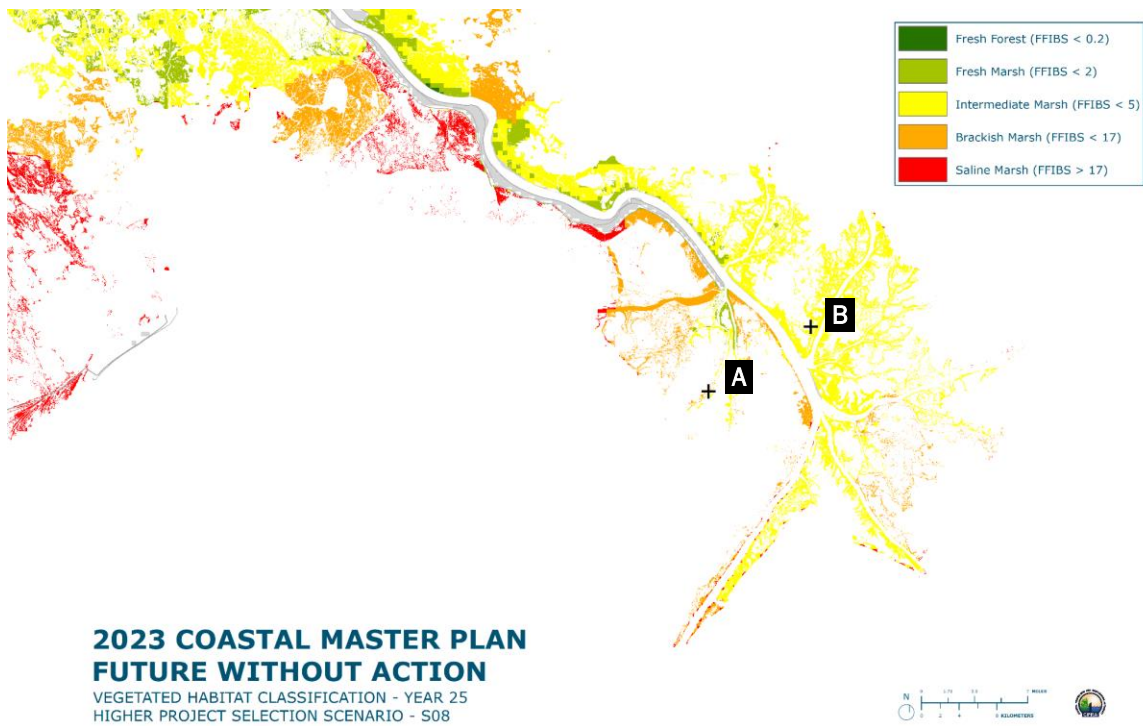


Figure 16. Wetland type (FFIBS score) distribution of the Bird's Foot Delta under scenario S08 in Year 25.

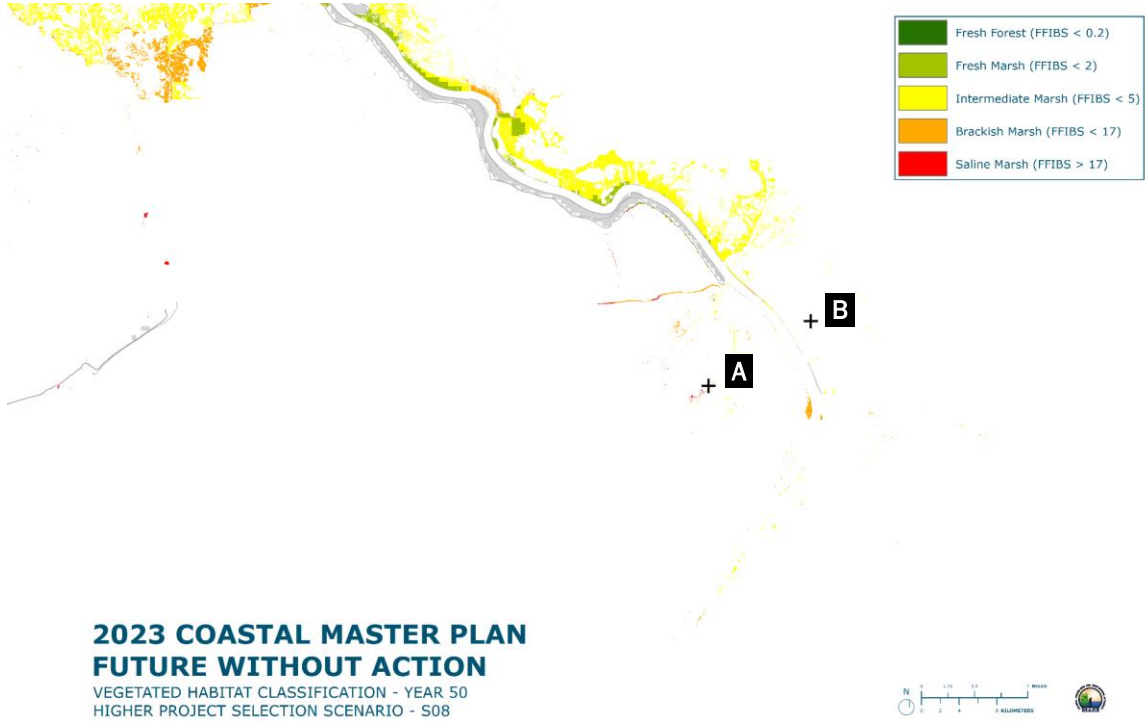


Figure 17. Wetland type (FFIBS score) distribution of the Bird's Foot Delta under scenario S08 in Year 50.

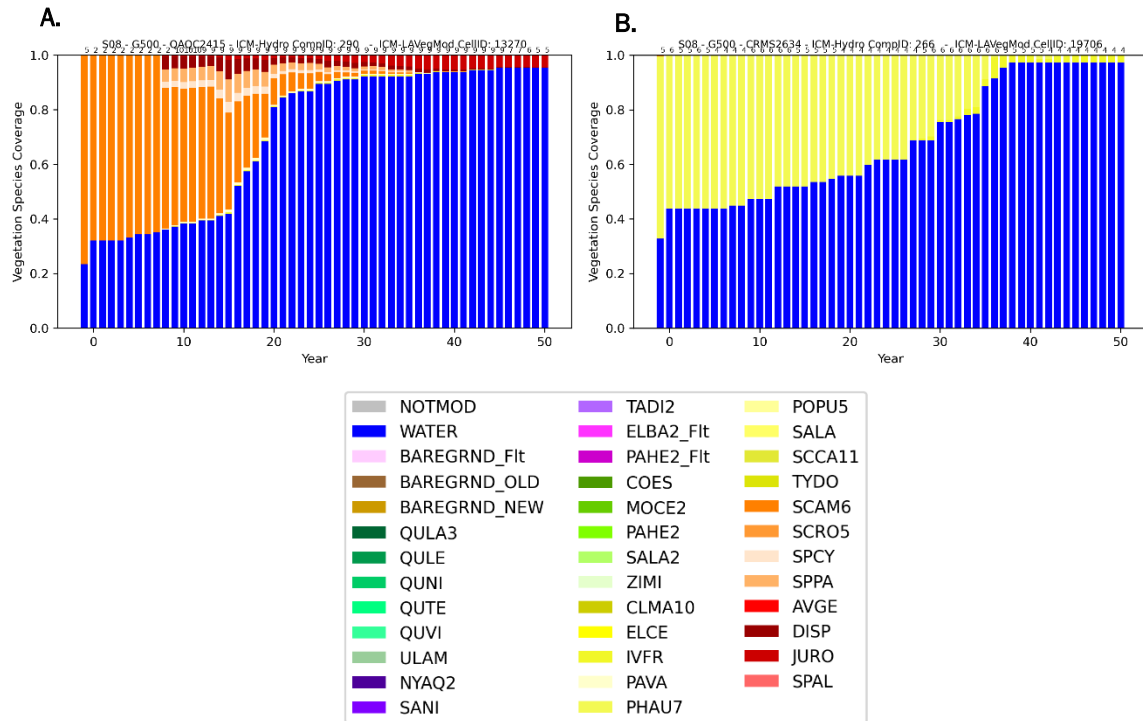


Figure 18. Change in vegetation cover under S08 is shown at representative points within the Bird’s Foot Delta. Point locations are shown in previous Bird’s Foot Delta map figures.

## 2.8 FWOA WETLAND MORPHOLOGY

### LOWER PROJECT SELECTION SCENARIO (S07)

The Maurepas and Lake Pontchartrain ecoregions are largely unchanged over the course of the 50-year simulation. On the Orleans Landbridge and the lower Pearl River Basin, there is only “speckled” land loss along interior marsh edges that mostly occurs in the last two decades, but the region as a whole remains intact. All marsh creation projects in the Lake Pontchartrain and Lake Borgne ecoregions are land in Year 50. Greater land loss is seen in the Chandeleur Sound ecoregion including the Biloxi Marshes. Progressive edge loss that mainly occurs in the last decade leaves much of the marsh fragmented.

The Lower Breton ecoregion has minor land loss, including some marsh edge erosion, and one area of concentrated land gain near Fort St. Philip which receives input from natural crevasses, increasing the mineral accretion rate. QAQC1693, close to the existing land but in open water of Breton Sound, does not become subaerial, but shows an increase in elevation over the course of the simulation (Figure 19).

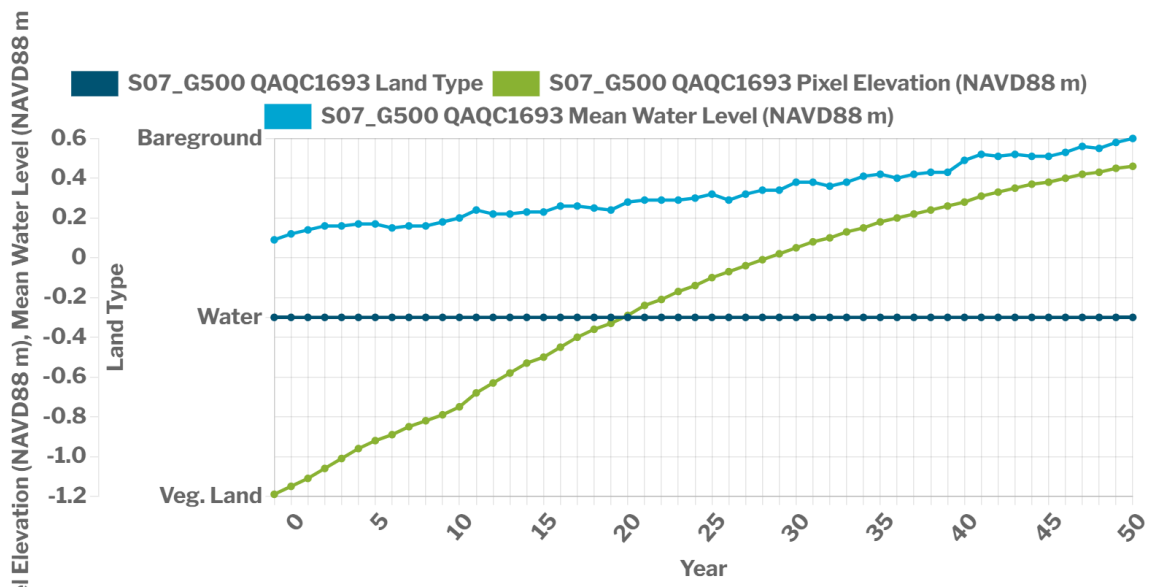


Figure 19. Inundation dynamics at QAQC1693 under S07.

The Upper Breton has areas that are influenced by the Mid-Breton Diversion and the Caernarvon Freshwater Diversion and build land, while areas more distant from the diversion are not influenced and lose land. These differences can be seen in the two plots below. CRMS0117, south of the Caernarvon diversion and west of Lake Lery, is not influenced by the Mid-Breton Diversion, and the elevation decreases (Figure 20). QAQC0387 is closer to the Mississippi River and the Caernarvon diversion. This location also remains open water but receives greater mineral accretion than CRMS0117 and increases in elevation. While both pixels are open water at the end of the simulation, the depth at CRMS0117 is about 0.5 m greater than QAQC0387. QAQC0329 is close to the Mid-Breton Diversion and shows a rapid increase in elevation in the first three decades resulting in a conversion from open water to land (Figure 21). Elevation continues to increase but at a lower rate. This location is in compartment 92 which is designated as 'active delta' and thus receives greater organic accretion once it converts to land (compared to areas with similar FFIBS scores).

Land changes are generally confined to the upper reaches of the ecoregion. The marsh in the lower portion of Upper Breton remains intact with only minor loss throughout the simulation.

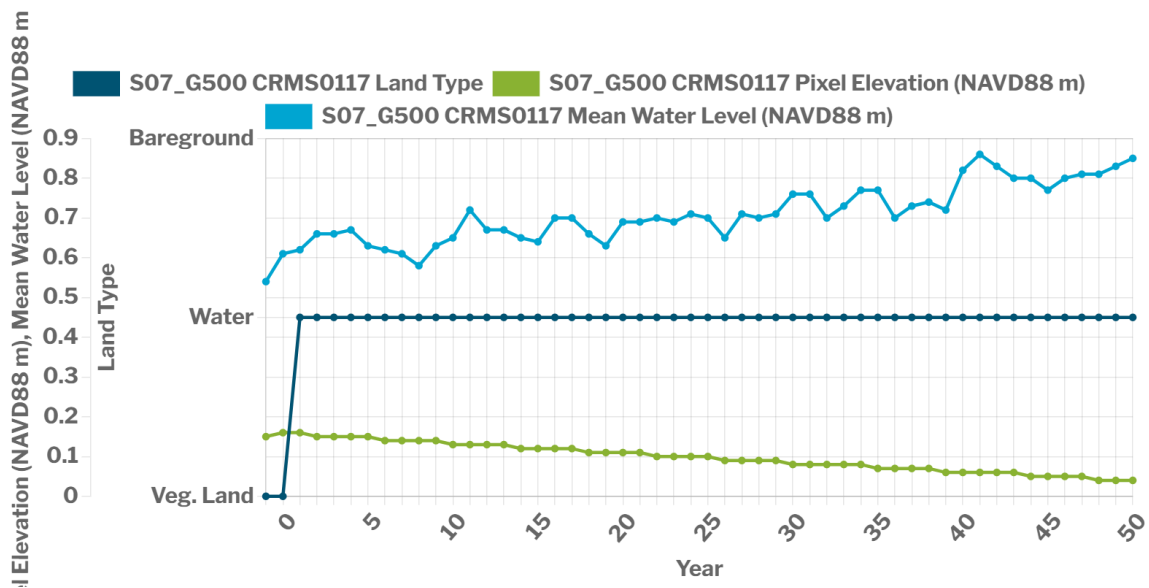


Figure 20. Inundation dynamics at CRMS0117 under S07.

Large areas of the Bird's Foot Delta convert to open water in the first three decades including marshes between Pass a Loutre and South Pass, and to the west of Southwest Pass, as deep subsidence drives elevation loss. This continues and by Year 50 most of the marshes between Southwest and South Passes and between Pass a Loutre and Main Pass have also been lost. There are a few, minor areas along channels, including Baptiste Collette, where land is built and is retained in Year 50.

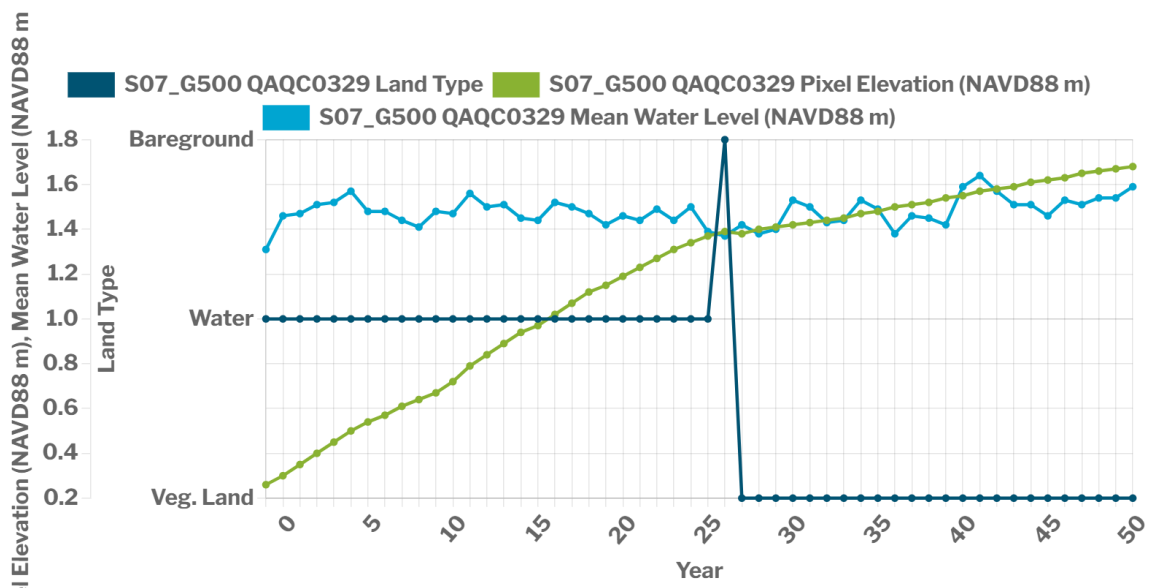


Figure 21. Inundation dynamics at QAQC0329 under S07.

## HIGHER PROJECT SELECTION SCENARIO (S08)

The upper part of the Pontchartrain Basin, especially in the Maurepas ecoregion, shows very little land loss during the 50-year simulation. Subsidence rates are generally low in this basin and in areas with very low FFIBS scores, accretion rates due to organic matter accumulation are greater than total subsidence leading to a gradual increase in elevation over time. Further, the area south of Lake Maurepas is designated as an active delta area associated with the River Reintroduction to Maurepas Swamp project that is included in FWOA. This increases the accretion rate in some areas to almost 2 cm/yr.

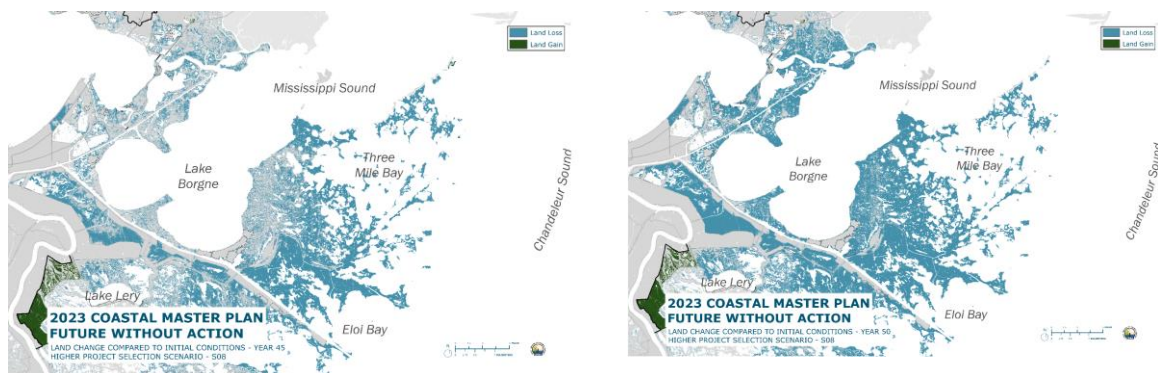


Figure 22. Cumulative land change by Year 45 (left) and Year 50 (right) for the Orleans Landbridge and Pearl River areas under S08. Polygon boundaries show the FWOA project footprints.

Around the shores of Lake Pontchartrain, some land loss occurs within the LaBranche wetlands. This occurs in the last five years of the simulation. Even though subsidence rates are low and low FFIBS scores result in high accretion and an increase in land elevation, rapid rates of water level rise in the last decade result in the inundation threshold being exceeded in parts of the LaBranche wetlands. However, the LaBranche East Marsh Creation project remains land at Year 50. On the north shore of Lake Pontchartrain some land loss also occurs in the marshes between Mandeville and Slidell. While there is scattered loss in the first two decades especially west of Bayou Lacombe, loss increases in the second half of the third decade and is greatest between Year 40 and 50. During this period the FFIBS scores increase and the area turns from intermediate to brackish west of Bayou Lacombe. The decrease in FFIBS score reduces organic accretion. Subsidence is low in this area and accretion is enough to increase the elevation of the marsh surface. However, as stage increases, lower elevation areas of marsh are lost to inundation. There is also loss due to marsh edge erosion in this area. Most of the Bayou Bonfouca restoration project remains intact except for one area of loss that occurs in Year 50.

Further east in the Pearl River Delta and the Orleans Landbridge there is similarly little land loss in the first three decades of the simulation with some isolated areas of loss occurring in Year 30. Loss

increases by Year 40 with almost all areas, except the interior of Bayou Sauvage and the Pearl River wetlands north of Hwy 90, experiencing some loss, including marsh edge erosion on some Lake Borgne shorelines. This loss is mainly in areas with brackish FFIBS scores. Fritchie Marsh area stays intermediate and therefore has higher accretion rates, as do the fresher areas with the Pearl River. Loss increases greatly in the last five years of the simulation, except in the areas with low FFIBS scores in the upper part of the Pearl River (Figure 22). Even though subsidence is low, and accretion is adequate to maintain or increase marsh elevation in many areas, sea level rise induced increases in stage result in inundation loss of wetlands. Most of the restoration projects in FWOA remain intact through Year 50 including the Golden Triangle, New Orleans Landbridge Shoreline Stabilization and March Creation, and various cells of marsh creation for the Hurricane & Storm Damage Risk Reduction System (HSDRRS) mitigation.

In the marshes north of the Mississippi River Gulf Outlet (MRGO), little land loss occurs in the first 20 years. These marshes are mostly brackish FFIBS scores with saline in the outer Biloxi Marshes. By Year 30, small, focused areas of loss occur mostly in the outer Biloxi Marshes and south of Bayou LaLoutre (Figure 23 left). These areas are subject to higher shallow subsidence (Chandeleur Sound ecoregion vs. Lake Borgne ecoregion) and deep subsidence also increases to the east. By Year 40 there has been extensive land loss in the CHS ecoregion with few marshes remaining (Figure 23 right). Accretion in these saline marshes is dominated by organic accumulation and in many areas balances rates of subsidence allowing marsh elevation to be maintained for several decades. However, the inundation threshold is lower for higher salinity marshes and so the effects of increased sea level rise on stage result in land loss earlier than in fresher marsh areas. By the end of the simulation, the western Biloxi Marshes are also subject to extensive inundations loss as sea level rise increases stage and inundation. The only land left at Year 50 is the Lake Borgne Marsh Creation (Increment 1) area which remains wetland, land along Bayou LaLoutre and fragmented wetlands in the eastern Biloxi Marshes.

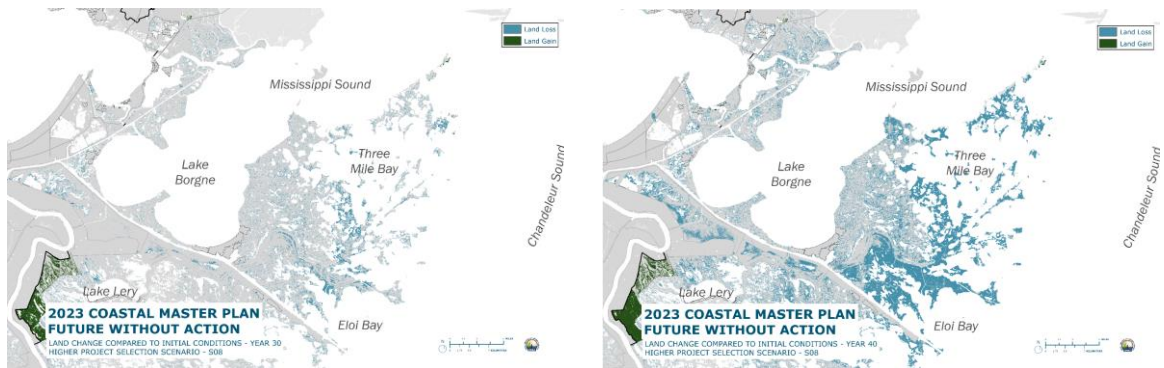


Figure 23. Cumulative land change by Year 30 (left) and Year 40 (right) for the marshes north of MRGO under S08. Polygon boundaries show the FWOA project footprints.

The upper sections of the Breton Basin are dominated by influence of the Mid-Breton Sediment Diversion. During the first decade of the simulation there is minor loss in the vicinity of the diversion associated with high stage. However, some bareground begins to emerge at Year 15, a high river flow year, and this is rapidly vegetated. More extensive bareground occurs in Year 19 west of the Caernarvon outfall area which then becomes vegetated the following year. More bareground emerges near the diversion in Year 26 and again it is rapidly vegetated. In Year 30, while new land is growing near the diversion, some loss occurs to the east of Caernarvon, north of Lake Lery. By Year 35 the compartment adjacent to the diversion, where land was lost during spin-up, is almost completely filled, and some land loss is occurring in outer marshes. The changes that occur after three decades are exemplified in plots from two selected points – one adjacent to the diversion (TRNS1301, Figure 24) where elevation in open water increases rapidly, and inundation decreases until the area becomes land and organic accretion continues to raise elevation. In the area north of Lake Lery at QAQC0398 (Figure 25), away from extensive sediment deposition, organic accretion marginally increases elevation, but inundation increases greatly and land is lost in Year 33, and elevation then gradually declines due to subsidence and little mineral deposition (Figure 6 bottom). This area is not designated as ‘active delta’ and so receives less organic matter accumulation rate (OMAR) (note change in scale on accretion axis) than compartments closer to the diversion despite having similar FFIBS scores.

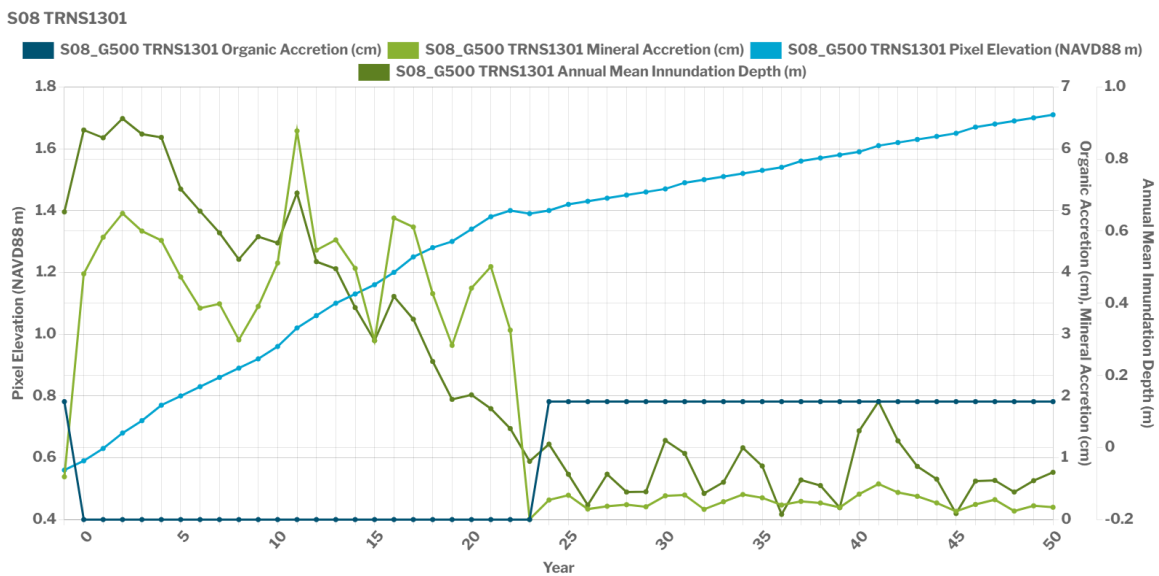


Figure 24. Accretion and inundation dynamics at TRNS1301, adjacent to the Mid-Breton Sediment Diversion outfall, under S08.

S08 QAQC0398

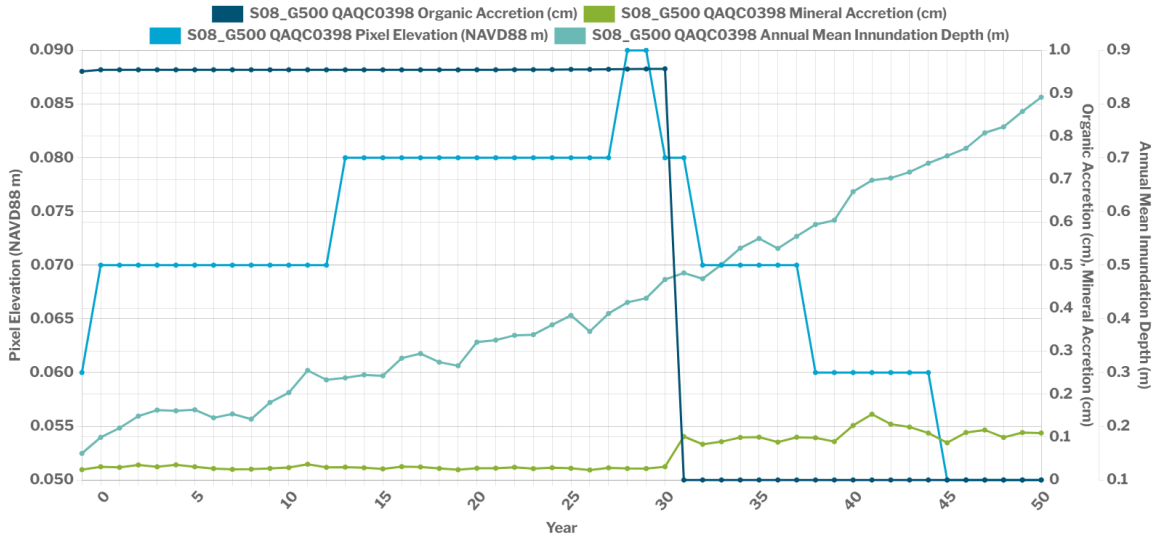


Figure 25. Accretion and inundation dynamics at QAQC0398, further afield from the Mid-Breton Sediment Diversion outfall, under S08.

By Year 40, while land is built near the diversion, land loss increases in marshes east of Delacroix. Organic accretion can maintain marsh elevation in the face of subsidence but rising stage increases inundation and leads to land loss. By Year 45 there is extensive loss between Bayou Terre aux Boeufs and MRGO, even while new land is still emerging near the diversion. By Year 50 there is extensive loss in the outer part of the Breton marshes and close to the Mississippi River near East Pointe a la Hache.

Within the Bird's Foot Delta some areas of land loss occur within the first decade to the west of Southwest Pass where very high subsidence rates lead to rapid lowering of the surface elevation, and brackish FFIBS scores result in less organic accretion. By Year 20 there is extensive loss between South Pass and Pass a Loutre. These are categorized as active delta and so receive high OMAR but subsidence is also really high (almost 2.5 cm/yr at CRMS0154) leading to inundation loss. By Year 30 this entire basin between the distributaries is lost to open water while marshes remain near Cubit's Gap, around Baptiste Collette and the outboard marshes of the Mississippi River near Ostrica and Fort St Philip. Land loss increases south of Venice and by Year 35 part of the Barataria Basin Ridge and Marsh Creation - Spanish Pass Increment project has turned to open water. By Year 45 there are few marshes left in the Bird's Foot Delta and loss is beginning in Baptiste Collete. The marshes near Fort St. Philip toward Baptiste Collete remain at Year 50; subsidence rates are lower and active delta designations mean higher organic accretion rates enabling marsh elevation to increase and slowing the increase in inundation depth due to sea level rise.

## 2.9 FWOA BARRIER ISLAND MORPHOLOGY

The ICM-BI model simulates the evolution of the barrier islands and headlands over the 50-year model simulation period as expected for scenarios S07 and S08. Processes included in the ICM-BI are: cross-shore retreat of the Gulf and bay shorelines, subsidence of the profiles, and application of relative sea level rise (sea level rise). As the barrier islands cross the threshold for auto-restoration, the restoration template is automatically applied, resulting in transgression and “managed retreat”.

In general, sediment volumes associated with auto-restoration are reasonable within the broad range of uncertainty associated with the prescribed templates, application of auto-restoration thresholds, and specific simplifications used within the modeling framework. Because ICM-BI uses cross-shore retreat informed by historical observations, it does not capture the influence of sediment input on long-shore or cross-shore sediment transport, which could impact the overall retreat rate and thus the restoration timing and/or volumes. Other specific processes that would influence the restoration volumes are the impact of storms, which could either cause earlier triggers due to accelerated erosion following a storm, or cause repeat restoration triggers if the timing of the storm follows a restored barrier. Evaluating all factors that influence sediment placement and restoration frequency is not straightforward due to insufficient data to quantify restoration influence on cross-shore retreat or isolate the impacts of storms. A series of sensitivity tests were conducted and are presented in Appendix D: Overview of Improvements to Landscape Modeling (ICM) for 2023, [Supplemental Material D.4.1: ICM-BI Model Sensitivity Tests on Future Without Action \(FWOA\)](#).

The barrier islands in the Pontchartrain region that are modeled with ICM-BI include Breton Island and the Chandeleur Islands, the latter of which are split into a northern and southern portion of the island chain (Figure 26).

All the barrier islands in the Pontchartrain region of the coast undergo cycles of cross-shore retreat and auto-restoration leading to transgression over time for both the S07 and S08 scenarios (Figure 27, Figure 28). The higher rate of sea level rise in the S08 scenario increases the rate of erosion, and for both Breton Island and the South Chandeleurs this leads to auto-restoration within 1-2 years of the end of the model round and thus a large subaerial footprint at Year 50. The main factor driving sediment volume placement during auto-restoration in this region is island size (Figure 29, Table 3), with the larger area of the North Chandeleurs leading to greater sediment volume placed during both individual auto-restoration actions and as a cumulative sediment volume total over 50-years. However, the South Chandeleurs cross the threshold for auto-restoration more frequently compared to either Breton Island or northern Chandeleurs.

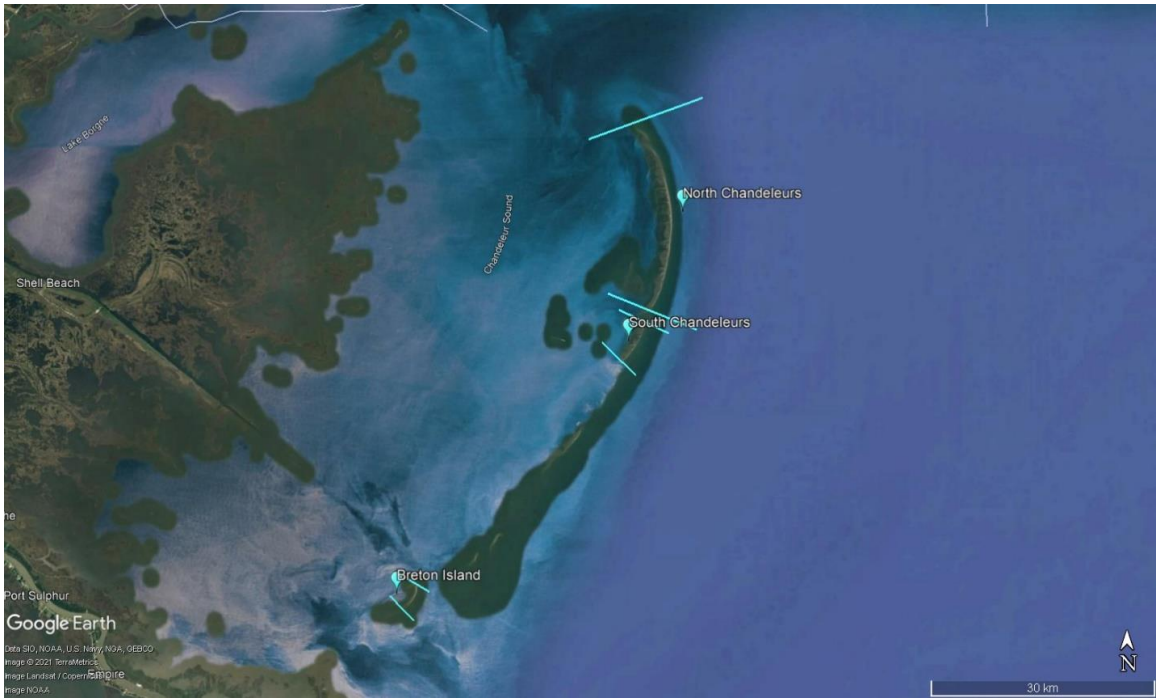


Figure 26. Barrier islands located within the Pontchartrain region of the coast. Background imagery from Google Earth.

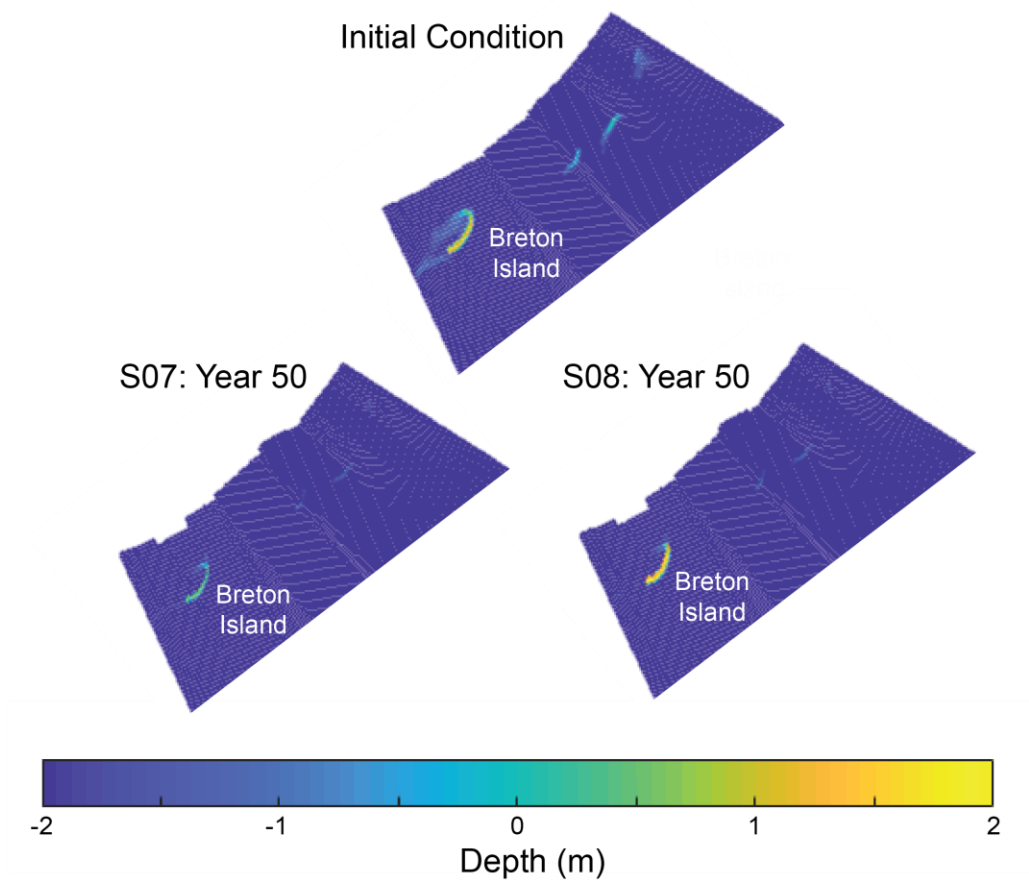


Figure 27. Elevation in MHW for the initial condition in the southern portion of the Pontchartrain region along with Year 50 results for S07 and S08. Depth is shown in meters (m).

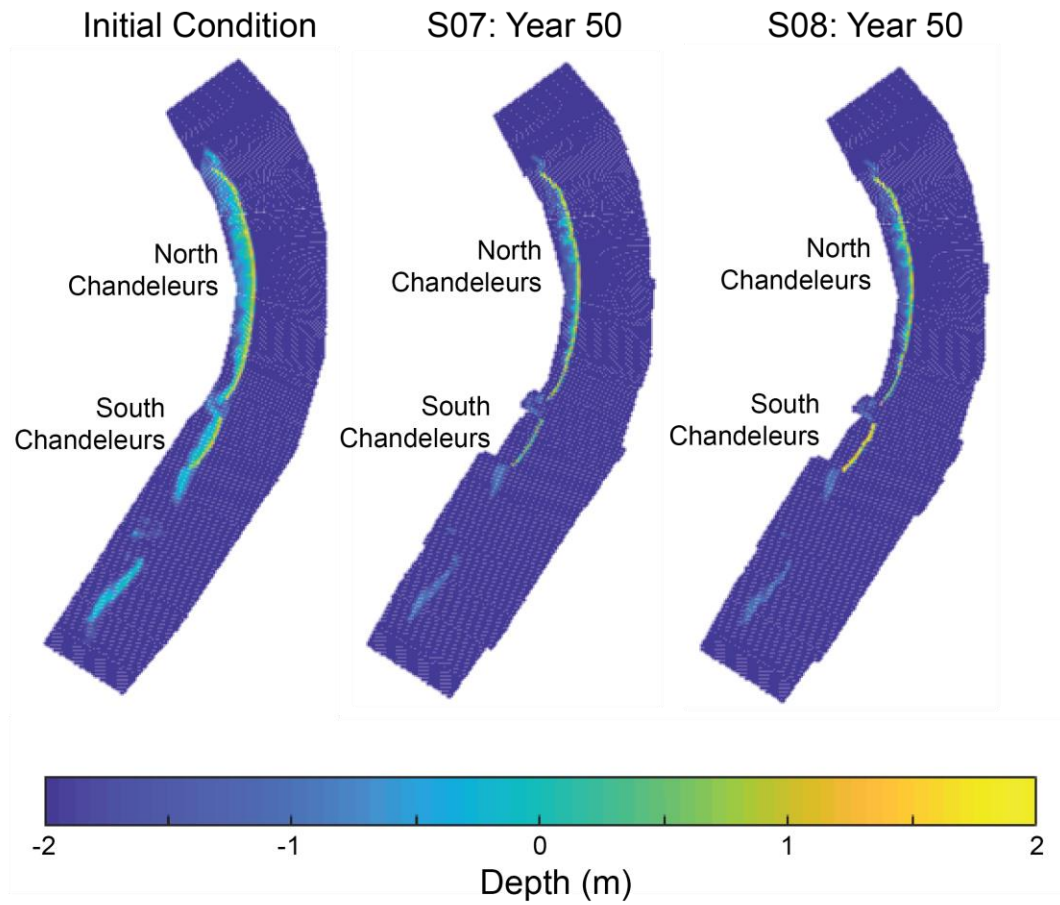


Figure 28. Elevation in MHW for the initial condition in the northern portion of the Pontchartrain region along with Year 50 results for S07 and S08. Depth is shown in meters (m).

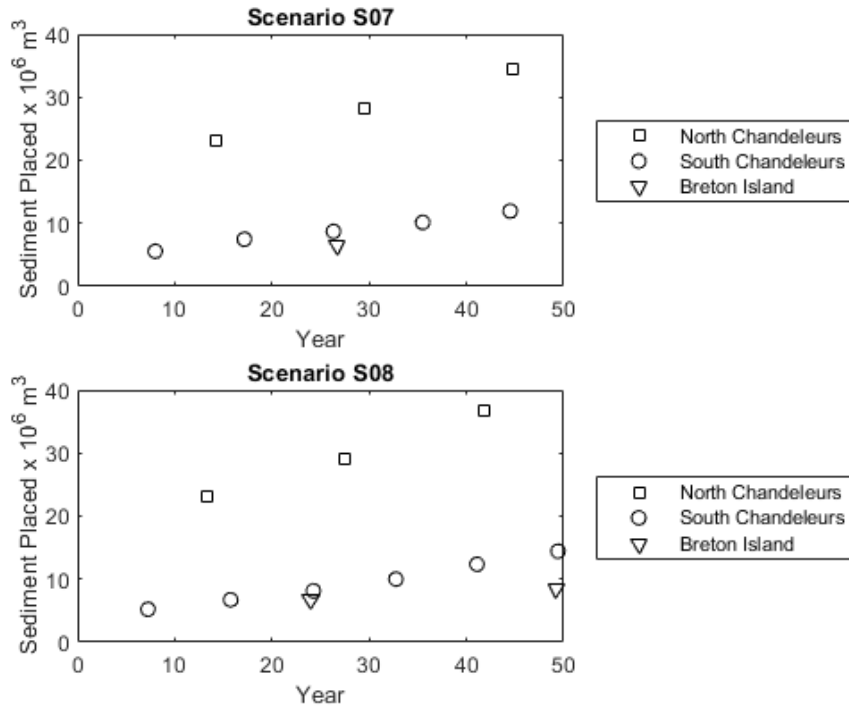


Figure 29. Summary of sediment volume placed in scenarios S07 and S08 for the Pontchartrain region of the coast.

Table 3. Summary of total sediment volume placed (10<sup>6</sup> m<sup>3</sup>) over FWOA simulation in scenarios S07 and S08 for the Pontchartrain/Breton region of the coast

Barrier Island or Headland	S07	S08
North Chandeleurs	85.53	88.78
South Chandeleurs	43.83	56.84
Breton Island	6.51	15.22

The Barrier Island Tidal Inlet (ICM-BITI) module calculates the link dimensions for each link in ICM-Hydro that represents a tidal inlet. The link dimensions calculated by ICM-BITI change as a function of the tidal prism of the basin the inlet is connected to. Each link within a basin has a designated sub-basin, whose tidal prism is used to calculate each link's corresponding dimensions. Tidal prism is a function of the backbarrier water area and the tidal range, both of which change over the course of the simulations. The change in link width and depth are both capped at 50% as compared to the initial size. These caps are applied separately, meaning the cap on width can be reached at a different time than the cap on depth. A minimum cap is also applied, which prevents the links from being smaller than 25% the initial size. The initial sizes were set by the ICM-Hydro team based on the bathymetry in the vicinity of the tidal inlet. All links maintain the original aspect ratio as they enlarge or reduce in size

in response to the tidal prism except for two, Barataria Pass (Link 532) and Caminada Pass (Link 529). These passes have hardened shorelines. Therefore, the links that represent these locations have a set width, and any changes in area are achieved by changing the depth. The depths used in ICM-Hydro and shown below are referenced to the mean water level. The BITI module outputs the absolute link size, and the mean water levels in ICM-Hydro compartments 494, 482, 316, 314, 306, and 303 are used to convert the calculated size to the depth.

Under S08, only one of the six tidal inlets within Pontchartrain/Breton reaches the maximum allowable width; this occurs in the last four years of the simulation; no inlets reach the maximum allowable depth. All inlets expand after the initial spin-up period (Figure 30).

Two tidal inlets within Pontchartrain/Breton reach the maximum allowable width. Link 141 reaches it in the fourth decade and Link 350 reaches it in the fifth decade. Link 350 also reaches the max depth towards the end of the simulation. The change in all other links is minimal (Figure 31).

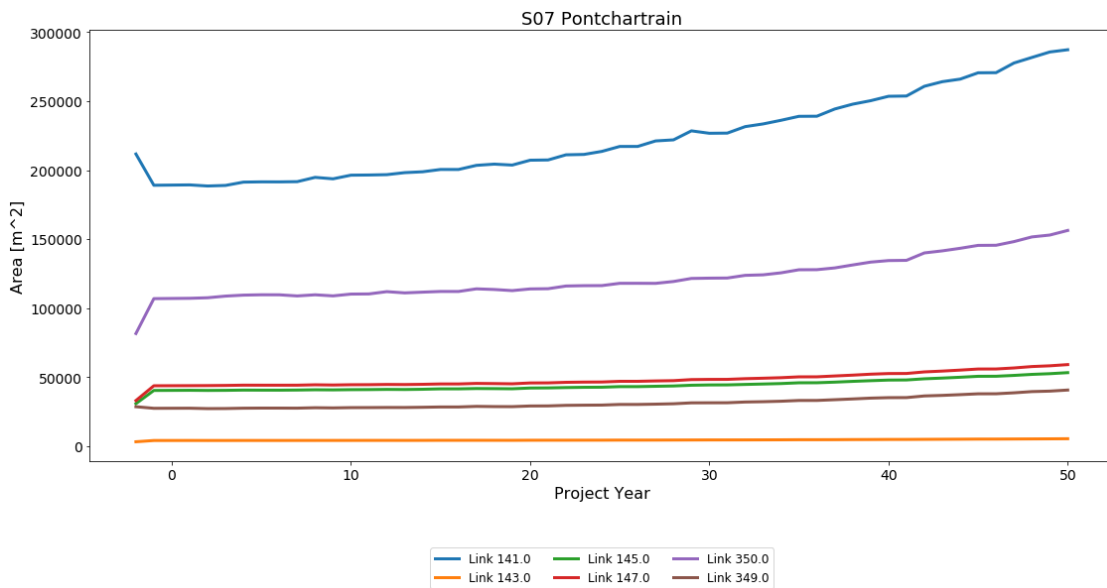


Figure 30. Tidal inlet cross-sectional area changes over time in Pontchartrain/Breton, under S07.

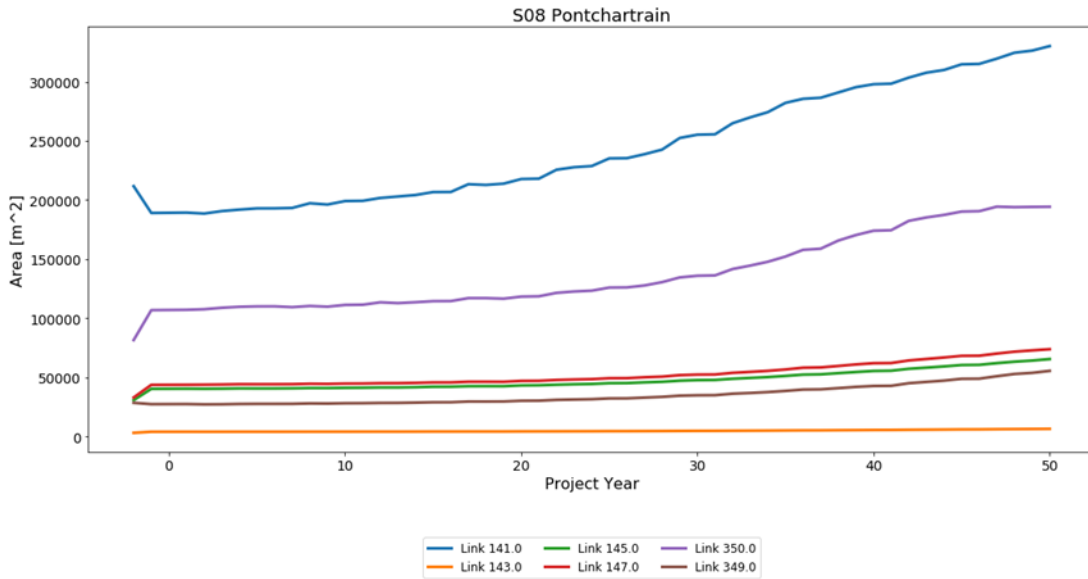


Figure 31. Tidal inlet cross-sectional area changes over time in Pontchartrain/Breton, under S08.

## 2.10 FWOA HABITAT SUITABILITY INDICES

### LOWER PROJECT SELECTION SCENARIO (S07)

The suitability of habitats across the Pontchartrain, Breton, and Bird’s Foot Delta region was relatively stable over the first half of the S07 environmental scenario for most fish, shellfish, and wildlife species. There was some variability in habitat suitability during this period that was attributed to interannual variability in freshwater discharges from the Pearl River, Mississippi River distributaries, and river diversions such as the Mid-Breton Sediment Diversion. This variability was particularly evident for oysters in the Biloxi Marsh area of the Chandeleur Sound ecoregion, which was influenced by Pearl River discharge. When Pearl River discharge was relatively high the freshwater inflow decreased salinities such that they were closer to optimal range, resulting in high suitability scores (i.e., 0.7 to 0.9, Figure 32); and when river discharge was relatively low, higher salinities from the Gulf of Mexico intruded to keep the suitability of these areas at moderate levels (0.4 to 0.6).

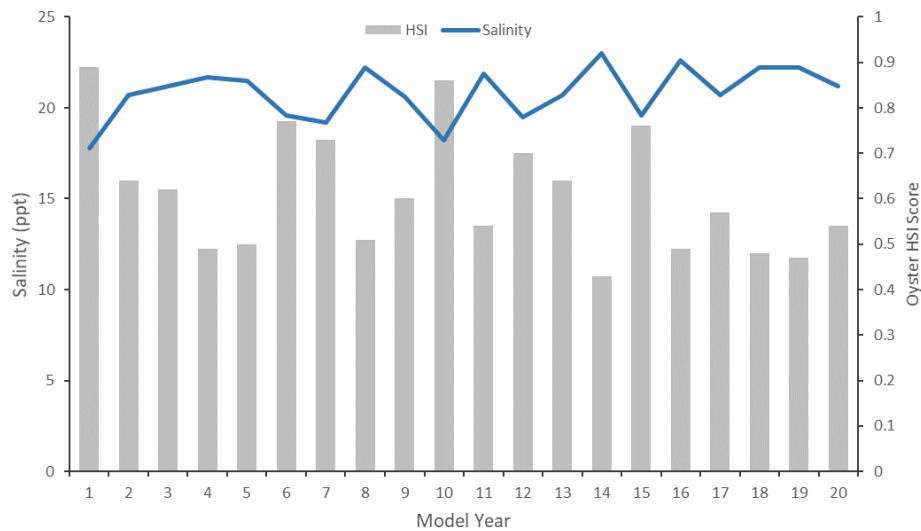


Figure 32. Oyster HSI scores compared to salinity simulated for the Bay Boudreau area over the first 20 years of the S07 environmental scenario. Scores range from 0.0, completely unsuitable habitat, to 1.0, optimal habitat.

Larger changes to habitat suitability occurred during the last half of the simulation primarily due to increased salinities and water levels from sea level rise. The effects of increased salinities were most apparent in the lower Pontchartrain Basin (i.e., the Lake Borgne ecoregion and the New Orleans Landbridge area of the Lake Pontchartrain ecoregion). Habitat suitability for species that are more common in salinities >5 ppt (i.e., brown shrimp, white shrimp, spotted seatrout) increased in these areas during the last half of the simulation (Figure 33). This pattern, however, was less evident for oysters because the Lake Borgne area was more directly exposed to freshwater inflow from the Pearl River, which lowered minimum monthly salinities below 2 ppt thus creating unsuitable conditions for oysters (suitability scores of 0.0). In contrast, habitat suitability for species more associated with low-salinity habitats, such as alligator, decreased somewhat over time in these areas.

Increased water levels had a negative effect on habitat suitability for alligator and seaside sparrow across the region. These species were specifically affected by increases in marsh inundation over time, which can greatly reduce nesting success. Alligator habitat suitability decreased primarily in the last half of the simulation, particularly in the Upper Breton ecoregion where the most suitable habitat occurred (Figure 34). By comparison, the impact on seaside sparrow habitat suitability was more pronounced and occurred immediately. Suitable habitat for seaside sparrow occurs at marsh elevations >0.09 m above mean water level. As water levels increased, the availability of such habitat was steadily reduced such that by the middle part of the simulation very little habitat remained.

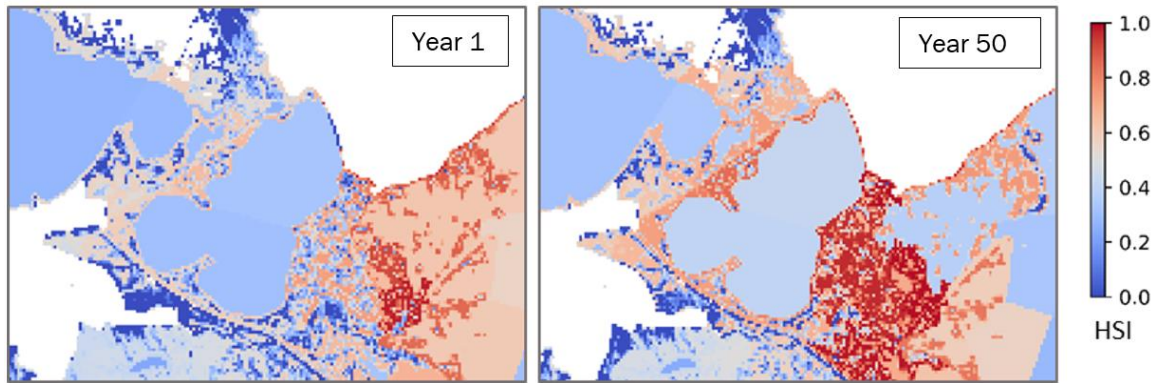


Figure 33. Small juvenile brown shrimp HSI scores across the Lake Borgne and Biloxi Marsh areas for Year 1 (left) and Year 50 (right) of the S07 environmental scenario. Scores range from 0.0, completely unsuitable habitat, to 1.0, optimal habitat.

Changes in wetland area did not have a large effect on species’ habitat suitability across most of the region. Extensive wetland loss over time in the Bird’s Foot Delta reduced habitat suitability for nearly all species, but particularly for species associated with low-salinity marsh habitats such as alligator, mottled duck, and largemouth bass. Habitat suitability also decreased for fish and shellfish near the outfall of the Mid-Breton Sediment Diversion because sediment deposited by the diversion converted fragmented marshes into a more solid marsh landscape with less open water habitat available for aquatic species (see dark blue area in lower left corner of Figure 33).

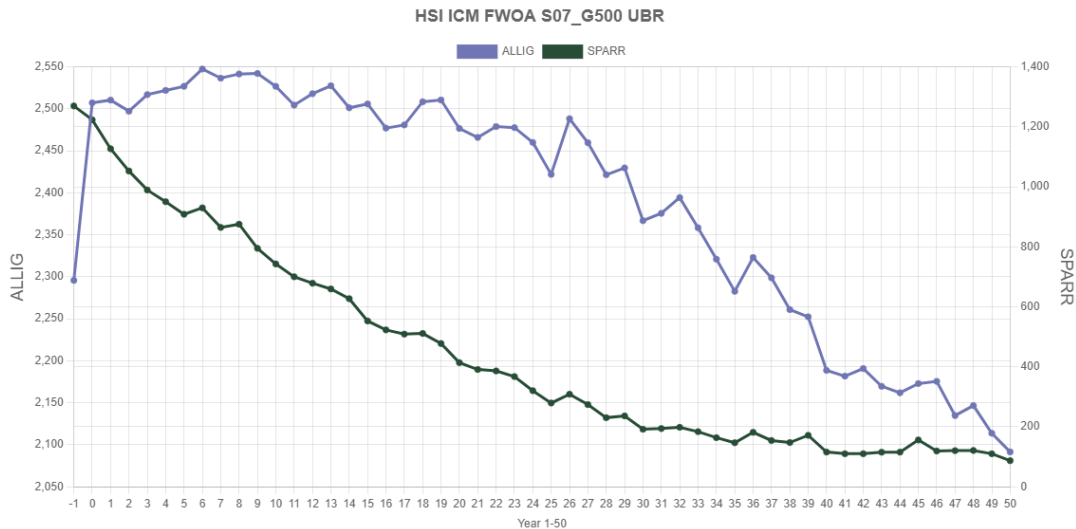


Figure 34. Total HSI score for alligator and seaside sparrow in the Upper Breton ecoregion over the 50-year S07 environmental scenario simulation. The total HSI score was calculated by summing the individual scores for each ICM model cell within the ecoregion.

## HIGHER PROJECT SELECTION SCENARIO (S08)

Large changes in habitat suitability occurred across most of the region in the S08 environmental scenario. These changes were primarily driven by extensive wetland loss that occurred in the Bird's Foot Delta, Upper Breton, and Lake Borgne ecoregions, as well as the Biloxi Marshes. Wetland loss generally resulted in reduced habitat suitability for fish, shellfish, and wildlife, because most of these species are dependent on marsh and associated shallow-water habitats during part of their life cycle. Seaside sparrow, in particular, was greatly affected because relatively little brackish and saline marsh, which are the most suitable habitat for the species, remained at the end of the simulation. There were instances, though, where wetland loss increased habitat suitability for certain species. For example, wetland loss converted areas of relatively solid marsh in Upper Breton and the Biloxi Marshes to a highly suitable, fragmented marsh-shallow water landscape. As a result, habitat suitability increased in these areas, especially for low-salinity species such as juvenile blue crab and mottled duck (Figure 35). However, as wetland loss progressed, these areas converted into mostly open water and habitat suitability decreased accordingly.

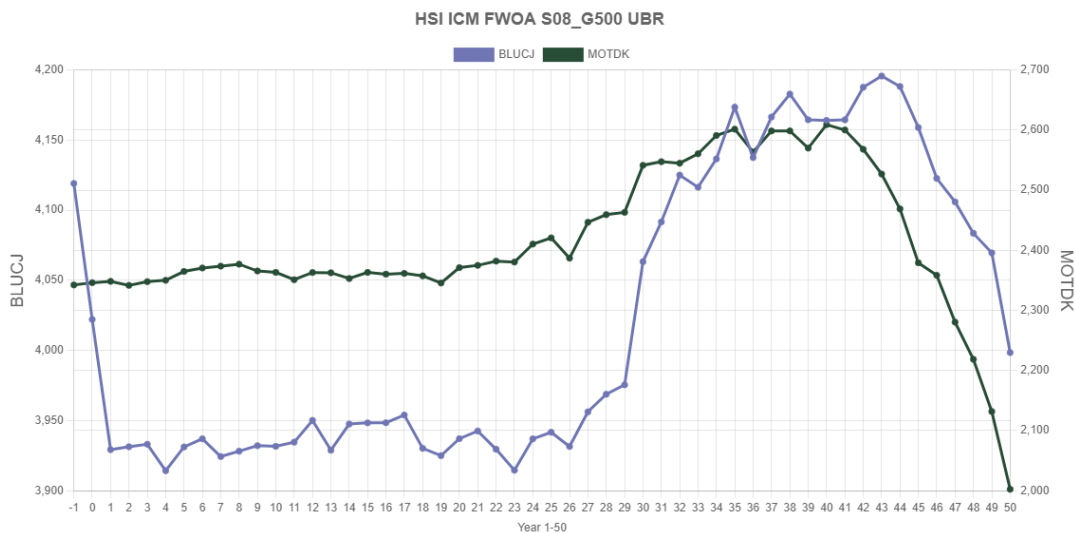


Figure 35. Total HSI score for juvenile blue crab and mottled duck in the Upper Breton ecoregion over the 50-year S08 environmental scenario simulation. The total HSI score was calculated by summing the individual scores for each ICM model cell within the ecoregion.

Habitat suitability was also affected by changes in salinity during the S08 environmental scenario. Salinities increased over time across much of the region, but particularly in the Lake Borgne ecoregion and the eastern half of the Lake Pontchartrain ecoregion. This resulted in relatively large increases in habitat suitability for higher-salinity species, such as brown shrimp, white shrimp, and spotted seatrout (Figure 36), and a decrease in suitability for low-salinity species, such as alligator and largemouth bass. Increased salinities did not have a large effect on oyster habitat suitability in Lake Borgne due to

the seasonal influence of freshwater discharge from the Pearl River. However, oyster habitat suitability did increase in the Chandeleur Sound ecoregion due to a decrease in salinities. High Mississippi River discharge during the last decade of the S08 environmental scenario decreased salinities across the southern part of Chandeleur Sound such that they were in the optimal range for oysters (i.e., annual average salinities of 10 to 15 ppt). As a result, oyster habitat suitability increased markedly toward the end of the simulation (Figure 37).

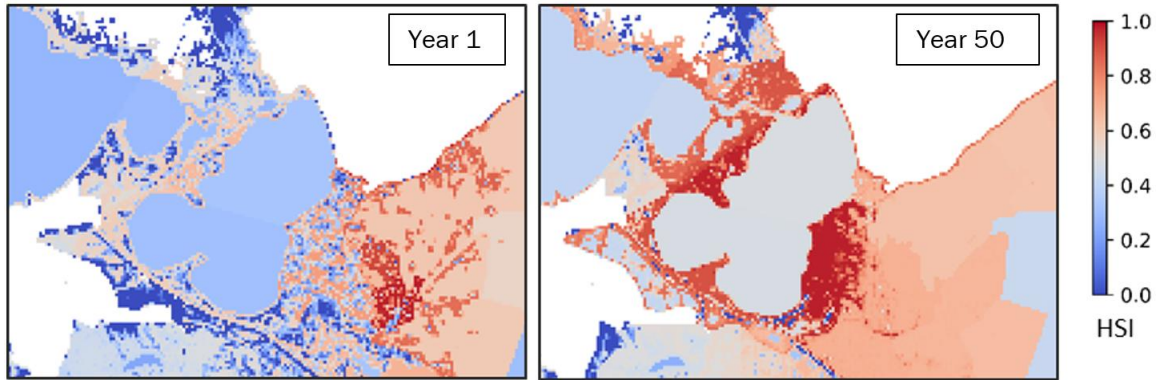


Figure 36. Small juvenile brown shrimp HSI scores across the Lake Borgne and Biloxi Marsh areas for Year 1 and Year 50 of the S08 environmental scenario. Scores range from 0.0, completely unsuitable habitat, to 1.0, optimal habitat.

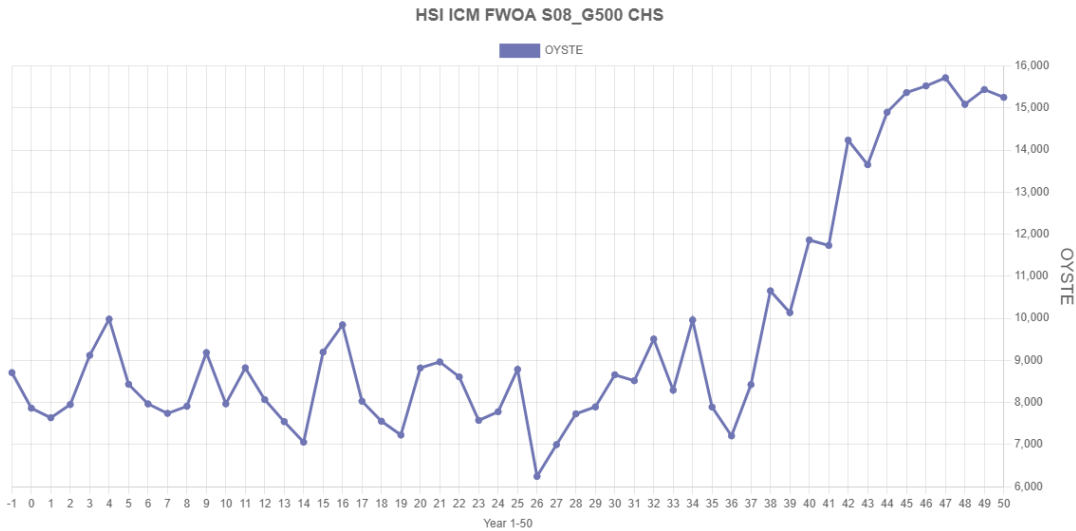


Figure 37. Total HSI score for oysters in the Chandeleur Sound ecoregion over the 50-year S08 environmental scenario simulation. The total HSI score was calculated by summing the individual scores for each ICM model cell within the ecoregion.

## 2.11 DISCUSSION

The higher rate of sea level rise for S08 manifests in higher stages compared to S07, observed across the entire region including the offshore as well as the entirety of the basins. This difference already manifests in a small yet noticeable degree for the latter part of the first decade and becomes increasingly substantial during the following decades.

The increased wetness of S08 compared to S07 leads to higher discharges in tributaries, which is especially of relevance for the Pontchartrain area. This could be an additional contribution to the relatively higher annual mean stage observed for S08 in areas in the vicinity of distributaries.

No significant differences can be found in tidal ranges when comparing S08 to S07 for the first 10 years. However, when comparing S08 to S07 during subsequent decades, higher tidal ranges can be observed for S08 throughout the Pontchartrain/Breton region. The overall pattern and spatial gradients in tidal range are near-identical for S07 and S08 apart from some small differences at the tributaries in the Pontchartrain area, which can most likely be attributed to different flow rates resulting from the higher rate of wetness in S08.

Overall, salinity patterns are similar between S07 and S08, both showing clear salinity gradients between the offshore and uppermost parts of the Pontchartrain and Breton basins. The effects of the Mid-Breton Sediment Diversion on salinity in the receiving area are very similar for both scenarios, which is in line with expectations regarding using the same Mississippi River hydrograph for both scenarios.

Although, there is a significant effect of the scenarios on land change, vegetation composition stays very similar under both scenarios (Figure 38 and Figure 39).

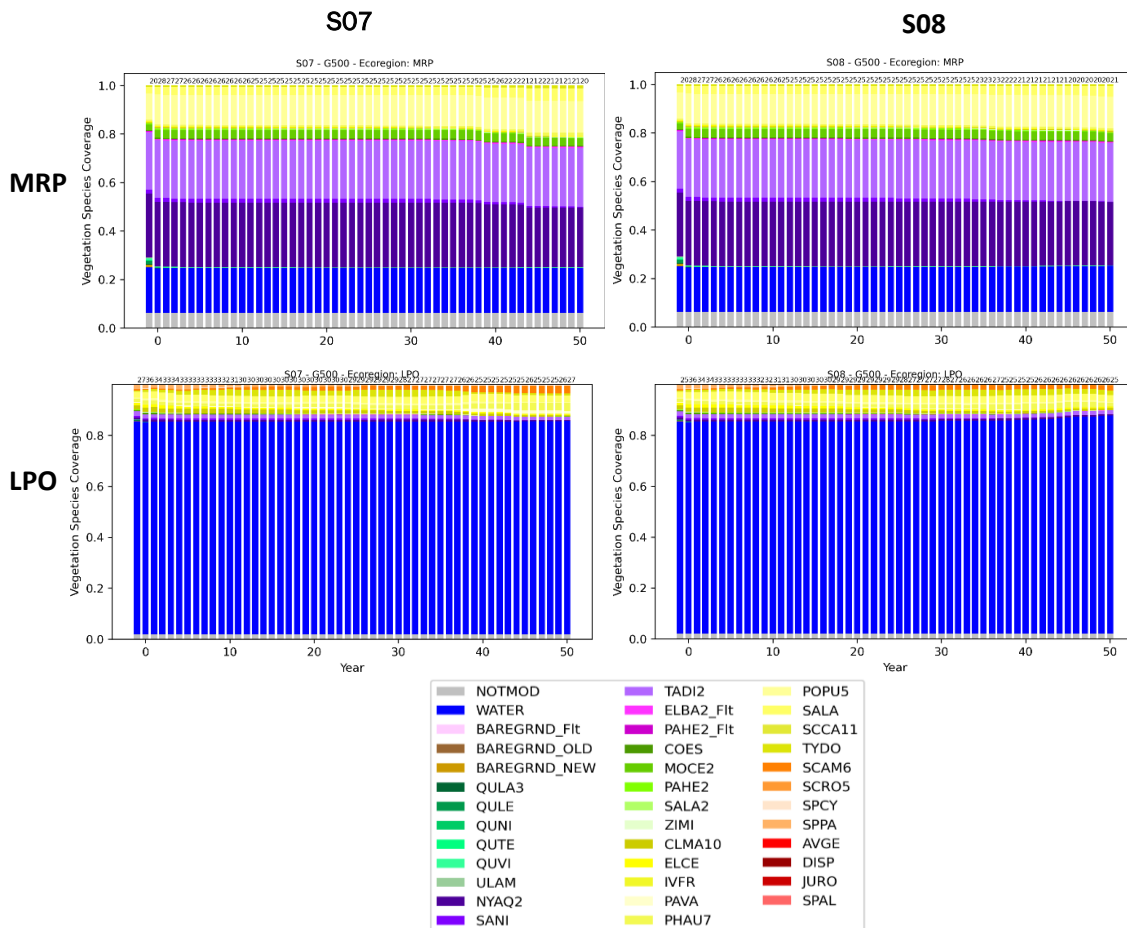


Figure 38. Comparison of vegetation cover change in the upper ecoregions of the Pontchartrain Basin between the two scenarios.

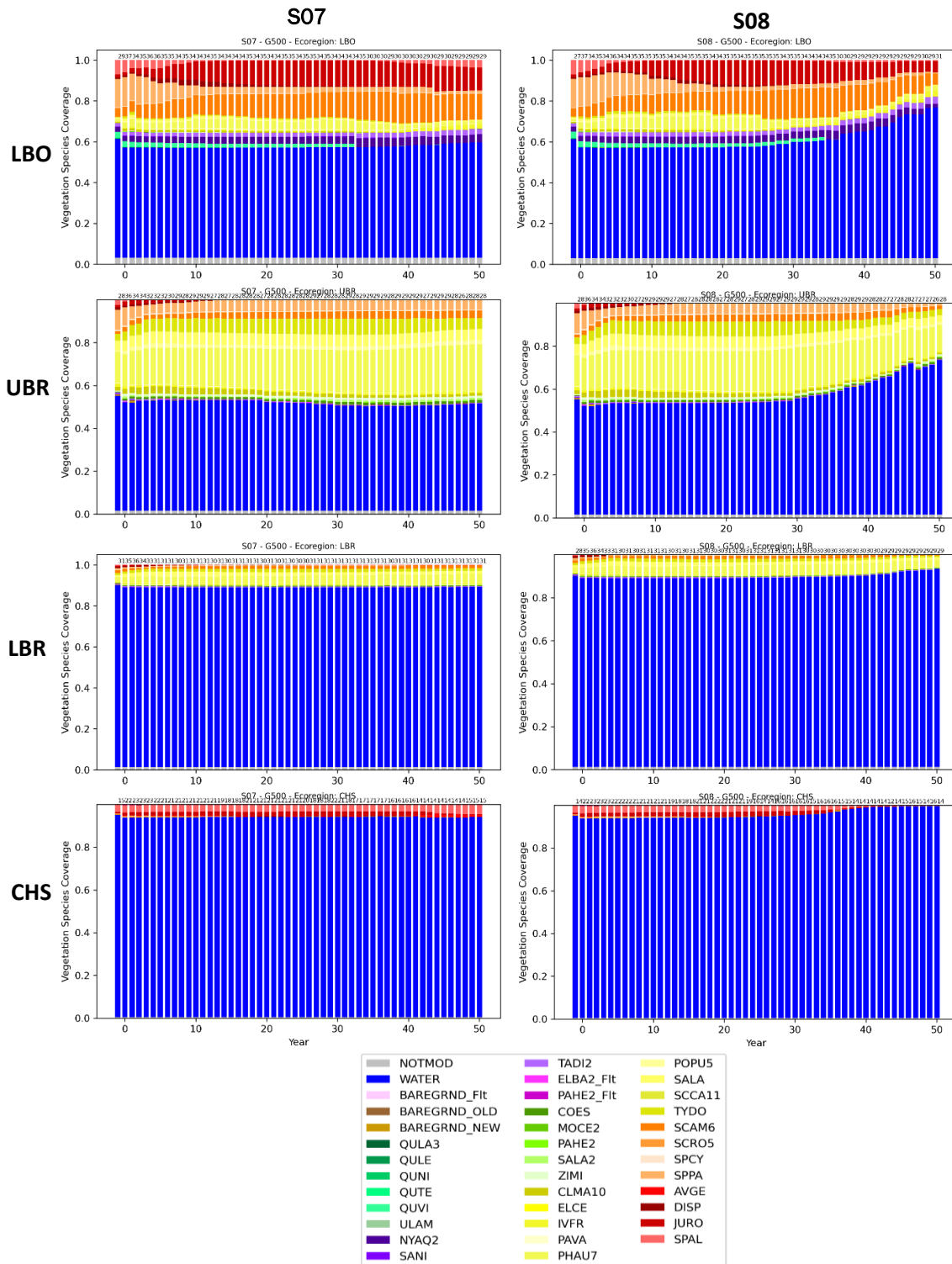


Figure 39. Comparison of vegetation cover change in the lower ecoregions of Pontchartrain and Breton basins between the two scenarios.

The differences in land loss between S07 and S08 in this region are extensive, especially on the Orleans Landbridge, the Central Wetlands, Biloxi Marshes and the outer marshes of the Breton Sound Basin. These areas show little land remaining by Year 50 in S08 but are largely intact at Year 50 in S07. Within region variations can be driven by the sea level rise component of the environmental scenarios but there are also locations where shallow subsidence varies substantially between the scenarios. For example, shallow subsidence in the CHS ecoregion, which includes much of the Biloxi Marshes, is 4 mm/yr higher in S08 compared to S07. These areas are more brackish/saline and so receive less organic accretion (compared to the fresher marshes of the upper estuary parts of the region), are distant from sources of mineral sedimentation and have a lower depth inundation threshold. These conditions hold for both scenarios but the higher shallow subsidence in S08 results in much greater inundation loss.

Differences between scenarios in terms of inundation factors are less in other areas. QAQC1598 is southeast of the Gulf Intracoastal Waterway (GIWW) on the Orleans Landbridge. Figure 40 shows that while elevation is similar between the two at the end of the simulation (reflecting similar accretionary processes and less difference among scenarios in subsidence) there is a greater increase in mean water level (driven by sea level rise) in S08 which results in loss at the end of the simulation in S08.

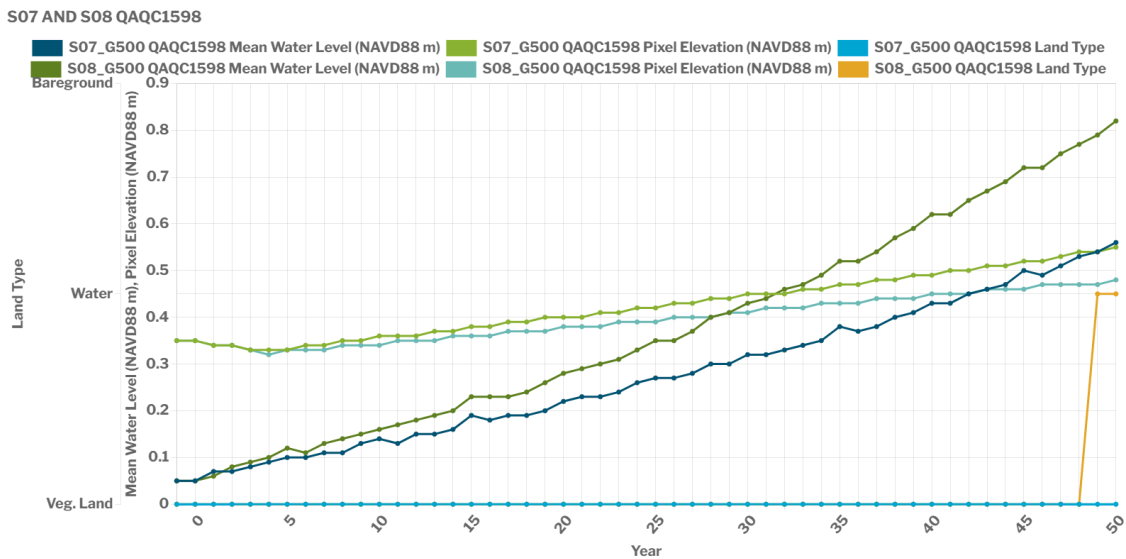


Figure 40. Comparison of conditions under S07 and S08 at QAQC1598 on the Orleans Landbridge.

TRNS1401, shown in Figure 41, in the lower part of the Bohemia Spillway has a difference of almost 1.5 mm in shallow subsidence between the two scenarios. As this area has FFIBS scores in the 6-7 range for both scenarios, organic accretion is relatively low (<0.9 cm/yr). Elevation decreases initially under both scenarios as the starting elevation is so high but once it reaches a level where inundation occurs and organic accretion contributes to elevation, under S07 the site maintains its elevation throughout the simulation as accretion is approximately in balance with subsidence. However, under

S08 accretion cannot keep pace and elevation gradually declines. The greater sea level rise in S08 adds to this and the marsh is lost to open water in Year 42. Although mineral accretion increases once the site is open water it is much less than the subsidence (by an order of magnitude) and the site loses elevation more rapidly.

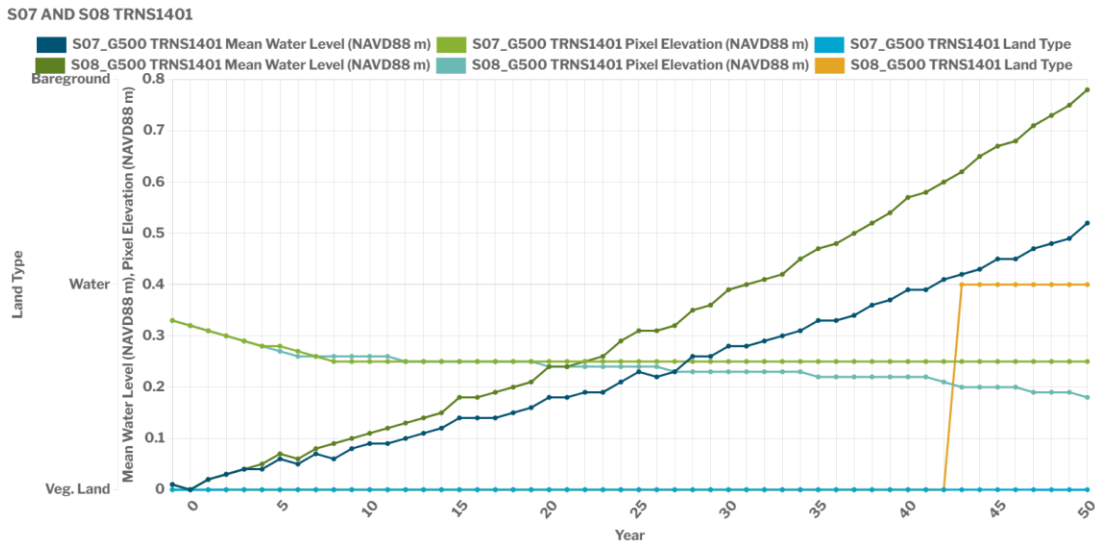


Figure 41. Comparison of conditions under S07 and S08 at TRNS1401 near the Bohemia Spillway.

The higher rate of sea level rise in the S08 scenario leads to all three islands within this region requiring auto-restoration at a slightly faster interval than for the S07 scenario, with the interval between restorations decreasing by 1-2 years (Figure 29). In addition, the amount of sediment volume required for each auto-restoration increases, as well. As a result, the sediment volume required over the 50-year time period (Table 3) for the North Chandeleurs increases by ~4%. For both Breton Island and the South Chandeleurs, the shorter period between auto-restoration events for the S08 scenario results in one additional auto-restoration occurring just before the end of the 50-year time period. As a result, the total amount of sediment volume required for these areas increases more substantially, with South Chandeleurs requiring ~30% more sediment volume and Breton Island requiring over twice as much sediment volume for the S08 scenario compared to the S07 scenario.

In S07, the general trend is that the inlet areas increase over time as the tidal prism increases. Across all basins, there are changes, both increases and decreases, during the spin-up period (i.e., ICM Years 1-2). The trends in S08 are similar to those in S07, but maximum caps are reached earlier in the simulation. The spin-up period changes are the same as those in S07 because the spin-up conditions are used for all scenarios are the same. Differences between S07 and S08 are seen across all basins. As expected, the links whose sub-basins contain the most marsh at the start of the simulation see some of the largest differences between S07 and S08 due to the differences in land (marsh) loss. Attenuation of the tidal signal is observed in each basin with the largest tidal range at the Gulf end

and decreasing moving up-basin. As land is lost and connectivity increases, less attenuation is observed. The tidal range increased over the course of the simulation. Greater increase is seen in S08 than S07 across all basins.

Tidal inlet cross-section area, under S08, of the two largest inlets within Pontchartrain/Breton, Link 141 and Link 350, diverge from the S07 results in the second decade and both end about  $5 \times 10^4 \text{ m}^2$  larger (Figure 42). All other inlets in the basin have smaller differences between the scenarios; they begin diverging in the third decade and end about 20% greater due to increased land loss and larger increase in tidal range. One exception is Link 143, which is small and whose sub-basin is open water at the start of the simulation. There is a small increase due to increase in the tidal range in that compartment.

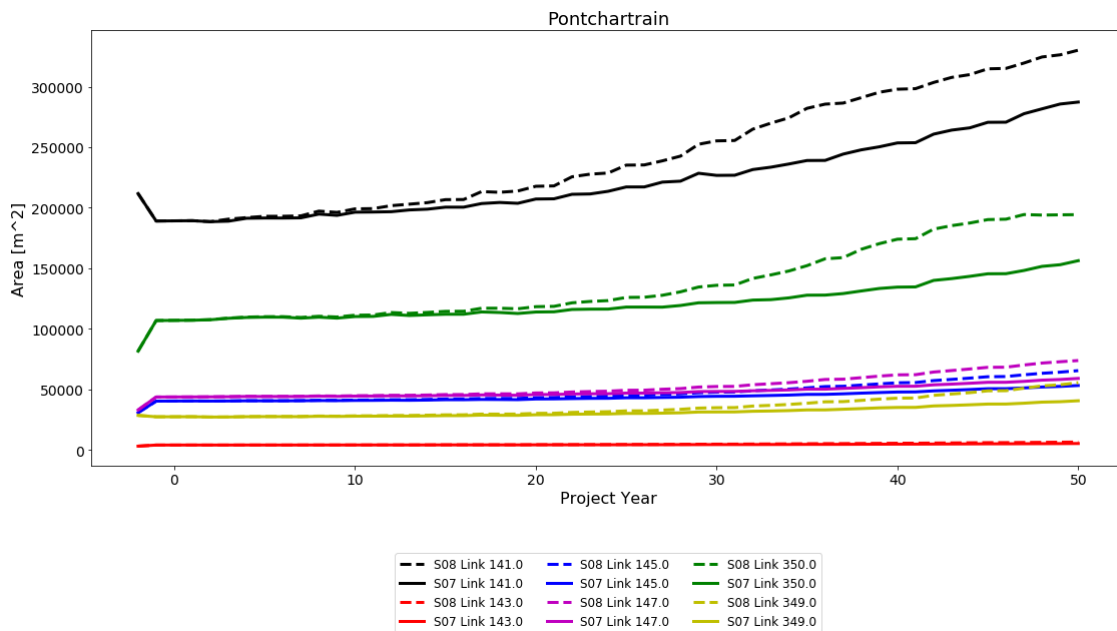


Figure 42. Tidal inlet cross-sectional area changes over time in Pontchartrain/Breton, under S07 and S08.

There is a difference in tidal range across the most Gulf-ward compartments in Pontchartrain/Breton across the two scenarios. Compartments to the east, which convey flow to the Rigolets and Lake Pontchartrain, have a greater tidal range than the compartments to the west in Breton Sound. The tidal range of the two scenarios diverges in the second decade, and the difference between them accelerates in the third decade (Figure 43).

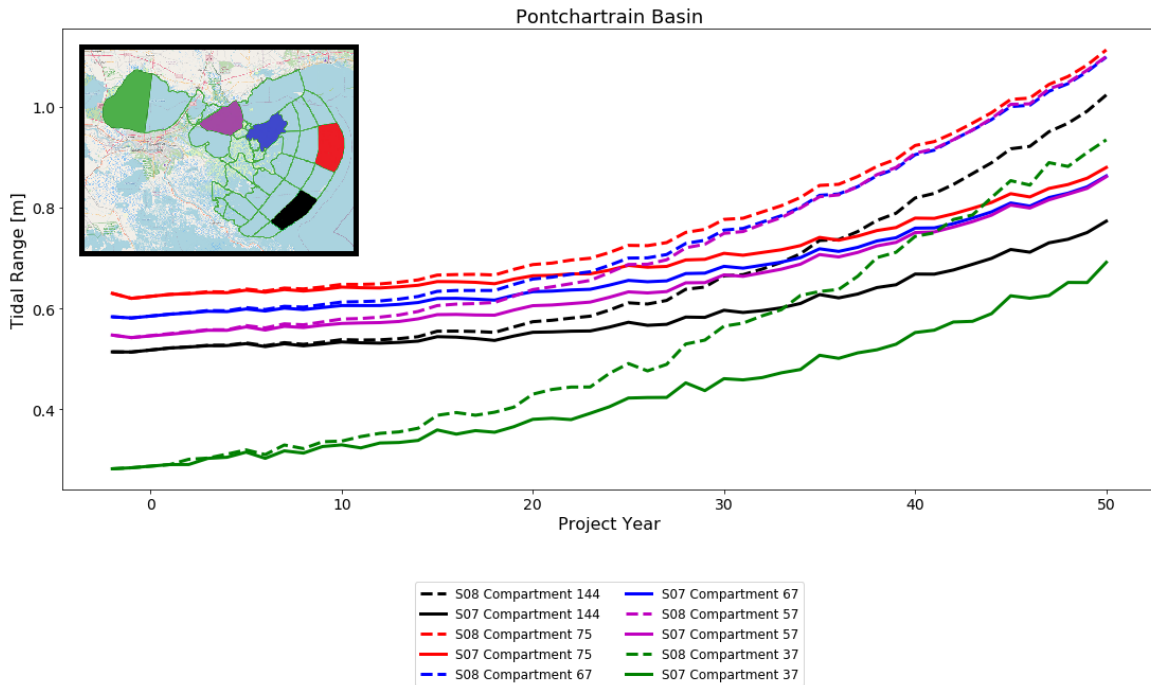


Figure 43. Tidal range for ICM-Hydro compartments contributing tidal prism to Barataria Basin tidal inlets.

Differences in habitat suitability between the S07 and S08 environmental scenarios were primarily related to differences in wetland loss rates. In the S07 scenario, most wetland acreage in the region is maintained through the 50-year simulation, and thus habitat conditions for fish, shellfish, and wildlife were relatively stable over time. By comparison, in the S08 scenario, most wetland acreage is lost and much of the remaining wetland habitat was comprised of swamp, fresh marsh, and intermediate marshes in the Lake Maurepas, Lake Pontchartrain, and Upper Breton ecoregions. These wetlands are more suitable habitat for the wildlife and the low-salinity fish and shellfish species included in the master plan. However, continued marsh fragmentation and increasing water levels and salinities over the S08 scenario would greatly reduce the suitability of these habitats. Similarly, though the higher-salinity fish and shellfish would benefit from the high degree of marsh fragmentation and increased salinities observed in the S08 scenario, over time there also would be a general reduction in habitat suitability for these species.

## 3.0 BARATARIA

### 3.1 INTRODUCTION

Barataria lies on the west bank of the Mississippi River, reaching to Port Fourchon and includes the west bank of New Orleans and popular fishing destinations of Lafitte and Venice. Barataria Basin is separated from the Gulf by a string of barrier islands that includes Grand Isle.

The ecosystem is characterized by extensive swamps in the upper basin and floating marshes near Lac des Allemands and Lake Salvador. Fresh marshes grade into intermediate, brackish, and salt marshes closer to the Gulf. Several remnant natural ridges are in the area, including Bayou L'Ours. The lower part of the basin is rimmed with barrier islands, separated by wide, and sometimes deep, inlets. The region includes Lake Boeuf and Salvador/Timken Wildlife Management Areas, the Elmer's Island Wildlife Refuge, and the Barataria Unit of Jean Lafitte National Historical Park and Preserve.

Basin hydrology has been extensively altered since European settlement. Levees built along the Mississippi River during the 19th century limited overbank flow during floods, and the basin was essentially isolated from the Mississippi River following the flood in 1927. Bayou Lafourche was cut off from the river in 1905, further limiting riverine inputs of sediment and freshwater to this region. Additional hydrologic changes to facilitate navigation included dredging the GIWW (1930's), Empire to the Gulf Waterway (1950), Segnette Waterway (1957), Barataria Waterway (1963), and Tiger Pass Waterway (1978). Along the Gulf, shoreline jetties were first constructed at Belle Pass in 1939, and jetties at Grand Isle on the Barataria Pass and the Empire Waterway were later added. Repeated storm impacts result in overwash, erosion, breaching, and fragmentation of barrier islands.

Since the 1990s, more than 60 restoration projects have been constructed in the Barataria Basin by local, state, and federal agencies; parishes; nongovernmental organizations; and private companies. This represents more projects and more expenditures for restoration than in any other basin. Some of these projects were built to support navigation or reduce flood risk. Examples include the Naomi Freshwater Diversion (1992), the West Pointe a la Hache Freshwater Diversion (1992), and the Davis Pond Freshwater Diversion (2002). Others addressed barrier island or headland erosion and fragmentation, including the massive Caminada Headland Beach and Dune Restoration that placed approximately 5.4 million tons of sediment transported from Ship Shoal onto the shoreline, and the Spanish Pass Increment of the Barataria Basin Ridge and Marsh Creation project that used sediment dredged from the Mississippi River. Further, the Mid-Barataria Sediment Diversion, a first-of-its-kind restoration project currently undergoing final design, has the capability to create and sustain thousands of acres of wetlands in the region.

The 2023 Coastal Master Plan assumes that the Mid-Barataria Sediment Diversion is actively

operated throughout the entire 50-year period of evaluation; and is therefore included in the FWOA. While the real-world operations will vary due to river stage and discharge, for modeling purposes, a single operational rule was followed for ICM simulations. When comparing FWOA against a future without currently funded projects (FWOCFP), where the diversion is not active, one can see a large area of newly built wetlands in the immediate outfall of the diversion where river sediments deposit in open water bodies, eventually becoming land after approximately 20 years of operation. In addition to the newly built subaerial land, large portions of existing wetlands throughout the middle portions of Barataria Basin (i.e., areas northwest of Little Lake) are maintained into the future, whereas they are projected to be lost if the diversion were not active. The land is maintained due to a combination of suspended sediments nourishing the wetlands and increased OMAR in these areas. It is important to keep in mind the sensitivity of these results to the exact operations of the diversion. Slight changes to the operational rules will impact the balance between sediment and freshwater delivery and inundation, which is one of many reasons why adaptively managing the operations will be critical to the long-term success of the project.

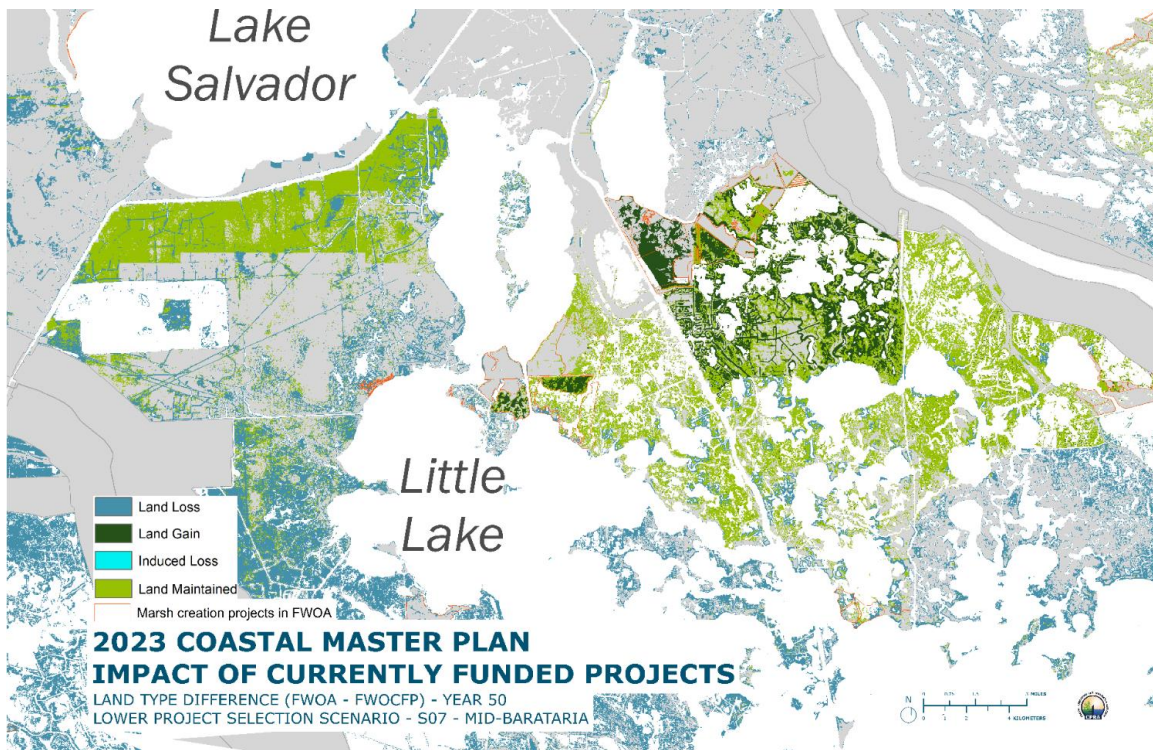


Figure 44. Land change, under S07, after 50 years in the outfall of the Mid-Barataria Sediment Diversion, as compared to a future without the diversion on. This diversion is included as an active project in FWOA.

## 3.2 FWOA STAGE

### LOWER PROJECT SELECTION SCENARIO (S07)

Under a future without action, there is a gradient in water level dynamics across the Barataria region. Timeseries plots show that lower parts of the basin mostly follow the astronomic tide, whereas upper portions are mostly influenced by seasonal trends and flows from diversion outfalls.

The stage in areas near diversion outfalls is impacted by diversion operation, as can be seen in timeseries plots indicating high stages around springtime driven by higher Mississippi River discharge rates.

### HIGHER PROJECT SELECTION SCENARIO (S08)

The trends and gradients of water levels under S08 in the Barataria region are consistent with those seen under S07; however, the magnitude of increases in water levels during later decades is greater due to the higher rates of sea level rise.

Additionally, under the higher rates of sea level rise in S08, there is a greater impact on linear features throughout the Barataria Basin. For instance, levees and hydraulic constraining features around Golden Meadow interact with tidal waters more frequently under S08 in later decades than they did in S07.

## 3.3 FWOA TIDAL RANGE

### LOWER PROJECT SELECTION SCENARIO (S07)

The tidal range follows an expected pattern with the largest ranges in the offshore, with a gradual decline of in tidal range towards the upper portions of Barataria basin.

### HIGHER PROJECT SELECTION SCENARIO (S08)

The trend in tidal ranges in Barataria under S08 are consistent with those seen under S07. One area of difference is in that the slight increase in tidal range in later decades is more pronounced under S08 than it was under S07.

### 3.4 FWOA SALINITY

#### LOWER PROJECT SELECTION SCENARIO (S07)

The overall pattern in the Barataria region follows a clear estuarine-gradient pattern; with near-zero salinity concentrations in the uppermost parts of the basin, with gradually increasing salinities towards the offshore with brackish and saline waters in the lower portions of the basins. This gradient, however, is augmented in the mid-basin due to the presence of the Mid-Barataria Sediment Diversion.

Salinity concentrations increase over time in the upper basin due to rising sea levels; however, the magnitude of the increase is quite small with salinities remaining under 1 ppt even after 50 years of sea level rise.

In the lower portions of the basin, there is a strong seasonal pattern to salinity though there is no clear sign of an increase over time; likely due to the mitigating effects of the Mid-Barataria Sediment Diversion. Closer to the diversion outfall, there is a marked increase in salinity spikes during later years when sea levels are higher. These spikes are temporary, however they increase in frequency even if the area is maintained as low salinity throughout the 50 year FWOA under S07.

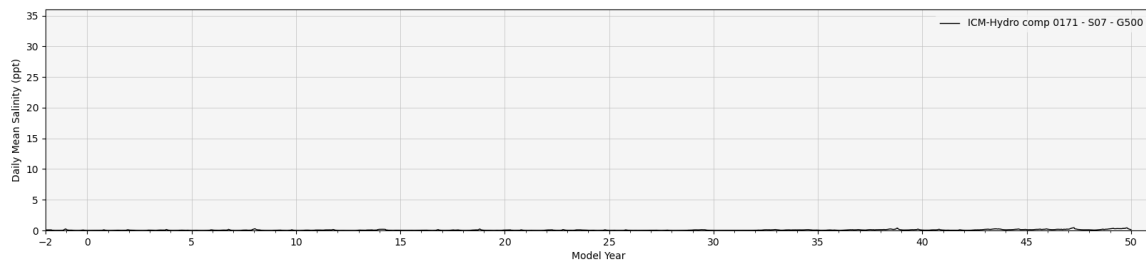


Figure 45. Salinity, under S07, in Lac des Allemandes (compartment 171); this demonstrates the slow increase in salinity intrusion in the upper basin, even though this area maintains a fresh condition.

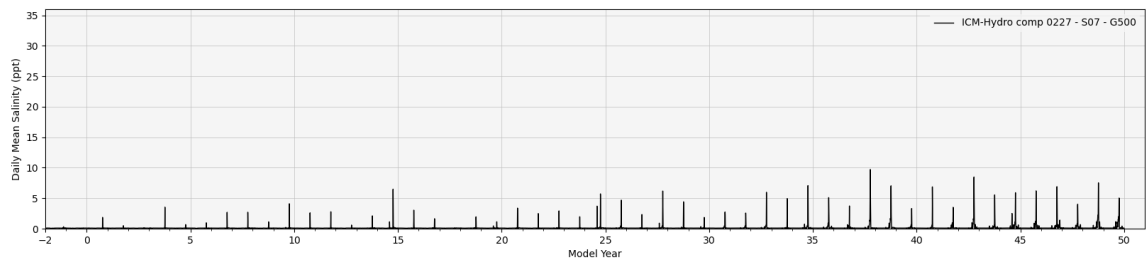


Figure 46. Salinity, under S07, in Wilkinson Canal (compartment 227); this demonstrates the mitigating impact on salinity intrusion due to the Mid-Barataria Sediment Diversion, which decreases over time due to sea level rise.

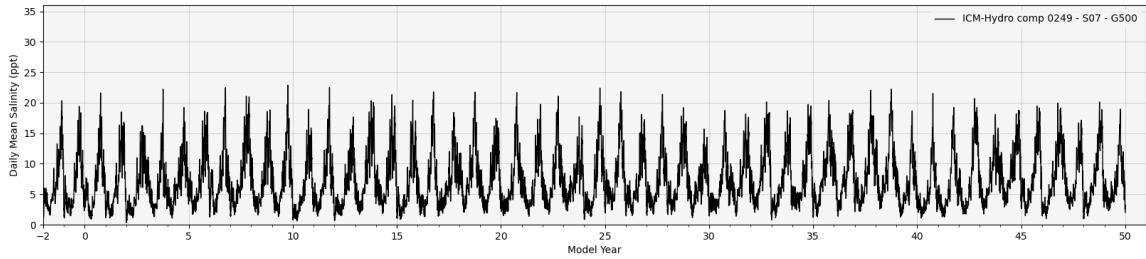


Figure 47. Salinity, under S07, in northern Barataria Bay (compartment 249); this demonstrates the seasonal fluctuations of Gulf-dominated waters, without a clear increase over time (likely due to mitigating effects of the Mid-Barataria Sediment Diversion).

### HIGHER PROJECT SELECTION SCENARIO (S08)

The cross-basin trends in salinity under S08 are quite similar as they were under S07. However, the mitigating effect of the Mid-Barataria Sediment Diversion on salinities in the mid-basin are less pronounced under S08 in the later decades than seen under S07.

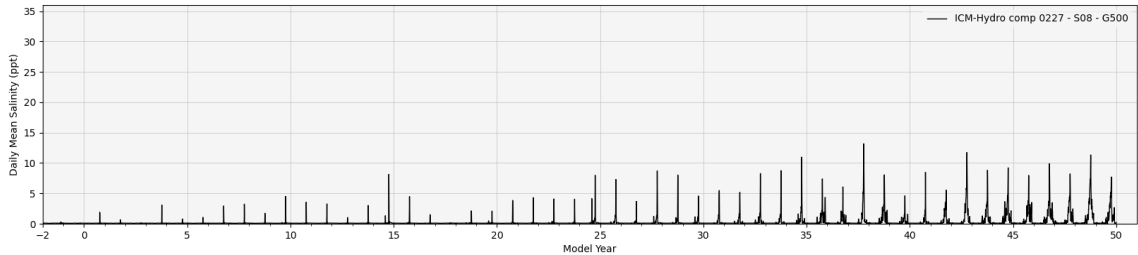


Figure 48. Salinity, under S08, in Wilkinson Canal (compartment 227); this demonstrates the mitigating impact on salinity intrusion due to the Mid-Barataria Sediment Diversion. This mitigation is less effective under S08 than it was under S07.

### 3.5 FWOA TOTAL SUSPENDED SOLIDS (TSS)

#### LOWER PROJECT SELECTION SCENARIO (S07)

Under S07, low TSS concentrations are found in upper portions of the Barataria region that are distant from river distributaries or diversion outfalls of any type (Figure 49). Higher TSS can be seen in areas around diversion outfalls and river distributaries. No substantial differences can be observed when comparing across decades. However, within diversion outfall areas, seasonal and interannual changes in TSS can be seen as a function of diversion operations. TSS concentrations decrease longitudinally in diversion outfalls, due to suspended sediments dropping out of suspension closer to the outfall

location (Figure 50 and Figure 51). Even in the upper portions of Barataria (Figure 49), strong seasonality of TSS concentrations corresponding to Mississippi River hydrograph and diversion operations indicates some seasonality up-basin may still be showing effects of downstream conditions.

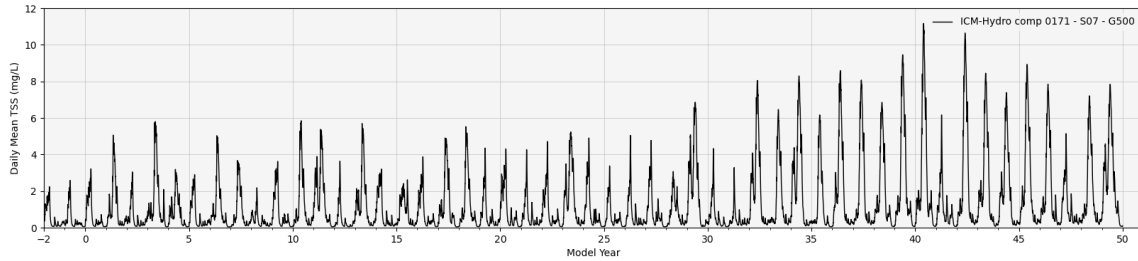


Figure 49. TSS, under S07, in Lac des Allemandes (compartment 171); this demonstrates the lower sediment concentrations in the areas of Barataria without river influences.

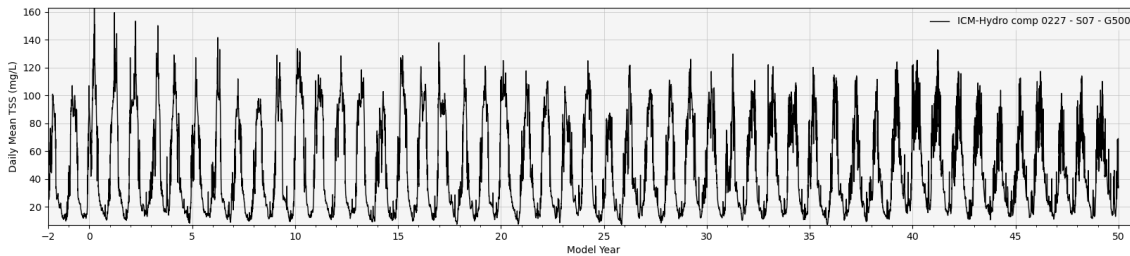


Figure 50. TSS, under S07, in Wilkinson Canal (compartment 227); this demonstrates the highest sediment concentrations in the immediate outfall area near the Mid-Barataria Sediment Diversion.

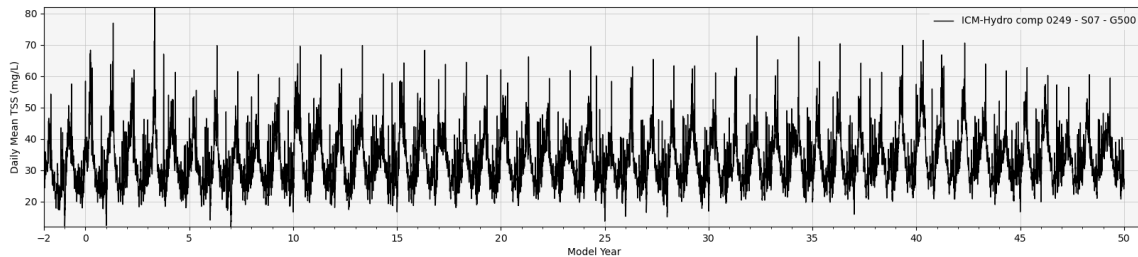


Figure 51. TSS, under S07, in northern Barataria Bay (compartment 249); this demonstrates the elevated TSS levels due the diversion, but a decrease in magnitude longitudinally from the Mid-Barataria Sediment Diversion outfall.

## HIGHER PROJECT SELECTION SCENARIO (S08)

Trends in TSS across the basin, and over time, are consistent in the Barataria region between S08 and S07. Impacts of access to riverine sediments is a driving factor in defining TSS dynamics throughout the basin.

### 3.6 FWOA WATER TEMPERATURE

## LOWER PROJECT SELECTION SCENARIO (S07)

Similar to other regions, there is a clear and persistent increase in temperature throughout Barataria over the 50-year FWOA simulation, under S07. This long-term increase is on the order of approximately 1 degree Celsius, and is evident in both the wintertime lows and summertime highs. Similar to Pontchartrain/Breton, there is a clear signature evident in areas impacted by the cooler winter waters in the Mississippi River (Figure 52), as compared to less river-connected portions of the basin, such as near Caminada Bay (Figure 53).

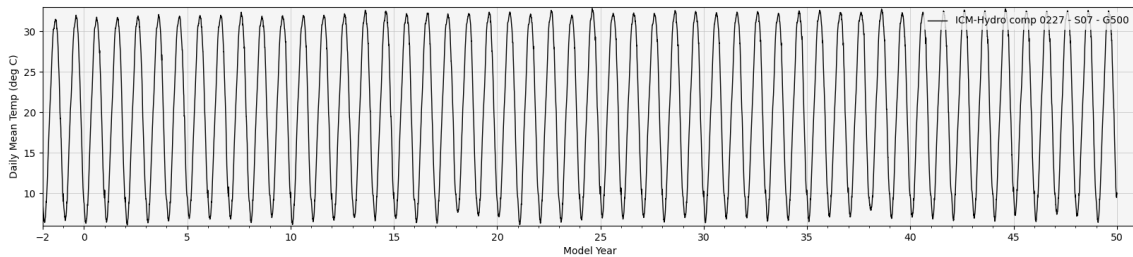


Figure 52. Water temperature, under S07, in Wilkinson Canal (compartment 227); this demonstrates the cooler winter minimums in areas connected to the Mississippi River; here as a result of the Mid-Barataria Sediment Diversion.

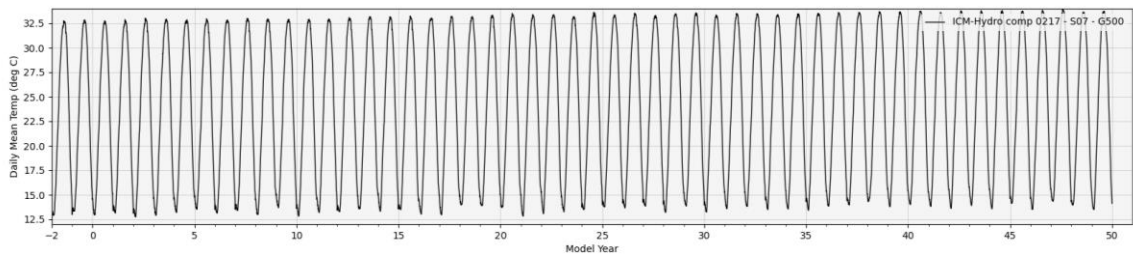


Figure 53. Water temperature, under S07, west of Caminada Bay (compartment 217); this demonstrates the warmer winter minimums in areas without direct connection to the Mississippi River.

## HIGHER PROJECT SELECTION SCENARIO (S08)

The Barataria region, much like the Pontchartrain/Breton region has similar temperature dynamics under S08 as compared to S07. However, the overall magnitude of increase over time is greater in S08, given the higher rates of temperature increases in the underlying climate change-derived scenario values. The higher degree of warming of S08 compared to S07 becomes more and more obvious over time. When comparing S08 to S07, consistently higher summertime highs and wintertime lows can be observed in the Barataria; the upper portions of Barataria are controlled by the more stable estuarine water temperature boundary and is less impacted by the fluctuating Mississippi River temperatures, as compared lower in the basin and in the areas impacted by the diversion outfall (Figure 54).

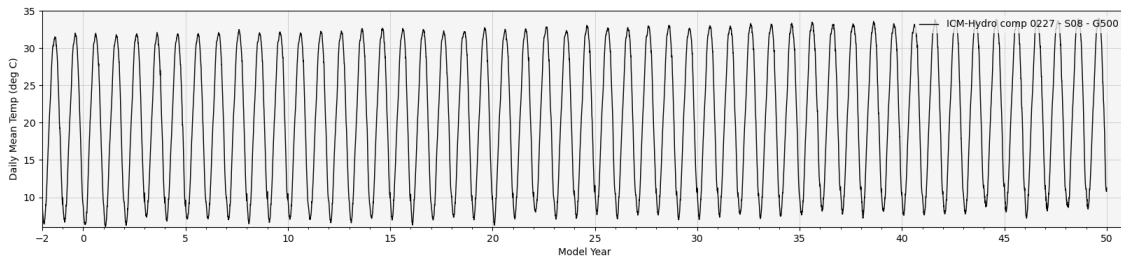


Figure 54. Water temperature, under S08, in Wilkinson Canal (compartment 227); this demonstrates the cooler winter minimums in areas connected to the Mississippi River, here as a result of the Mid-Barataria Sediment Diversion.

## 3.7 FWOA VEGETATION

### LOWER PROJECT SELECTION SCENARIO (S07)

In the Barataria Basin, UBA remains relatively stable as forested wetland under S07 (Figure 55 and Figure 56). This is demonstrated with CRMS0217 (Point A in Figure 57). At CRMS0217 the forest is stable, but in the marsh PAHE2 is replaced with POPU5. MBA shows slightly more land loss and this coincides with loss of swamp and flotant. However in most areas of MBA no land loss is observed as demonstrated with CRMS0211, where PAHE2 remains dominant (Point B in Figure 57). In northern lower Barataria there is a marked difference between the west and the east. In LBAnw, land is relatively stable under the influence of the Mid-Barataria Sediment Diversion, and fresh and intermediate marshes expand. This is illustrated by QAQC1313, where deltaic species COES, SALA2, ZIMI, PHAU7, and POPU5 all expand (Point C in Figure 57). In contrast in LBAnw, brackish marshes are lost at the same time that intermediate marsh converts to brackish marsh. This is illustrated with QAQC1209 (Point D in Figure 57). At QAQC1209, there is a low rate of loss when the site is dominated by SALA in the first 3 decades. SALA is decreasing and partially replaced with PHAU7 and TYDO as loss accelerates in the fourth decade. After SCAM6 invades in Year 39, the loss rate accelerates even more in the last decade. This difference between east and west disappears in the southern half of lower

Barataria where salt marsh is lost at very high rates (example CRMS0175, Point E in Figure 57).

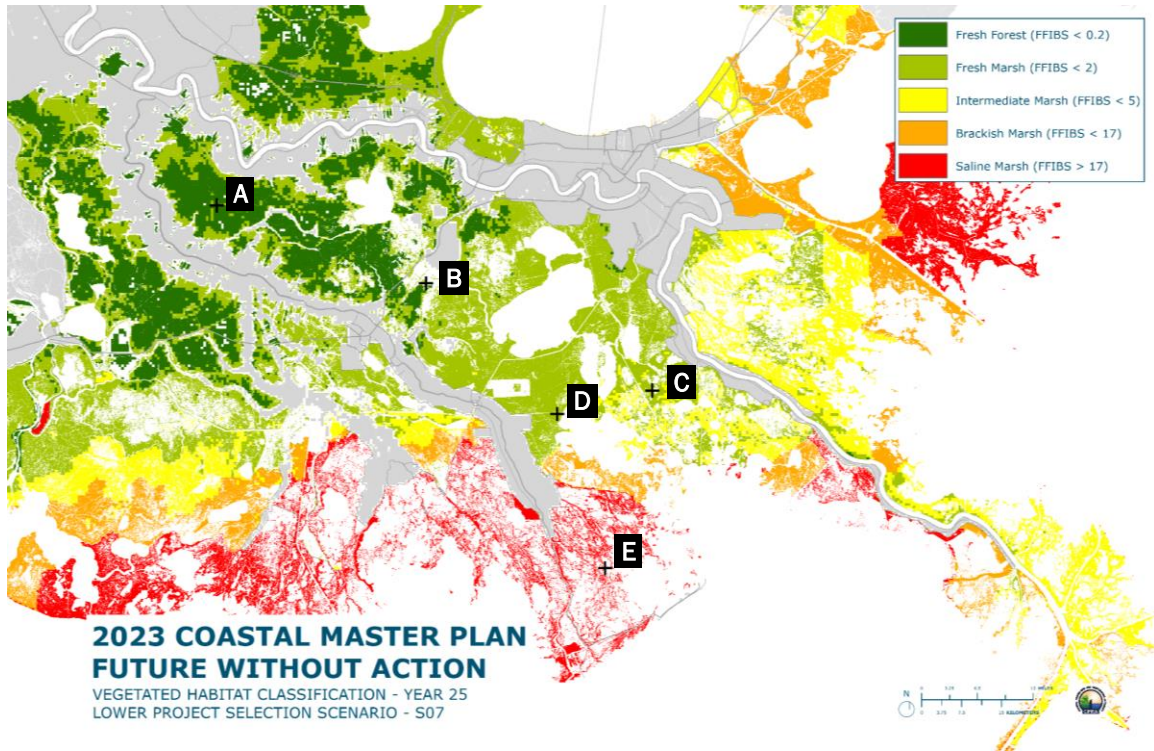


Figure 55. Wetland type (FFIBS score) distribution of the Barataria Basin under scenario S07 in Year 25.

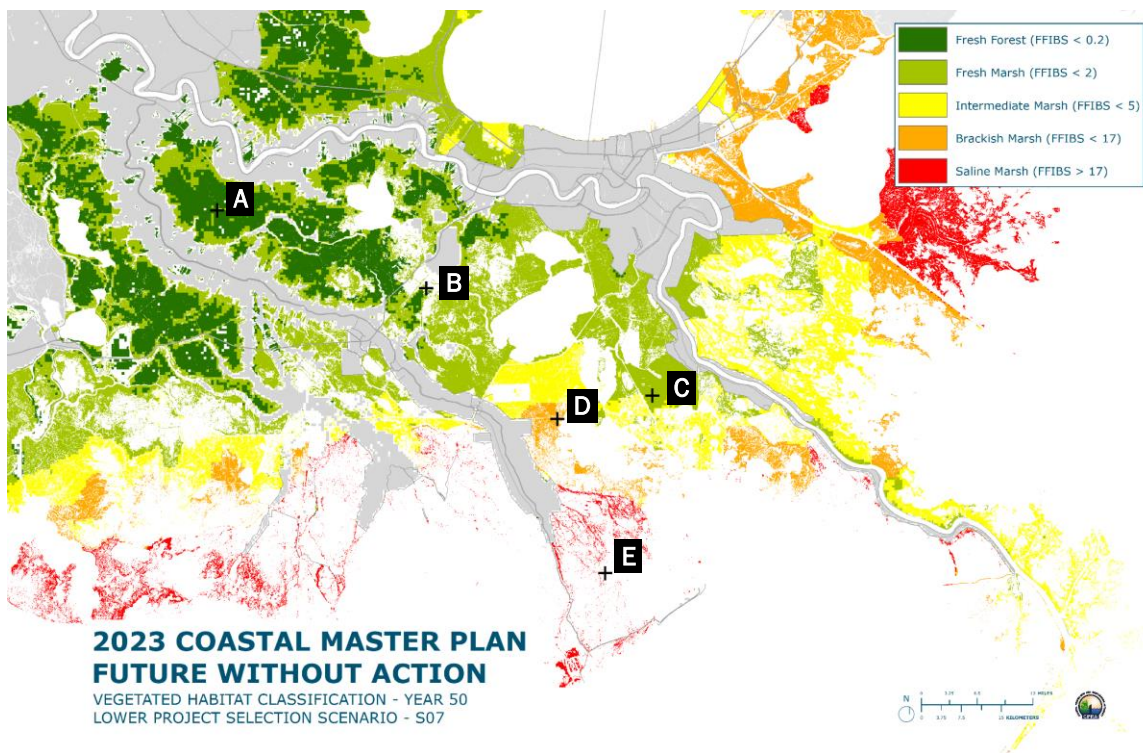


Figure 56. Wetland type (FFIBS score) distribution of the Barataria Basin under scenario S07 in Year 50.

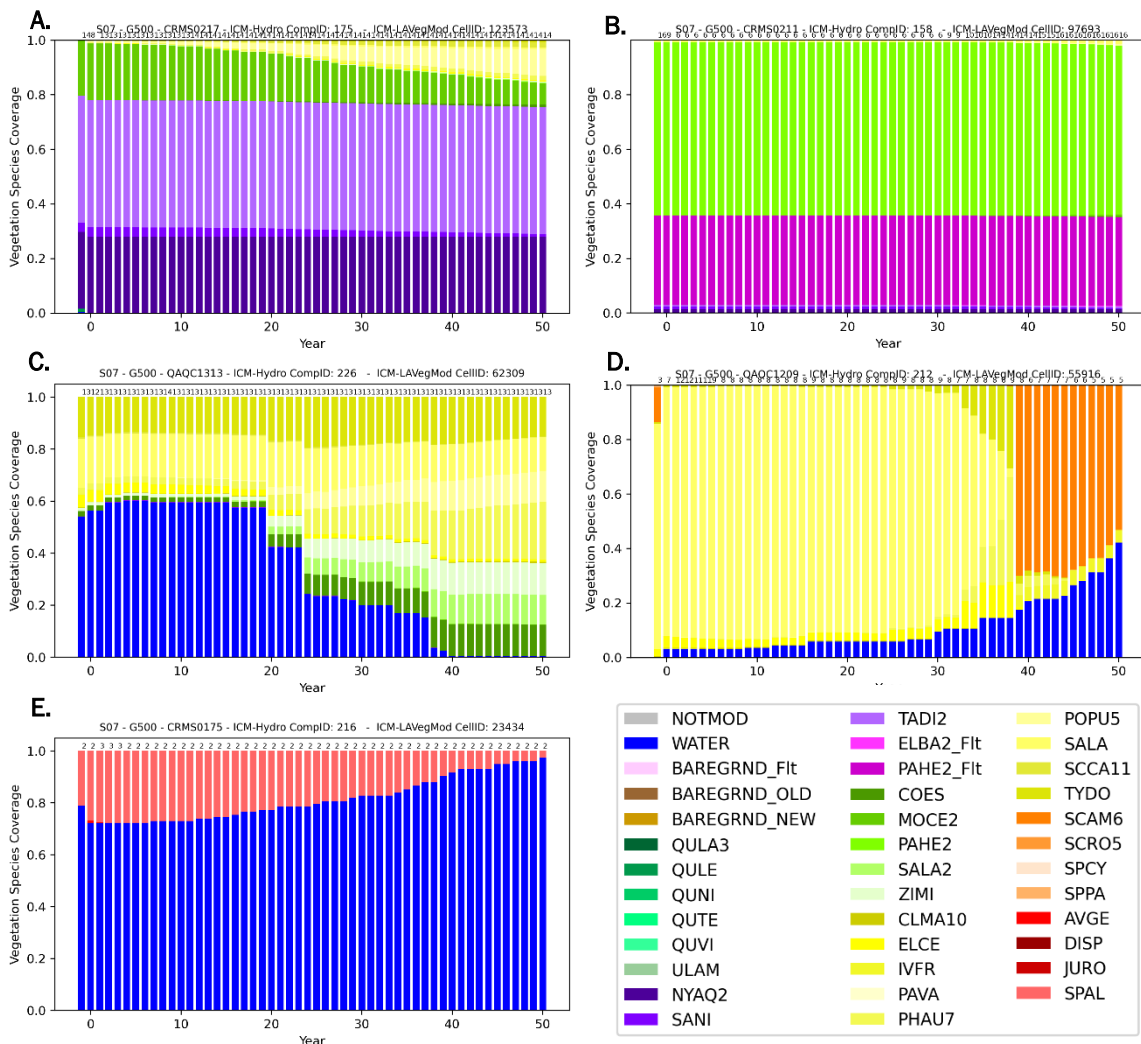


Figure 57. Change in vegetation cover under S07 is shown at representative points for different locations throughout Barataria Basin. Point locations are shown in previous Barataria region map figures.

## HIGHER PROJECT SELECTION SCENARIO (S08)

UBA remains relatively stable forested wetland under S08 (Figure 58 and Figure 59). This is demonstrated with CRMS0217 (Point A in Figure 60). At CRMS0217 the forest is stable, but in the marsh PAHE2 is replaced with POPU5. MBA shows slightly more land loss and this coincides with loss of swamp and flotant. However in most areas no land loss is observed as demonstrated with CRMS0211 (Point B in Figure 60). In northern lower Barataria there is a marked difference between the west and the east. In LBAnE, land is relatively stable for the first 25 years under the influence of the Mid-Barataria Sediment Diversion. However, in the last 25 years even with the diversion in place, land is lost primarily in brackish and intermediate marshes farther away from the diversion. At

QAQC1313 closer to the diversion (Point C in Figure 60), there is deltaic expansion dominated by PHAU7 in Year 46. In contrast, in LBA<sub>nw</sub>, marshes become progressively more saline up estuary as marshes down estuary are lost. This change is illustrated with QAQC1209 (Point D in Figure 60). At QAQC1209, there is a low rate of loss when the site is dominated by SALA in the first two decades. SALA is decreasing and partially replaced with PHAU7 and TYDO as loss accelerates in the third decade. When SCAM6 starts increasing rapidly in Year 33, the loss rate accelerates even more with little marsh remaining in the last decade. This difference between east and west disappears in the southern half of lower Barataria where salt marsh is lost at very high rates (example CRMS0175, Point E in Figure 60).

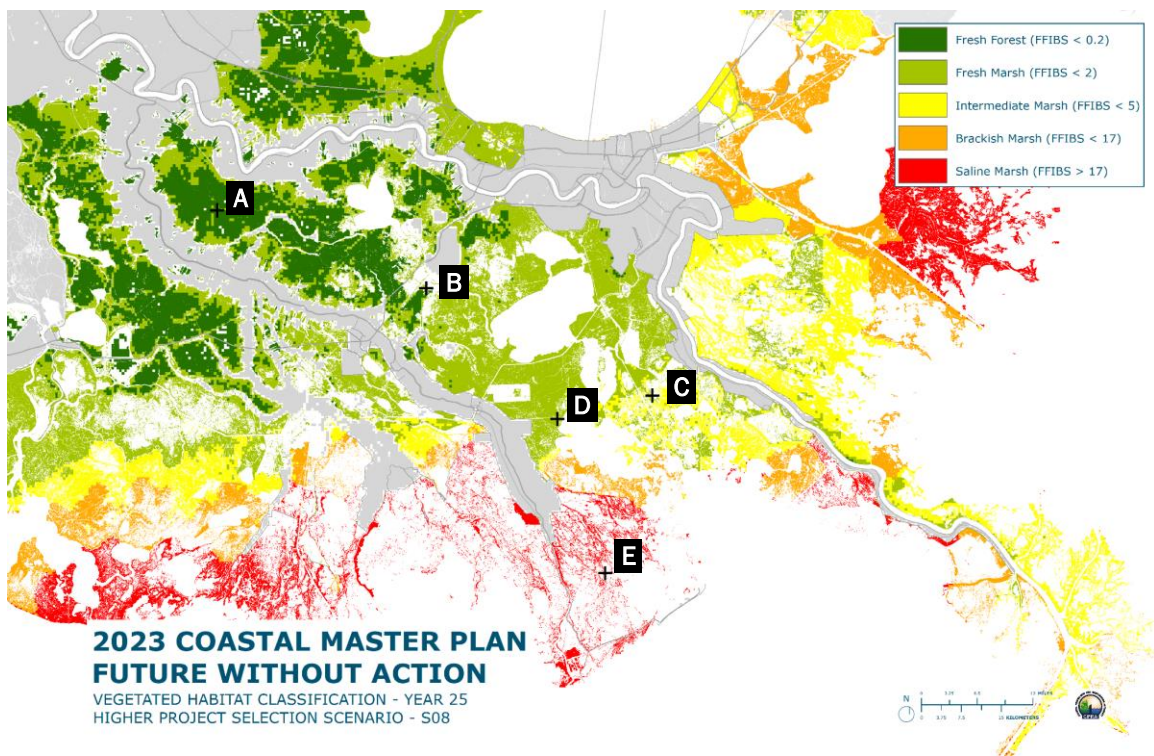


Figure 58. Wetland type (FFIBS score) distribution of the Barataria Basin under scenario S08 in Year 25.

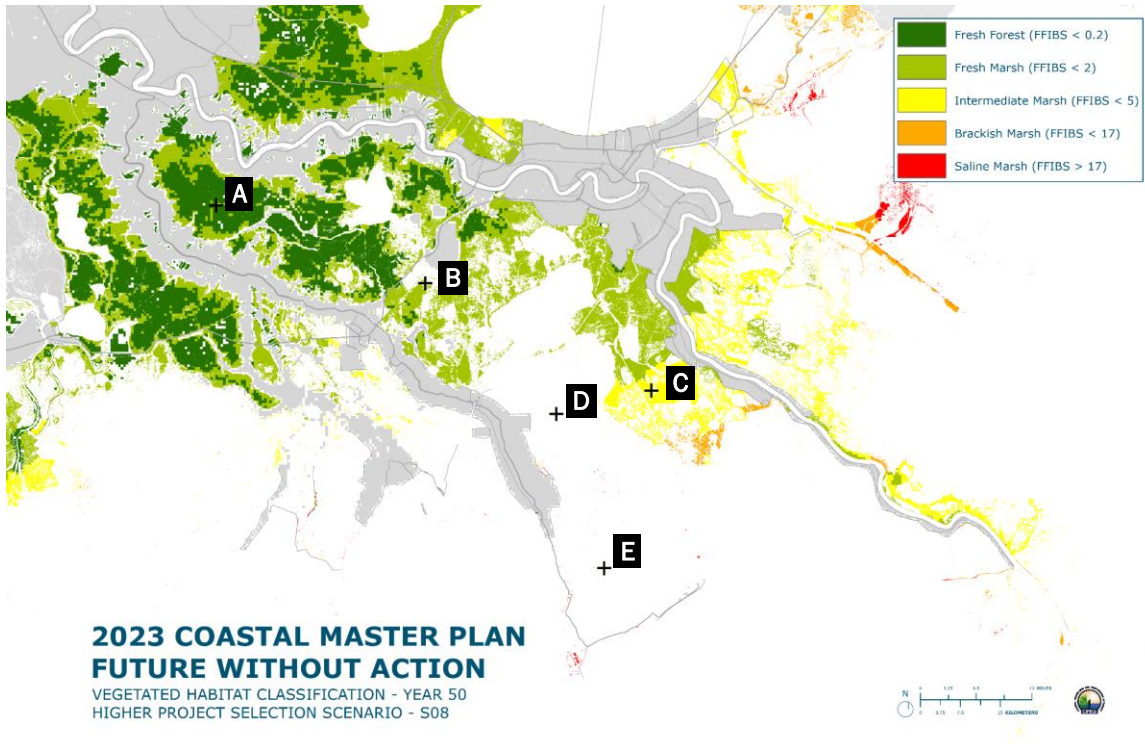


Figure 59. Wetland type (FFIBS score) distribution of the Barataria Basin under scenario S08 in Year 50.

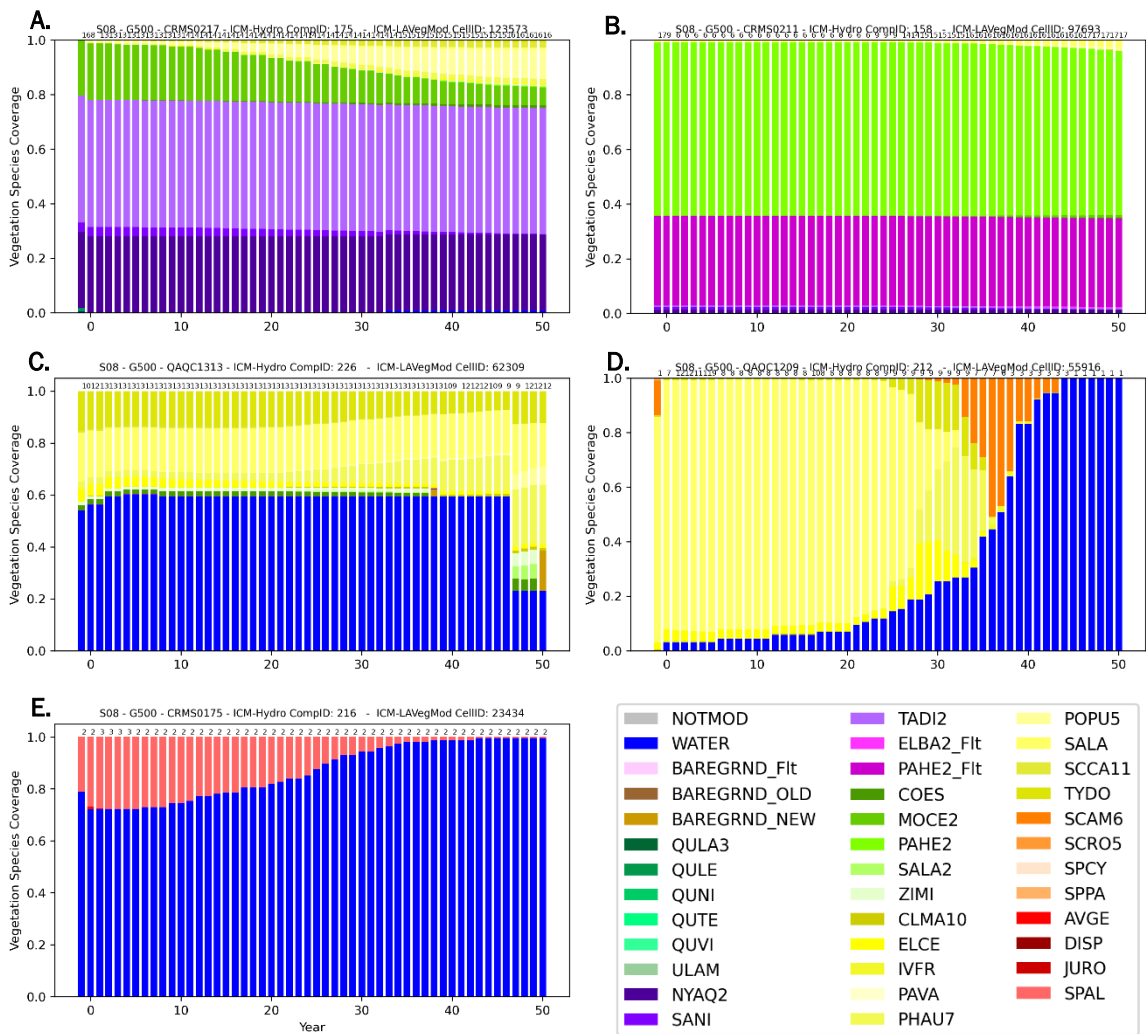


Figure 60. Change in vegetation cover under S07 is shown at representative points for different locations throughout Barataria Basin. Point locations are shown in previous Barataria region map figures.

### 3.8 FWOA WETLAND MORPHOLOGY

#### LOWER PROJECT SELECTION SCENARIO (S07)

Barataria experiences little change in the first three decades. There is minor land loss along marsh edges in the lower reaches of the region, especially around the edge of Barataria Bay, and there is land gain in compartment 226 due to the operation of the Mid-Barataria Sediment Diversion. This pattern continues in the last two decades with increased land loss in lower Barataria. There is land loss in the southeast portion, particularly in areas less influenced by the diversion, such as around the

Port Sulphur Canal in the southeast, between Bayou L'Ours and Bayou Lafourche on the western side of the bay and on the western side of Little Lake. Mid-Barataria and upper Barataria experience little change. There is small land gain from the Davis Pond Freshwater Diversion. There are also small pockets of flotant loss west of Lake Salvador near Gheens. The Northwest Turtle Bay Marsh Creation remains intact in Year 50, while the Spanish Pass increment of the Barataria Basin Ridge Marsh Creation converts to open water over the later portion of the last decade.

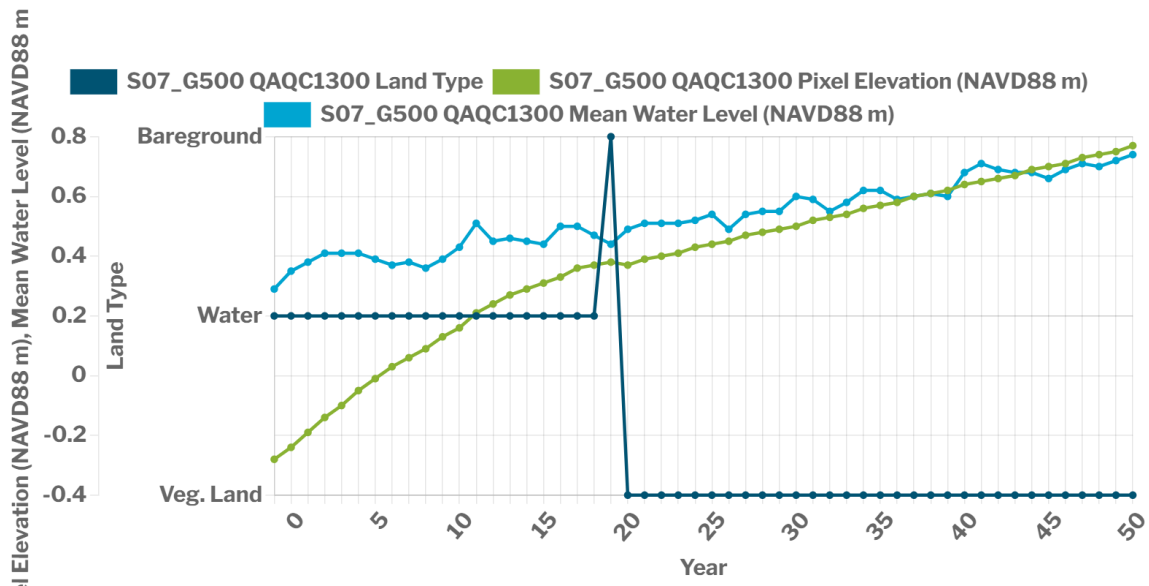


Figure 61. Inundation dynamics at QAQC1300 under S07.

The impact of the diversion is clear in compartment 226. QAQC1300, which is within Veg Cell 70704, illustrates the land building process. This pixel receives high levels of mineral deposition in the first two decades until it transitions to bareground and becomes vegetated (Figure 61). Once vegetated, the organic accretion is the primary driver of elevation gain, and the elevation gain matches the mean water level increase. The area remains predominantly fresh with a mix of fresh and intermediate species and a FFIBS score of about 1.5 (Figure 62).

Note that it is expected that bareground shows up in the Morph results (Figure 61) and not in LAVegMod (Figure 62). LAVegMod results are at the end of the LAVegMod “year.” What comes in as new bareground leaves as vegetated land.

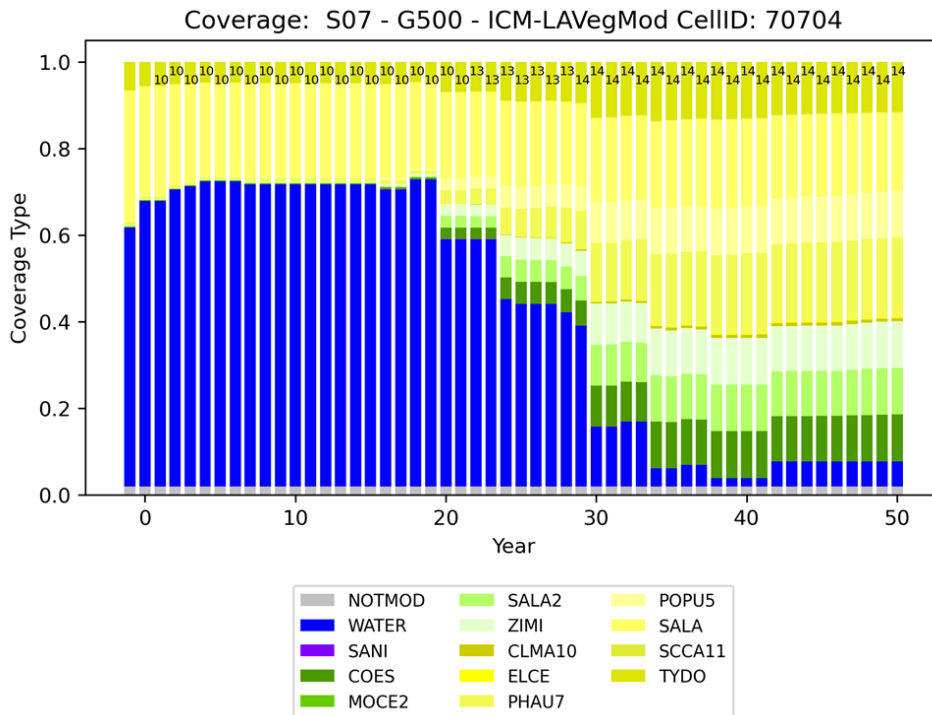


Figure 62. Vegetation coverage in grid cell 70704 (includes QAQC1300) under S07.

### HIGHER PROJECT SELECTION SCENARIO (S08)

In the first decade there is little change in the upper part of the Barataria Basin (north of the GIWW). There is some edge erosion around the shores of Lake Salvador and some new land develops in fragmented marsh areas near the Davis Pond Diversion. Mineral sediment deposition rates here are high in open water and total accretion actually decreases when pixels convert to marsh as the compartment is not designated active delta. This can lead to a change back to open water after several years as stage increases. The general pattern of gain near Davis Pond continues and isolated areas of loss occur west of Lake Cataouatche, north of Lake Salvador and southwest of Des Allemands by Year 15. By Year 30 most of the pockets of loss have increased in size. Land loss increases in the first part of the last decade, especially between Gheens and Lake Salvador. By Year 45 the loss is confined to marsh areas and the flotant in this part of the basin remains intact. However, in the last five years of the simulation land loss occurs in areas previously stable (Figure 63).

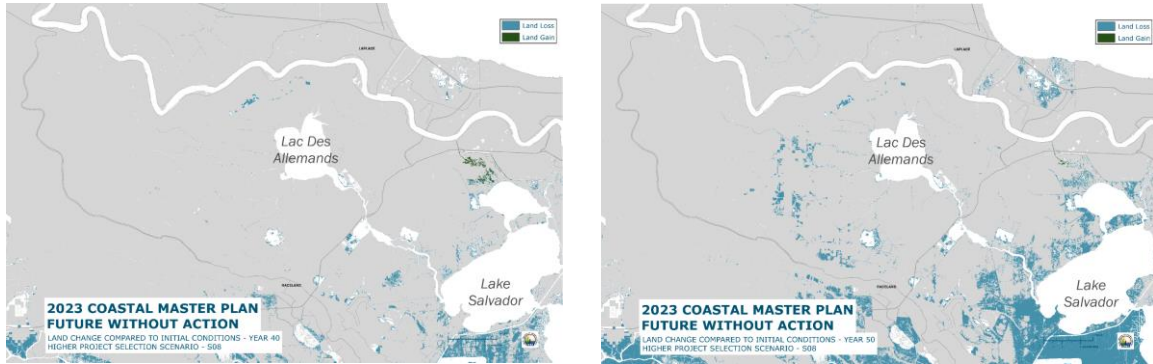


Figure 63. Cumulative land change by Year 40 (left) and Year 50 (right) for the upper Barataria Basin under S08.

There is loss in some fresh marsh areas of the upper basin (e.g., near Chackbay) and more extensive loss south of Lake Cataouatche. Some of the land built near Davis Pond converts back to open water leaving only minor net gain by Year 50. Further, some of the flotant west of Lake Salvador turns to open water (see Figure 63). This occurs in Year 47 of the simulation. Salinity for compartment 159 which covers the area southwest of Lake Salvador is higher than the compartments to the north and northwest. In Year 47 the salinity increases to a peak of 10 ppt (apparently associated with a storm impact as stage also peaks). The marshes in this area are fresh and intermediate.

The lower basin shows little change in the first decade of the simulation. There is scattered land loss in the marshes near the Mid-Barataria Sediment Diversion as well as in the southwest part of the basin. In Year 15, some flotant is lost to open water near Delta Farms. This appears to be associated with high salinity (up to almost 10 ppt in compartment 204) associated with a storm impact. By Year 20, while scattered land loss occurs through the lower basin, some land gain is apparent close to the Mid-Barataria Sediment Diversion, in an area bounded to Wilkinson Canal to the east, Bayou Dupont to the North, and the Barataria Waterway. By Year 30 there is widespread loss between Bayou L'Ours and Bayou Lafourche and near the Port Sulphur Canal, mostly in areas with brackish or saline FFIBS scores. By Year 35 the marshes around Delta Farms, which are intermediate, also show land loss, while land gain continues close to the Mid-Barataria Sediment Diversion (Figure 64). In Year 37, large areas of bareground emerge near the Mid-Barataria Sediment Diversion which become vegetated the following year. By Year 40 land loss is extensive on the western side of the basin including the Delta Farms area while the Mid-Barataria Sediment Diversion appears to maintain marshes on the eastern side, north of the Bay Batiste area. This land loss on the western side of the basin becomes more complete in the last decade of the simulation with some loss between Wilkinson Canal and the Barataria Waterway, south of the immediate influence of the Mid-Barataria Sediment Diversion (see Figure 64).

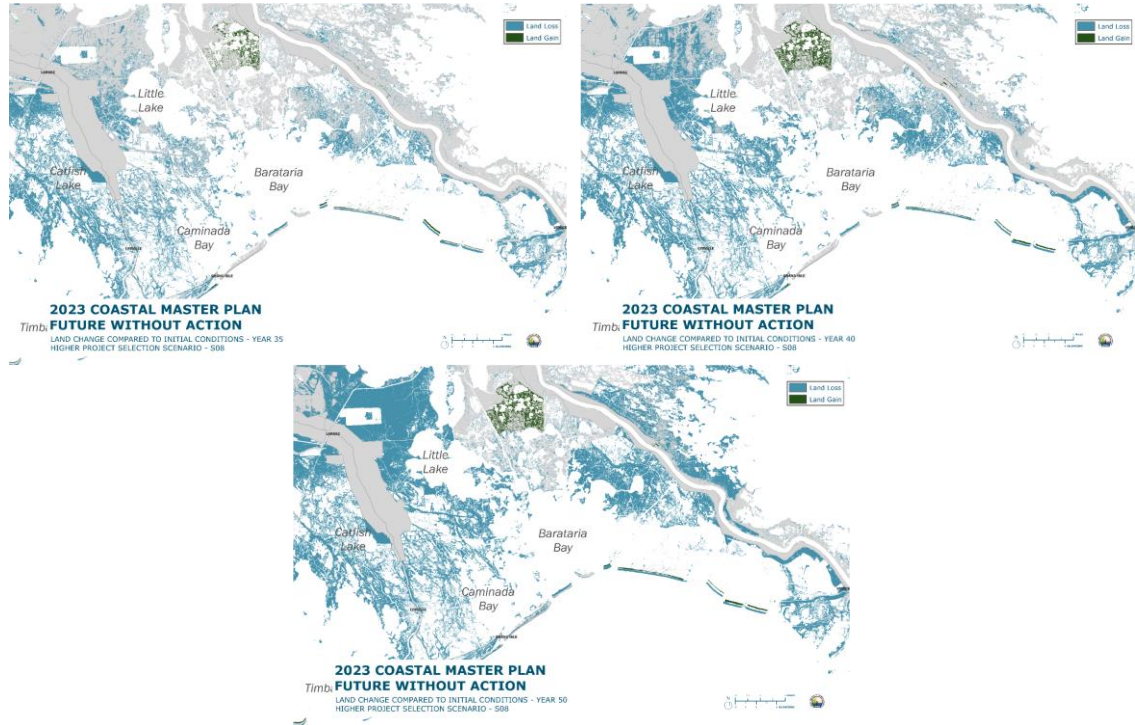


Figure 64. Cumulative land change by Year 35 (top left), Year 40 (top right) and Year 50 (bottom) for the lower Barataria Basin under S08.

These dynamics of changing elevation, accretion and inundation is illustrated for specific locations in the graphs below. CRMS 4529 is on the northeast side of Bay Batiste on the lower eastern side of the basin (Figure 65). For the first three decades of the simulation accretion, dominantly organic, maintains or even slightly increases marsh elevation against subsidence of approximately 8 mm/yr. However rising water levels increase inundation until the marsh is lost to open water in Year 30. Thereafter, when organic accretion is no longer present elevation declines and inundation depths further increase. In contrast, QAQC1313 (near the Bayou Dupre ridge on the eastern side of the Barataria Waterway) starts as open water and experiences high rates of mineral sediment deposition (over 5 cm in some years) and bed elevation increases over time (Figure 66). As bed elevation increases sediment deposition also declines until in Year 40 bareground emerges and organic accretion becomes dominant. While this is lower in magnitude than the sediment deposition in open water in the earlier decades, surface elevation continues to increase throughout the remainder of the simulation. Inundation does increase but remains below the inundation threshold for marsh loss (as the area is very low salinity with a FFIBS score of ~2).

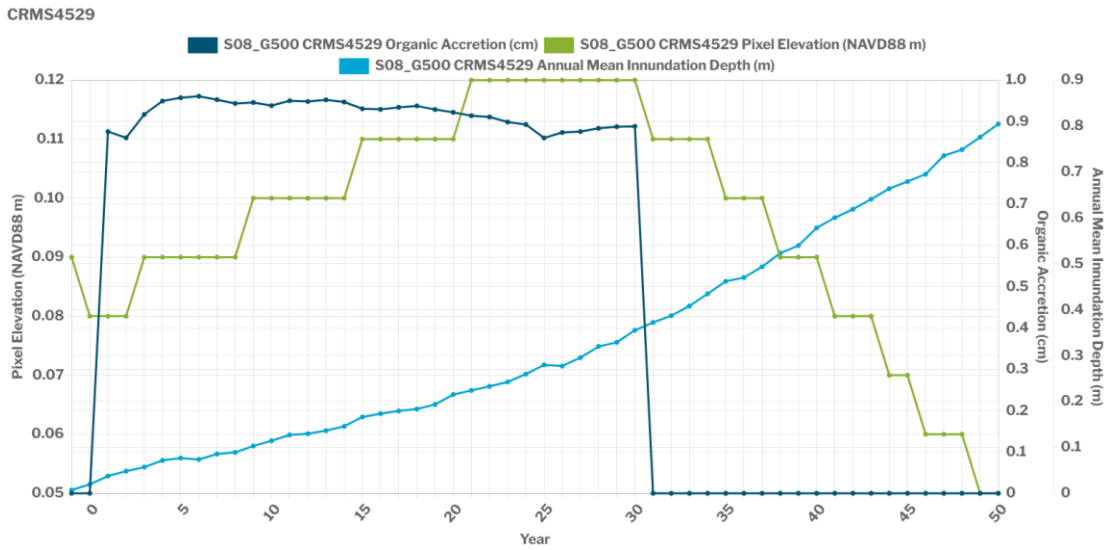


Figure 65. Organic accretion and inundation dynamics at CRSM4529 under S08.

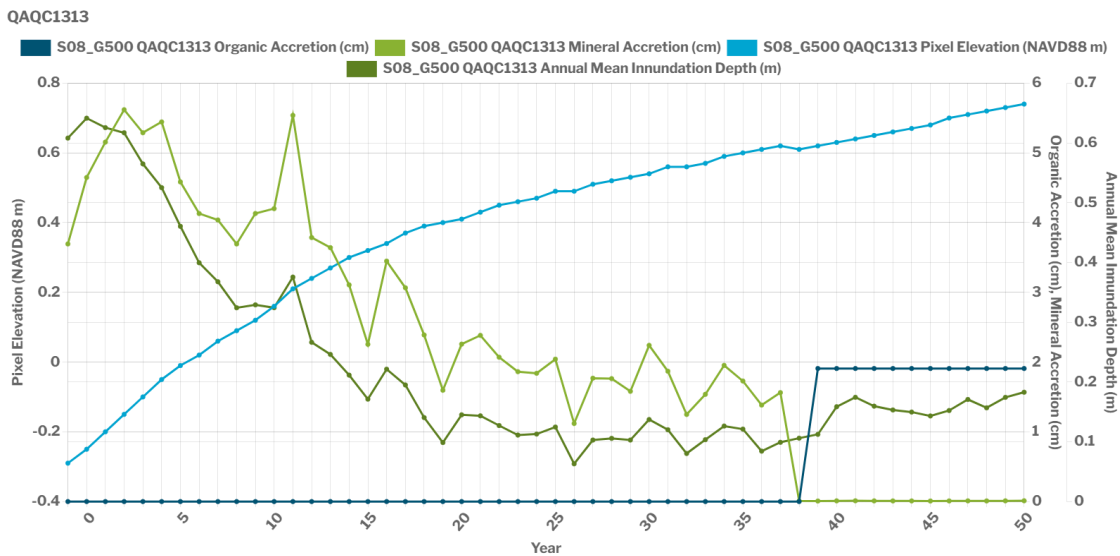


Figure 66. Organic and mineral accretion and inundation dynamics at QAQC1313 under S08.

There are several restoration projects apart from the Mid-Barataria Sediment Diversion included in the FWOA. Barataria Basin Ridge and Marsh Creation - Spanish Pass Increment is lost to open water by Year 50, and Northwest Turtle Bay Marsh Creation western component is lost in Year 48. However, the eastern component remains land at Year 50, as does Large-Scale Barataria Marsh Creation.

### 3.9 FWOA BARRIER ISLAND MORPHOLOGY

The barrier islands in the Barataria region that are modeled with ICM-BI include: Grand Isle, Grand Terre, East Grand Terre, Grand Pierre, Shell Island, Pelican Island, and Scofield Island. In addition, there are three headland features in this region including West Belle Pass, Caminada Headland, and Chaland Headland (Figure 67).



Figure 67. ICM-BI barrier islands and headlands within the Barataria region of the coast. Background imagery from Google Earth.

Because of the assumption that coastal protection action will be taken to preserve Grand Isle in place, the cross-shore retreat rate for this location is set to zero and the barrier island's elevation keeps pace with relative sea level rise, reflecting anthropogenic intervention to maintain elevation. As a result, the footprint and location of Grand Isle are preserved in both the S07 and S08 scenarios (Figure 68). The remaining barrier islands in this region of the coast, including Grand Terre, East Grand Terre, Grand Pierre, Shell Island, Pelican Island, and Scofield Island, all undergo transgression toward the mainland through cycles of cross-shore erosion, relative sea level rise, and auto-restoration (Figure 68, Figure 69).

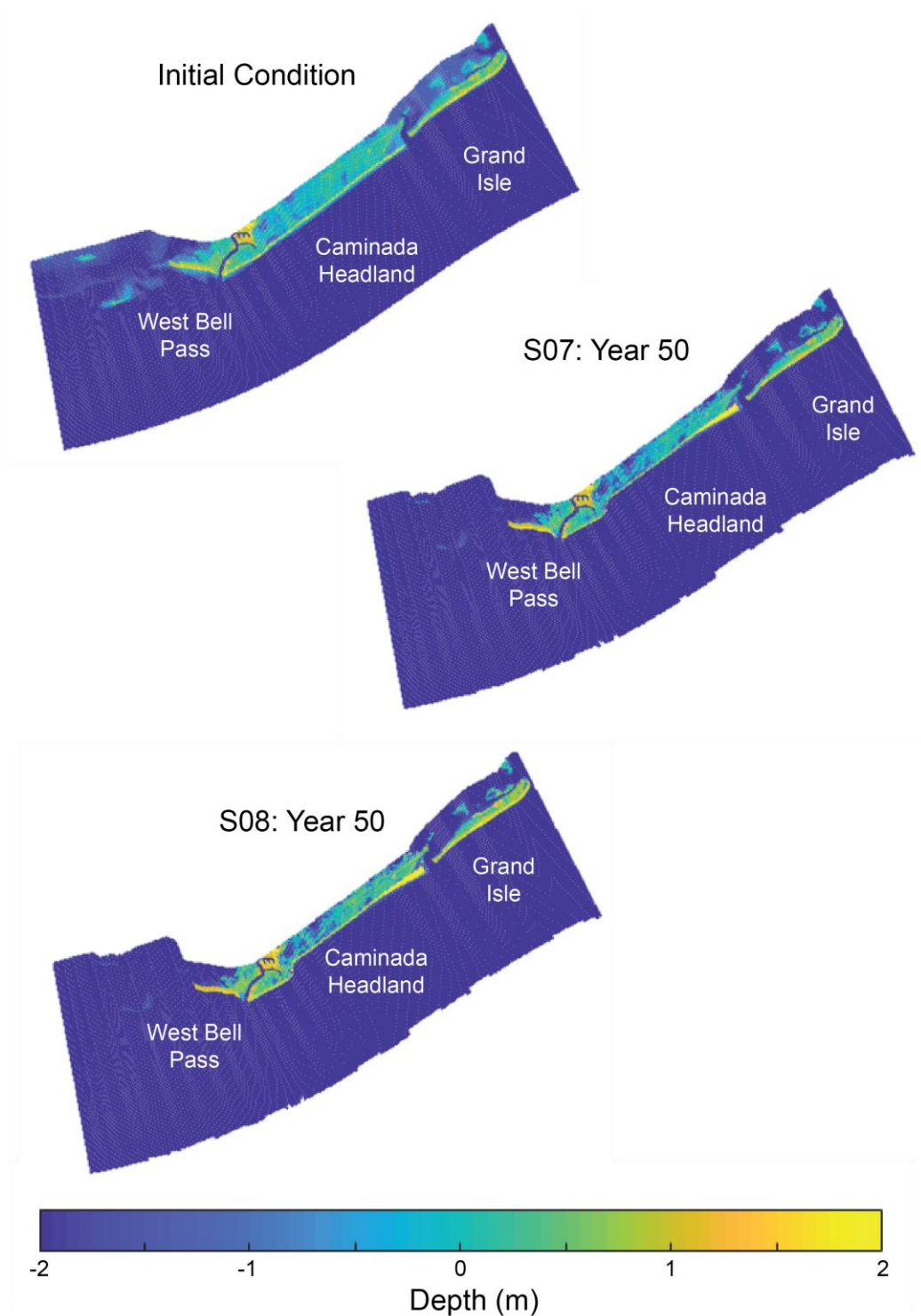


Figure 68. Elevation, relative to mean high water, for the initial condition in the eastern portion of the Barataria region along with Year 50 results for S07 and S08. Depth is shown in meters.

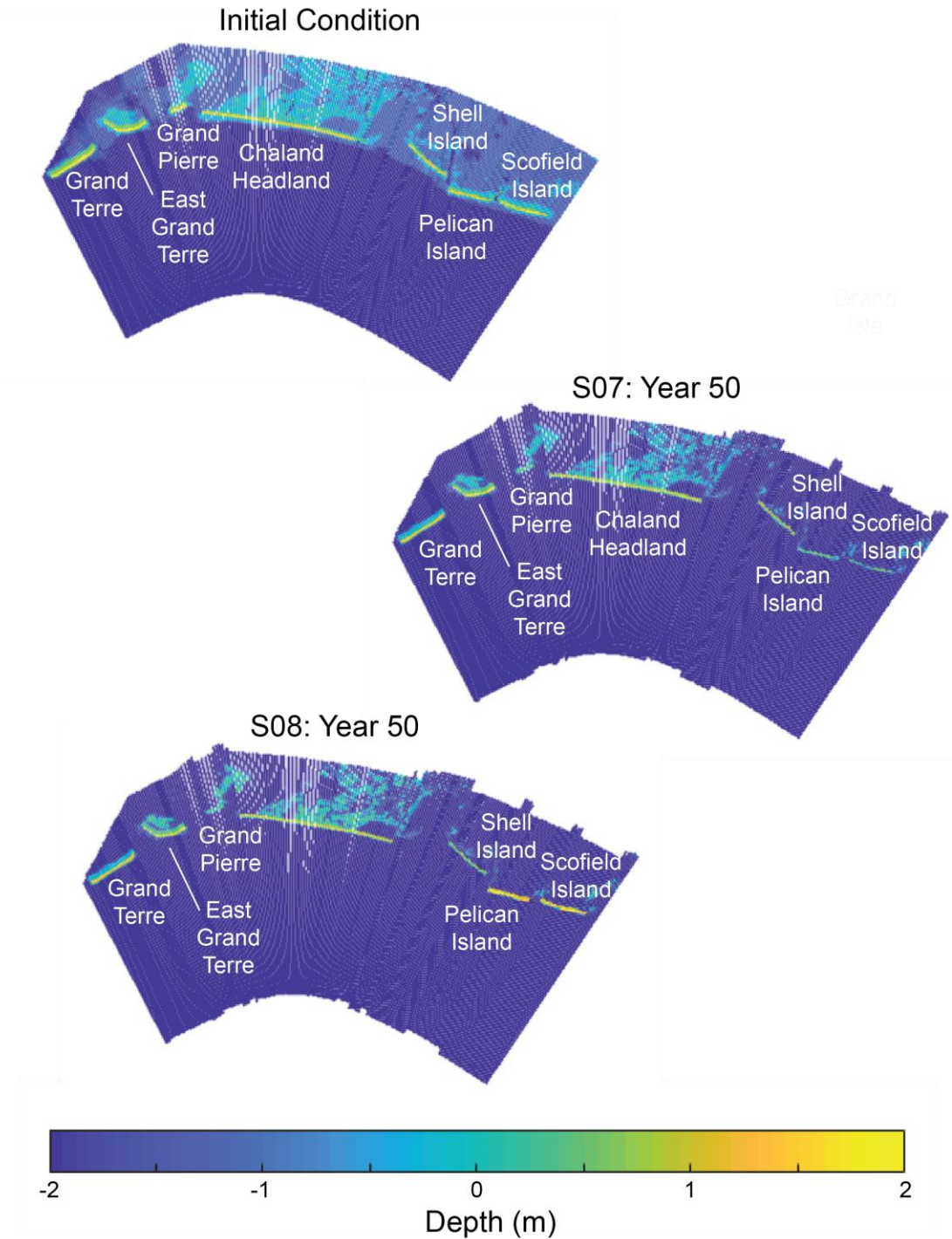


Figure 69. Elevation, relative to mean high water, for the initial condition in the western portion of the Barataria region along with Year 50 results for S07 and S08. Depth is shown in meters.

The exception to this behavior is Grand Terre, which due to a relatively low cross-shore retreat rate did not reach the threshold for auto-restoration (Figure 70, Table 4) and remains relatively intact at the end of the 50-year model run for both scenarios. There are three locations that are modeled as headlands in this region of coast, including West Belle Pass, Caminada Headland, and Chaland Headland. Except for the area near Port Fourchon, each of these headlands were allowed to retreat landward over cycles of cross-shore retreat and auto-restoration, leading to overall landward migration of the Gulf shoreline. This behavior was most pronounced at the Caminada Headland, which owing to a high rate of cross-shore retreat was auto-restored more frequently than any of the other barrier shorelines, with auto-restoration occurring approximately every 4-5 years. Due to this high frequency of restoration and the large size of the headland, the overall sediment volume placed during auto-restoration at the Caminada Headland is higher than for any other barrier island and headland (Figure 68, Table 4). As with other regions of the coast, the shallow areas around the barrier islands that are outside of the restoration footprints deepen over time with relative sea level rise, and the condition of the islands at the end of the 50-year model runs are strongly a function of the time that has elapsed since the last auto-restoration occurred.

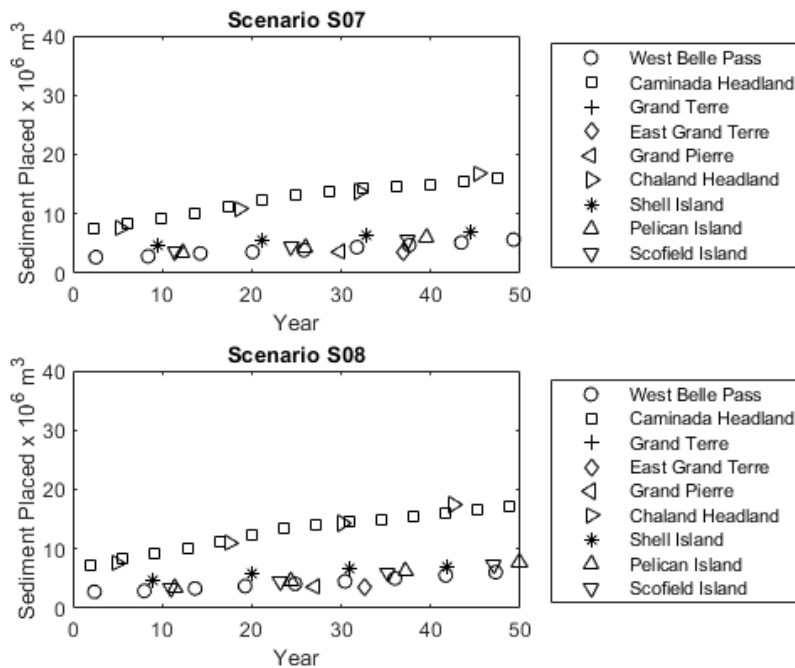


Figure 70. Sediment placement volumes for barrier islands within the Barataria region of the coast.

Five of the nine tidal inlets in Barataria Basin reach their maximum allowable cap on either depth, width, or both (Figure 71). Link 529, Caminada Pass, reaches the max depth during the model spin-up, and since the width is set, the inlet area does not change at all after the spin-up period. Link 532, Barataria Pass, reaches the max depth in the third decade. Link 535 and Link 538 reach the max width at the end of the fourth decade and reach the max depth towards the end of the fifth decade.

Link 540 reaches the max width in the last decade. Links 554, 551, 555, and 556 expand gradually throughout the simulation and do not reach the 50% limit.

Table 4. Summary of total sediment volume placed ( $10^6 \text{ m}^3$ ) over FWOA simulation in scenarios S07 and S08 for the Barataria region of the coast

Barrier Island or Headland	S07	S08
West Belle Pass	36.27	37.95
Caminada Headland	168.84	189.35
Grand Isle	n/a	n/a
Grand Terre	0	0
East Grand Terre	3.57	3.69
Grand Pierre	3.63	3.65
Chaland Headland	48.99	50.45
Shell Island	23.33	24.05
Pelican Island	13.8	22.05
Scotfield Island	13.95	21.43

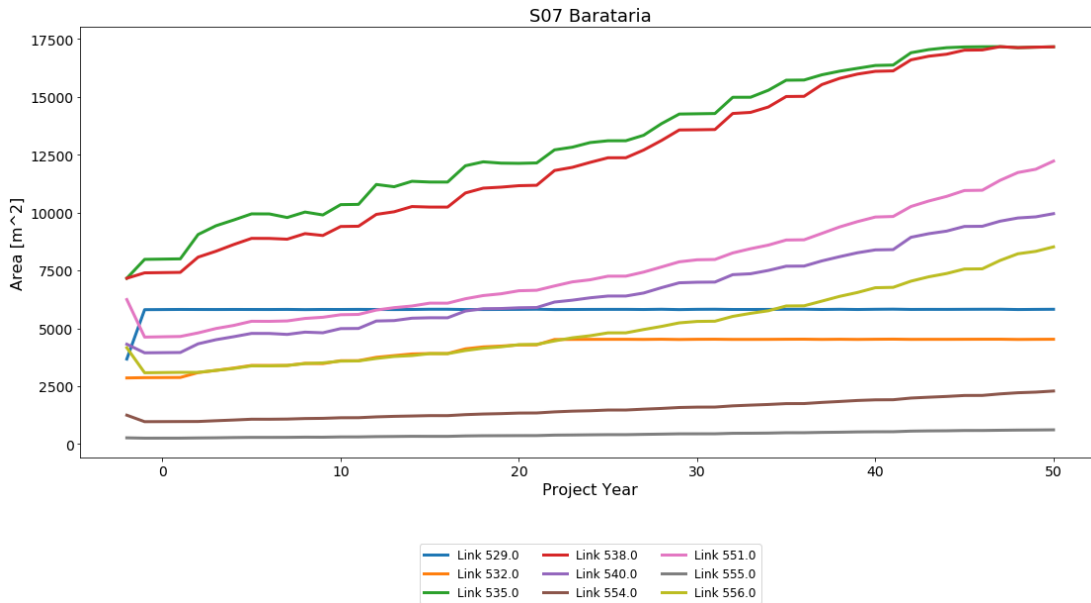


Figure 71. Tidal inlet cross-sectional area changes over time in Barataria, under S07.

Under S08, all tidal inlets within Barataria reach either the max depth, max width, or both (Figure 72). Link 529, Caminada Pass, reaches the max depth during the spin-up and remains at that area throughout the simulation since the width is set. Similarly, Link 532, Barataria Pass, reaches the max depth towards the end of the second decade and remains at that size. Links 535 and 538 follow a

similar pattern as their respective sub-basins contain many of the same ICM-Hydro compartments; the max width is reached at the end of the third decade, and max depth is reached at the beginning of the fourth decade. Link 540 reaches both max width and depth in the last decade. Link 554, Link 551, and Link 556 only reach the max width in the last decade and do not reach the max depth. Link 555 reaches the max depth in the last decade and does not reach the max width; this link is small and has the largest depth to width ratio.

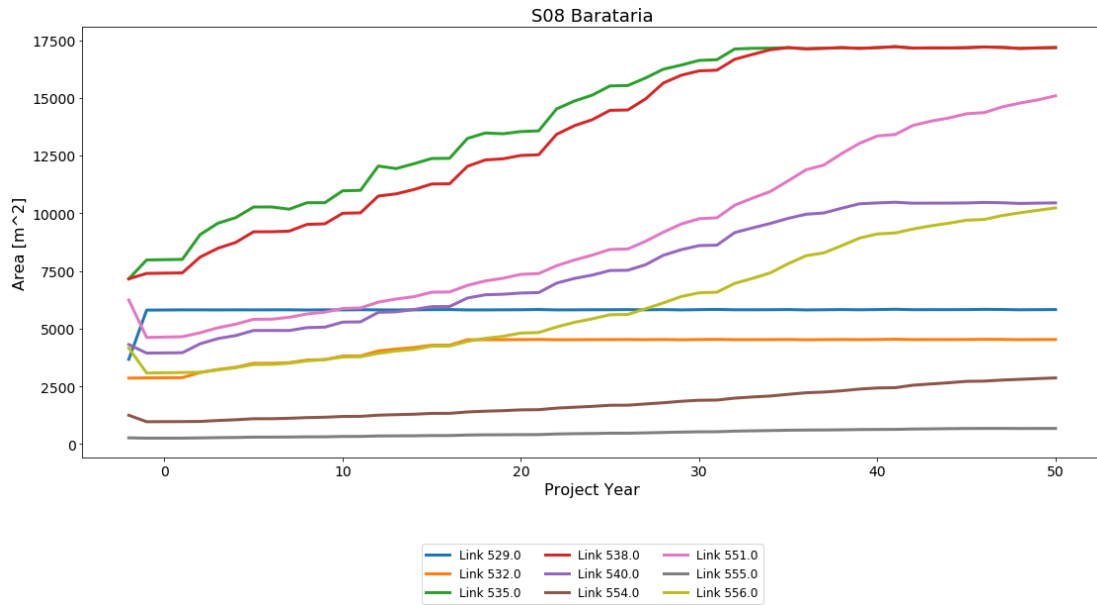


Figure 72. Tidal inlet cross-sectional area changes over time in Barataria, under S08.

### 3.10 FWOA HABITAT SUITABILITY INDICES

#### LOWER PROJECT SELECTION SCENARIO (S07)

Patterns of habitat suitability for fish and shellfish across the lower Barataria region were generally related to the influence of the Mid-Barataria Sediment Diversion in the S07 environmental scenario. In the southeastern part of the basin (i.e., the Lower Barataria-Northeast and Lower Barataria-Southeast ecoregions), habitat suitability for fish and shellfish was relatively stable over most of the simulation because the diversion maintained a relatively consistent salinity regime. There was some interannual variability in diversion discharge, but this did not greatly affect salinities or habitat suitability in the southeastern basin. For example, oyster suitability scores in northeast Barataria Bay ranged from 0.5 to 0.75 over the first 20 years of the simulation, except Year 1 when salinities during the spring-summer dropped below 2 ppt for a short period of time and thus the area received a score of 0.0 (Figure 73). Otherwise, the most notable change in fish and shellfish habitat suitability in the southeastern basin was the large decrease near the diversion outfall, where the area was converted into a relatively solid marsh landscape with little open water habitat available.

The diversion had less of an influence in the southwestern part of the basin (i.e., LBA<sub>nw</sub> and LBA<sub>sw</sub>) and this is where most of the change in habitat suitability occurred for fish and shellfish. Increased salinities as a result of sea level rise were more apparent in this part of the basin. Consequently, the marsh and open water habitats in the areas north and west of Little Lake became more suitable over time for higher-salinity species, such as brown shrimp (Figure 74), and less suitable for low-salinity species, such as largemouth bass. Wetland loss was also greater in the southwest part of the basin. In the areas north and west of Little Lake, relatively solid marshes were converted into a fragmented marsh landscape, which represented optimal marsh habitat conditions for fish and shellfish and thus contributed to the increased habitat suitability in the area. In areas closer to the Gulf of Mexico, continued wetland loss resulted in a landscape that was predominantly open water, which decreased the suitability of the area for the wetland dependent fish and shellfish species (Figure 74).

Compared to fish and shellfish, the wildlife species showed much greater change in habitat suitability over time in the Barataria region. In some cases, these changes were attributed to changes in marsh habitat type. For example, the areas north of Little Lake became more suitable over time for gadwall because of an increase in intermediate marsh coverage, which is considered optimal habitat for the species (Figure 75). Otherwise, changes in habitat suitability for wildlife species were attributed to increased water levels as a result of sea level rise. Increased water levels resulted in increased marsh inundation, which caused large decreases in habitat suitability for alligator across the region. Increased water levels also increased water depths, which changed the amount of suitable shallow water habitat for gadwall and mottled duck. The direction of this change depended on the elevation of the habitat at the start of the simulation. In lower-elevation marshes, such as in the eastern side of the region, water depths became too deep over time, greatly reducing the amount of shallow water habitat and thus habitat suitability for these species. However, in higher-elevation marshes, such as those north and west of Lake Salvador and Little Lake, the increase in water depths was relatively small and resulted in an increase in the amount of suitable shallow water habitat in these areas for gadwall and mottled duck (Figure 76).

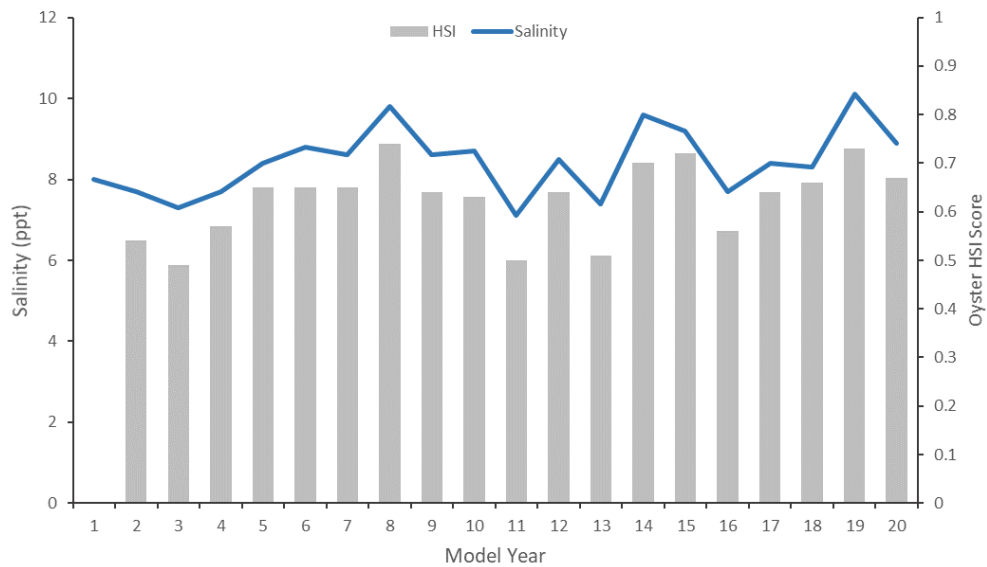


Figure 73. Oyster HSI scores compared to salinity simulated for northeast Barataria Bay over the first 20 years of the S07 environmental scenario. Scores range from 0.0, completely unsuitable habitat, to 1.0, optimal habitat. Note: this FWOA simulation used a lower river stage for controlling diversion operation than other FWOA simulations.

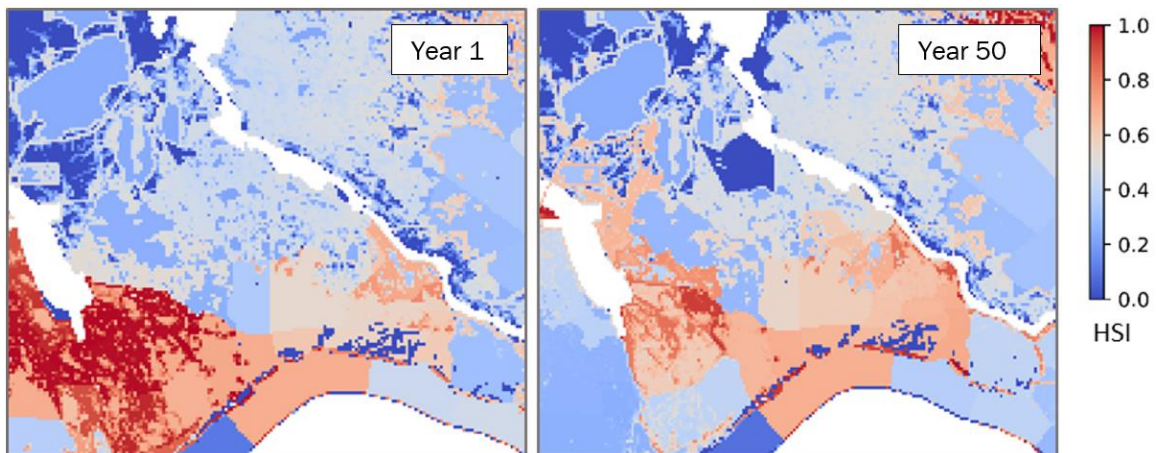


Figure 74. Small juvenile brown shrimp HSI scores across the lower Barataria region for Year 1 (left) and Year 50 (right) of the S07 environmental scenario. Scores range from 0.0, completely unsuitable habitat, to 1.0, optimal habitat.

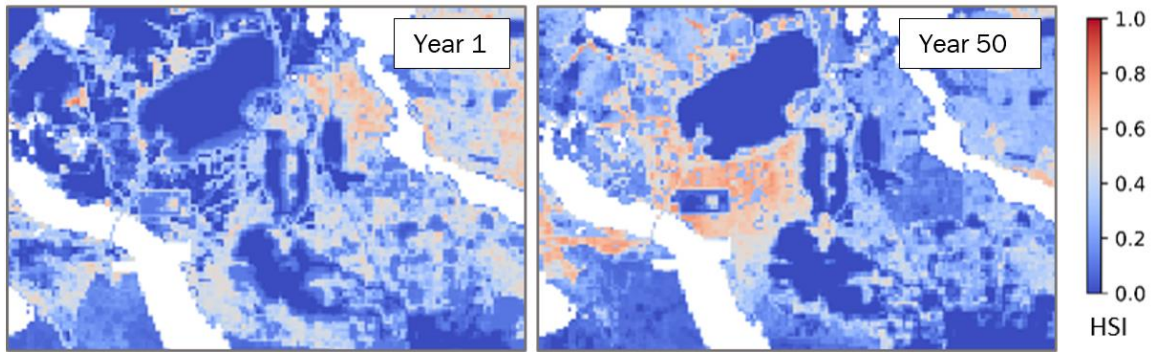


Figure 75. Gadwall HSI scores across the middle Barataria region for Year 1 (left) and Year 50 (right) of the S07 environmental scenario. Scores range from 0.0, completely unsuitable habitat, to 1.0, optimal habitat.

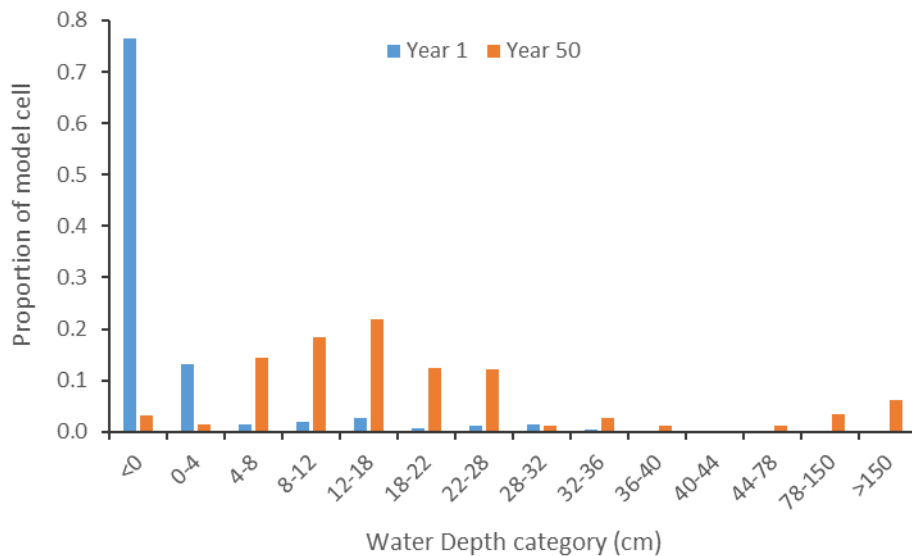


Figure 76. Water depths simulated for a model cell west of Lake Salvador for Year 1 and Year 50 of the S07 environmental scenario. Water depth categories are used for gadwall HSI calculations, with depths from 18 to 32 cm representing the most suitable water depths.

## HIGHER PROJECT SELECTION SCENARIO (S08)

The S08 environmental scenario simulation also showed distinct spatial patterns in habitat suitability. In the southeastern part of the Barataria region, habitat suitability for most fish, shellfish, and wildlife was relatively unchanged over much of the simulation (e.g., oysters and juvenile blue crab, Figure 5). This was largely due to the influence of the Mid-Barataria Sediment Diversion, which maintained a large amount of wetland habitat as well as consistent salinity conditions. However, because of the high rate of relative sea level rise in the scenario, there was a notable loss of wetlands during the last

two decades of the simulation in the Lower Barataria-southeast ecoregion and adjacent parts of the Lower Barataria-northeast ecoregion. This resulted in a decrease in habitat suitability in the area over the last decade of the simulation for wetland dependent species (Figure 77).

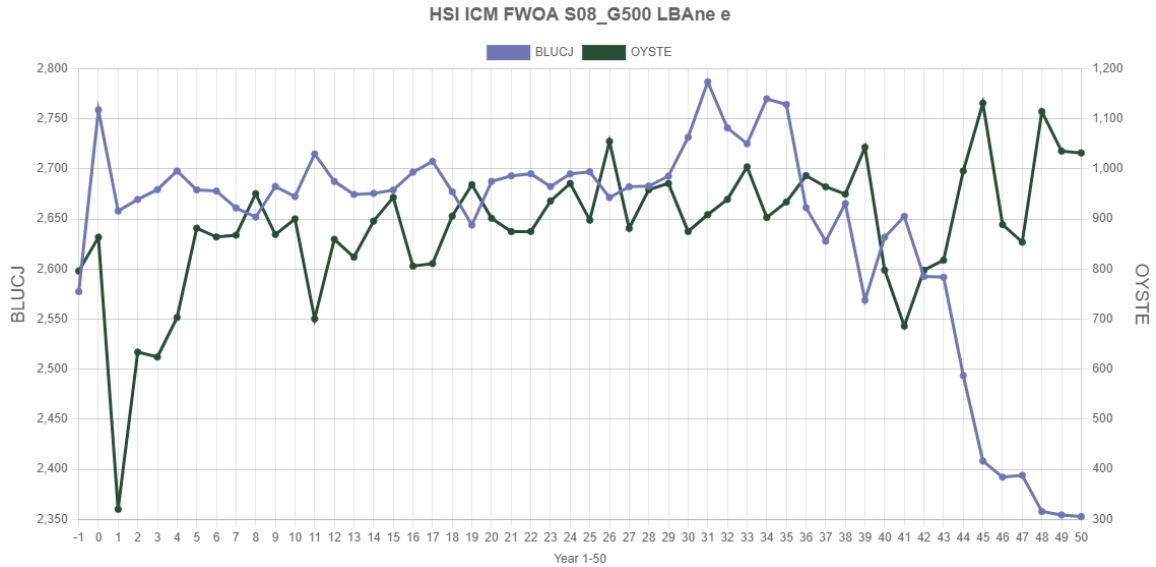


Figure 77. Total HSI score for juvenile blue crab and eastern oyster in the Lower Barataria - northeast ecoregion over the 50-year S08 environmental scenario simulation. The total HSI score was calculated by summing the individual scores for each ICM model cell within the ecoregion.

In the southwestern part of the Barataria region, there was a general decrease in habitat suitability for most fish, shellfish, and wildlife species due to extensive wetland loss (e.g., small juvenile brown shrimp, Figure 78). This decrease was relatively steady over time in the Lower Barataria-southwest ecoregion, as the highly-fragmented marshes in this ecoregion were gradually converted to mostly open water by the end of the simulation. In the Lower Barataria-northwest ecoregion, habitat suitability increased over the first three decades of the simulation because the relatively solid marshes in the area were converted into highly-suitable fragmented marshes. However, suitability then declined over the last decade as the marshes were converted into mostly open water (Figure 79). Salinities also increased considerably in the ecoregion during this time, and contributed to the greater decline in suitability seen for low-salinity species, such as juvenile blue crab, as compared to higher-salinity species, such as brown shrimp (Figure 79).

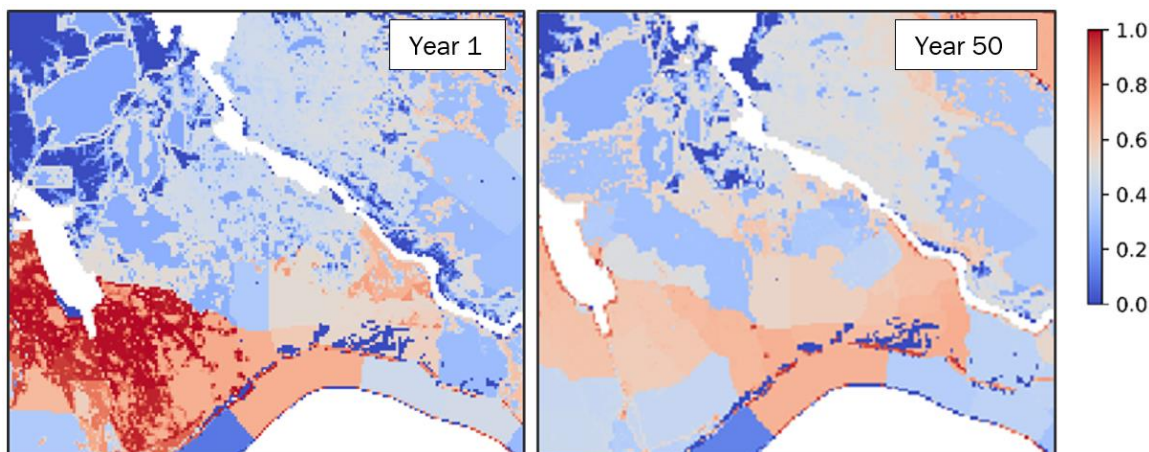


Figure 78. Small juvenile brown shrimp HSI scores across the lower Barataria region for Year 1 (left) and Year 50 (right) of the S08 environmental scenario. Scores range from 0.0, completely unsuitable habitat, to 1.0, optimal habitat.

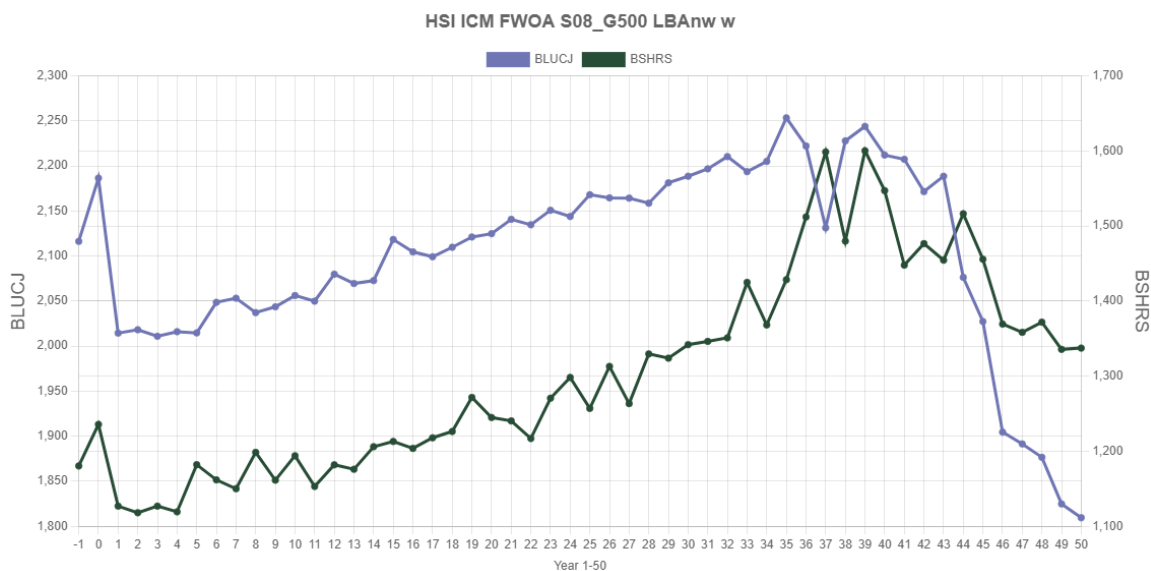


Figure 79. Total HSI score for juvenile blue crab and small juvenile brown shrimp in the Lower Barataria - northwest ecoregion over the 50-year S08 environmental scenario simulation. The total HSI score was calculated by summing the individual scores for each ICM model cell within the ecoregion.

While habitat suitability generally decreased over time throughout most of the lower Barataria region, there was an increase in suitability in the upper Barataria region. This was primarily due to small areas of wetland loss in the Mid-Barataria ecoregion, which created new aquatic habitat particularly for low-salinity species such as alligator, largemouth bass, and juvenile blue crab. In addition, as a result of the sea level rise in the scenario there was an increase in marsh water depths across much of the

Mid-Barataria and Upper Barataria ecoregions, which created more suitable habitat for gadwall and mottled duck in these areas.

### 3.11 DISCUSSION

Although, there is a significant effect of the scenarios on land change, vegetation composition stays very similar under both scenarios (Figure 80 and Figure 81).

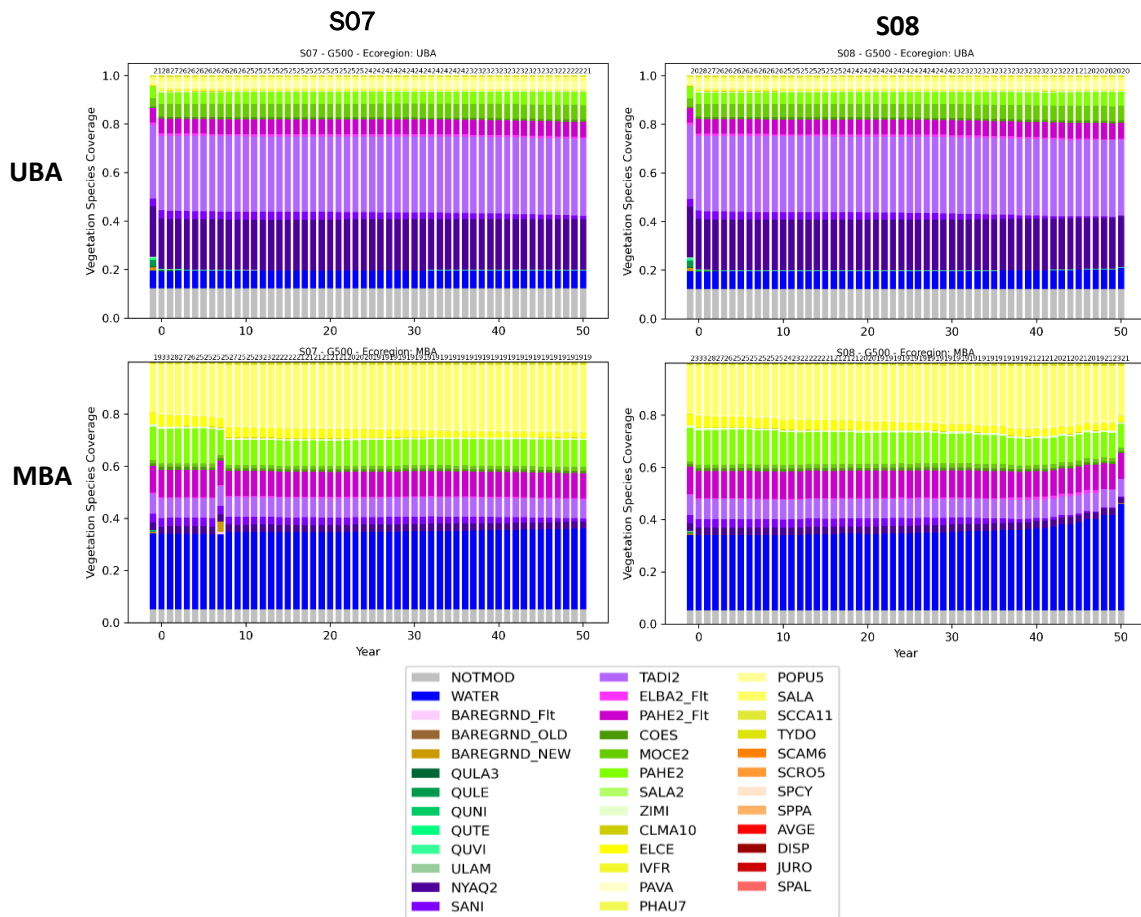


Figure 80. Comparison of vegetation cover change in the upper ecoregions of Barataria Basin between the two scenarios.

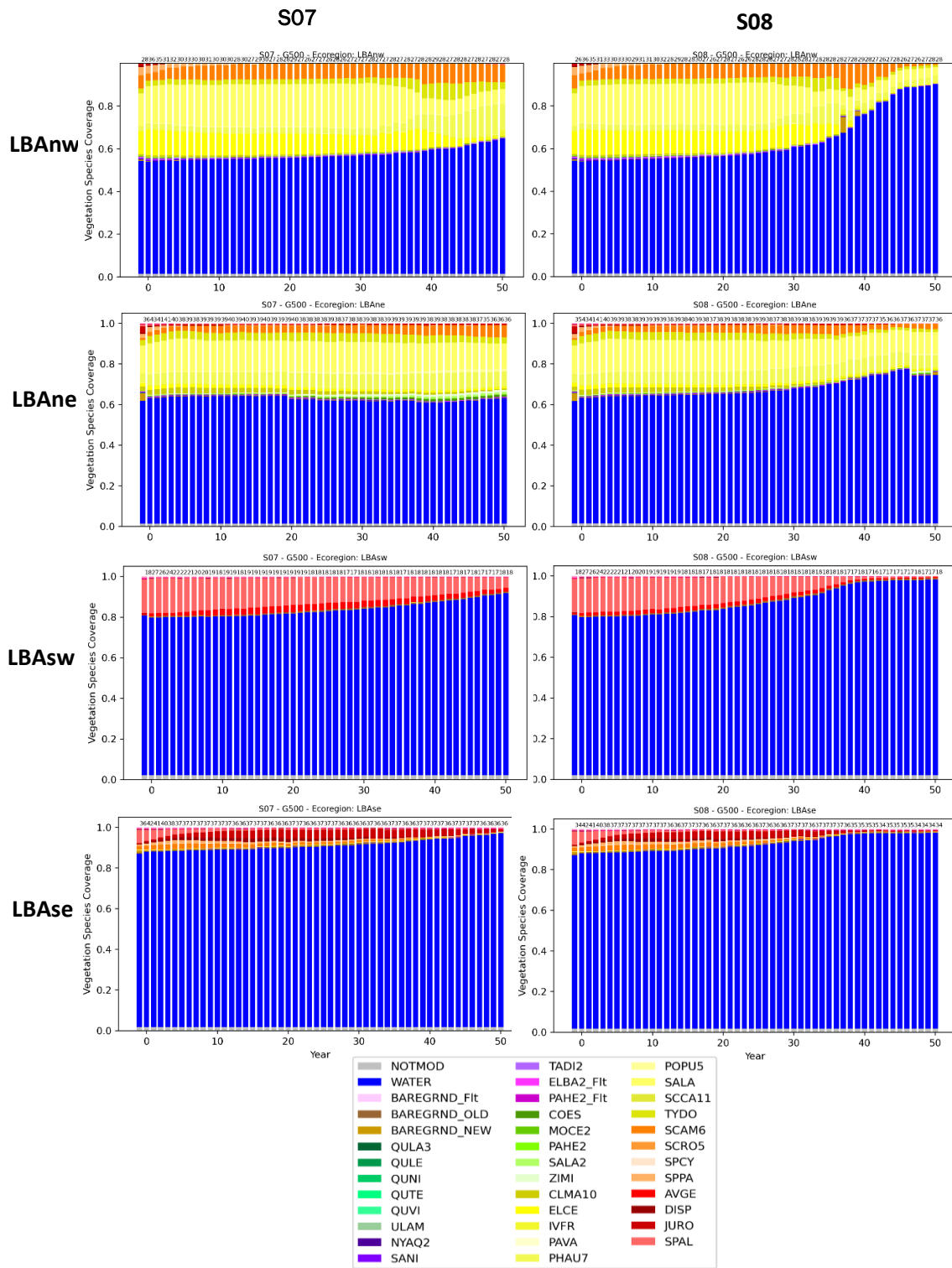


Figure 81. Comparison of vegetation cover change in the lower ecoregions of Barataria Basin between the two scenarios.

There is much more extensive loss in Barataria for S08 than for S07 especially in the mid-western part of the basin north of Little Lake and west of Lake Salvador and on the east near Port Sulphur. However, the response close to the Mid-Barataria Sediment Diversion is somewhat similar. CRMS0225 illustrates this (Figure 82). The location is land throughout in both scenarios and elevation increases sufficient to keep pace with increasing water levels due to high organic accretion as the area is designated active delta.

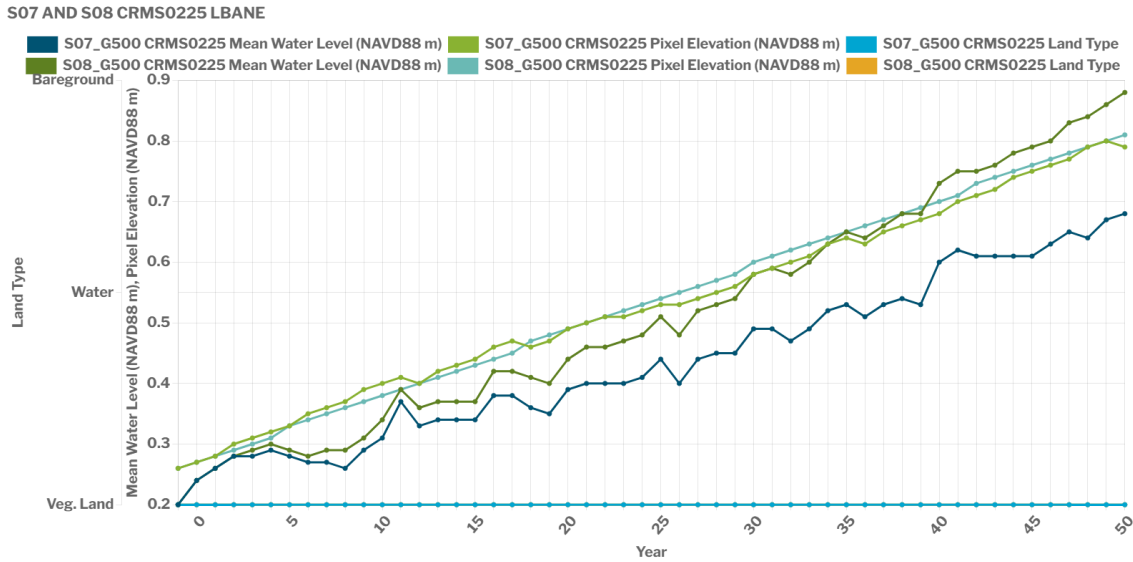


Figure 82. Comparison of S07 and S08 conditions at CRMS0225 in LBANE.

While many areas show loss by Year 50 in both scenarios, the mechanisms may be different. At QAQC1435 between the East and West Bayou L’Ours ridges the starting elevation is high and as the marsh is not inundated in the first years of the simulation there is no organic or mineral accretion and elevation decreases for both scenarios (Figure 83). As water levels rise the marsh is inundated and organic accretion is sufficient to balance total subsidence. However rising water levels result in land loss in Year 41 in the higher scenario. In the lower scenario, lower sea level rise and subsidence rates allow the marsh to be below the inundation threshold. At Year 46 the location switches from land to water in the lower scenario due to marsh edge erosion which also results in a loss of elevation of 25 cm. Such loss would also have occurred in S08 had the area still been vegetated at that time.

S07 AND S08 QAQC1435 LBASW

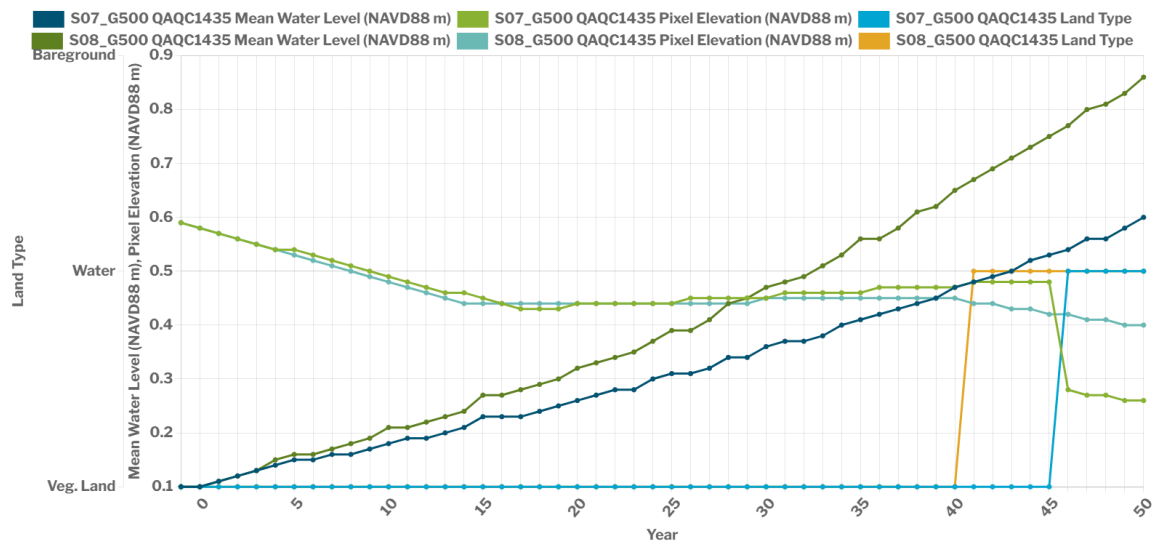


Figure 83. Comparison of S07 and S08 conditions at QAQC1435 in LBASw.

For the barrier islands within the Barataria Basin, the cross-shore retreat rate of the Gulf shoreline and shoreface, combined with direct effects of the increased rate of sea level rise, leads to more rapid erosion and natural island loss in the S08 scenario, as compared to S07. As a result, the barrier islands transgress farther in this scenario and the sediment volumes required during individual auto-restoration events is higher than for the S07 scenario (Figure 68, Figure 69, Figure 70, and Table 4). For Pelican Island and Scofield Island, the increased rate of sea level rise leads to a higher number of auto-restoration events occurring in the 50-year period of the model, leading to substantial increases (> 50%) in the total sediment volume placed. For the other barrier islands and headlands, the higher rate of relative sea level rise leads to greater sediment volume placement during individual auto-restoration events with more modest overall increases (1-2%) in the total sediment volume placed at those locations over the modeled period.

Caminada Headland, where auto-restoration for the southeastern portion of the barrier island was parameterized to “hold the line”, maintains its position. Similarly, Grand Island follows the expected modeled behavior and does not transgress. Some minor unrealistic behaviors – expected based on initial testing – occurred with the model runs, including jaggedness of the shoreline introduced for some islands during auto-restoration. Neither of these issues are expected to significantly impact the results of either the ICM or ADCIRC model runs. However, the jaggedness worsened during interpolation of the ICM-BI point cloud to the 30-m ICM-Morph grid. Because the ADCIRC grid is sensitive to the increased jaggedness, the higher resolution DEM output of the ICM-BI grid is provided directly to ADCIRC to resolve the issue, and all results shown in this report are taken directly from the ICM-BI output.

Differences in tidal inlet areas for the two scenarios are seen throughout the simulation, but by the end of the 50-year period, five of nine inlets in Barataria have reached their maximum size regardless of scenario. Link 551, Link 540, Link 556, and Link 554 are still expanding either in width, depth, or both at the end, and therefore, have different areas depending on the scenario. The largest difference is in Link 551, whose sub-basin is the area adjacent to the lower Mississippi River. This area has differences in land loss and tidal range between the scenarios, and the area in S08 is 16% larger than S07 in ICM-Year 52.

There is a distinct change between the two scenarios, with a greater increase in tidal range in S08 compared to S07. Since Barataria Basin is less open compared to Terrebonne Basin, the tidal attenuation is maintained throughout the entire simulation. In Year 50 there is about a 0.08 m difference between the upper and lower compartments, regardless of scenario (Figure 84).

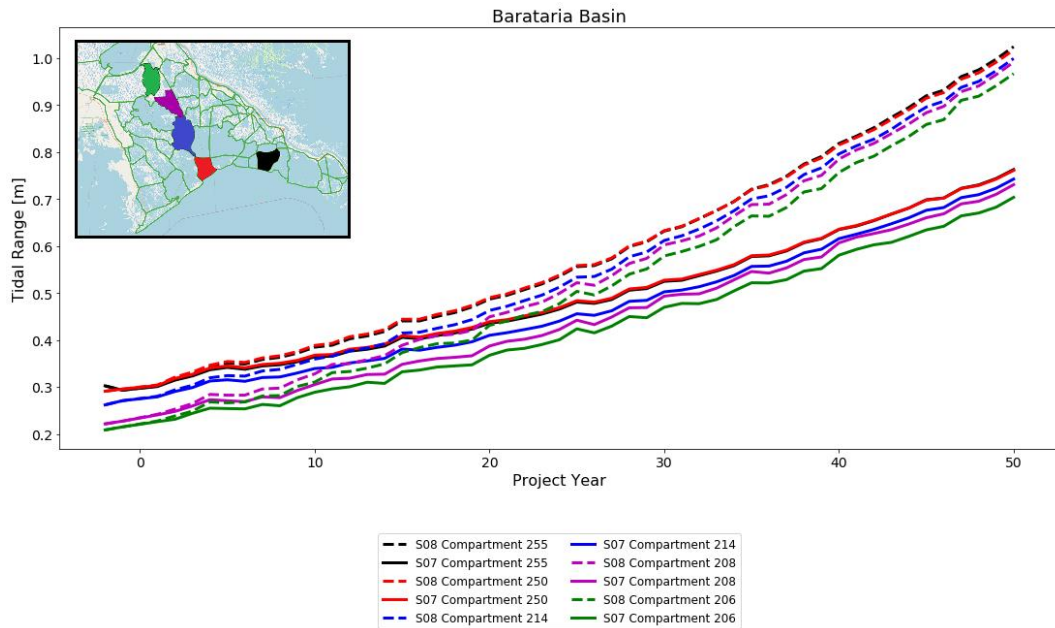


Figure 84. Tidal range for ICM-Hydro compartments contributing tidal prism to Barataria Basin tidal inlets.

The asymmetrical partitioning works as expected in ICM-BITI, and inlet dimensions respond to the changes that occur within their assigned sub-basins. For example, in the Barataria Basin, the sub-basins for Links 535 and 538, which boarder East Grand Terre, make up a large portion of the basin interior. Most of the land loss occurs in this area, and the inlet areas increase as the tidal prism increases (blue and purple lines in Figure 84). In contrast, the sub-basins for Links 554 and 555, which boarder Pelican Island, are small and the backbarrier basin already has ample open water in the initial conditions. The tidal prism in these sub-basins only modestly increases over the 50-year simulation, which is reflected in the small change in inlet area (gray and yellow lines in Figure 85).

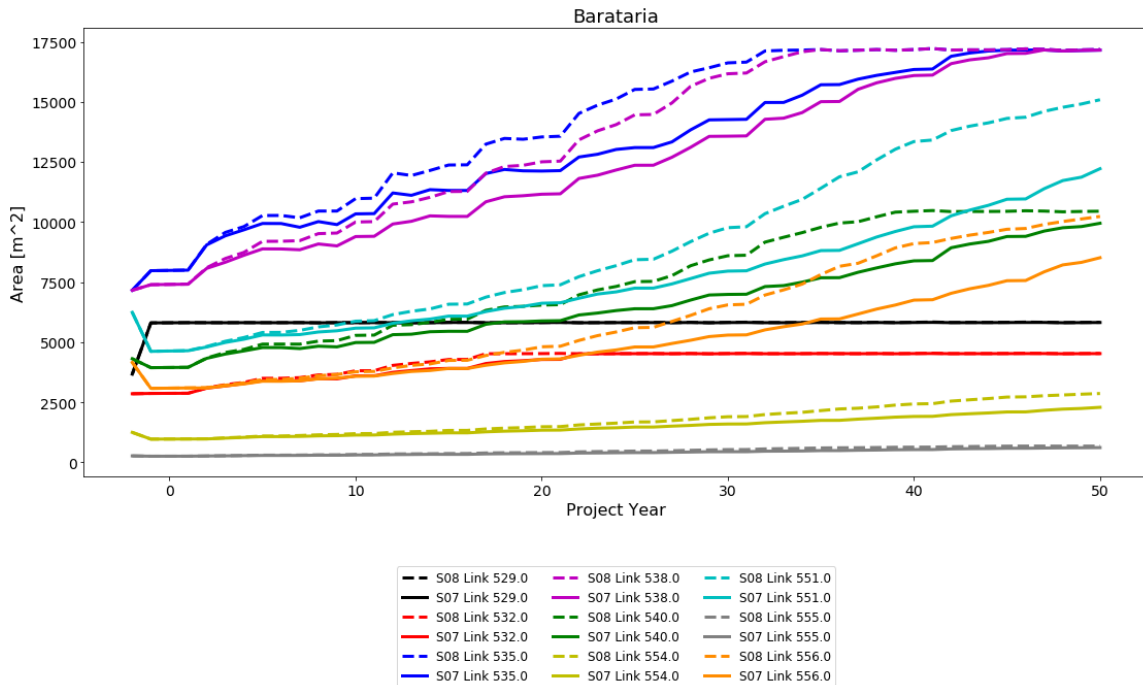


Figure 85. Tidal inlet cross-sectional area changes over time in Barataria, under S07 and S08.

The higher rate of relative sea level rise used in the S08 environmental scenario caused a greater change in habitat suitability in the Barataria region compared to the S07 environmental scenario. Wetland loss and increased salinities were much more extensive in the S08 scenario and extended farther north into the region, especially on the western side. These factors had a large effect on habitat suitability for species, and particularly higher-salinity species. In the S07 scenario, much of the marsh habitat was lost in the areas nearest the Gulf; however, there was some habitat expansion into the middle part of the region due to marsh fragmentation and increased salinities. By comparison, in the S08 scenario most of the marsh habitat south of Lake Salvador was lost, and the habitats that remained at the end of the simulation were primarily open waters, and swamp, fresh marsh, and intermediate marsh in the upper Barataria region and near the Mid-Barataria Sediment Diversion. These habitats were generally suitable for low-salinity species, but were relatively low quality habitat (HSI scores <0.6) for higher-salinity species. As a result, while there was a northward contraction of habitat for fish, shellfish, and wildlife in both scenarios, the contraction was more extreme in the S08 scenario and there was a relative lack of highly-suitable habitat for higher-salinity species.

# 4.0 TERREBONNE

## 4.1 INTRODUCTION

The Terrebonne region spans from Morgan City to Highway 1 and is filled with an interconnected web of bayous after which many of its small towns are named. It extends from Bayou Lafourche in the east to the Atchafalaya Basin floodway, Fourleague Bay, and Oyster Bayou on the west. The region has a series of barrier islands across the Terrebonne and Timbalier bays, including Timbalier Island and the Isles Dernieres Barrier Islands Refuge.

The ecosystem includes extensive bottomland hardwood and swamp forests in the Verret Basin and floating marshes in the Penchant Basin. While there is a fresh-to-saline gradient across the region, salt and brackish marshes are more prevalent in eastern Terrebonne. The Verret and Penchant basins receive freshwater from the Atchafalaya River. Areas east of the Bayou Terrebonne Ridge receive freshwater primarily from rainfall and from Atchafalaya River inflow to the GIWW via the Houma Navigation Canal (HNC) and Grand Bayou Canal. Flows to the east from the Atchafalaya River through the GIWW are an important source of freshwater to the marshes of the eastern and central Terrebonne region. Freshwater flows south through openings, such as Bayou Copesaw, Minors Canal, the HNC, Bayou Terrebonne and, further to the east, Grand Bayou Canal. This water flow helps to maintain the estuarine gradient from fresh to salt across the southern part of the region.

Land loss was extensive during the 20th century in part due to ongoing deltaic subsidence, saltwater intrusion along the HNC and other canals, historic oil and gas activity, and natural deterioration of barrier islands.

## 4.2 FWOA STAGE

### LOWER PROJECT SELECTION SCENARIO (S07)

As in the Central Coast region, stages in areas of the Terrebonne region that are directly east of the Atchafalaya River are heavily influenced by seasonal discharge cycles (Figure 86). Stages in the Upper Penchant Basin and along the GIWW east to the HNC display a seasonal trend that follows the annual flood cycle. Conversely, marshes and open water areas in the southern and eastern Terrebonne Basin generally follow seasonal trends in the tidal boundary. Stages throughout the region increases over the long-term with sea level rise, and there is a slight spatial gradient with higher mean stages in more inland marsh compartments.

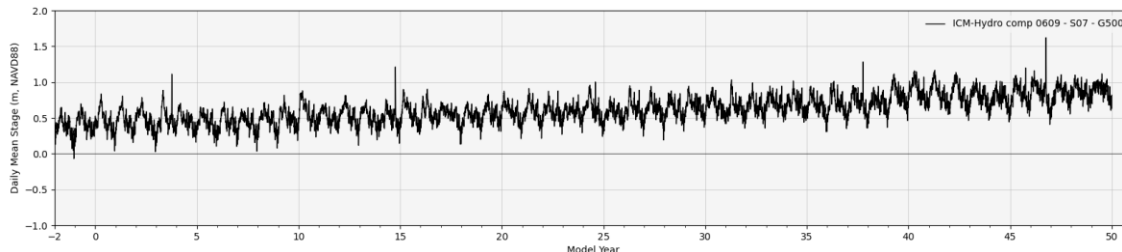


Figure 86. Stage in compartment 609, under S07, representative of the Terrebonne region directly influenced by the Atchafalaya River where seasonal discharge trends are evident.

## HIGHER PROJECT SELECTION SCENARIO (S08)

Stages for S08 in the Terrebonne region are as expected given the S07 results. Stages in the Upper Penchant Basin and along the GIWW east to the HNC display a seasonal trend that follows the annual flood cycle, while marshes and open water areas in the southern and eastern Terrebonne Basin generally follow seasonal trends in the tidal boundary. Stages throughout the region increases at a greater rate than in S07, reflecting this scenario’s higher sea level rise rate.

### 4.3 FWOA TIDAL RANGE

## LOWER PROJECT SELECTION SCENARIO (S07)

Seasonal variations in stages near the Lower Atchafalaya River produce a seasonal trend in daily water level variability, with higher daily ranges during lower flow periods and lower ranges during higher flow periods when the distribution of river discharge throughout the basin opposes inland tidal propagation. Tidal ranges across the Central Terrebonne Basin are generally lower than in more Gulfward areas. For this scenario, long-term increases in tidal range with sea level rise are only evident in more Gulfward open water and marsh compartments, especially east of the HNC and in Terrebonne Bay (Figure 87).

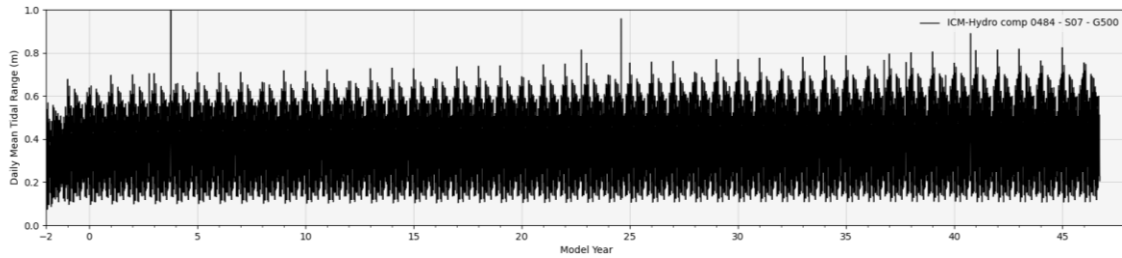


Figure 87. Tidal range in compartment 484, under S07, showing the long-term increase in tidal range in Terrebonne Bay with sea level rise.

## HIGHER PROJECT SELECTION SCENARIO (S08)

Tidal ranges are similar to those modeled with S07. Tidal range in the region is primarily controlled by the seasonal variability in the Gulf boundary conditions in the lower region and Atchafalaya River flow variability in the upper region. As compared against S07, there are greater long-term increases to tidal range under S08 in locations closer to the Gulf. However, in more interior portions of the basin little long-term change to tidal range is seen. There are slight decreases in tidal range within the Morganza to the Gulf alignment near Houma through time (Figure 88), presumably due to more frequent system closures than in S07.

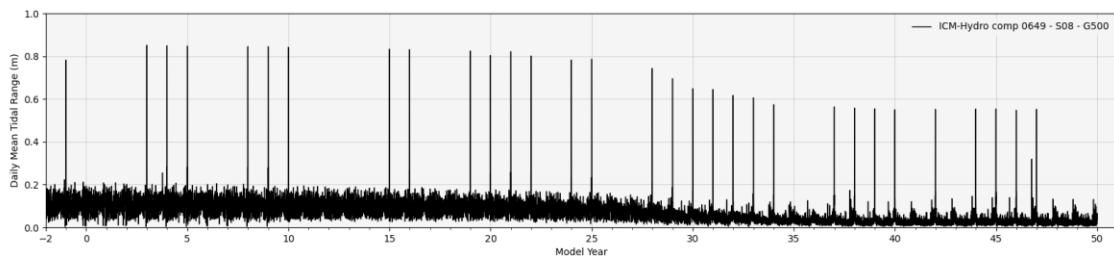


Figure 88. Tidal range in compartment 649, under S08, showing the slight long-term decreases in tidal ranges.

## 4.4 FWOA SALINITY

### LOWER PROJECT SELECTION SCENARIO (S07)

As in the Central Coast region, salinities in the Terrebonne region are influenced by the Atchafalaya River, though with areas east of the HNC impacted to a lesser degree. In the Penchant Basin and Upper and Central Terrebonne, salinities follow a seasonal cycle that peaks during late summer and fall when discharges are lowest, with salinities decreasing to near 0 ppt during spring floods (Figure 89). In the marshes of Lower Terrebonne, salinities are higher, though still subject to significant seasonal variation with seasonal river discharge variability. Sea level rise associated with this scenario

does not appear to result in any long-term trends in salinities in this region.

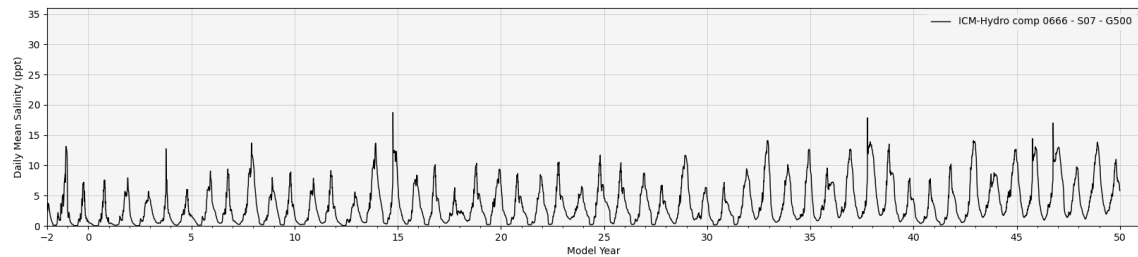


Figure 89. Salinity in compartment 666, under S07, showing the seasonal patterns resulting from Atchafalaya River discharge.

Salinities in Terrebonne and Timbalier Bays as well as in the upper basin west of Bayou Lafourche show greater interannual variability, though also with no clear trend that could be associated with sea level rise.

## HIGHER PROJECT SELECTION SCENARIO (S08)

Salinities in S08 are very similar to those simulated in S07. Salinities are influenced by the Atchafalaya River flows, which is more pronounced in the west and upper basin adjacent to Atchafalaya River and GIWW. Salinities in the lower basin are much higher in the Gulfward direction. The overall salinity is slightly lower for S08 when compared to S07.

## 4.5 FWOA TOTAL SUSPENDED SOLIDS (TSS)

### LOWER PROJECT SELECTION SCENARIO (S07)

TSS in the Terrebonne region is also subject to the influences of Atchafalaya River discharges. In the Penchant Basin and Terrebonne west of the HNC, TSS increases seasonally with spring floods, though with peak values typically lower than in the Central Coast regions that are closest to the Atchafalaya and Wax Lake Outlet. A small portion of the Central Terrebonne Basin shows a long-term reduction in peak seasonal TSS values (Figure 90), which may be related to depletion of sediment supplies in major flowpaths from the Atchafalaya.

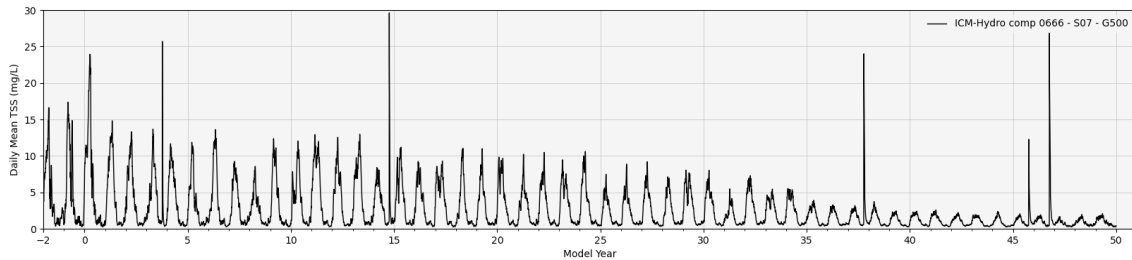


Figure 90. TSS in compartment 666, under S07, showing the slight long-term reductions in peak seasonal TSS values.

## HIGHER PROJECT SELECTION SCENARIO (S08)

TSS spatial variability in S08 is similar to S07, subject to the influences of Atchafalaya River discharges. Unlike in S07, TSS does vary more over the long-term in more inland marsh compartments, with significant reductions in peak TSS values in the last decade of simulation (Figure 91). These could potentially be related to greater marsh submergence decreasing erosion and TSS.

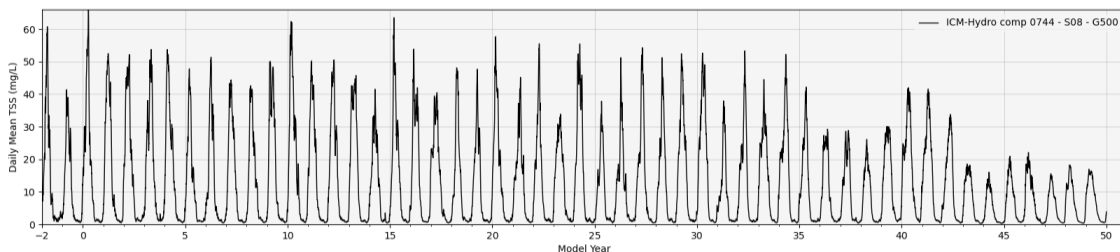


Figure 91. TSS in compartment 744, under S08, showing the reductions in peak values in the last decade of simulation.

## 4.6 FWOA WATER TEMPERATURE

### LOWER PROJECT SELECTION SCENARIO (S07)

Water temperatures in the Terrebonne region are as expected, showing the typical seasonal cycle with no evident spatial variability across the region. Temperatures are consistent over time, with slight increases associated with scenario-dependent warming. Long-term increases in yearly minimum temperatures are greater than long-term increases in yearly maximums.

### HIGHER PROJECT SELECTION SCENARIO (S08)

Temperatures in the S08 scenario are as expected, showing the same seasonal patterns in S07 with no spatial variability. A long-term increasing trend is more evident with this scenario's higher

temperature increases. As with S07, long-term increases in yearly minimum temperatures are greater than long-term increases in yearly maximums.

## 4.7 FWOA VEGETATION

### LOWER PROJECT SELECTION SCENARIO (S07)

The Verret Basin experiences no substantial changes under S07 and stays as a swamp (Figure 92 and Figure 93). Although the area remains dominated by TADI2 and NYAQ2 there is some loss of trees (primarily SANI) and replacement by marsh species as illustrated by CRMS5536 (Figure 94). At CRMS5536, SANI decreases as PAHE2 increases. In the PEN region, there is loss of PAHE2\_FLT as well as brackish marsh species. The loss of PAHE2\_FLT as well as the relative stability of ELBA2\_FLT is demonstrated with QAQC0795 (Figure 94). This decrease in PAHE2\_FLT is primarily due to its lower salinity tolerance relative to ELBA2\_FLT. The conversion of intermediate to brackish marsh followed by land loss is illustrated with QAQC0738. At QAQC0738 the marsh is dominated by TYDO in the first 15 years. In the next 10 years, TYDO and SALA were replaced by SCAM6 and PHAU7. This change in vegetation cover changes the FFIBS score from 2.73 (intermediate marsh) in Year 13 to 5.2 (brackish marsh) in Year 25. In WTB and ETB, loss occurs primarily in brackish and saline marshes. Marsh loss is less severe along the bay rims of WTB than in the interior and all of ETB. The relative stability of the WTB bay rim is illustrated with CRMS0332, which shows minor land loss during the first 30 years and moderate land loss in the last 20 years. In contrast, CRMS0336 demonstrates the rapid loss of saline marsh in ETB.

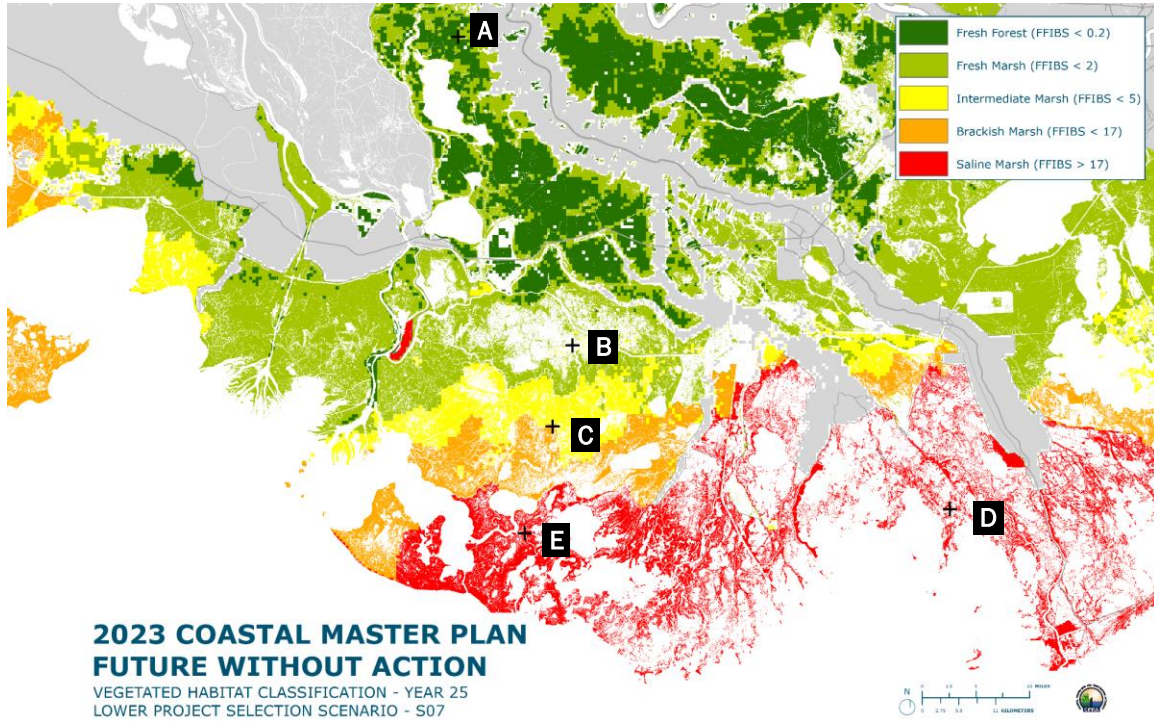


Figure 92. Wetland type (FFIBS score) distribution of the Terrebonne region under scenario S07 in Year 25.

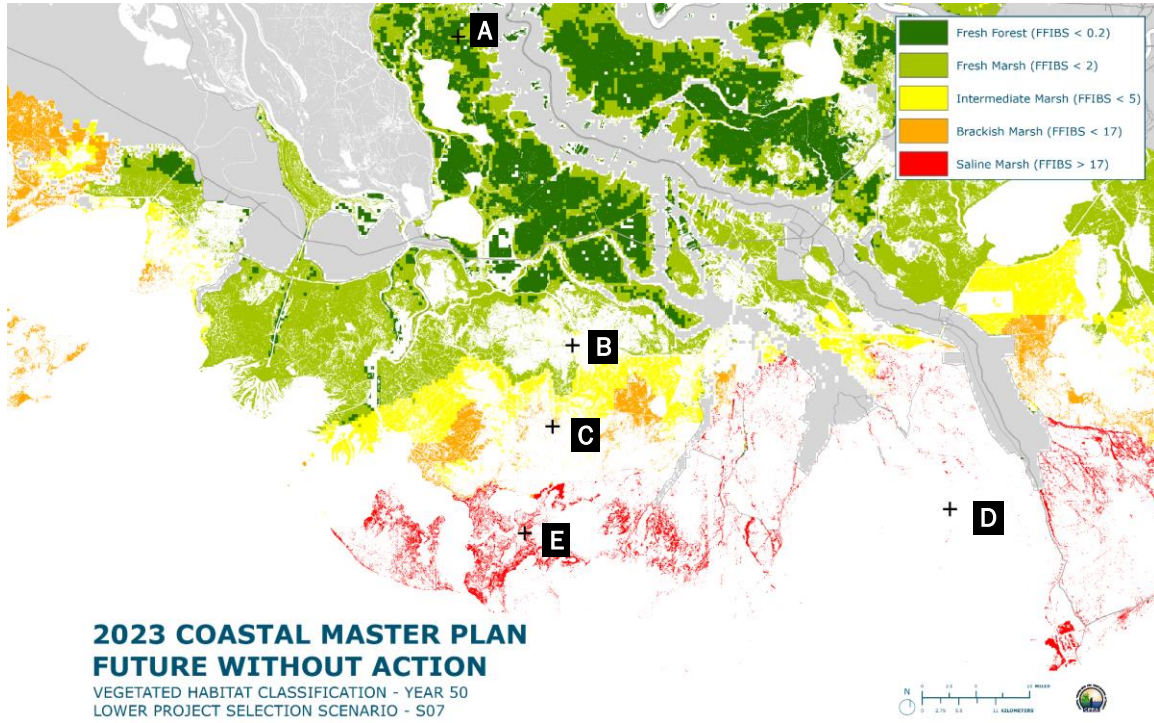


Figure 93. Wetland type (FFIBS score) distribution of the Terrebonne region under scenario S07 in Year 50.

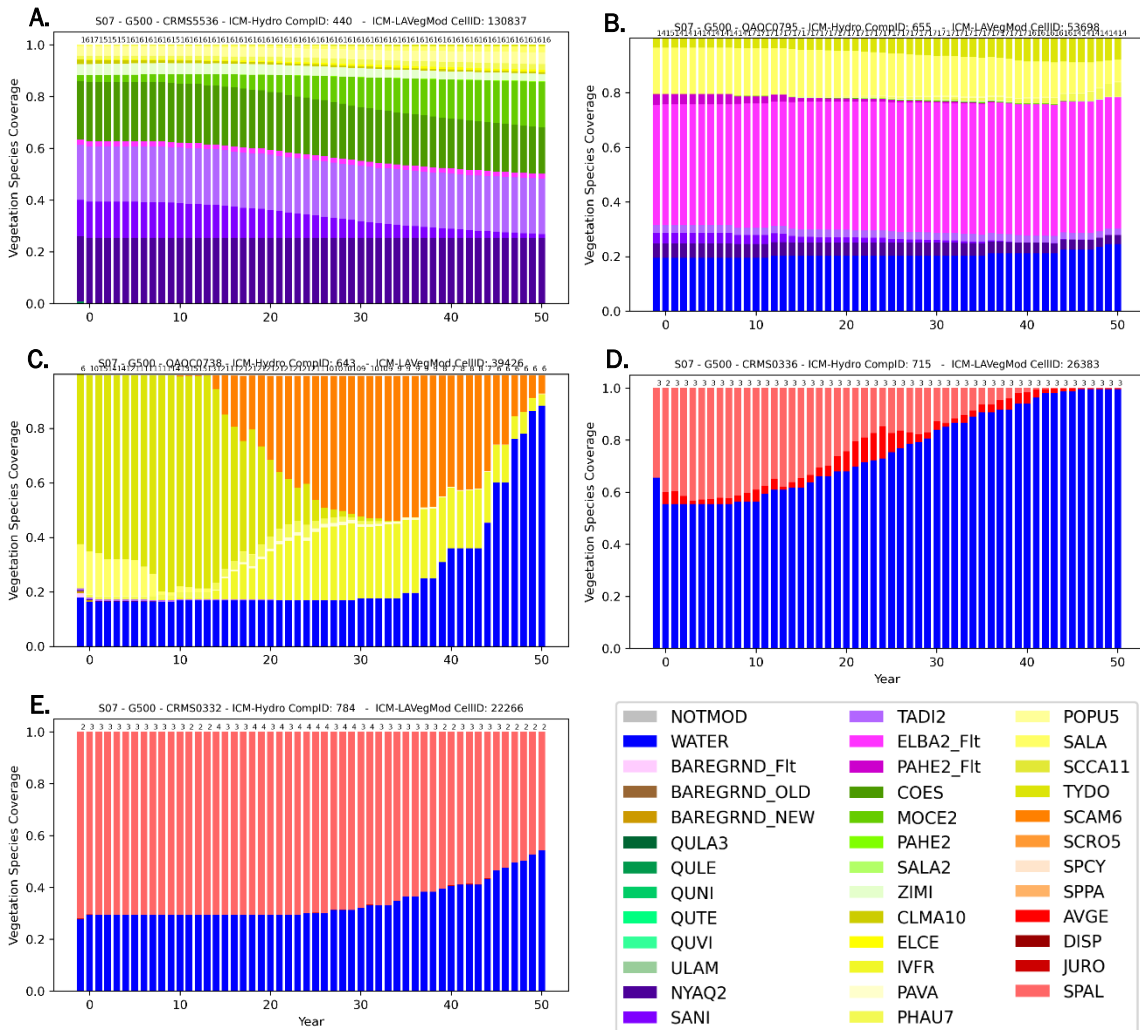


Figure 94. Change in vegetation cover under S07 is shown at representative points in the Terrebonne region. Point locations are shown in previous Terrebonne region map figures.

## HIGHER PROJECT SELECTION SCENARIO (S08)

The Verret Basin experiences no substantial changes under S08 and stays as a swamp (Figure 95 and Figure 96). Although the area stays dominated by TADI2 and NYAQ2 there is some loss of trees (primarily SANI) and increases in marsh species as illustrated by CRMS5536 (Figure 97). At CRMS5536, SANI decreases as PAHE2 increases. In the PEN, there is widespread loss except for areas near the Atchafalaya River and the areas occupied by ELBA2\_FIT. The interior loss and survival of ELBA2\_FIT is illustrated with QAQC0795 (Figure 97). QAQC0795 shows very little change in vegetation cover over the first thirty years, then cover of all species (except ELBA2\_FIT) declines

rapidly over the next 10 years due to increasing inundation. In the real world, this loss of attached marsh would expose the flotsam to wave action and it is unlikely that it would survive. However, this erosion effect is not captured by the model and therefore ELBA2\_FLT survives as the area remains relatively fresh (average annual salinity stays below 2 ppt). At QAQC0738 the marsh is dominated by TYDO in the first 15 years. Over the next five years, TYDO and SALA were replaced by SCAM6 and PHAU7. This change in vegetation cover changes the FFIBS score from 2.7 (intermediate marsh) in Year 13 to 5.3 (brackish marsh) in Year 22. After Year 26, marsh loss accelerates and only a few pixels of marsh remain after Year 33. In WTB and ETB loss occurs steadily in brackish and saline marshes (Figure 95 and Figure 96) with most brackish and saline marshes gone by Year 40. Only slivers of marsh along the ridges remain. Marsh loss occurs earlier in ETB than in WTB. CRMS0332 in WTB shows moderate land-loss from Year 15 to Year 34 and rapid land loss from Year 35 to 42 after which very little marsh remains. In contrast, CRMS0336 in ETB demonstrates rapid loss of saline marsh between Year 8 and 30.

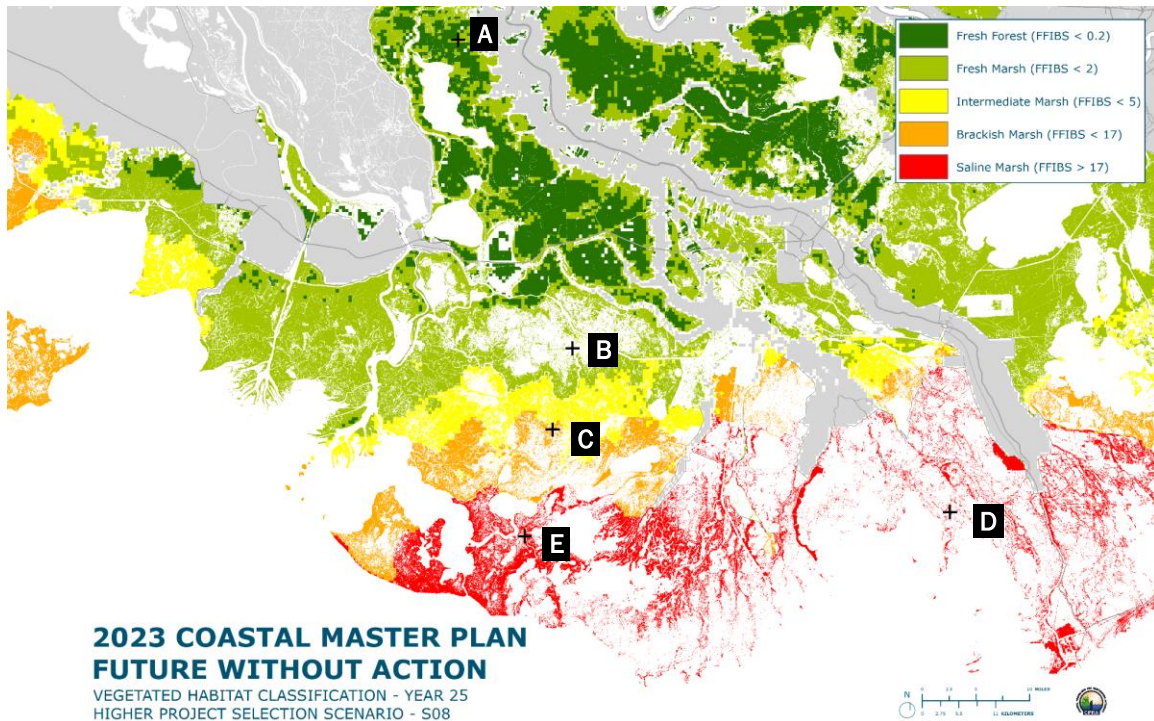


Figure 95. Wetland type (FFIBS score) distribution of the Terrebonne region under scenario S08 in Year 25.

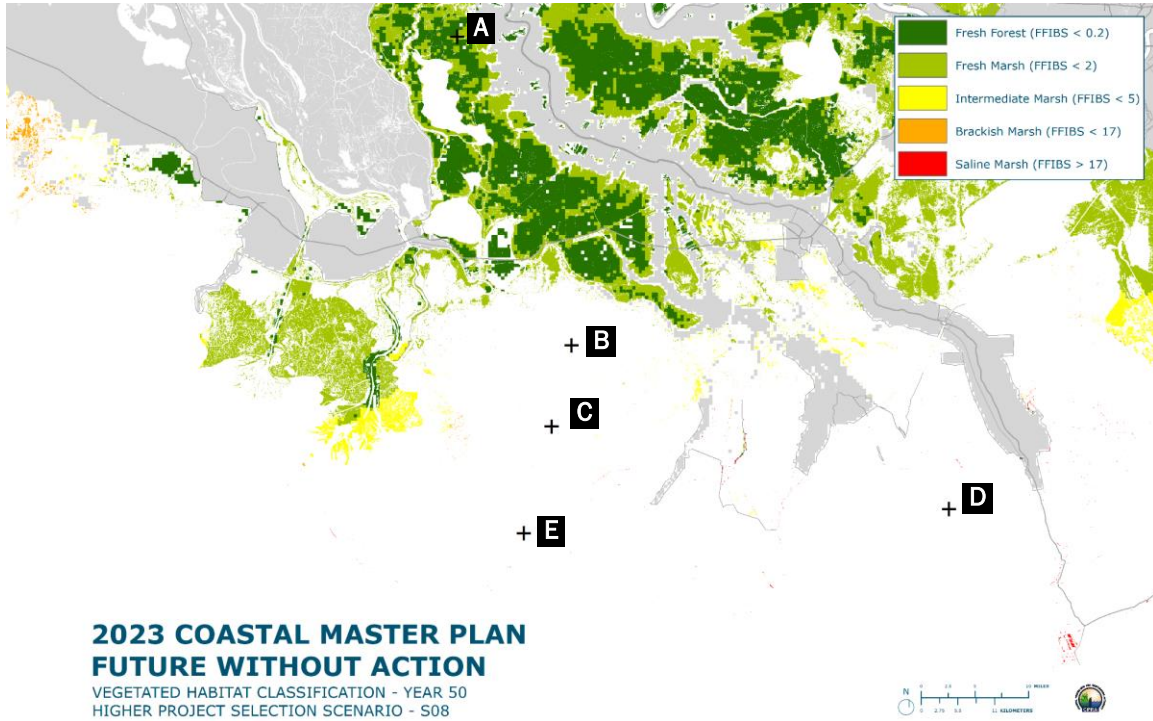


Figure 96. Wetland type (FFIBS score) distribution of the Terrebonne region under scenario S08 in Year 50.

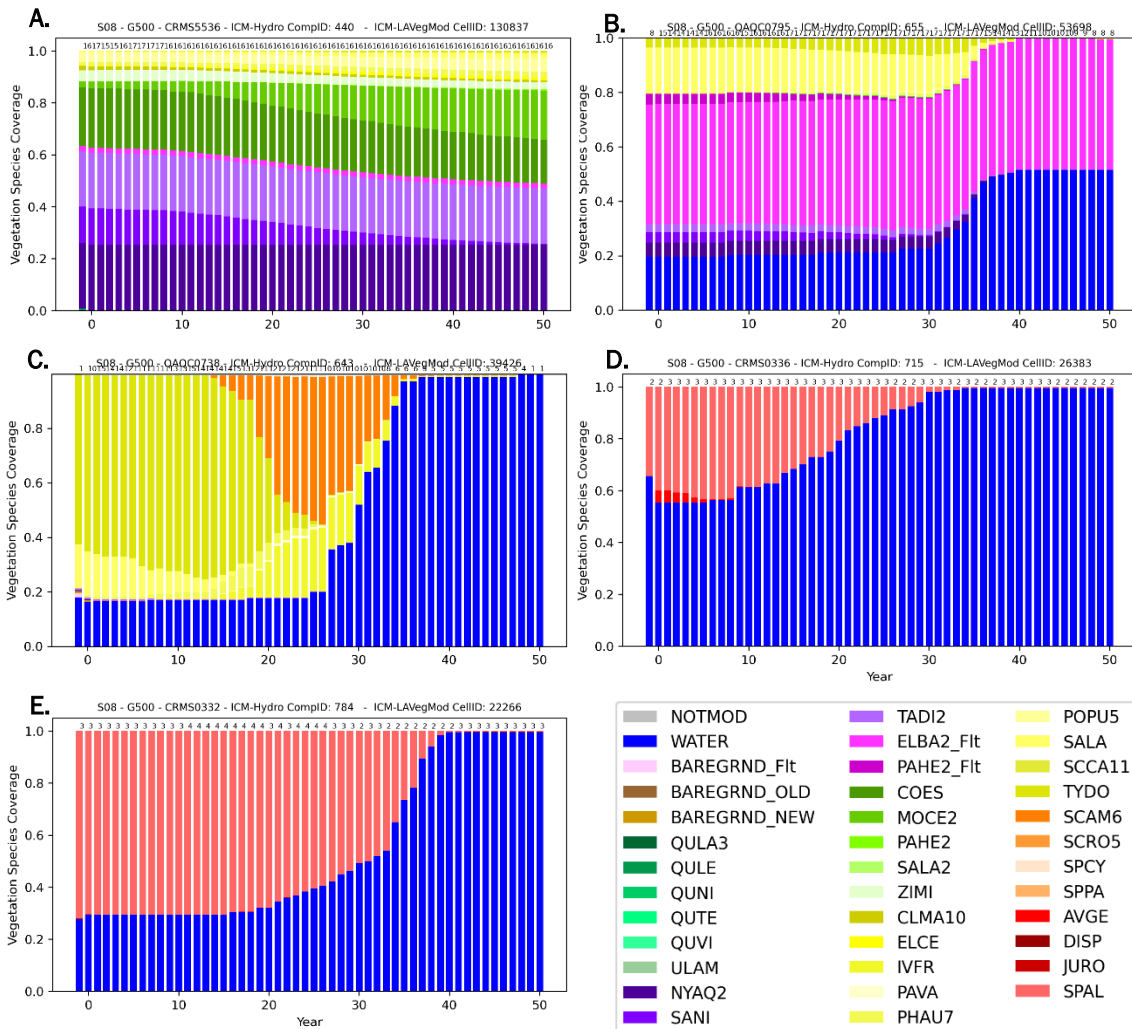


Figure 97. Change in vegetation cover under S08 is shown at representative points in the Terrebonne region. Point locations are shown in previous Terrebonne region map figures.

## 4.8 FWOA WETLAND MORPHOLOGY

### LOWER PROJECT SELECTION SCENARIO (S07)

Within the first five years, there is concentrated loss in compartment 640 in the Penchant ecoregion. There is flotant loss in the western region in the first decade, in the eastern region in the second decade, and in the central region in the third decade; although some flotant in the central and upper eastern area remain throughout the whole simulation. Land loss in the lower portion of the ecoregion, between Fourleague Bay and Lake Decade, greatly increases over the last two decades. The area to the west, closer to the Atchafalaya Delta, remains somewhat intact with most loss occurring along

marsh edges. QAQC0738 and CRMS0365 illustrate the differences between the lower and western portions, respectively. The starting elevation of CRMS0365, closer to the Atchafalaya, is 0.24 m higher, and the mean salinity remains below 2.09 ppt (the lower end of intermediate), allowing for greater inundation tolerance (Figure 98). However, the elevation is not keeping pace with the increase in mean water level. QAQC0738, west of Lake Penchant, experiences a steady increase in salinity from the lower to upper end of intermediate and a loss of elevation once the vegetation, and therefore organic accretion, is lost (Figure 99). The Lost Lake Marsh Creation is intact, but the Bayou Decade Marsh Creation is lost in the last five years of the simulation.

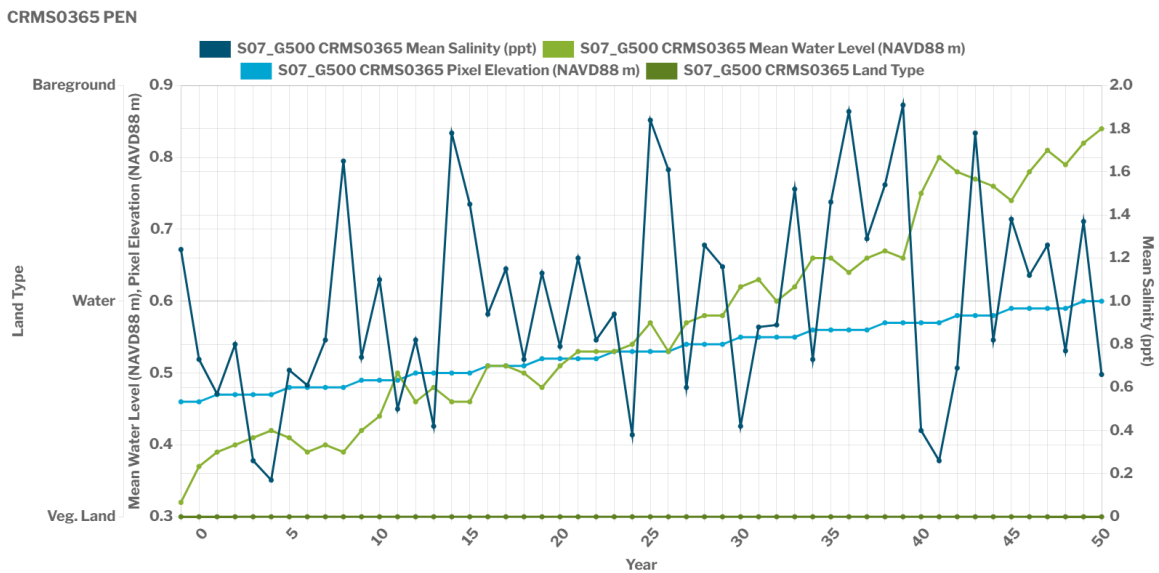


Figure 98. Salinity and inundation dynamics at CRMS0365 under S07.

In the first five years, there is concentrated land loss in compartments 634 and 635 south of the GIWW and little loss elsewhere. Land loss follows a speckled pattern throughout the first two decades, impacting the lowermost reaches around the margins of Terrebonne Bay and south of Sister Lake, most heavily. By the end of the third decade, these already fragmented lower basin marshes have largely converted to open water, and the central portion of the Western Terrebonne ecoregion begins to follow the speckled loss pattern, e.g., marshes between Lake Mechant and the HNC. In the fourth decade, there is loss in the upper reaches, particularly in the area around Grand Bayou Canal southwest of Larose and Cut Off, and in the upper Lake Boudreaux Basin south of Houma. In the last decade, land loss is extensive, and the only remaining marsh in the western and eastern ecoregions is highly fragmented in the mid-reach of Western Terrebonne, e.g., between Sister Lake and Fourleague Bay and west of Lake Mechant. The Terrebonne Basin Ridge Marsh Creation converts to open water at the beginning of the last decade, and the Small Dredge Program project east of Catfish Lake converts to open water in Year 50.

QAQC0738 PEN

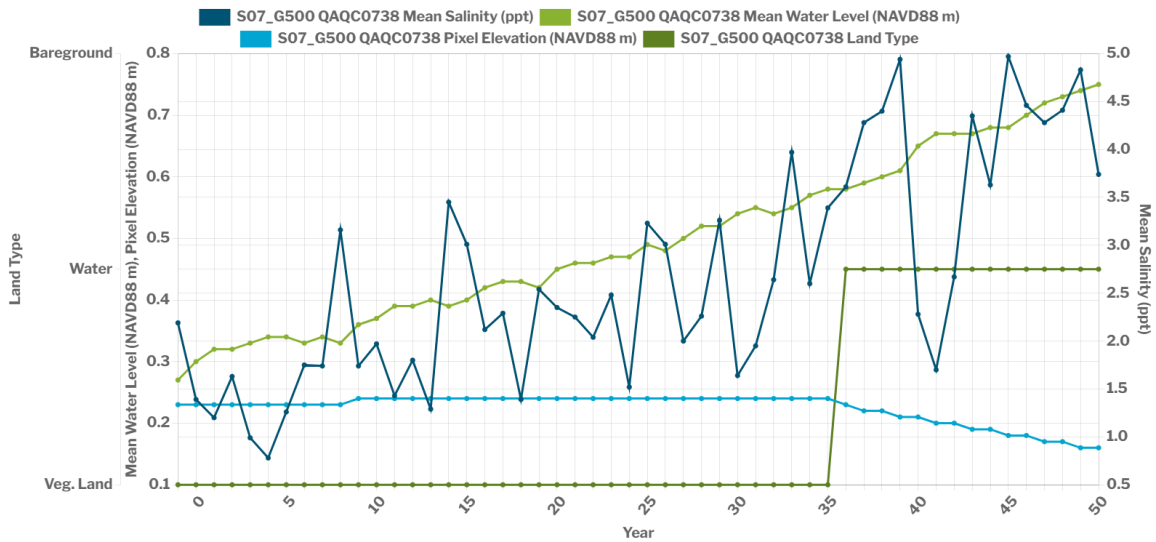


Figure 99. Salinity and inundation dynamics at QAQC0738 under S07.

QAQC1012, on the northern margin of Terrebonne Bay near Bayou de Jean Charles, and TRNS0801, southwest of Dulac and west of the HNC, are located along a similar latitude but have different patterns of change. Both exhibit a progressive conversion from land to water, as the mean water level increases by about 0.5 m (Figure 100 and Figure 101). Terrebonne Bay is more open to the Gulf and experiences higher salinities, which lead it to be dominated by AVGE (Figure 102). The salinity near Bayou Grand Caillou and the HNC is lower, and the area becomes dominated by SPAL (Figure 103).

QAQC1012 ETB

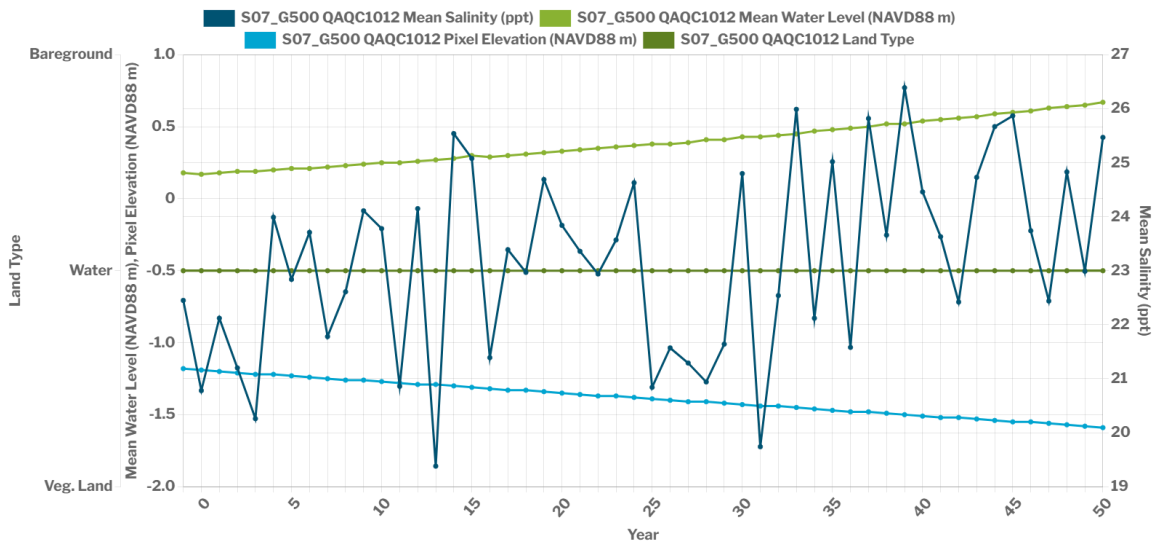


Figure 100. Salinity and inundation dynamics at QAQC1012 under S07.

TRNS0801 WTE

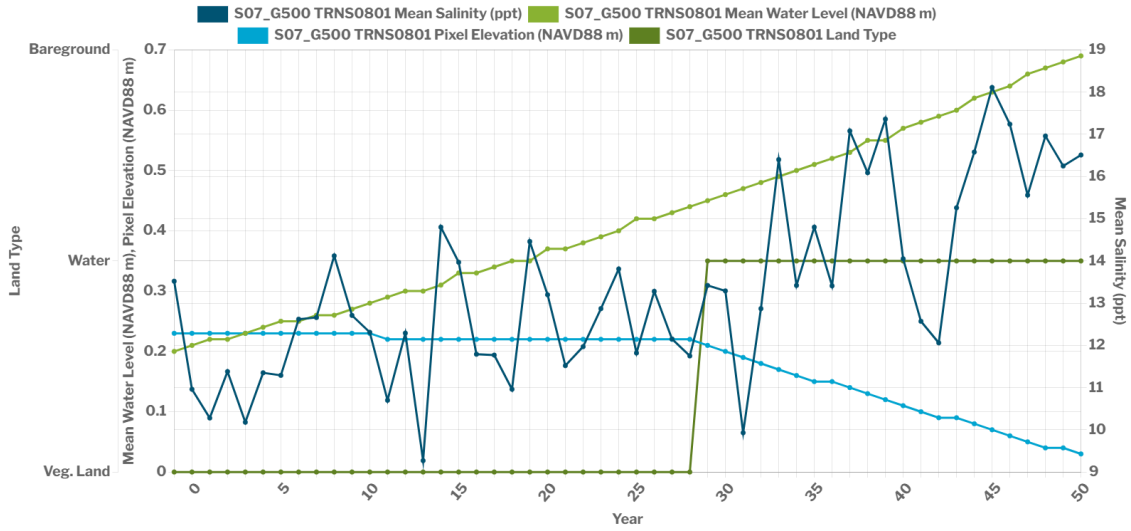


Figure 101. Salinity and inundation dynamics at TRNS0801 under S07.

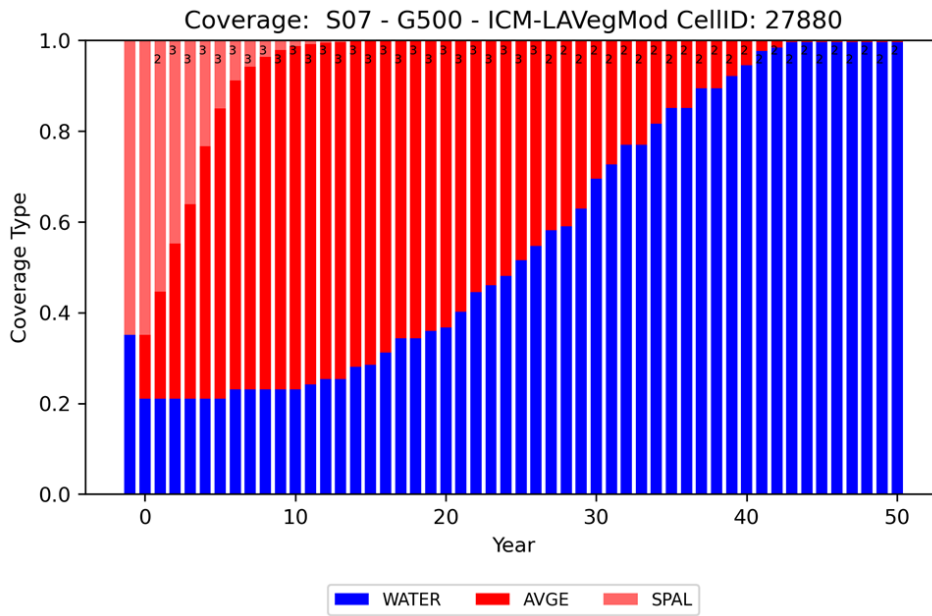


Figure 102. Vegetation change in grid cell 27880 (includes QAQC1012) under S07.

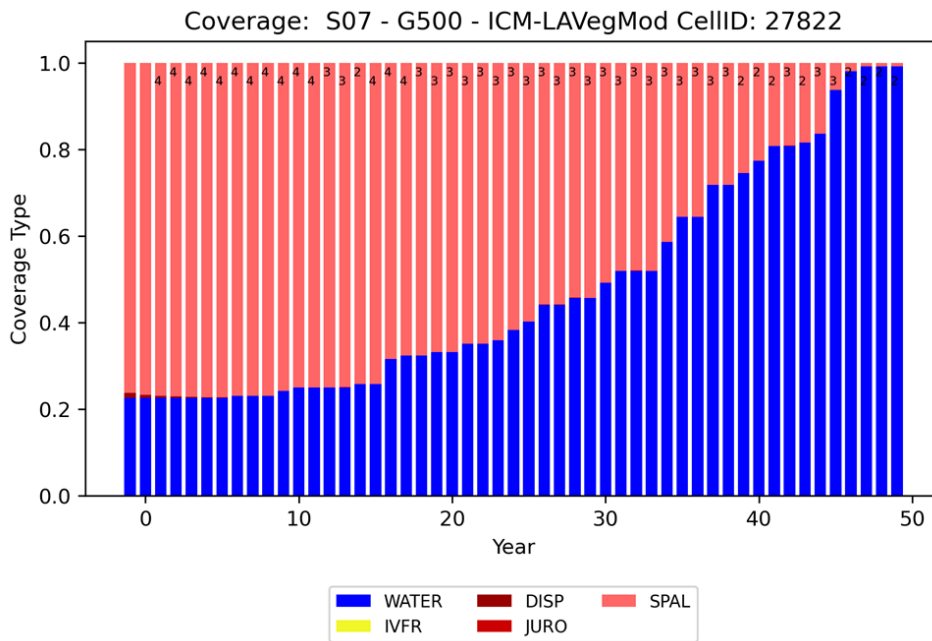


Figure 103. Vegetation change in grid cell 27822 (includes TRNS0801) under S07.

### HIGHER PROJECT SELECTION SCENARIO (S08)

The Verret Basin shows very little loss of land during the 50-year simulation. The area is dominated by fresh forested wetlands, and high FFIBS scores result in relatively high organic accretion rates that allow surface elevation to increase over time as subsidence rates are very low. Marsh edge erosion results in some land loss around channel margins near Lake Palourde and between Grassy Lake and Lake Verret. Marsh edge erosion rates are relatively low, although in some places they are greater than 1 m/yr and isolated land loss is apparent in the first few decades of the simulation.

In the marshes north and east of Houma (i.e., north of the GIWW), there are some areas of land loss in the first two decades, e.g., around Lake Houma. These are due to excessive water levels in the area which has complex hydrology. By Year 30 much of the wetland area between the Bayou Blue Ridge and the Bayou Terrebonne ridge has been lost. Between Year 20 and Year 30 the area just north of the GIWW, near Lake Long, experiences increasing FFIBS scores (from fresh to intermediate). CRMS2939, northwest of Lake Long, maintains a FFIBS score of less than 2 and accretion is able to keep pace with local subsidence, maintaining elevation in relation to North American Vertical Datum of 1988 (NAVD88). However, increasing water levels result in inundation loss at Year 30. By Year 40 much of the area has intermediate FFIBS scores. By Year 45 most of the land between Company Canal and the GIWW is open water but wetlands remain southwest of Lake Fields and between Bayou Blue Ridge and Bayou Lafourche. Marshes which survive in these basins by Year 50 mostly have lower

FFIBS scores which allows for higher accretion rates.

Land loss is scattered in the first 10 years of the simulation in the area between Bayou Lafourche and the HNC. In some areas around the shores of Terrebonne Bay, marsh edge erosion rates are high – several m per year, and this begins to manifest in land loss. Most of the outer saline marshes are lost in the next decade. Subsidence rates are relatively high, greater than 1 cm/yr and while organic accretion dominates in areas which are vegetated, water levels rise rapidly and marshes are lost due to inundation. CRMS0338, just east of Lake Chien, shows how elevation declines rapidly following the loss of marsh in Year 15, despite continuing mineral deposition (Figure 104).

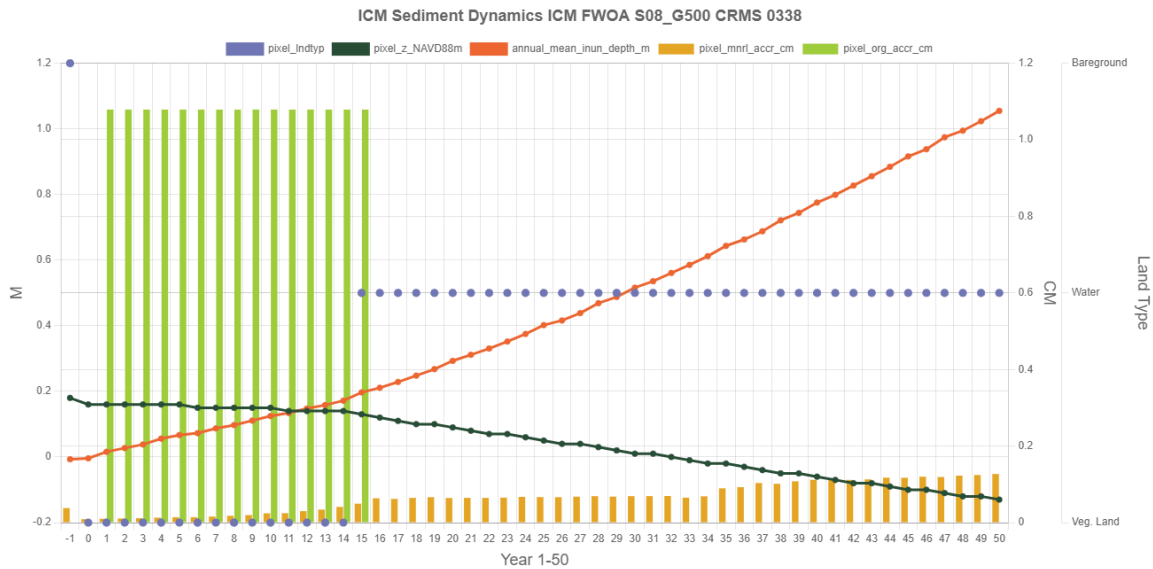


Figure 104. Sediment dynamics at CRMS0338 under S08.

As the outer marshes are lost, marsh loss increases further inland in the Lake Boudreaux Basin and west of Cut Off. These areas are brackish FFIBS scores in the third decade of the simulation which means they have relatively low rates of organic accretion for Delta Plain marshes. Subsidence rates are relatively high in S08 in ETB and WTB (4.5 and 4.3 mm respectively for shallow subsidence) with deep subsidence of 8 mm in the Lake Boudreaux area. This means that marsh elevation decreases while water levels rise leading to extensive inundation loss by Year 30. Only small areas of marsh remain, e.g., near Grand Bois, by Year 40, and these are diminished by Year 50. Two FWOA restoration projects in this area are also lost to open water: Terrebonne Basin Ridge and Marsh Creation - Bayou Terrebonne Increment turns to open water in Year 30/31, and Small Dredge Program marshes near Catfish Lake are lost in Year 34.

To the west, between the HNC and the Atchafalaya, there is minimal scattered land loss in the first decade of the simulation. By Year 15 land loss has increased in the lower saline marshes, north of the Isles Dernieres, north of Falgout Canal and in the marshes north of Lost Lake. Some areas of flotant

have also converted to open water north of Lake Penchant and between Avoca Island Cutoff and Fourleague Bay. For example, a focused area of flotant transition to open water, east of Bayou Copesaw near the GIWW, occurs in Year 15 and appears to be associated with a storm which increases the 2-week maximum salinity to more than 8 ppt exceeding the threshold of 5.5 ppt for loss of flotant (Figure 105).

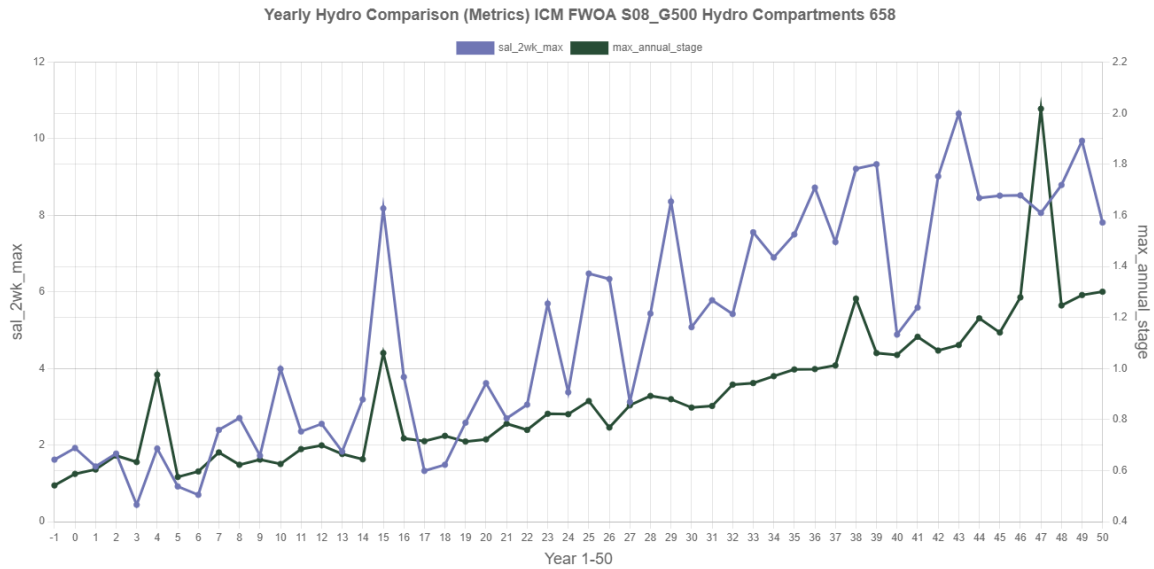


Figure 105. Maximum 2-week salinity and mean annual stage compartment 658 under S08.

Land loss continues in these areas. By Year 25, most of the lower saline marshes have transitioned to open water and loss is increasing south of Lake Decade. As subsidence rates are high in this area, most marshes lose elevation despite relatively high accretion rates, and rising stage results in inundation loss. This effect spreads further north toward Bayou Penchant by Year 30. CRMS 0290 shows this pattern well for the Penchant marshes (Figure 106).

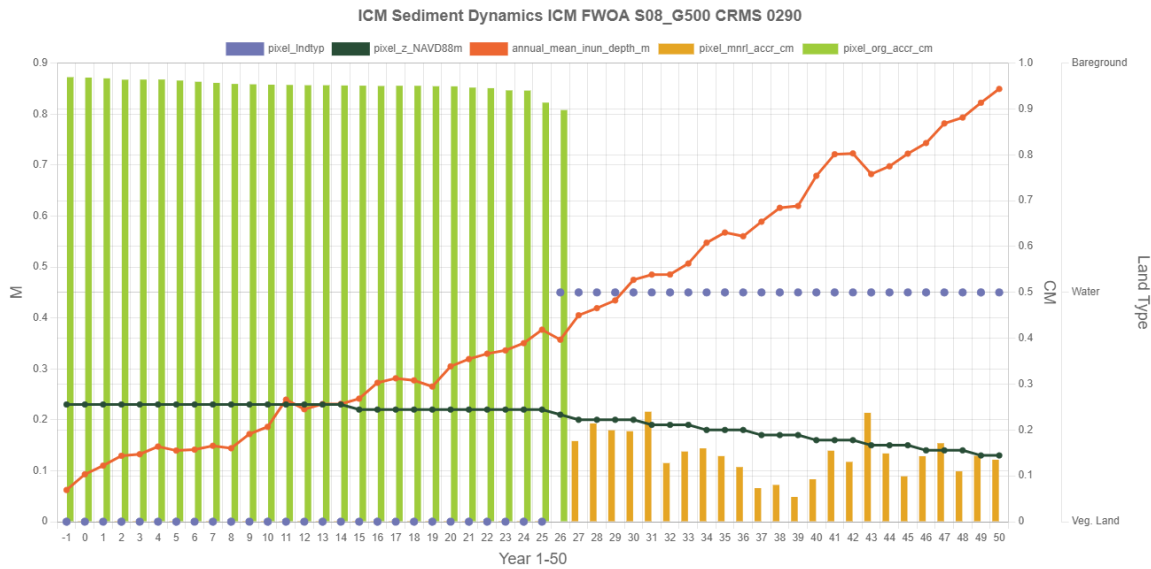


Figure 106. Sediment dynamics at CRMS0290 under S08.

Salinity increases from 1-2 ppt in the first few decades to 4-6 in the last decade, and FFIBS scores remain less than 5. However, rapid water level increase results in the loss of marshes, which with organic accretion were able to maintain elevation. Following conversion to open water inundation rates continue to increase despite contributions from mineral accretion and a ~50% reduction in subsidence as shallow subsidence does not apply to open water areas. By Year 35 the remaining marshes are to the west near the Atchafalaya, including some of Point au Fer, and north of Bayou Penchant between Bayou Copesaw and Minors Canal, with isolated marsh east of Lake Mechant. Two FWOA restoration projects in the area are also lost during this period. The Bayou Decade Ridge Restoration and Marsh Creation project transitions to open water in Year 34, as does the western portion of Lost Lake Marsh Creation and Hydrologic Restoration. However, the eastern portion of the Lost Lake project is lost at Year 37.

In the last decade, extensive areas of flotant convert to open water in FWOA Year 43, especially in compartments 744 and 655 east of Bayou Copesaw. There is a peak in 2-week salinity in Year 43, which exceeds 5.5 ppt in compartment 655. By Year 50, flotant remains north of the GIWW and north of Bayou Penchant west of Turtle Bayou where the salinity threshold for loss of flotant is not met. Some marshes remain in the west of the Penchant Basin in areas where FFIBS scores and salinities stay low due to the influence of the Atchafalaya River and organic accretion is able to maintain or even build elevation in the face of subsidence (which is also lower in this area due to the gradient in deep subsidence in western Terrebonne). Fresh conditions also mean that inundation thresholds are high. CRMS0301 illustrates this dynamic, although the station is slightly east of the area that remains as wetland by Year 50 (Figure 107). The area remains fresh with FFIBS scores less than 2 and elevation stays relatively stable. However, when inundation depths approach 0.5 m the marsh is lost.

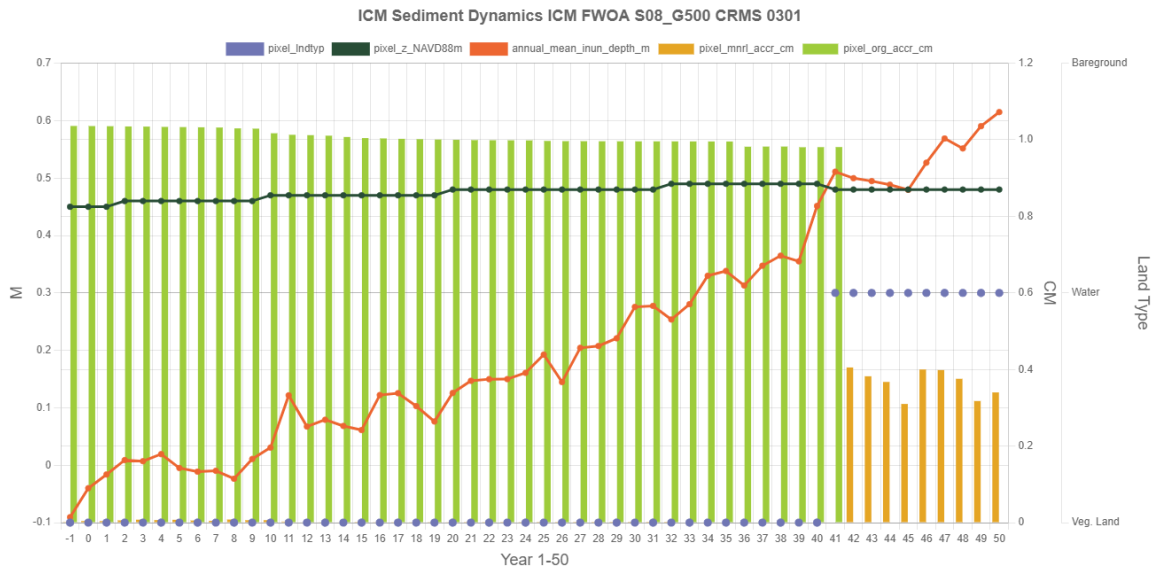


Figure 107. Sediment dynamics at CRMS0301 under S08.

## 4.9 FWOA BARRIER ISLAND MORPHOLOGY

The barrier islands in the Terrebonne region that are modeled with ICM-BI include: Raccoon Island, Whiskey Island, East/Trinity Island, and Timbalier Island (Figure 108). Because of the coastal protective structures constructed at Raccoon Island, the cross-shore retreat rate of the Gulf shoreline and uppermost shoreface (<3 m) in the ICM-BI model is set to zero. In contrast, the lower shoreface and the bay shoreline are allowed to retreat. In addition, no auto-restoration is applied to this barrier island. As a result, Raccoon Island narrows in place for both the S07 and S08 scenarios, with continued erosion of the bay shoreline and steepening of the shoreface (Figure 109).



Figure 108. ICM-BI barrier islands located within the Terrebonne region of the coast. Background imagery from Google Earth.

At Timbalier, Whiskey, and East/Trinity Islands, erosion of the upper and lower shoreface and auto-restoration in the model contributes to the islands' transgression over time (Figure 109). The shallow areas in the lee of the islands and along the flanks that are not part of a restoration footprint deepen with time because of subsidence and sea level rise. The number of auto-restorations and the volume of sediment placed varied by island and scenario (Figure 110). The volume of sediment placed at an island is increasing over time because of relative sea level rise and an increase in accommodation space. The subaerial footprint of each island at any point in time depends strongly on when auto-restoration last occurred. For example, for Timbalier Island in the S08 scenario restoration occurs in Year 49 (Figure 110) which results in a large subaerial footprint in Year 50 (Table 5).

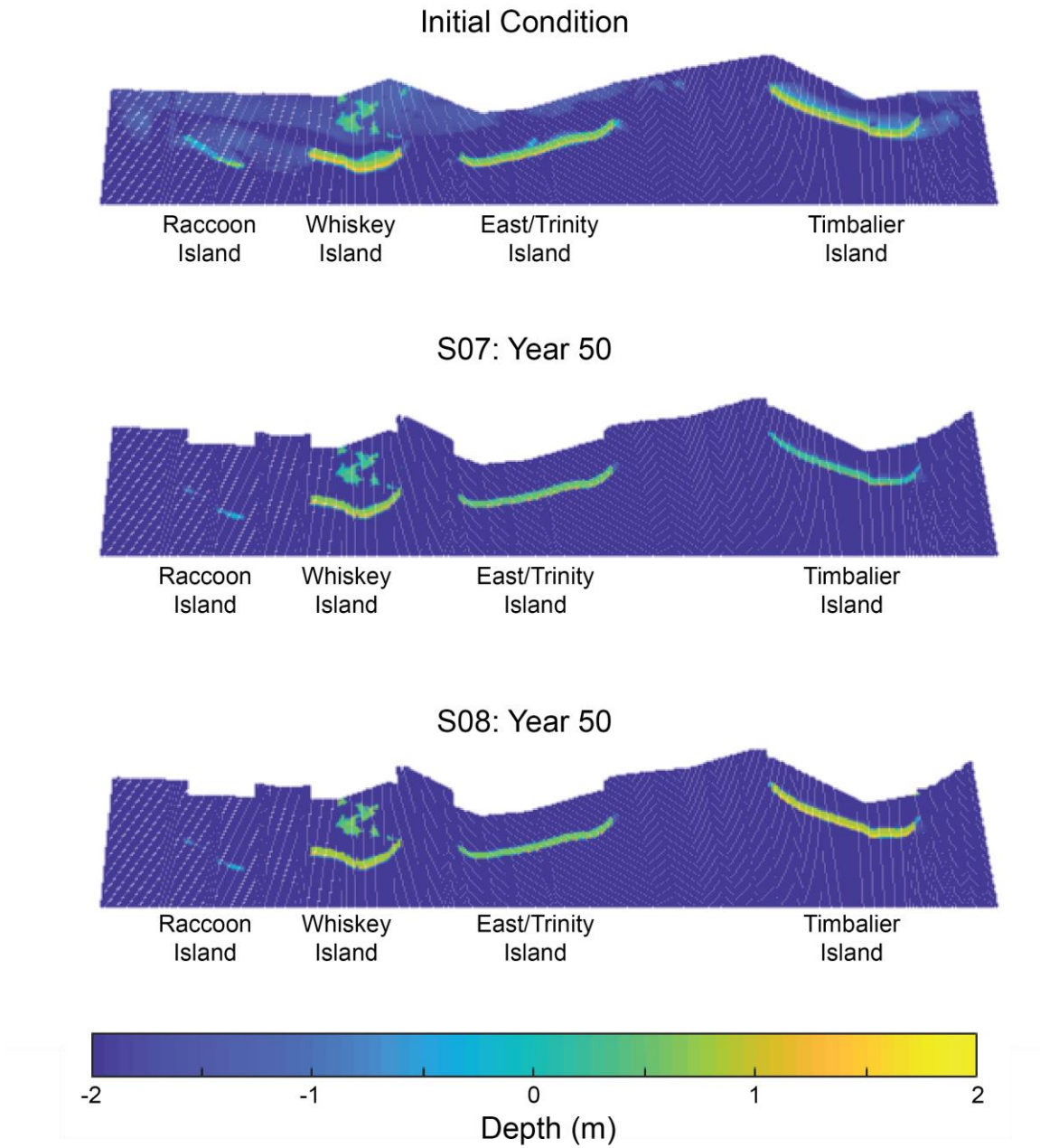


Figure 109. Elevation, relative to mean high water, for the initial condition in the Terrebonne region along with Year 50 results for S07 and S08. Depth is shown in meters.

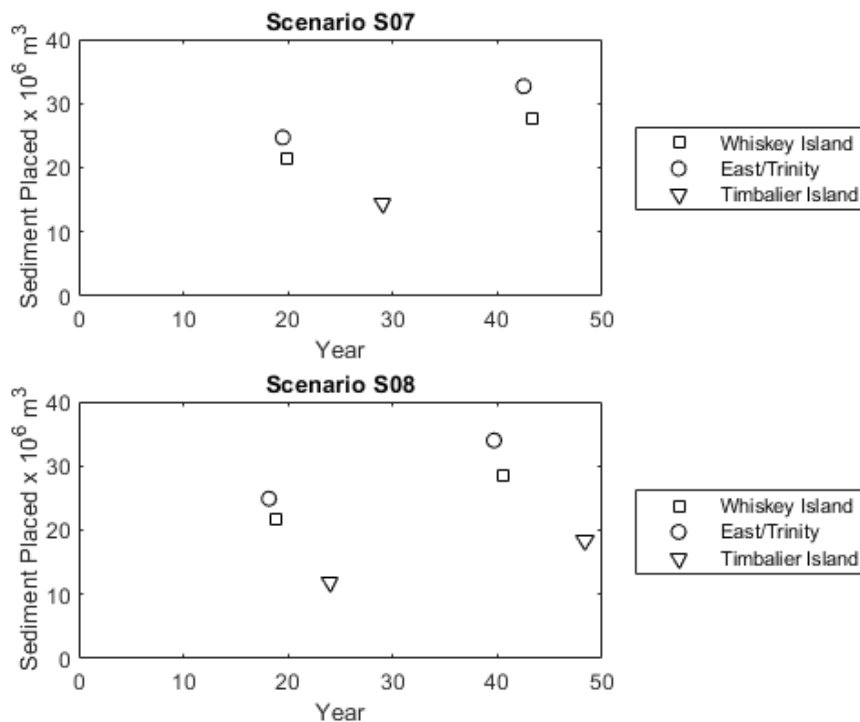


Figure 110. Sediment placement volumes for barrier islands within the Terrebonne region of the coast.

Table 5. Summary of total sediment volume placed (10<sup>6</sup> m<sup>3</sup>) over FWOA simulation in scenarios S07 and S08 for the Terrebonne region of the coast

Barrier Island or Headland	S07	S08
Raccoon Island	n/a	n/a
Whiskey Island	48.92	50.21
East/Trinity	57.39	58.88
Timbalier Island	14.42	30.25

Under S07, the general trend is that the inlet areas increase over time as the tidal prism increases. Across all basins, there are changes, both increases and decreases, during the spin-up period (i.e., ICM-Years 1-2). The trends under S08 are similar to those in S07, but maximum caps are reached earlier in the simulation. The spin-up period changes are the same as those in S07 because the spin-up conditions are used for all scenarios are the same. Differences between S07 and S08 are seen across all basins. As expected, the links whose sub-basins contain the most marsh at the start of the simulation see some of the largest differences between S07 and S08 due to the differences in land

(marsh) loss. Attenuation of the tidal signal is observed in each basin with the largest tidal range at the Gulf end and decreasing moving up-basin. As land is lost and connectivity increases, less attenuation is observed. The tidal range increased over the course of the simulation. Greater increase is seen in S08 than S07 across all basins.

Under S07, the two smallest inlets reach their minimum size during the spin-up, while the other links increase appreciably (Figure 111). Link 907 remains at the minimum size until ICM-Year 29 when it begins to expand. Link 906 (western-most link) reaches the maximum cap for both width and depth during the spin-up and remains at the maximum size for the remainder of the simulation. Links 908 and 910 behave similarly and reach the max width in the beginning of the fourth decade and reach the max depth at the end of the fifth decade.

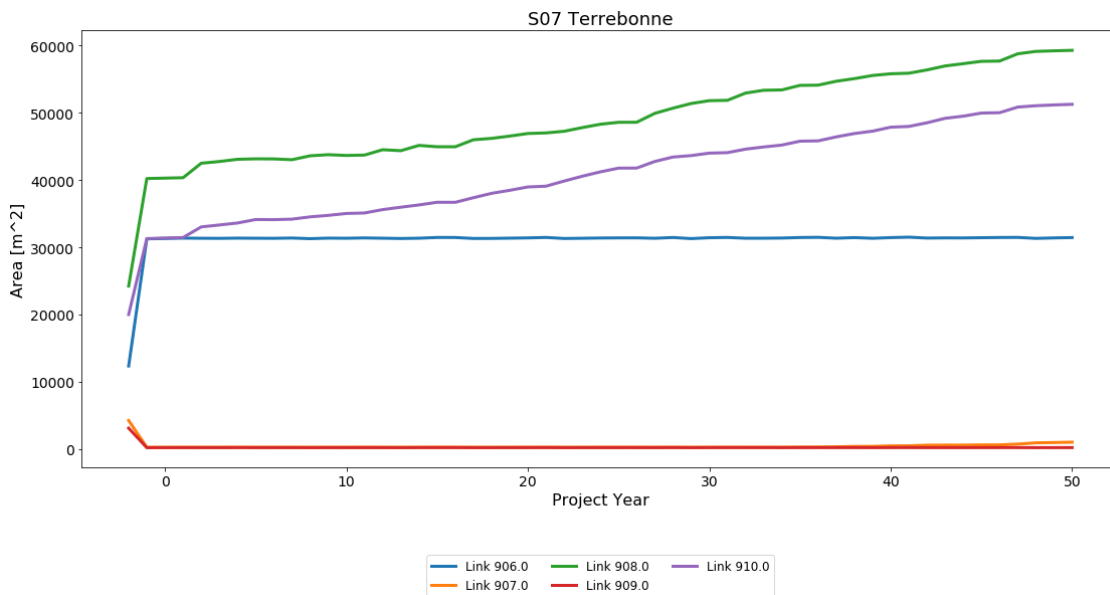


Figure 111. Terrebonne tidal inlet cross-sectional area changes over time, under S07.

Under S08, Links 908 and 910 reach the max width in the third decade, and the max depth is reached in the fourth decade (Figure 112). Link 910 reaches the max depth and width in the spin-up and remains at the maximum size for the remainder of the simulation. Links 907 and 909 reach the minimum size in the spin-up period. Link 907 begins to deepen at the end of the third decade and widen in the fourth decade. Link 909 remains at the minimum width and depth.

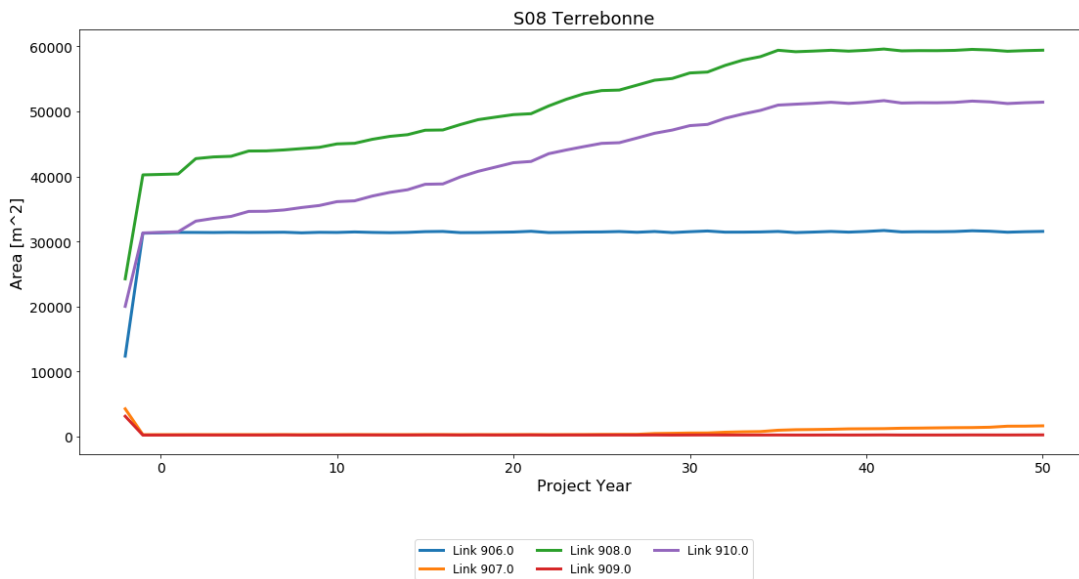


Figure 112. Terrebonne tidal inlet cross-sectional area changes over time, under S08.

## 4.10 FWOA HABITAT SUITABILITY INDICES

### LOWER PROJECT SELECTION SCENARIO (S07)

Habitat suitability for fish, shellfish, and wildlife in the Eastern and Western Terrebonne ecoregions was relatively stable until the last half of the S07 environmental scenario. During that time, suitability decreased for most species due primarily to the effects of extensive wetland loss around Terrebonne and Timbalier Bays. This wetland loss did not greatly affect the wildlife species because most of the highly-suitable habitat for these species occurred elsewhere in the Terrebonne region, but there were large decreases in habitat suitability for juvenile fish and shellfish due to the loss of marsh nursery habitat (e.g., small juvenile brown shrimp, Figure 113). In some cases, the decrease in habitat suitability was lessened by the presence of other nursery habitats. For example, newly-formed open waters near upper Terrebonne Bay remained moderately suitable for small juvenile brown shrimp (HSI scores of 0.4 to 0.5; Figure 113) because of the availability of oyster reef nursery habitat in these areas, which otherwise would have had lower suitability (scores 0.2 to 0.3).

Increased salinities contributed to changes in fish and shellfish habitat suitability in these parts of the region. In the areas nearest the Gulf of Mexico, salinities increased such that marsh and open water habitats became less suitable for fish and shellfish such as small juvenile brown shrimp and oysters, which have optimal salinity ranges from about 10 to 20 ppt. Meanwhile, in the upper Eastern and Western Terrebonne ecoregions, salinities increased such that habitat became more suitable. As a result of the increased salinities and wetland loss, the location of highly-suitable habitat (HSI scores  $\geq 0.7$ ) for several fish and shellfish species shifted north over time in the region (Figure 113).

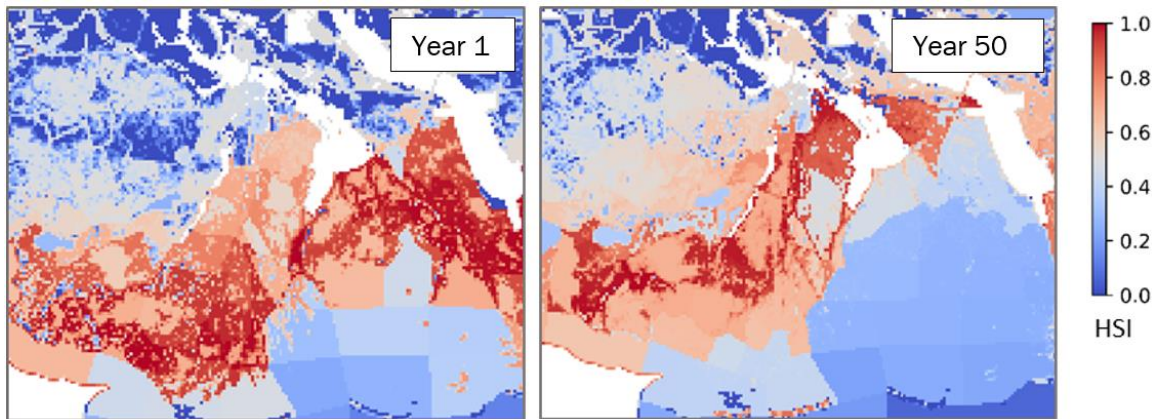


Figure 113. Small juvenile brown shrimp HSI scores across the Terrebonne region for Year 1 (left) and Year 50 (right) of the S07 environmental scenario. Scores range from 0.0, completely unsuitable habitat, to 1.0, optimal habitat

In contrast with the Eastern and Western Terrebonne ecoregions, habitat suitability for most species increased over time in the Penchant ecoregion. For fish and shellfish, this was mostly due to wetland loss in the southern part of the ecoregion, which resulted in a highly-suitable fragmented marsh landscape, and increased salinities, which benefitted higher-salinity species such as brown shrimp and spotted seatrout. For gadwall and mottled duck, increased suitability was due to increased water levels. Across much of the region, and in particular the higher-elevation marshes of the eastern and western parts of the ecoregion, increased water levels inundated marsh habitats such that the amount of suitable shallow water habitat increased over time (Figure 114 and Figure 115). In the lower-elevation marshes and flotant habitats of the northern and southern parts of the ecoregion, however, water depths became too deep over time and habitat suitability decreased accordingly (Figure 115).

Compared to the rest of the Terrebonne region, the Verret and Upper Verret ecoregions showed very little change in habitat conditions and thus habitat suitability for species over the simulation. The exception to this was for crayfish, which had a large decrease in habitat suitability in the Verret ecoregion over time (Figure 116). This was due to a decrease in water depths during the January to August seasonal period. Much of the Verret ecoregion experienced regular episodes of mineral deposition over time that increased wetland elevations such that they were infrequently flooded or flooded to low levels. While the lack of flooding would support crayfish burrowing activities, it would not support crayfish as they emerge from their burrows to forage and mate.

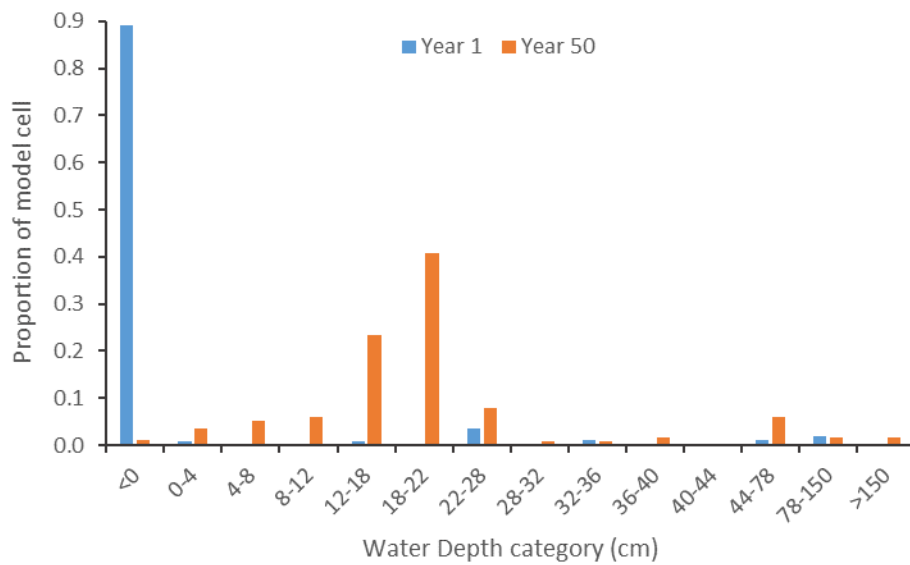


Figure 114. Water depths simulated for a model cell in the western Penchant ecoregion for Year 1 and Year 50 of the SO7 environmental scenario. Water depth categories are used for gadwall HSI calculations, with depths from 18 to 32 cm representing the most suitable water depths.

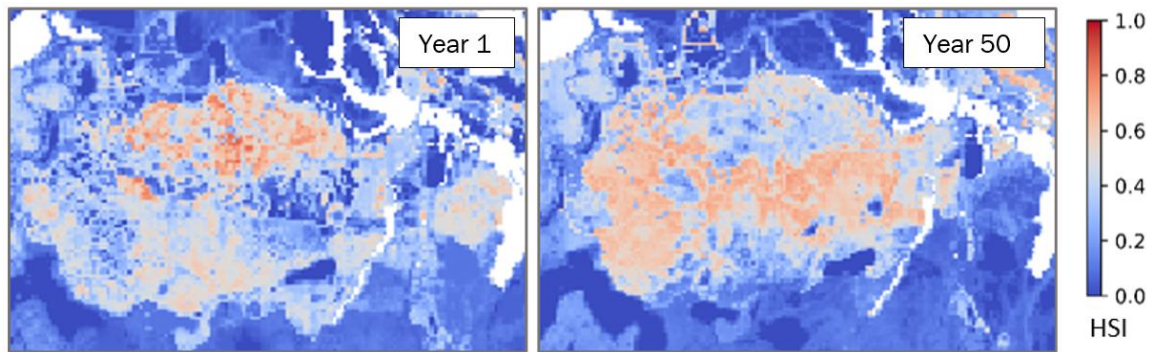


Figure 115. Gadwall HSI scores across the Penchant ecoregion for Year 1 (left) and Year 50 (right) of the SO7 environmental scenario. Scores range from 0.0, completely unsuitable habitat, to 1.0, optimal habitat.

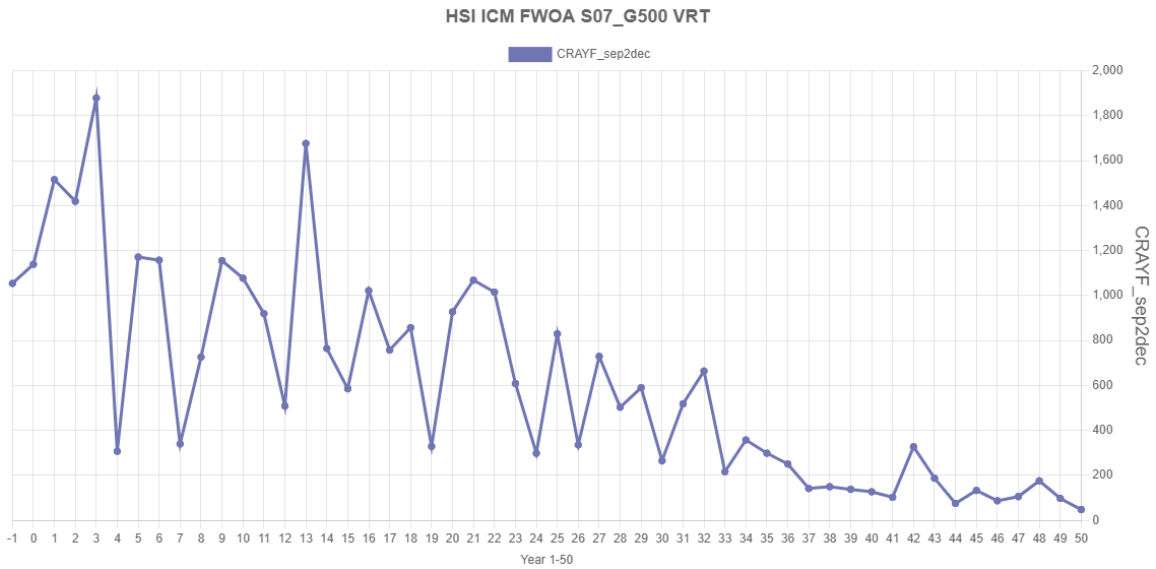


Figure 116. Total HSI score for crayfish in the Verret ecoregion over the 50-year S07 environmental scenario simulation. The total HSI score was calculated by summing the individual scores for each model cell within the ecoregion.

## HIGHER PROJECT SELECTION SCENARIO (S08)

While habitat conditions remained stable in the Verret and Upper Verret ecoregions under the S08 environmental scenario, the high rates of wetland loss in the rest of the Terrebonne region greatly reduced the amount of habitat for fish, shellfish, and wildlife. In the Eastern and Western Terrebonne ecoregions, habitat suitability for fish and shellfish steadily decreased over time as most wetlands were lost and the ecoregions were converted to primarily open water habitat (Figure 117). However, this decline slowed during the last two decades of the simulation and for some species there was a slight increase in habitat suitability during this time. The increase was likely due to the fragmentation of the remaining marshes in the upper part of the Eastern Terrebonne ecoregion, which provided new habitat for fish and shellfish at the end of the simulation.

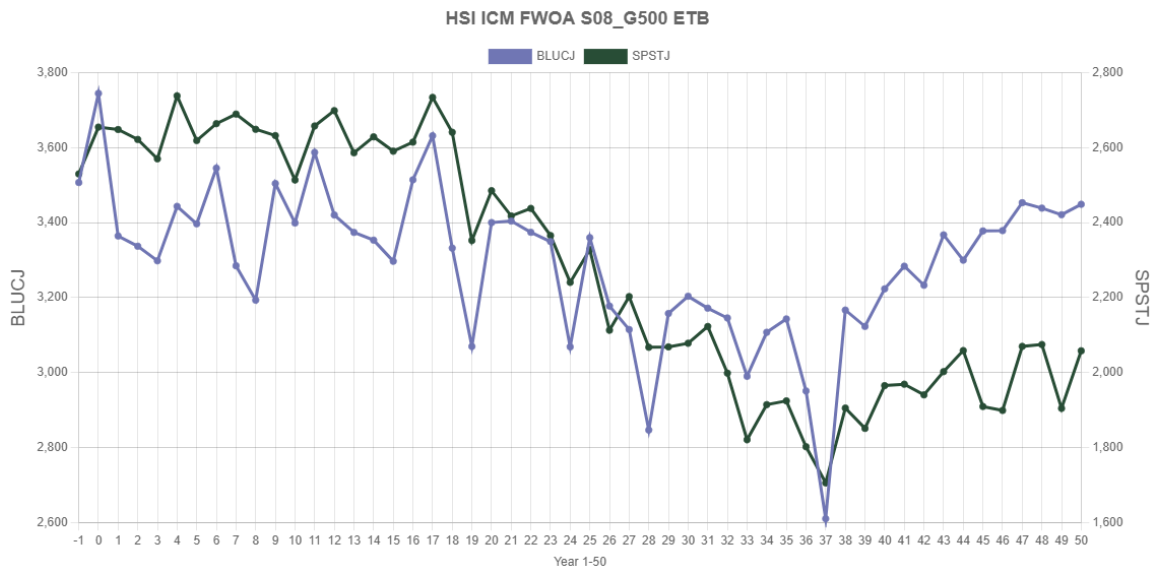


Figure 117. Total HSI score for juvenile blue crab and juvenile spotted seatrout in the Eastern Terrebonne ecoregion over the 50-year S08 environmental scenario simulation. The total HSI score was calculated by summing the individual scores for each model cell within the ecoregion.

Changes in salinities also contributed to the patterns of habitat suitability for fish and shellfish. Salinities increased over time to >20 ppt across most of the Eastern and Western Terrebonne ecoregions, which reduced the suitability of the open water and remaining marsh habitats for most species. However, the increase in salinities was moderated during the last decade of the simulation by high river discharge. The relative lack of wetlands across the region may have allowed freshwater to flow across a wider area and decrease salinities by about 5 ppt in the Eastern and Western Terrebonne ecoregions. As a result, salinities were reduced to more optimal levels for higher-salinity species such as brown shrimp and oyster, and thus habitat suitability increased somewhat around Terrebonne and Timbalier Bays during the last decade (Figure 118).

In the Penchant ecoregion, a slightly different pattern occurred relative to wetland loss. Compared to the Eastern and Western Terrebonne ecoregions, the Penchant ecoregion was primarily solid marsh at the beginning of the simulation and this marsh was converted into a highly suitable, fragmented marsh–shallow water landscape during the first half of the simulation. As a result, habitat suitability for fish, shellfish, and wildlife increased in the Penchant ecoregion during this time (Figure 119). However, similar to the other ecoregions, most of this wetland habitat was lost and the Penchant ecoregion was converted into primarily open water at the end of the simulation. This resulted in a general decline in habitat suitability over the last two decades, though the magnitude of this decline was different among species due to the influence of other important environmental factors. There was a large decline in habitat suitability for gadwall and mottled duck because, as sea level rise rates increased during the latter half of the simulation, the remaining open water habitats became too deep for these species. Habitat suitability for fish and shellfish did not decline much, however, because

these open water habitats still had value to these species, and salinities were maintained at suitable levels by the mix of freshwater from the Atchafalaya River and saline water from the Gulf of Mexico.

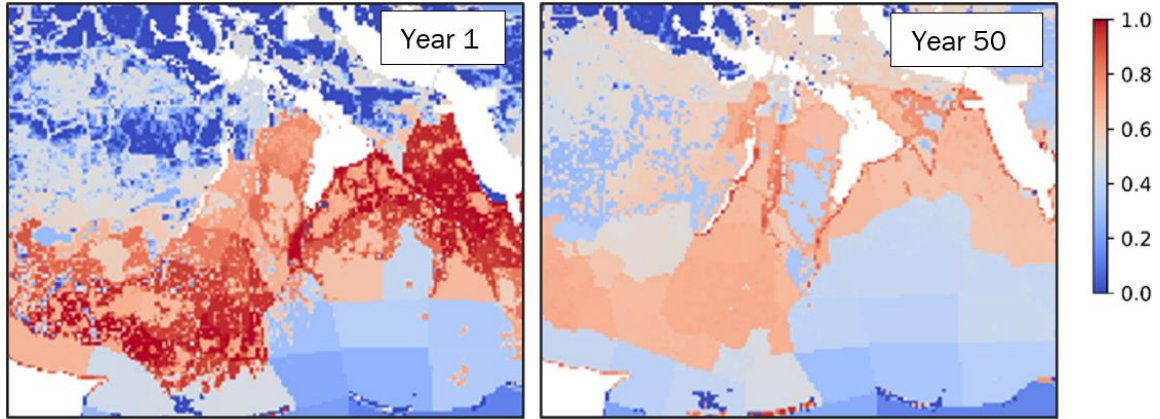


Figure 118. Small juvenile brown shrimp HSI scores across the Terrebonne region for Year 1 (left) and Year 50 (right) of the S08 environmental scenario. Scores range from 0.0, completely unsuitable habitat, to 1.0, optimal habitat.

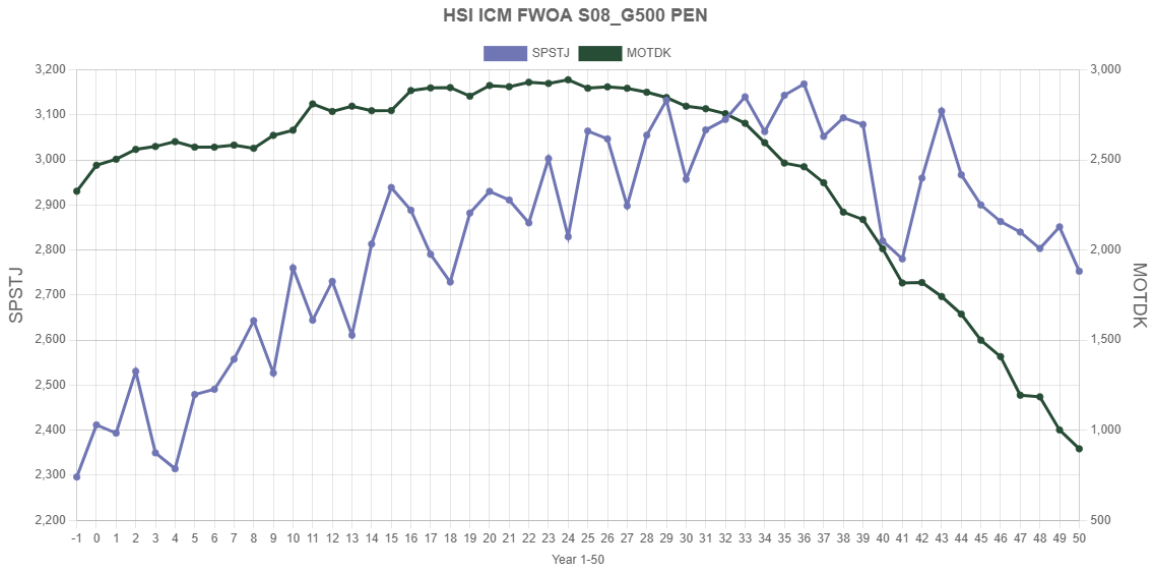


Figure 119. Total HSI score for juvenile spotted seatrout and mottled duck in the Penchant ecoregion over the 50-year S08 environmental scenario simulation. The total HSI score was calculated by summing the individual scores for each model cell within the ecoregion.

## 4.11 DISCUSSION

Although, there is a significant effect of the scenarios on land change, vegetation composition stays very similar under both scenarios (Figure 120).

The greatest difference between the two scenarios for this region is increased land loss in S08. However, the differences are not the same throughout the basin. Marshes are lost in eastern Terrebonne in both scenarios, in the southerly portions of western Terrebonne, and in the southern part of the Penchant Basin (north of Lake Decade to Fourleague Bay). There is extensive loss in and Lake Long/Lake Fields sub-basin in S08 which is largely intact in S07. Within the Penchant Basin areas near the Atchafalaya and south of the Bayou Black ridge remain intact in S07 and are lost in S08. There is little loss in the Verret Basin in either scenario. While some loss of flotant to open water occurs in S07, between Lake Theriot and the Turtle Bayou area, there is more extensive loss of flotant east of Turtle Bayou in S08.

As there is so little land left in ETB by Year 50 for S08 it is difficult to find a land location that behaves similarly between the two scenarios. QAQC1091 is located in open water close to the Bayou Pointe aux Chenes ridge southeast of the intersection with Grand Bayou Canal. Pixel elevation decreases similarly over time for both scenarios as no shallow subsidence is applied to open water areas (which does vary by scenario) and although mineral accretion is not the same the rates are very low (Figure 121). Inundation at the end of the simulation is higher for S08 than S07 due to sea level rise.

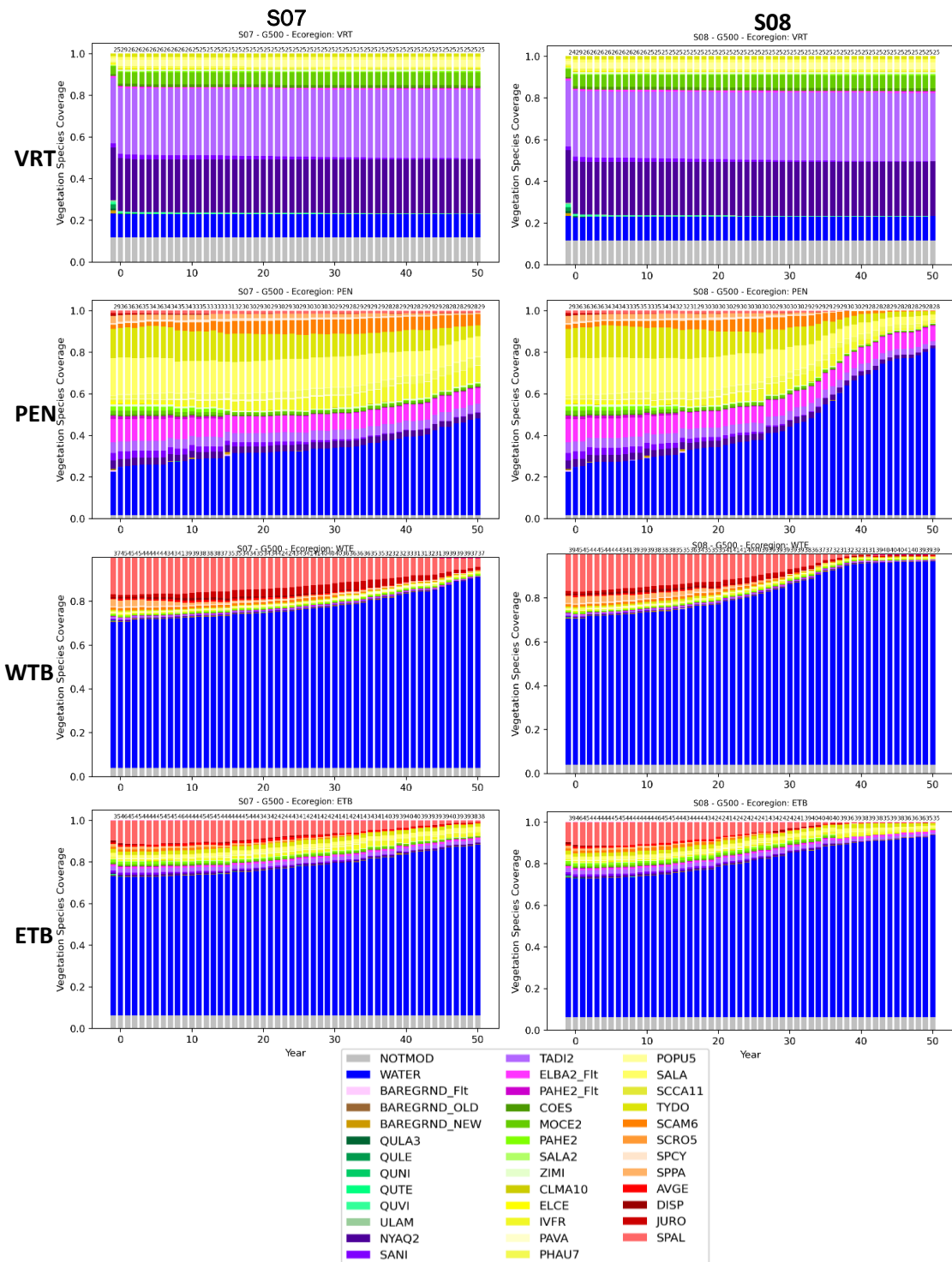


Figure 120. Comparison of vegetation cover change in the Terrebonne region between the two scenarios, by ecoregion. Ecoregion vegetation coverages for the lower scenario (S07) on left, and higher scenario (S08) on the right.

S07 AND S08 QAQC1091 ETB

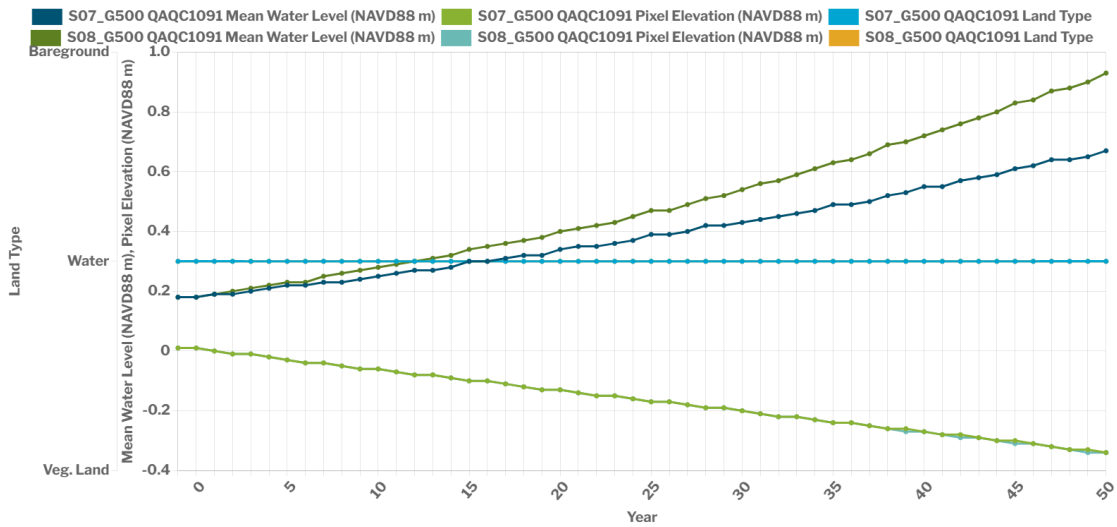


Figure 121. Comparison of S07 and S08 conditions for QAQC1091 in ETB.

CRMS0322 is in WTB close to Fourleague Bay and south of Old Oyster Bayou. This location is land through the simulation under S07 but is lost to open water under S08 in Year 34 (Figure 122). There is a >2 mm/yr difference between the scenarios for shallow subsidence, and S08 thus shows a greater decline in elevation being 20 cm lower in S07 than S08 in Year 50. The decline in elevation in the later decades is due to the loss of organic accretion when the area turns to open water in S08. Mineral accretion does increase but it is much lower than the organic contribution when the site is vegetated. The more rapid rise in water level due to higher sea level rise in S08 results in the loss due to inundation. In S07 inundation depth at Year 50 is still below the threshold depth for loss.

S07 AND S08 CRMS0322 WTE

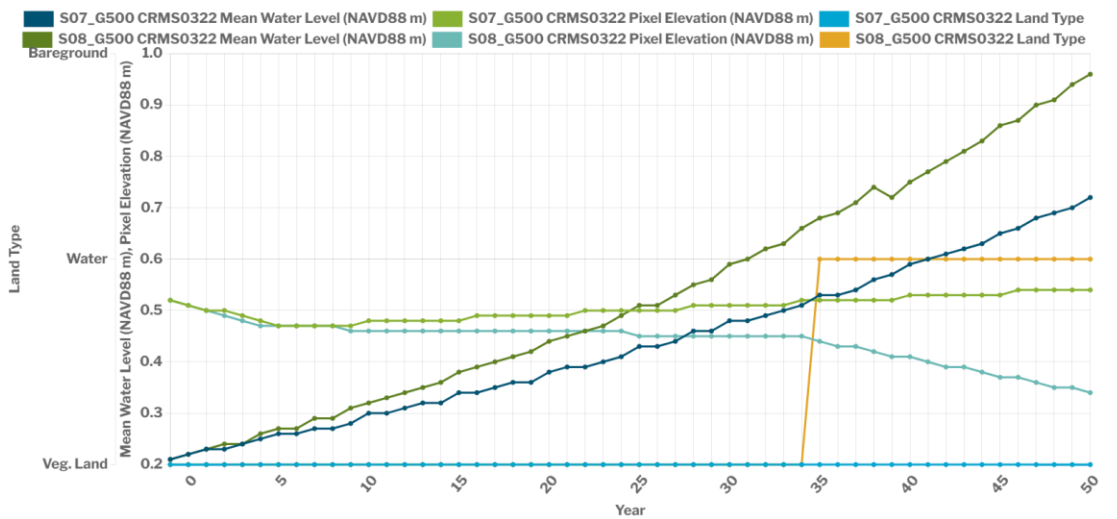


Figure 122. Comparison of S07 and S08 conditions for CRMS0322 in WTB.

In contrast to CRMS0322 which is saline in both scenarios throughout, QAQC0721 in PEN has low FFIBS scores throughout. It is located west of Turtle Bayou, between Bayou Penchant and the GIWW. Deep subsidence is fairly low in this area (~3 mm/yr) and although there is a difference of almost 2.5 mm/yr in shallow subsidence among the scenarios, the organic accretion gradually increases elevation in both S07 and S08, although the increase is less in S08 (Figure 123). This, in combination with rising water levels due to higher sea level rise means the site crosses the inundation threshold in Year 34 in S08 when mean annual inundation is more than 45 cm. Once the marsh turns to open water elevation begins to decrease due to the loss of organic accretion.

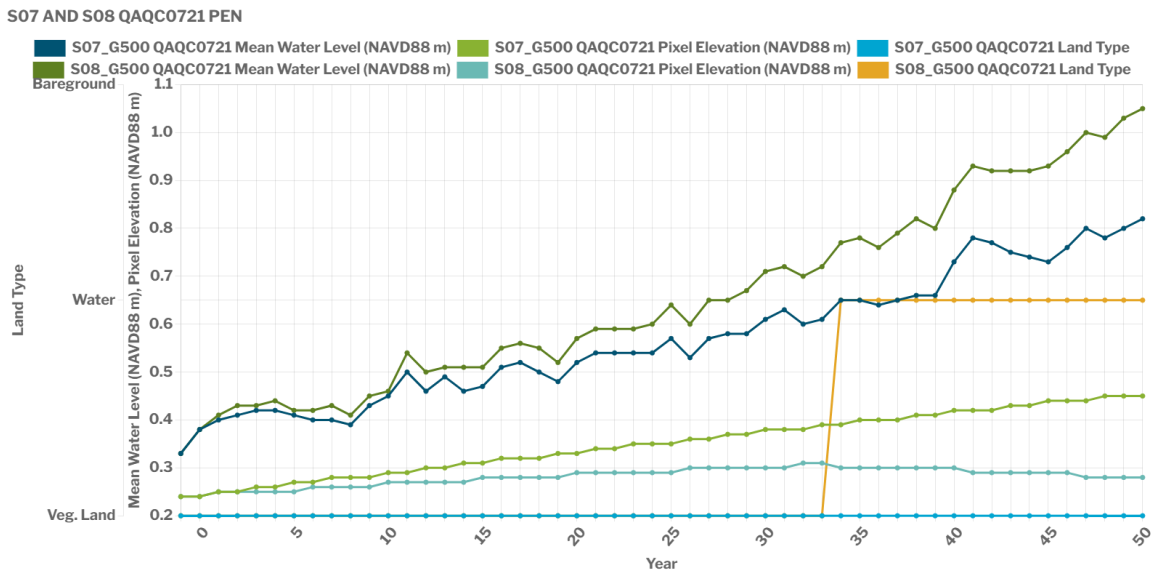


Figure 123. Comparison of S07 and S08 for QAQC0721 in PEN.

Raccoon Island follows expected modeled behavior and does not transgress. Some minor unrealistic behaviors – expected based on initial testing – occurred with the model runs, including jaggedness of the shoreline introduced for some islands during auto-restoration. In addition, the flanks of Timbalier Island do not restore correctly for a few profiles (specifically, the template is applied to the boundary of the profiles rather than at the location of the island). Neither of these issues are expected to significantly impact the results of either the ICM or ADCIRC model runs. However, the jaggedness worsened during interpolation of the ICM-BI point cloud to the 30-m ICM-Morph grid. Because the ADCIRC grid is sensitive to the increased jaggedness, the higher resolution DEM output of the ICM-BI grid is provided directly to ADCIRC to resolve the issue, and all results shown in this report are taken directly from the ICM-BI output.

As a result of the increased sea level rise in the S08 scenario, Raccoon Island has a smaller subaerial footprint at the end of the 50-year model run than in the S07 scenario (Figure 109). For the same reason, auto-restoration occurs 1-5 years earlier in the S08 scenario than in the S07 scenario for Whiskey, East/Trinity, and Timbalier Islands. Because the volume of sediment placed during each

restoration is slightly higher in the S08 scenario compared to the S07 scenario (Figure 110), the total amount of sediment placed over the 50-year model run is somewhat higher for Whiskey and East/Trinity Islands (increase of 1-2  $10^6$  m<sup>3</sup>, or ~2% of total sediment volume placed). In the case of Timbalier Island, the increased sea level rise rate leads to two restorations occurring over the 50-year period of S08 compared to one restoration occurring for S07. As a result, more than twice the volume of sediment is placed at Timbalier Island for the S08 scenario compared to the S07 scenario.

The cross-sectional area of several tidal inlets diverge from S07 to S08 during the first decade. The sub-basins of these links contain most of the upper basin marsh loss. The area of these links remain the same through the end the simulation because the maximum caps are met. An additional inlet diverges slightly starting in the fourth decade. This difference is due to the difference in tidal range between the scenarios, as its sub-basin contains no land from the beginning. All other inlets are the same between the scenarios due to minimum or maximum caps being reached.

The tidal range in all compartments increases with time in both scenarios. Much of the interior of Terrebonne Basin is open water, and there is little difference in the tidal range of the interior compartments by the third decade. As more land loss occurs and there is greater connectivity, there is less tidal attenuation. The two upper-most compartments shown in Figure 124, Compartments 710 and 512, start with different tidal ranges. By the end of the fourth decade in S08, attenuation has decreased, and the two compartments have the same tidal range (green and purple lines in Figure 124). For S07, this change does not occur until the last two years.

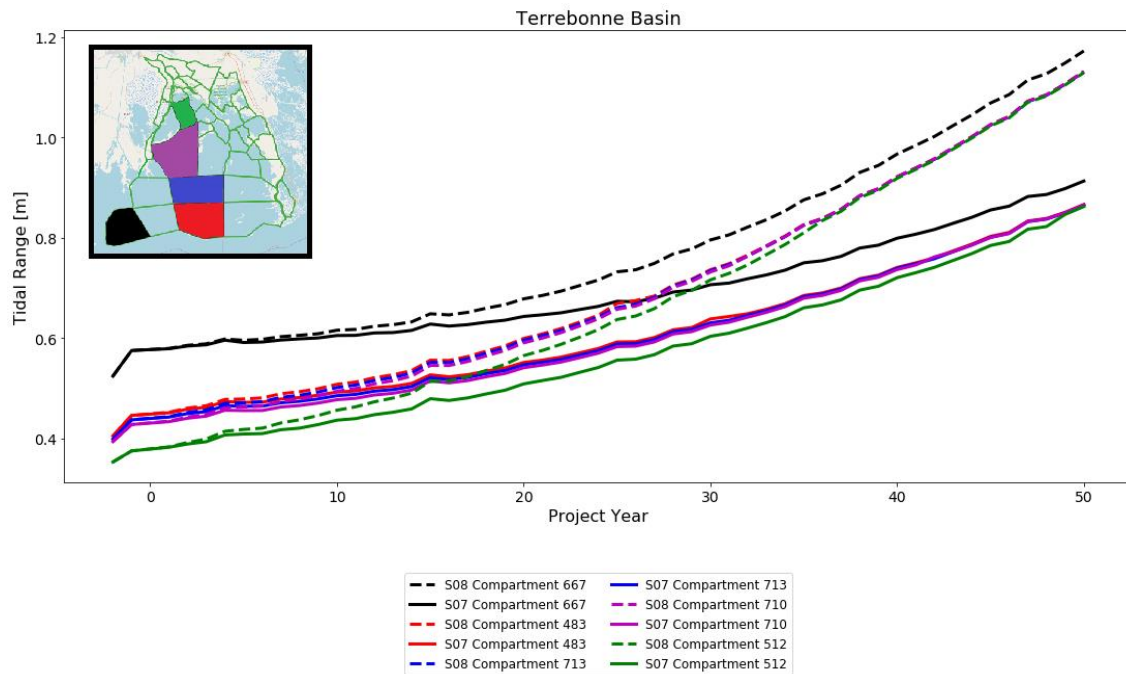


Figure 124. Tidal range for ICM-Hydro compartments contributing tidal prism to Terrebonne Basin tidal inlets.

Both the S07 and S08 environmental scenario simulations saw large reductions in the amount of fish, shellfish, and wildlife habitat in the Terrebonne region. The Eastern and Western Terrebonne ecoregions were similarly affected by extensive wetland loss in both scenarios, which caused the loss of most highly-suitable habitat (HSI scores  $\geq 0.7$ ) outside of the uppermost parts of the ecoregions. The effects of the two scenarios were slightly different, however, in the Penchant ecoregion. Marsh fragmentation, increased water depths, and increased salinities generally resulted in an increase in habitat suitability for fish, shellfish, and wildlife over the S07 scenario simulation. This was also observed over the first half of the S08 scenario simulation; however, the effects of high rates of relative sea level rise and associated wetland loss in the scenario ultimately reduced habitat suitability for most species. Some of the negative effects of the S08 scenario were mitigated by the incidental introduction of freshwater, which helped keep salinities in the open water habitats more suitable for the fish and shellfish. Despite this, relatively little highly-suitable habitat remained in the Terrebonne region at the end of the S08 scenario, except for perhaps oysters.

# 5.0 CENTRAL COAST

## 5.1 INTRODUCTION

The Central Coast includes the areas around the Atchafalaya River Delta, spanning from Freshwater Bayou to the eastern banks of the Atchafalaya River, including Abbeville and salt domes like Avery and Weeks Island. The region features a series of connected bays that lead to the Gulf. Notable features include Marsh Island and the Atchafalaya River and Wax Lake deltas. The Central Coast of Louisiana is the “Gateway to the Atchafalaya Basin,” and the landscape is shaped by the Atchafalaya River, which branches off the Mississippi River and carries up to 30% of its flow below the Old River Control Structure west of Simmesport. The Central Coast is one area of the state that is building land through active growth of the Atchafalaya River and the Wax Lake deltas. Because of the proximity to the Gulf and the influence of the Atchafalaya River, the ecosystems in this region are diverse and include freshwater swamps and saline marshes, as well as some of the most prominent areas of actively building deltas in the United States; the Atchafalaya River Delta and the Wax Lake Outlet.

## 5.2 FWOA STAGE

### LOWER PROJECT SELECTION SCENARIO (S07)

In areas near the Atchafalaya River and Wax Lake Outlet, stages increase with sea level rise; however, high seasonal variability with river discharge still dominates stages during early decades. Conversely, stages in open water compartments within the Atchafalaya Bay complex not directly adjacent to the deltas generally track the stages imposed at the Gulf boundary, with sea level rise superimposed on the seasonal mean stage cycle. With the sea level rise imposed in this scenario, the mean annual stages begin to exceed typical annual peak stages in initial years by approximately Year 40 (Figure 125). There is a slight spatial gradient with higher mean stages in more inland marsh compartments.

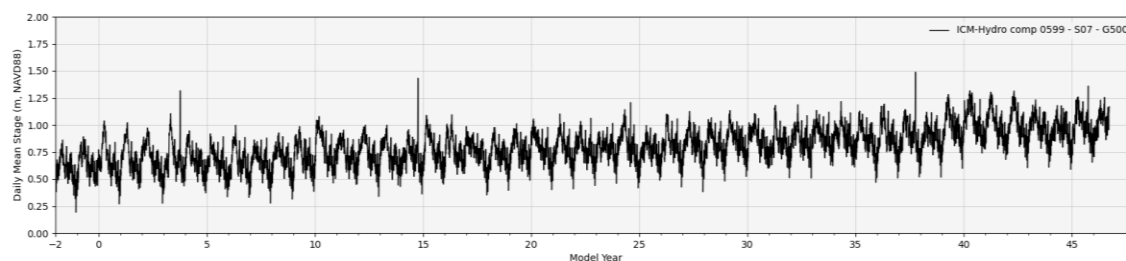


Figure 125. Stage, under S07, in compartment 599, representative of the Central Coast region directly influenced by the Atchafalaya River and Wax Lake Outlet where seasonal discharge trends are evident.

## HIGHER PROJECT SELECTION SCENARIO (S08)

Stages for S08 in the Central Coast region are as expected given the S07 results. In more western areas with less Atchafalaya River and Wax Lake Outlet influence, stages vary seasonally along with the Gulf boundary, though with greater long-term increases associated with this scenario's higher sea level rise rate. Areas more directly influenced by the Atchafalaya River and Wax Lake Outlet have seasonal trends more influenced by yearly discharge cycles, with similar long-term increasing trends.

### 5.3 FWOA TIDAL RANGE

## LOWER PROJECT SELECTION SCENARIO (S07)

Tidal ranges throughout the Central Coast region are as expected, with trends that tie directly to the seasonal and long-term trends in stages discussed above. In open water compartments in the Atchafalaya Bay complex, tidal ranges have slight seasonal variability and show a slight long-term increasing trend with sea level rise. In the more coastal marsh compartments where stages are still primarily influenced by tides, tidal range also follows a seasonal cycle with higher ranges during the summer and fall when daily mean stages are greater and lower ranges during the winter when daily mean stages are lower. Tidal ranges in more Gulfward compartments also show a slight long-term increasing trend with sea level rise. In Central Coast areas directly adjacent to and more influenced by the Atchafalaya River and Wax Lake Outlet, tidal ranges also vary seasonally, though with lower variability during river flood periods.

## HIGHER PROJECT SELECTION SCENARIO (S08)

Tidal ranges are similar to those modeled with S07. Tidal range in the region is primarily controlled by the seasonal variability in the Gulf boundary conditions except for areas between and adjacent to the Atchafalaya River and Wax Lake Outlet, where variability decreases during annual floods. In more inland marsh compartments, tidal ranges are slightly decreased in later years beginning approximately at Year 37 (Figure 126).

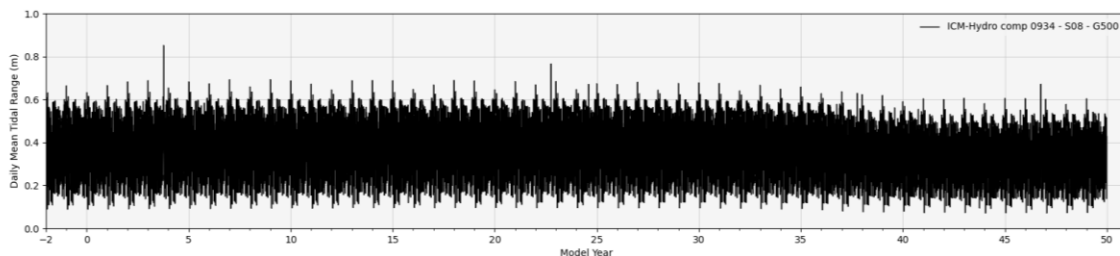


Figure 126. Tidal Range, under S08, in compartment 934, showing the decrease in tidal range in later years.

## 5.4 FWOA SALINITY

### LOWER PROJECT SELECTION SCENARIO (S07)

Salinities in the entire Central Coast region are influenced by the Atchafalaya River. In offshore areas and even the far western portions of the Atchafalaya Bay complex, salinities follow a seasonal cycle that peaks during late summer and fall when discharges are lowest. In marsh areas between and directly adjacent to the Atchafalaya River and Wax Lake Outlet, river discharges are sufficient to maintain fully fresh conditions for the full simulation. In the Atchafalaya and Wax Lake deltas, salinities also vary with river discharge, increasing from 0 ppt during low flow periods (Figure 127). Sea level rise does not appear to result in any long-term trends in salinities in this region.

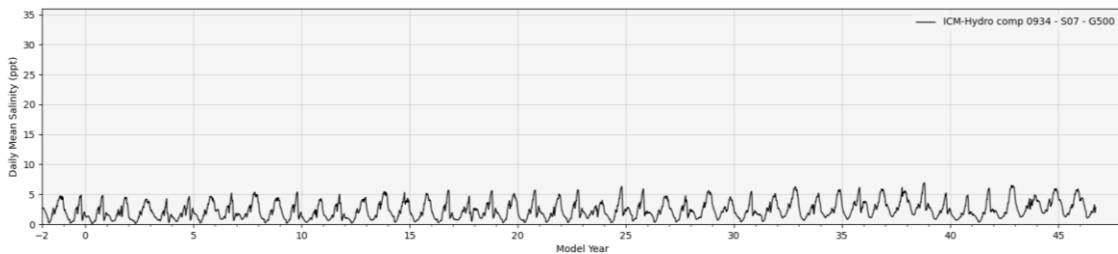


Figure 127. Salinity, under S07, in compartment 934, showing the seasonal patterns resulting from Atchafalaya River discharge.

### HIGHER PROJECT SELECTION SCENARIO (S08)

Salinities in the Central Coast region in S08 are very similar to those simulated in S07. Seasonal patterns in each area are the same, primarily influenced by the varying seasonal Atchafalaya discharge. Areas that are completely fresh in initial years do start to see higher salinities by approximately Year 30, indicating that the higher sea level rise in S08 does start to increase saline intrusion (Figure 128).

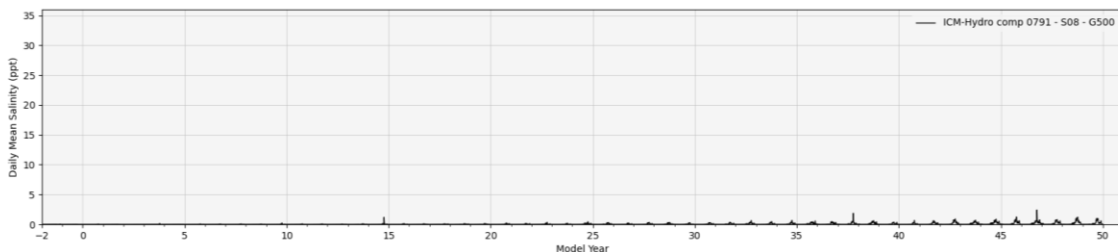


Figure 128. Salinity, under S08, in compartment 791, showing the slight saline intrusion in later years that is driven by this scenario's higher rate of sea level rise.

## 5.5 FWOA TOTAL SUSPENDED SOLIDS (TSS)

### LOWER PROJECT SELECTION SCENARIO (S07)

TSS in the Central Coast is generally high and also subject to the influences of Atchafalaya River and Wax Lake Outlet discharges. TSS in the Atchafalaya Bay Complex increases seasonally with spring floods, with peak annual values increasing closest to the deltas. TSS delivery to marsh compartments between and adjacent to the Atchafalaya River and Wax Lake Outlet is high, with little reduction in peak values compared to the river itself. There are no evident long-term trends in TSS related to sea level rise and stage trends.

### HIGHER PROJECT SELECTION SCENARIO (S08)

TSS variability through time in S08 is similar to S07, also primarily controlled by seasonal river discharge cycles with the magnitude of TSS peaks diminishing with distance from the Atchafalaya River and Wax Lake Outlet. Unlike in S07, TSS does vary over the long-term in more inland marsh compartments, with significant reductions in peak TSS values in the last decade of simulation (Figure 129). These could potentially be related to greater marsh submergence decreasing erosion and TSS.

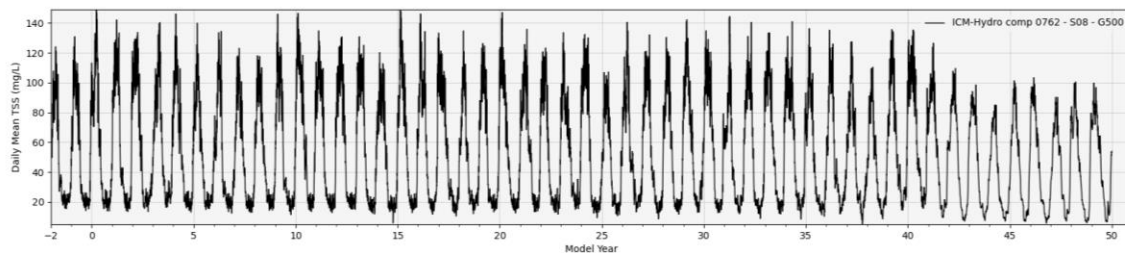


Figure 129. TSS, under S08, in compartment 762, showing the reductions in peak values in the last decade of simulation.

## 5.6 FWOA WATER TEMPERATURE

### LOWER PROJECT SELECTION SCENARIO (S07)

Water temperatures in the Central Coast region mimic the typical seasonal cycle in air temperature, with no evident spatial variability across the region. Temperatures are consistent over time, with slight increases associated with representative concentration pathway scenario-dependent warming. Long-term increases in yearly minimum temperatures are greater than long-term increases in yearly maximums.

## HIGHER PROJECT SELECTION SCENARIO (S08)

Temperatures in the S08 scenario are as expected, showing the same seasonal patterns in S07 with no spatial variability. A long-term increasing trend is more evident with this scenario's higher temperature increases. As with S07, long-term increases in yearly minimum temperatures are greater than long-term increases in yearly maximums.

### 5.7 FWOA VEGETATION

## LOWER PROJECT SELECTION SCENARIO (S07)

In the TVB ecoregion, the total acreage of brackish marsh stays relatively stable over the 50-year simulation. However, brackish marsh was lost at about the same rate that intermediate marsh was converted to brackish marsh (Figure 130 and Figure 131). This is mostly due to the loss of SPPA, TYDO, SALA, and PHAU7, while at the same time SCAM6 increased. Loss of brackish marsh on Marsh Island is illustrated by CRMS0499 (Point A in Figure 133). CRMS0499 shows decreasing SPPA, some increase in SCAM6, with a gradual change in total land area. Land loss in the last 20 years of the simulation also includes brackish marsh north of Cote Blanche Bay. This loss is demonstrated with CRMS1650 west of Vermilion Bay (Point B), which loses SPPA and gains SCAM6 as marsh is lost. At the same time, swamp is converted to intermediate marsh from west to east within the same area. An example is CRMS0513 (north of the GIWW, Point C), which shows the slow decrease in SANI and the slow increase in SALA at the western end of TVB where swamp remains the dominant.

In the vicinity and to the west of Wax Lake Outlet (Point D) fresh marsh expands for the first 40 years, but at the same time brackish and saline marshes are slowly lost on Point au Fer (Point F). These changes on Point au Fer are illustrated with CRMS0309, which shows decreasing SPAL and increasing JURO with accelerated loss in the last six years of the simulation. The increase in fresh marsh is due to expansion of ZIMI, SALA and to a lesser extent SALA2. In the Atchafalaya delta (Point E), TYDO and PHAU7 increase. This is demonstrated with CRMS6304, which slowly gains land, but changes from ELCE to PHAU7 dominated. Some of the stable fresh marsh in ATD may be misleading. For example, TRNS0403 is classified as fresh because of its FFIBS score throughout the simulation (Figure 132). However, this site has a mix of swamp, fresh, and intermediate species that changes over time (SANI decreases, ZIMI and SALA increase). These changes slowly increase the FFIBS score but not enough to change from fresh to intermediate marsh.

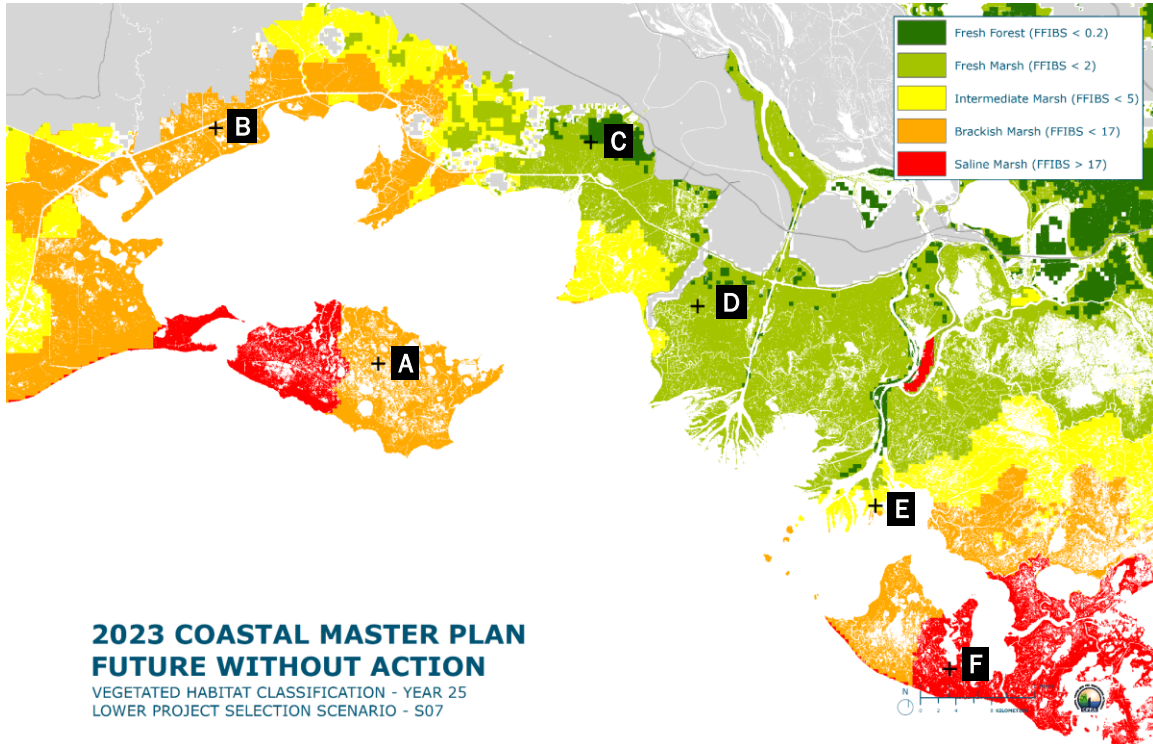


Figure 130. Wetland type (FFIBS score) distribution of the Central Coast region under scenario S07 in Year 25.

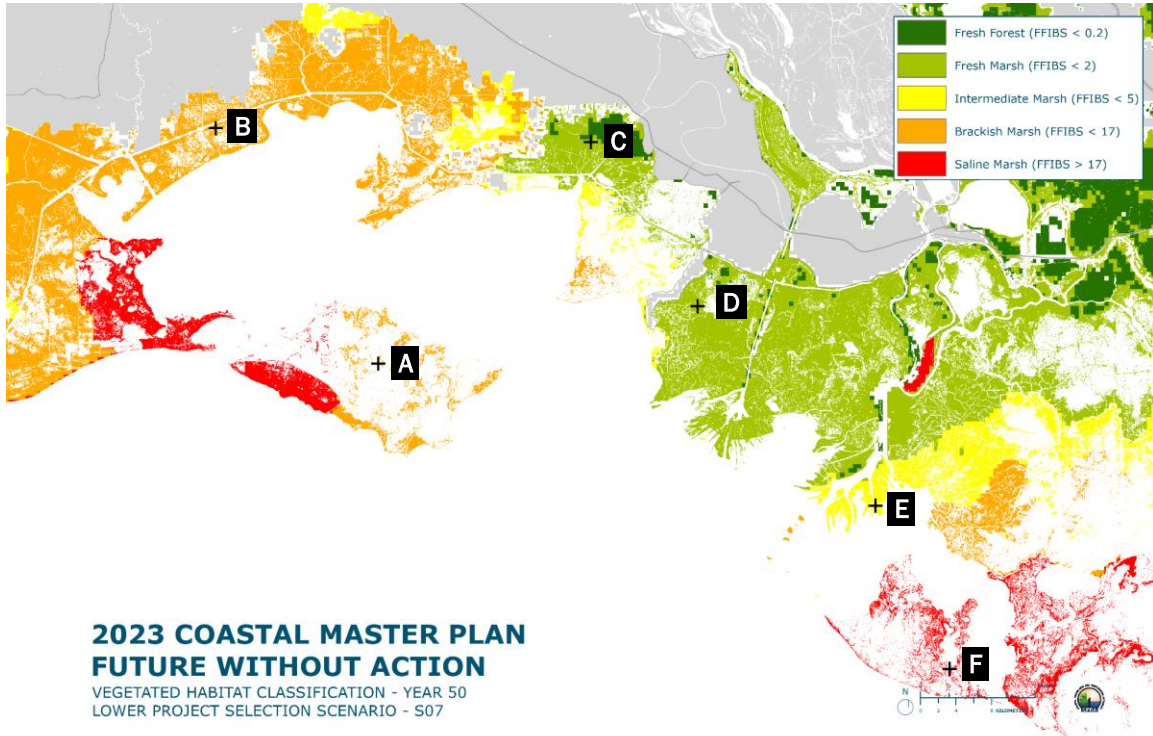


Figure 131. Wetland type (FFIBS score) distribution of the Central Coast region under scenario S07 in Year 50.

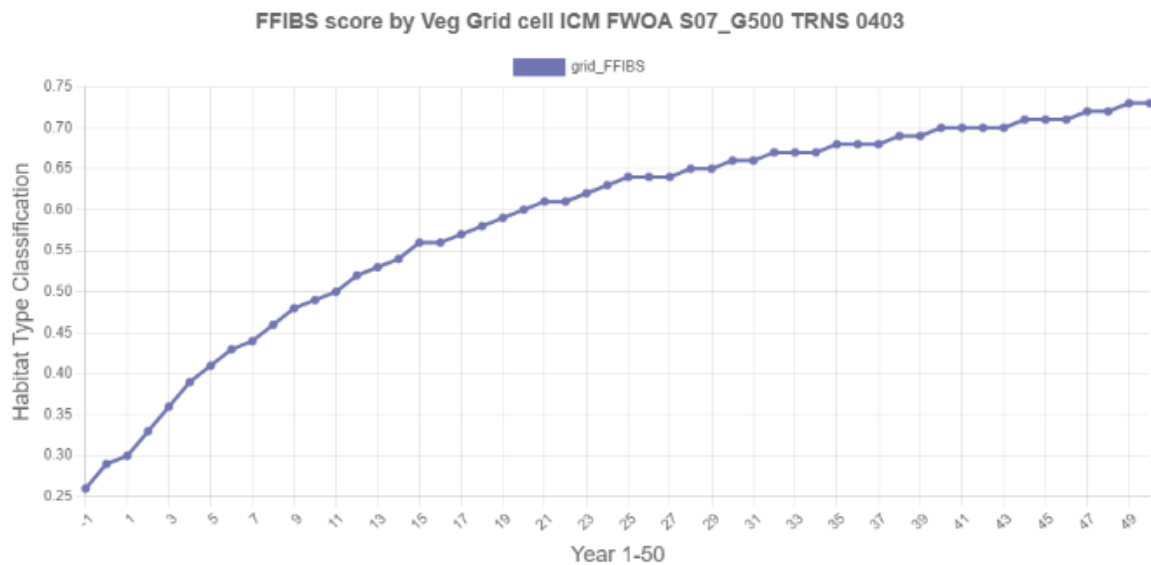


Figure 132. Changes in species composition and corresponding changes in FFIBS score for TRNS0403, west of the Wax Lake Outlet (Point D in previous maps).

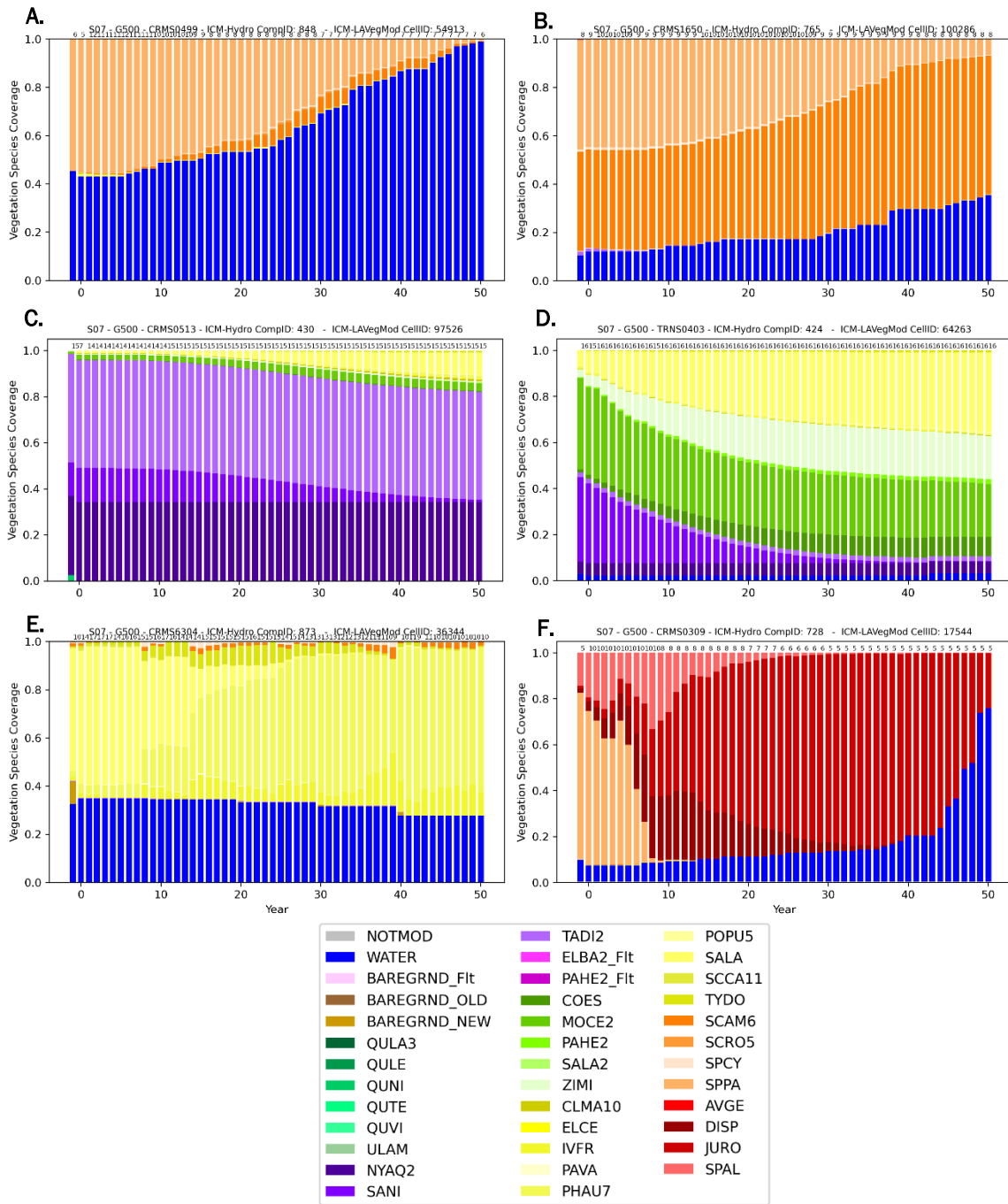


Figure 133. Change in vegetation cover under S07 is shown at representative points in the Central Coast region. Point locations are shown in previous Central Coast region map figures.

## HIGHER PROJECT SELECTION SCENARIO (S08)

In the TVB ecoregion, land is relatively stable in the first decade and decreases slightly in the next two decades under S08. During the second and third decade most of the loss occurs in brackish marshes, while at the same time intermediate marshes are converting to brackish marshes. In the last two decades land loss occurs both in brackish and intermediate marshes (Figure 134 and Figure 135). The loss in brackish marshes is shown for CRMS0499 and CRMS1650 (Figure 136). Loss in the TVB brackish marshes is primarily due to loss of SPPA, while conversion of intermediate marsh is driven by increases in SCAM6 and decreases of PHAU7 and PAVA. Throughout the 50 years there is also a steady decline in swamp, primarily due to steady decreases in TADI2 and SANI as exemplified by CRMS0513.

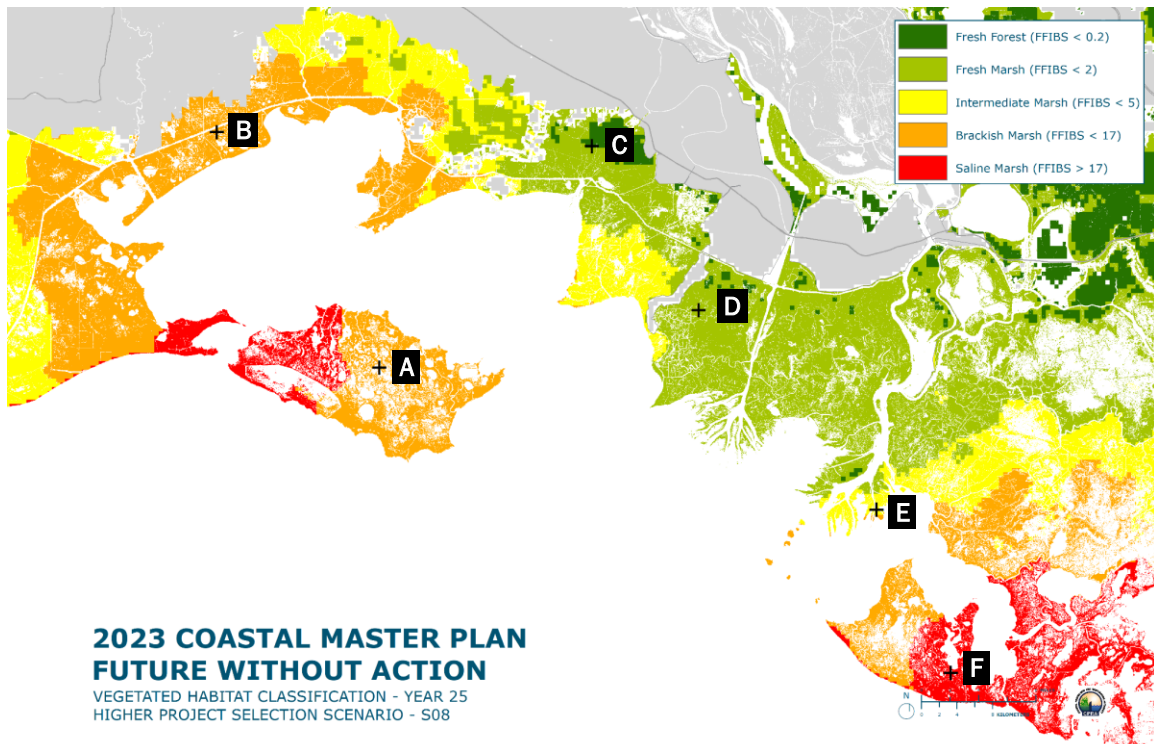


Figure 134. Wetland type (FFIBS score) distribution of the Central Coast region under scenario S08 in Year 25.

In the ATD ecoregion, land is relatively stable for the first three decades, because loss of brackish marshes on Point au Fer are balanced by expansion of fresh marshes. In the last two decades all the brackish and saline marshes on Point au Fer are lost as are fresh marshes primarily south of the intra-coastal waterway. The land loss on Point au Fer is illustrated by CRMS0309. While the relative stability of the fresh marsh is illustrated by CRMS6304 and TRNS0403. These two sites also illustrate that significant changes in species composition occur. With the delta (CRMS6304) increasingly dominated by PHAU7 and SCAM6, and the basin west of Wax Lake Outlet (TRNS0403) from dominance by SANI to

ZIMI to SALA.

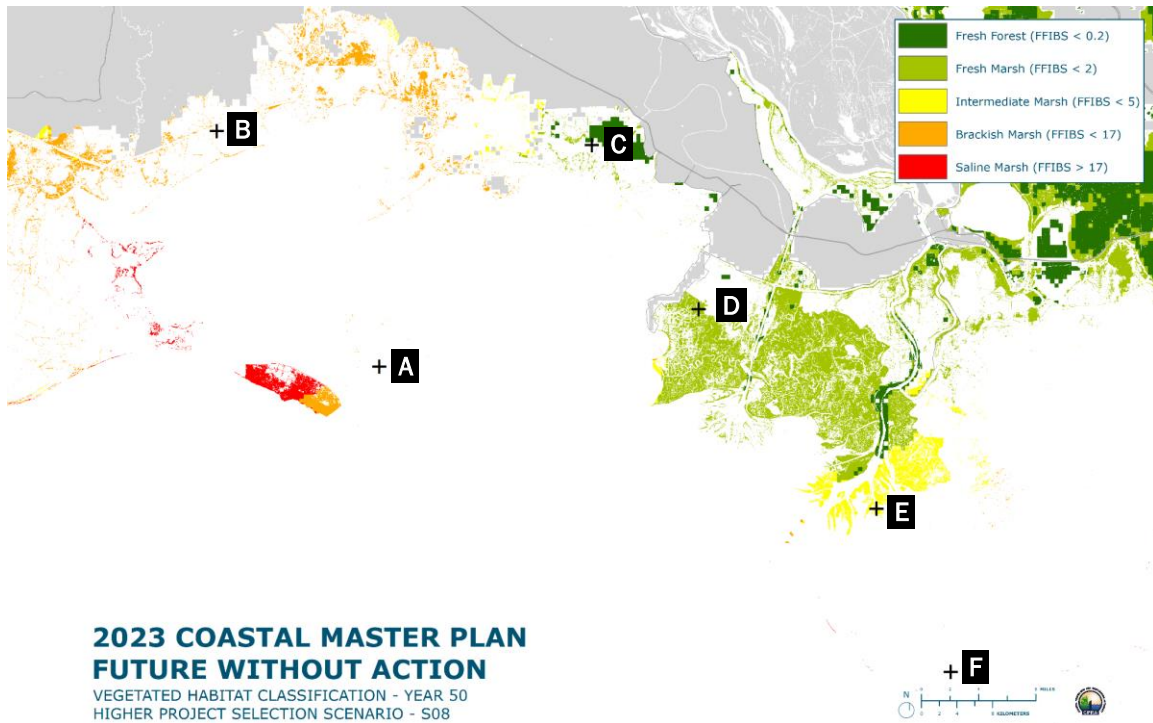


Figure 135. Wetland type (FFIBS score) distribution of the Central Coast region under scenario S08 in Year 50.

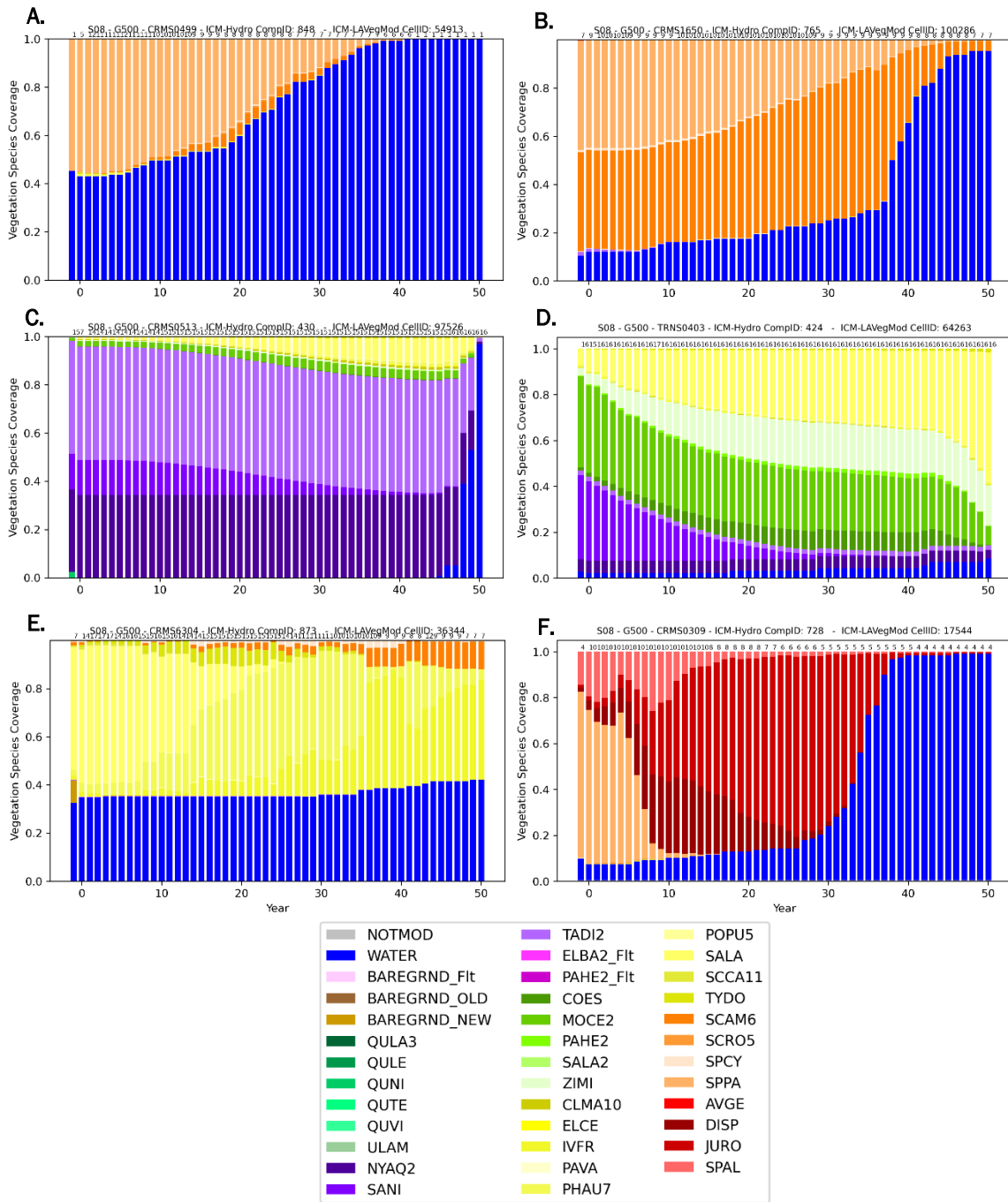


Figure 136. Change in vegetation cover under S08 is shown at representative points in the Central Coast region. Point locations are shown in previous Central Coast region map figures.

## 5.8 FWOA WETLAND MORPHOLOGY

### LOWER PROJECT SELECTION SCENARIO (S07)

The Teche/Vermilion ecoregion undergoes little change until the fourth decade. There is concentrated land loss in the area between the Jaws and Bayou Salé, and little of this land is remaining in Year 50. CRMS0544 is centrally located in this area and demonstrates the progressive loss of elevation until converting to open water in Year 46 (Figure 137).

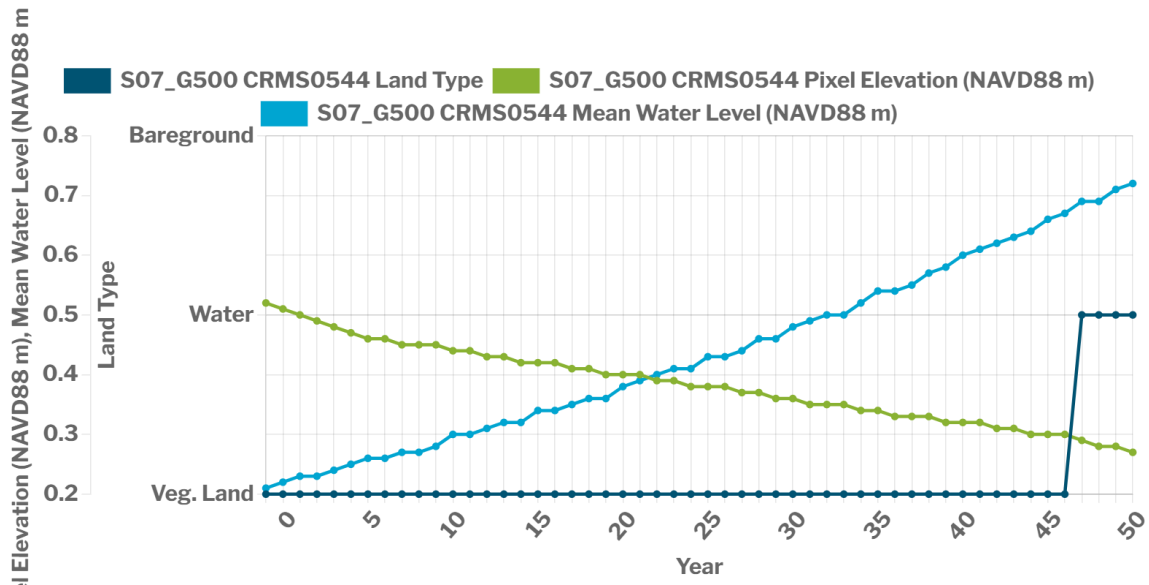


Figure 137. Elevation dynamics at CRMS0544 under S07.

Towards the west (east of Freshwater Bayou Canal) the lower elevations convert to open water, as demonstrated in the transect shown in Figure 138. TRNS0300 is the gulf-most point with increasing numbers moving inland. The three points with the higher starting elevations are maintained and remain land (Figure 138). TRNS0301 has the lowest elevation and converts to open water in Year 33, and TRNS0303 converts to open water in the last year of the simulation. Cole's Bayou Marsh Restoration remains intact in Year 50.

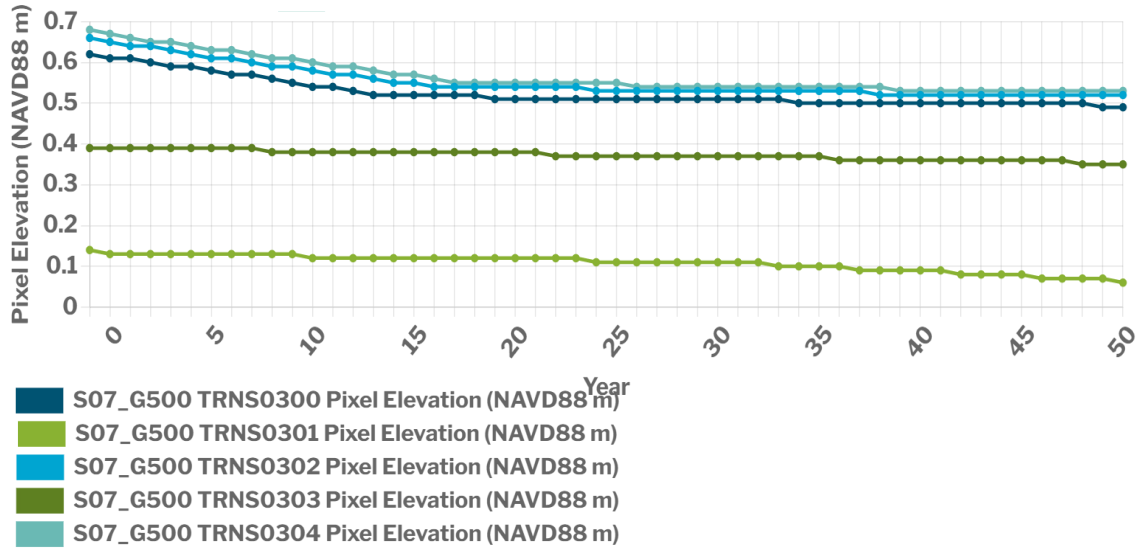
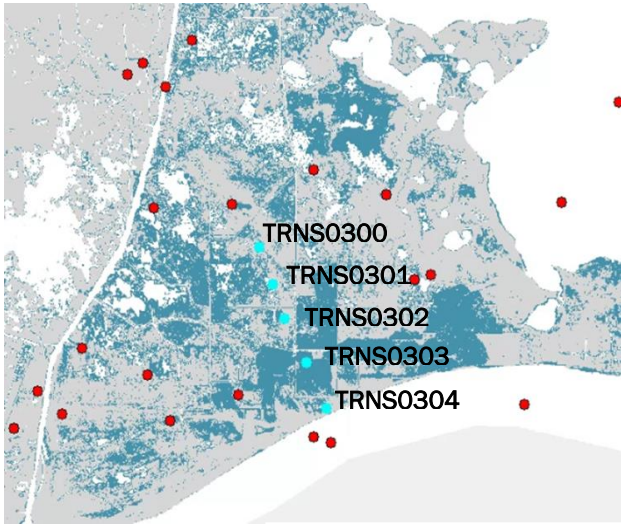


Figure 138. Changes in pixel elevation over time for points along Transect03 - location of points shown in top figure.

In the Atchafalaya Delta ecoregion, the first decade brings minor land building in the Wax Lake Delta and little change elsewhere. The lower Wax Lake Delta continues to build land with the largest land gain occurring in the second decade. This land remains through the end of the 50-year period. Areas in the upper reaches fill in progressively, and an example of this progressive growth is shown in Veg cell 48422 (Figure 139). Concentrated loss occurs in ICM-Hydro compartments 448 and 832 south of the GIWW and west of the Wax Lake Outlet in the last decade. Parts of the main stem of both deltas infill in the third and fourth decades. The west side of the Atchafalaya Delta (towards Wax Lake Delta) gains land, while the eastside and outfall islands lose land along the marsh edges.

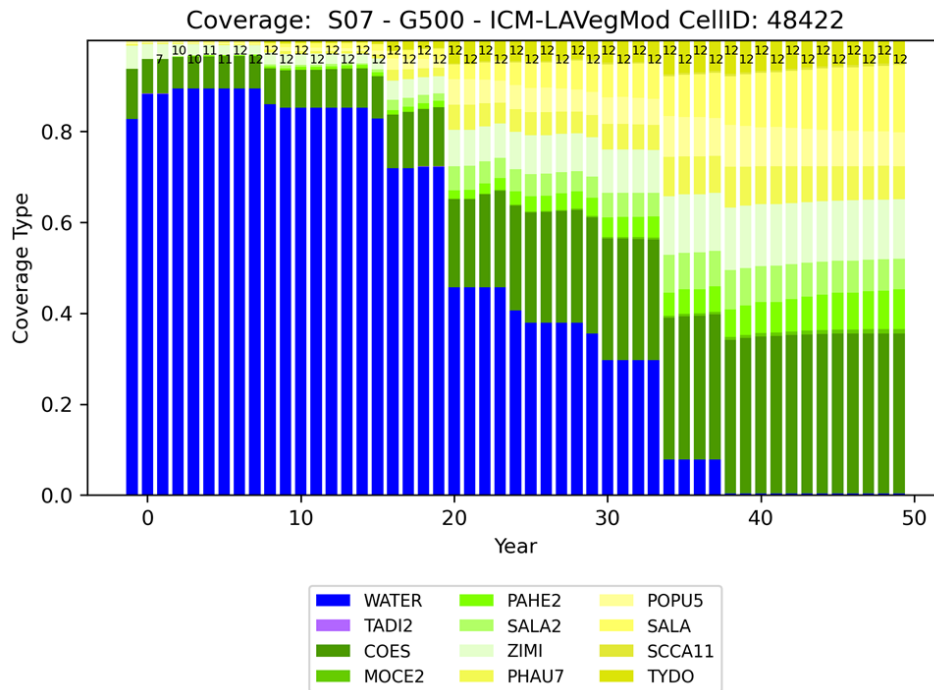


Figure 139. Progressive increase in vegetated cover at grid cell 48422 under S07.

The area surrounding Yellow Bayou (in the lower Atchafalaya Basin) infills in the second and third decades and then begins to lose land in the last decade. The land south of Fourleague Bay has dispersed land loss in the interior for the first four decades, which increases in the last decade, leaving little land by the end of the period. QAQC2204 demonstrates the progression in this area (Figure 140). There is a small deficit between accretion and subsidence, leading to a 0.06 m decrease in elevation over the 50-year period, but the increase in water level drives an increase in inundation, and it converts to open water in the last decade.

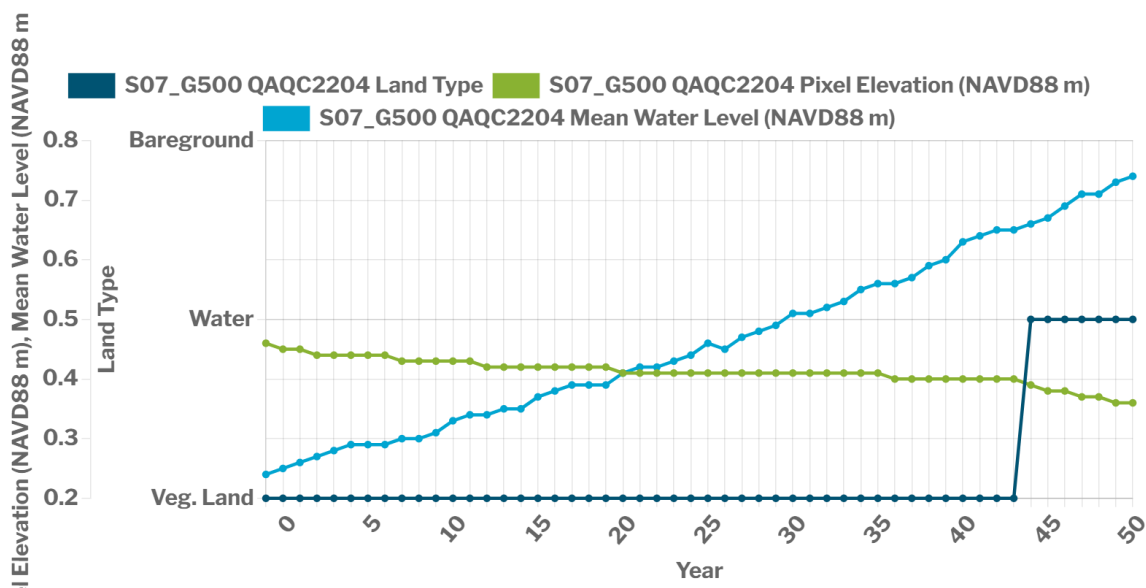


Figure 140. Elevation dynamics at QAQC2204 under S07.

## HIGHER PROJECT SELECTION SCENARIO (S08)

The first two decades of the simulation show little change in land/water across most of the region. There is some isolated land building in the Atchafalaya and Wax Lake deltas and scattered land loss in marshes surrounding West Cote Blanche Bay and Vermilion Bay (including the interior marshes of Marsh Island). A larger area of land building occurs in the lower Atchafalaya Basin in the Yellow Bayou area as sediment accumulates. Although subsidence rates are relatively high here (~1 cm/yr), largely due to shallow subsidence in the ATD ecoregion, mineral sediment deposition contributes over 10 cm of accretion at QAQC2237 in some years during the first decade, and elevation increases by almost 1 m. By Year 30 there is land loss in the outer Wax Lake Delta and outer parts of the Atchafalaya Delta. Loss is extensive across Marsh Island, and between the Jaws and the Bayou Sale ridge. These areas are subject to relatively high subsidence (around 1 cm/yr) and are classified as being in the Chenier Plain for organic matter accretion calculations. This reduces the amount of organic accretion in herbaceous marshes for a given FFBS score compared to the Delta Plain. In this region the ATD ecoregion including the areas east of the Bayou Sale ridge is considered Delta Plain and thus vegetated marshes receive higher rates of organic accretion. As deep subsidence rates decrease east to west from that ridge to Freshwater Bayou, marshes to the west of the TVB ecoregion are more likely to be able to maintain elevation with these lower accretion rates.

Areas of previously scattered land loss become more focused by Year 35 as exemplified Figure 141. Similarly areas of loss occur by Year 35 on the Rainey Refuge and in the marshes around Cypremort Point.

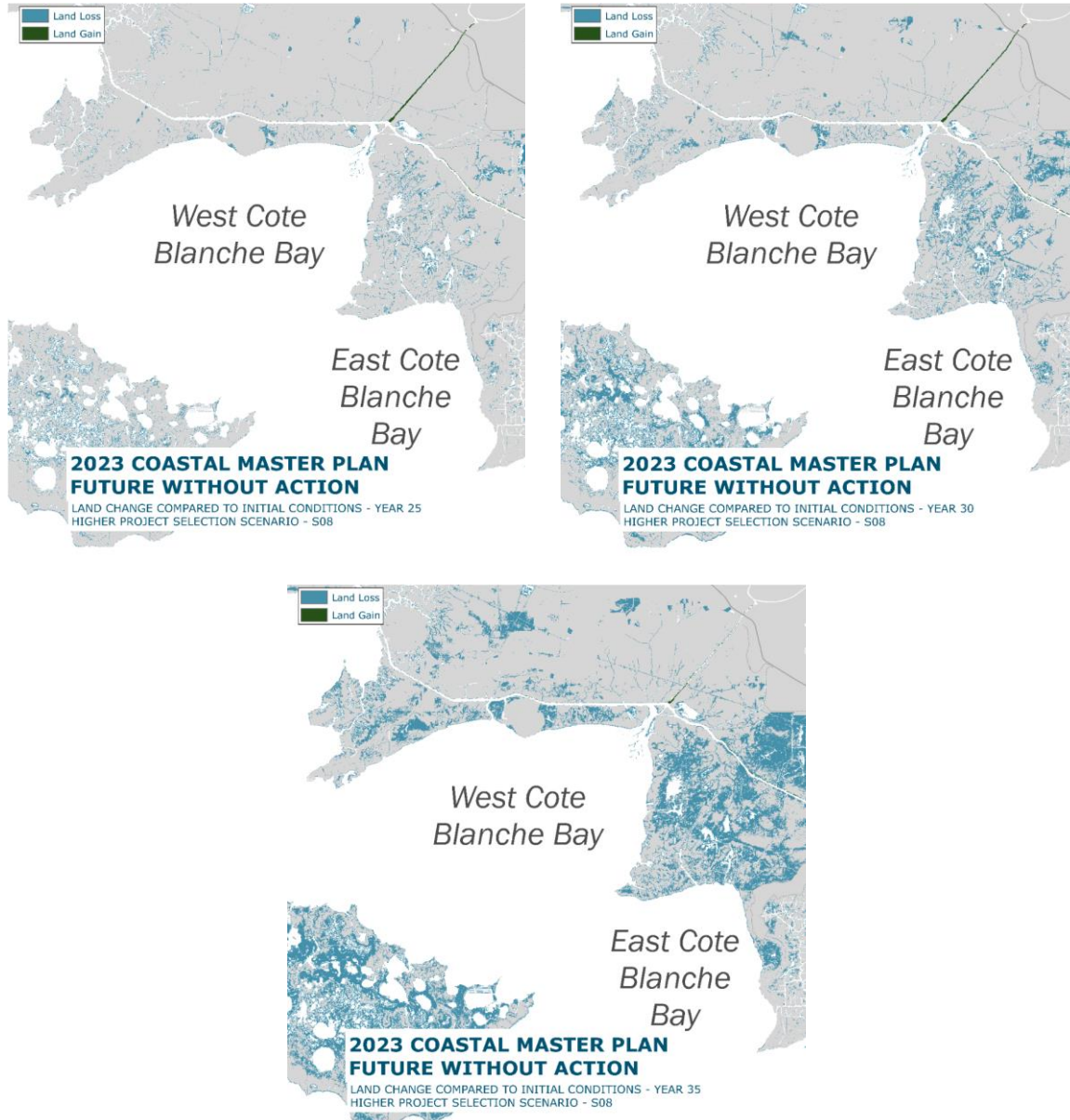


Figure 141. Cumulative land loss for part of the Central Region for Years 25 (top left), 30 (top right), and 35 (bottom) under S08.

An example of the complex dynamics near the Atchafalaya River is shown in Figure 142. The maps show land loss and land gain for Years 30 (Figure 142 top left) and Year 32 (Figure 142 top right) for the area including TRNS0602 (Figure 142 lower). Organic accretion maintains elevation in the area, but inundation increases until land is lost in FWOA Year 32. Once the area becomes open water mineral sediment deposition dramatically increases and subsidence is reduced to only ~3 mm/yr (as shallow subsidence does not apply to open water areas). Thus elevation increases, and inundation levels decline but are not sufficient low for the area to once again vegetate.

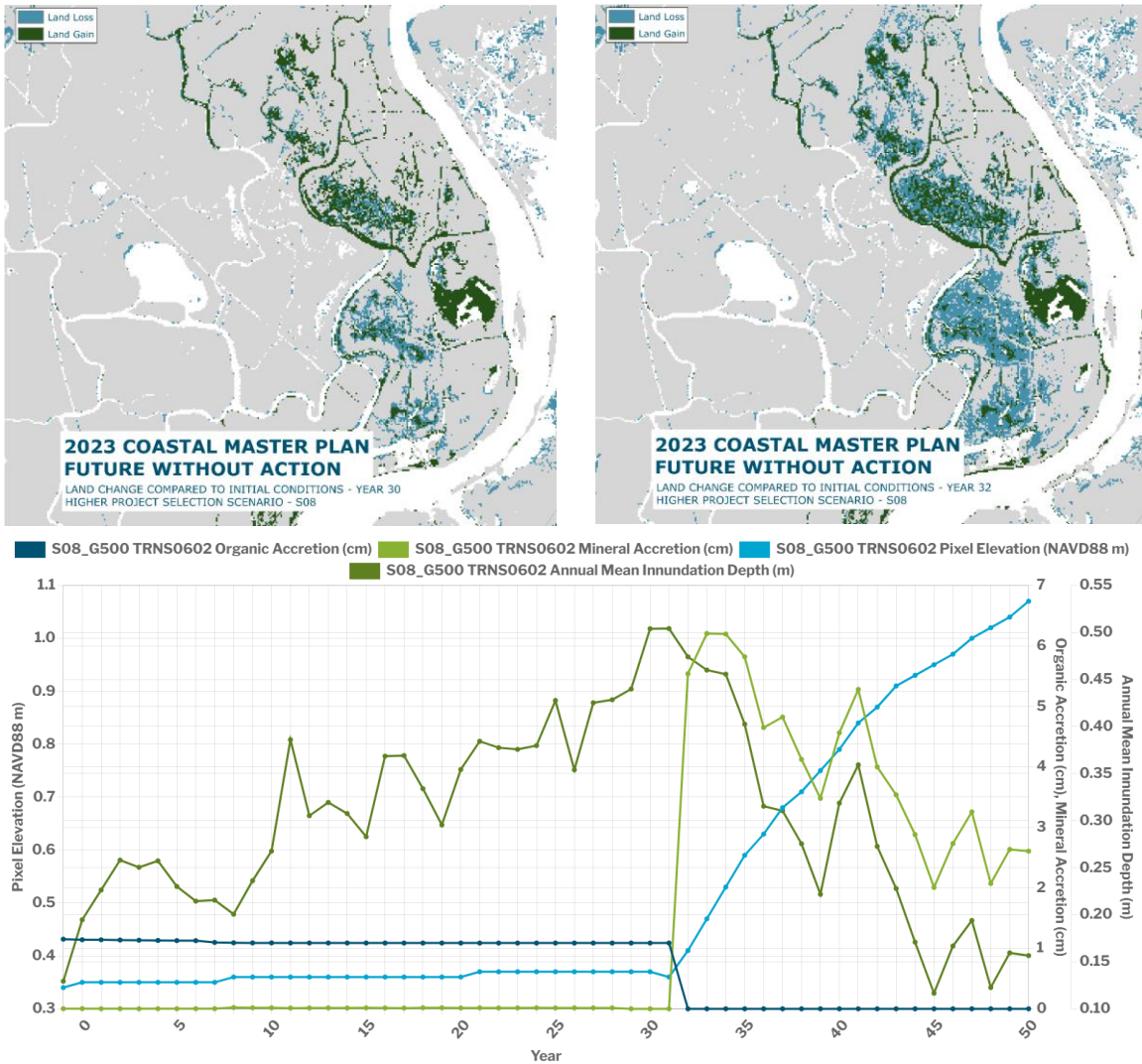


Figure 142. Cumulative land loss for S08 by Year 30 (top left) and Year 32 (top right) for an area near the Atchafalaya River in ATD, with inundation-induced loss conditions at TRNS0602 (lower panel).

Loss continues and by Year 40 in the TVB ecoregion with lower organic accretion rates there is extensive loss, with marshes remaining mainly north of GIWW and in parts of the Rainey Refuge area west of Vermilion Bay. With some exceptions, the marshes in ATD are largely intact. Figure 143A shows land loss in eastern TVB and western ATD at Year 40 with three selected points to illustrate different aspects of the dynamics. CRMS0542 starts with high elevation (Figure 143B) and negative inundation values (Figure 143C). CRMS0513 has a lower starting elevation (Figure 143B) but also has negative inundation at the start of the simulation (Figure 8C). Negative inundation means that the mean annual water level is less than the surface elevation. Early in the simulation (through Year 19 for

CRMS0542 and Year 6 for CRMS0513) they are also not flooded resulting in no contribution from organic accretion (Figure 8D). Thus, subsidence rates of 9-9.5 mm/yr reduce elevations at both sites. As the stage rises both stations begin to be flooded and organic accretion begins. CRMS0513 begins as forested wetland (FFIBS score of <0.1 until Year 20) and so received a high rate of organic accretion (Figure 143D). Organic accretion declines as FFIBS score increases before stabilizing at Year 28 and even though FFIBS score still increases organic accretion remains fairly stable. This means that elevation is relatively stable until rising water levels result in loss at Year 47. CRMS0542 has a higher FFIBS score and so lower rates of organic accretion once the marsh begins to flood (Figure 143D). Accretion cannot maintain elevation however and elevation continues to gradually decline until marsh is lost at Year 48. In contrast, TRNS0403 is in ATD and has a subsidence rate of 14 mm/yr but increases elevation throughout the simulation due to its designation as an active delta area (compartment 424) and resulting high organic accretion rates (Figure 143D). It remains vegetated through Year 50 with increased elevation and a lower increase in inundation depth (Figures 8B and 8C).

By Year 50 loss in TVB is even more extensive with some isolated marshes remaining including two areas that remain fresh near the Charenton Canal. Many marshes remain in ATD likely due to areas remaining fresh and the active delta designation. The Wax Lake Delta, however, is lost to open water as are parts of the Atchafalaya Delta.

The Coles Bayou project is included in FWOA in this region. The northern unit converts to open water at Year 42 and the southern unit at Year 44.

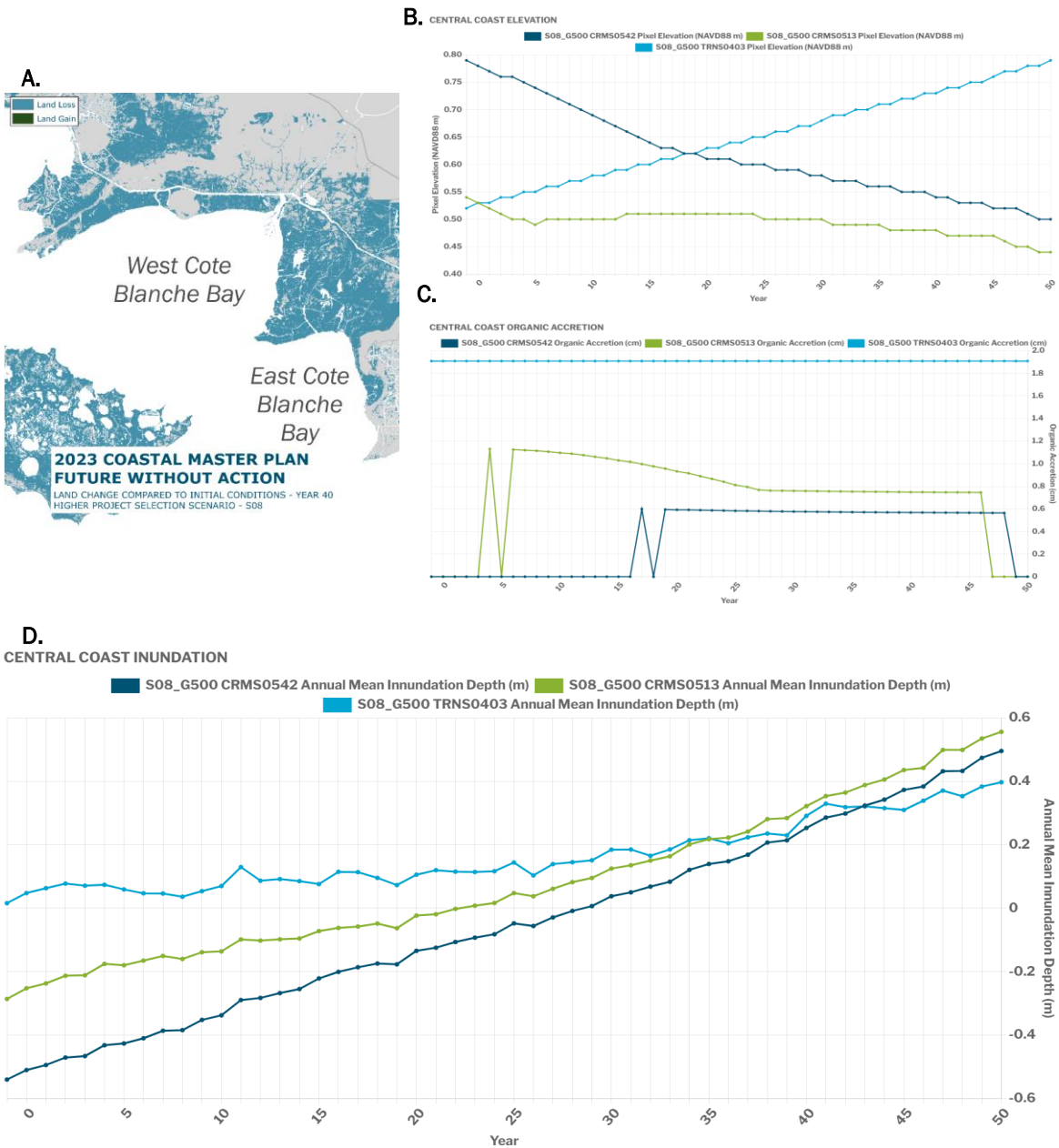


Figure 143. Cumulative land loss by Year 40 for S08 in eastern TVB and western ATD (A); land elevation (B); organic accretion (C); mean annual inundation depth (D) for CRMS0542, CRMS0513 and TRNS0403 under S08.

## 5.9 FWOA HABITAT SUITABILITY INDICES

### LOWER PROJECT SELECTION SCENARIO (S07)

The Central Coast ecoregions showed markedly different trends in habitat suitability in the S07 environmental scenario. Because of the relatively consistent inflow from the Atchafalaya River in the simulation, habitat conditions and thus habitat suitability in the Atchafalaya Basin and Atchafalaya Delta ecoregions were relatively stable over time. The small areas of wetland loss and gain that occurred caused localized increases or decreases in habitat suitability, but did not impact overall suitability across the ecoregions. Increased water levels, however, did have a notable effect in the Atchafalaya Delta, as habitat suitability for alligator decreased over time due to increased marsh inundation, and habitat suitability for gadwall and mottled duck increased due to an increase in suitable shallow water habitat. Increased water levels did not appear to affect habitat conditions in the Atchafalaya Basin, as greater rates of sediment deposition likely helped offset the increased stage. Unlike in the Verret ecoregion, this sediment deposition did not greatly affect seasonal water depths in the Atchafalaya Basin ecoregion and consequently habitat suitability for crayfish was relatively unchanged over time (Figure 144).

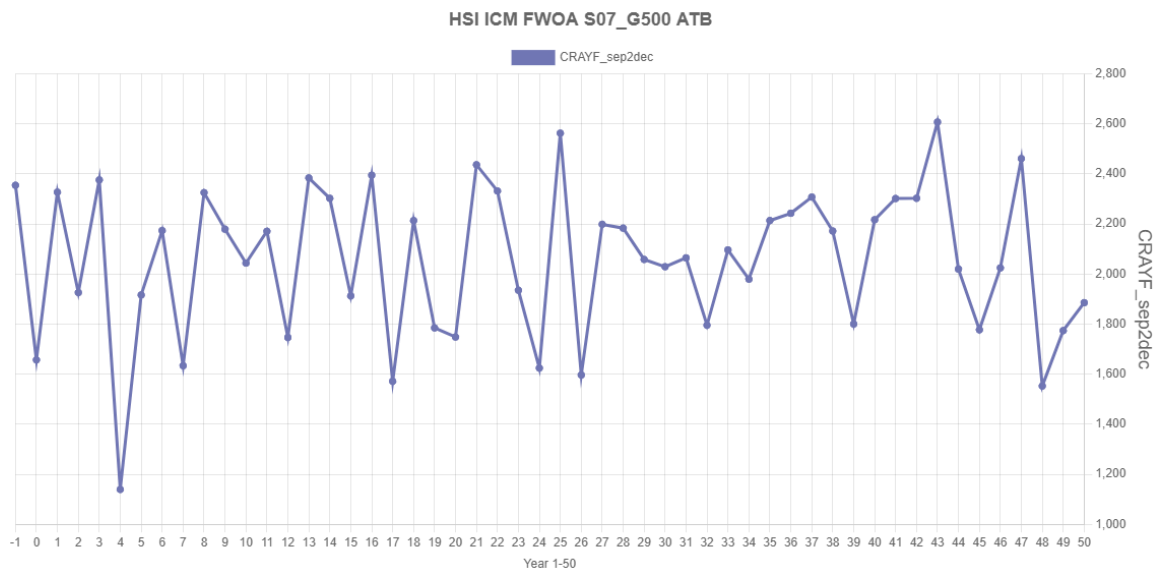


Figure 144. Total HSI score for crayfish in the Atchafalaya Basin ecoregion over the 50-year S07 environmental scenario simulation. The total HSI score was calculated by summing the individual scores for each model cell within the ecoregion.

By comparison, the Teche/Vermilion/Bays ecoregion showed large changes in habitat suitability over time for most fish, shellfish, and wildlife. These changes were due to wetland loss, and increased salinities and water levels from sea level rise. Increased salinities were most evident in Vermilion Bay and adjacent marshes during the last half of the simulation. Though the increase in salinities was minor (about 2 to 4 ppt), it contributed to increased habitat suitability for oysters, brown shrimp, and spotted seatrout in the Vermilion Bay area, with highly suitable habitat (HSI scores  $\geq 0.7$ ) expanding north into the marshes around Weeks Bay by the end of the simulation (Figure 145).

Extensive wetland loss in the Teche/Vermilion/Bays ecoregion contributed to the increased habitat suitability over time for many species. In most areas, the wetland loss resulted in a fragmented marsh landscape that was more suitable nursery habitat for juvenile fish and shellfish. Habitat suitability on Marsh Island decreased, though, because the island was mostly highly suitable fragmented marsh at the start of the simulation and then converted into mostly open water near the end of the simulation. Wetland loss also created new shallow water habitat in areas that were formerly solid marsh, which resulted in increased habitat suitability in these areas for gadwall and mottled duck (Figure 146).

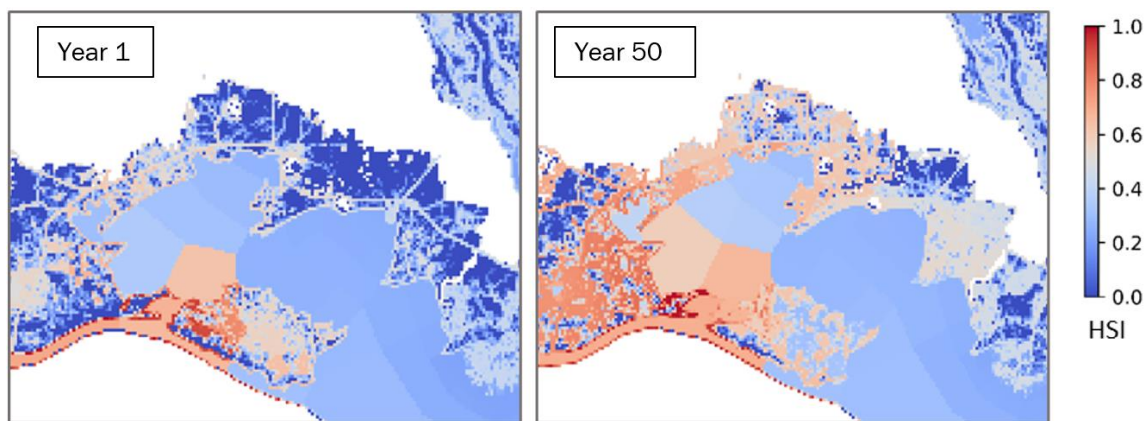


Figure 145. Small juvenile brown shrimp HSI scores across the Teche/Vermilion/Bays ecoregion for Year 1 and Year 50 of the S07 environmental scenario. Scores range from 0.0, completely unsuitable habitat, to 1.0, optimal habitat.

Increased water levels from sea level rise negatively affected habitat suitability for alligator and seaside sparrow in the Teche/Vermilion/Bays ecoregion. Increased water levels resulted in increased marsh inundation, which can greatly affect nesting success for these species. Decreased habitat suitability for alligator primarily occurred during the second half of the simulation; however, the reduction in seaside sparrow habitat was much more immediate and pronounced (Figure 147). Suitable habitat for seaside sparrow occurs at marsh elevations  $>0.09$  m above mean water level. As water levels increased, the availability of such habitat was steadily reduced such that by the third decade of the simulation most habitat was lost.

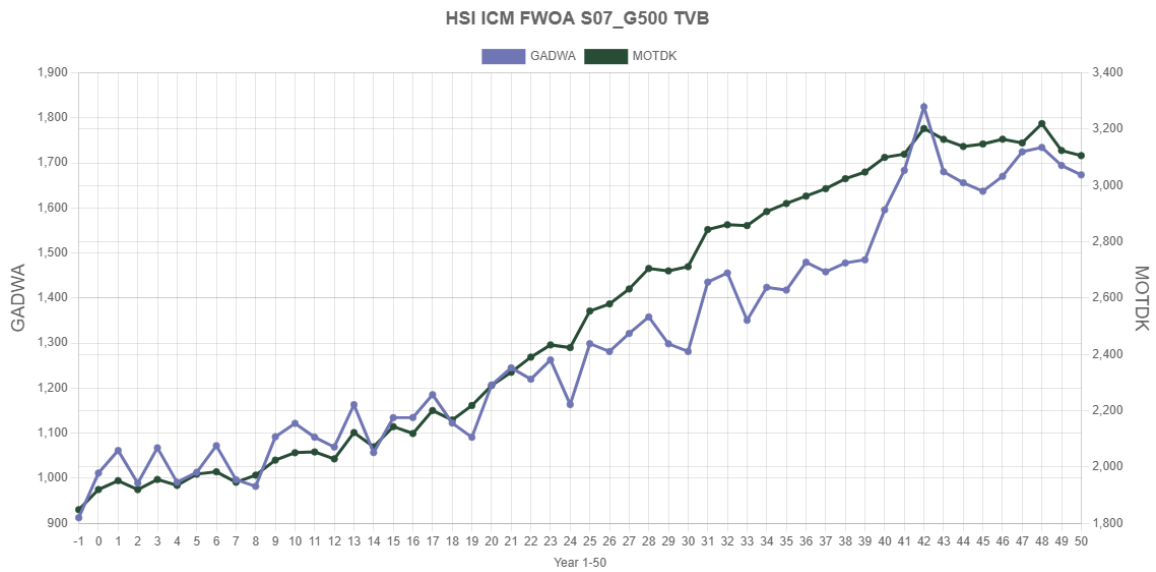


Figure 146. Total HSI score for gadwall and mottled duck in the Teche/Vermilion/Bays ecoregion over the 50-year S07 environmental scenario simulation. The total HSI score was calculated by summing the individual scores for each model cell within the ecoregion.

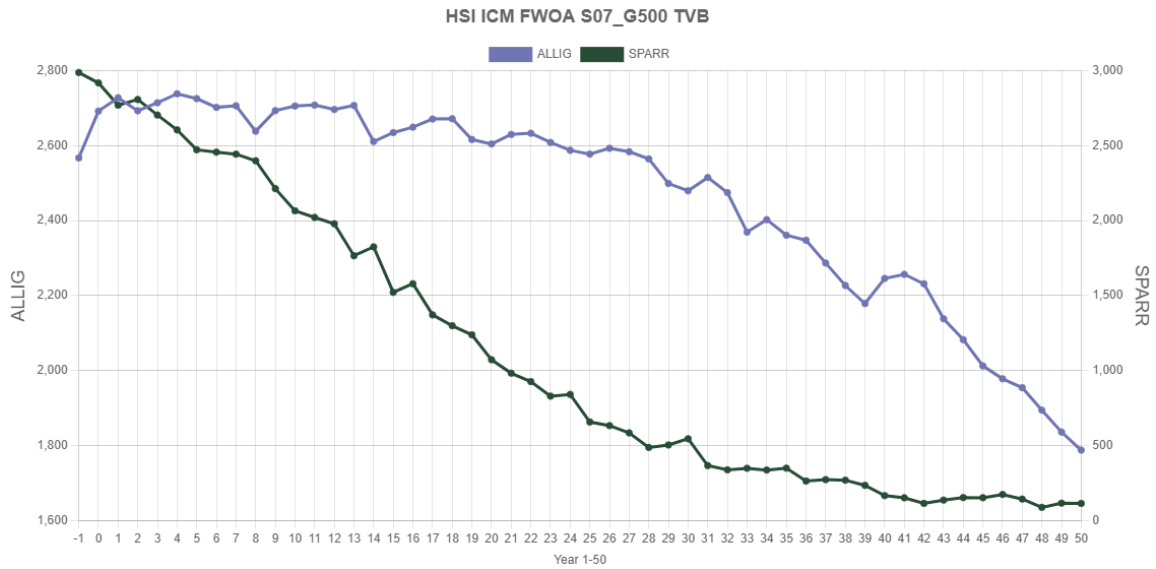


Figure 147. Total HSI score for alligator and seaside sparrow in the Teche/ Vermilion/Bays ecoregion over the 50-year S07 environmental scenario simulation. The total HSI score was calculated by summing the individual scores for each model cell within the ecoregion.

## HIGHER PROJECT SELECTION SCENARIO (S08)

While the suitability of habitats in the Atchafalaya Basin ecoregion remained relatively stable over the S08 environmental scenario simulation, there was some notable changes in the Atchafalaya Delta ecoregion. Habitat suitability increased over time for most fish and shellfish primarily due to wetland loss, which converted areas of solid marsh into a more suitable fragmented marsh-shallow water landscape. Habitat suitability for gadwall and mottled also increased throughout much of the simulation due to the increase in shallow water habitat (Figure 148). However, this increase was not apparent over the last two decades of the simulation, and suitability decreased over this time for mottled duck. This was due to the high rate of sea level rise in the scenario, which progressively increased water depths across the ecoregions. Mottled duck was more affected considering this species primarily utilizes the shallowest depths (<40 cm), whereas gadwall utilizes a wider range of water depths (though depths between 12-32 cm are most suitable) and thus would be less affected initially by the increased water depths.

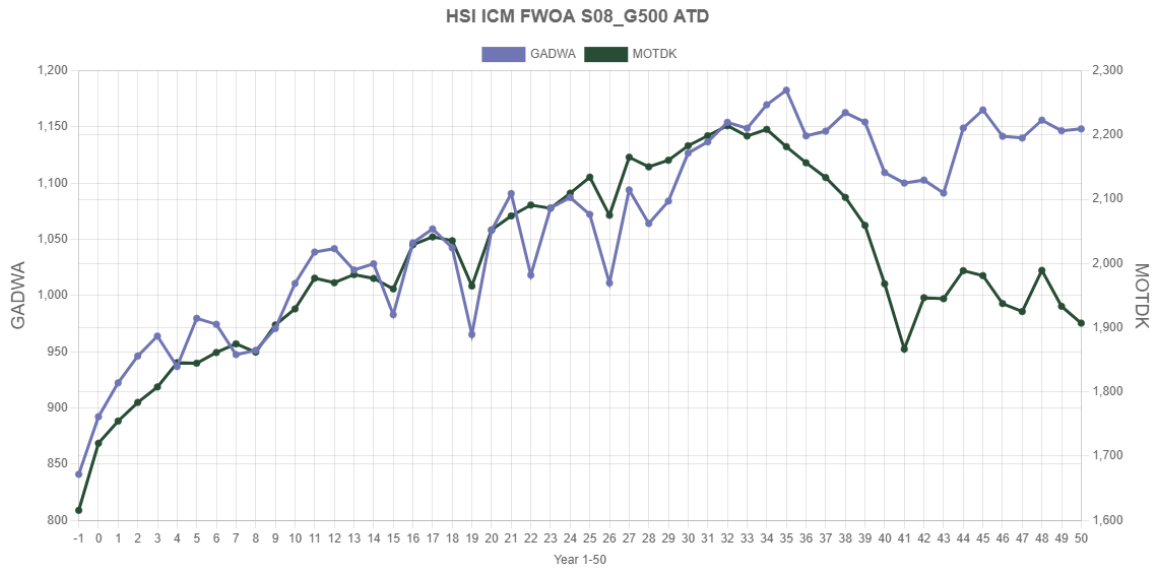


Figure 148. Total HSI score for gadwall and mottled duck in the Atchafalaya Delta ecoregion over the 50-year S08 environmental scenario simulation. The total HSI score was calculated by summing the individual scores for each model cell within the ecoregion.

Habitat suitability showed a much bigger change over time in the Teche/Vermilion/Bays ecoregion. This, again, was primarily due to extensive wetland loss that occurred in the ecoregion. Wetland loss further fragmented marshes resulting in an increase in suitability for the fish, shellfish, and wildlife species during the first three decades of the simulation. As this wetland loss progressed, though, most marsh was converted into open water and habitat suitability decreased accordingly over the last two decades of the simulation. Water levels and salinities also increased greatly during this time period in the ecoregion. These factors contributed to the decrease in habitat suitability for wildlife species by increasing water depths, marsh inundation, and reducing the acreage of more suitable fresh and intermediate marsh habitats. Fish and shellfish, by comparison, were less affected by these factors, and increased salinities allowed for an expansion of suitable habitat into Vermilion Bay for brown shrimp and oysters (Figure 149).

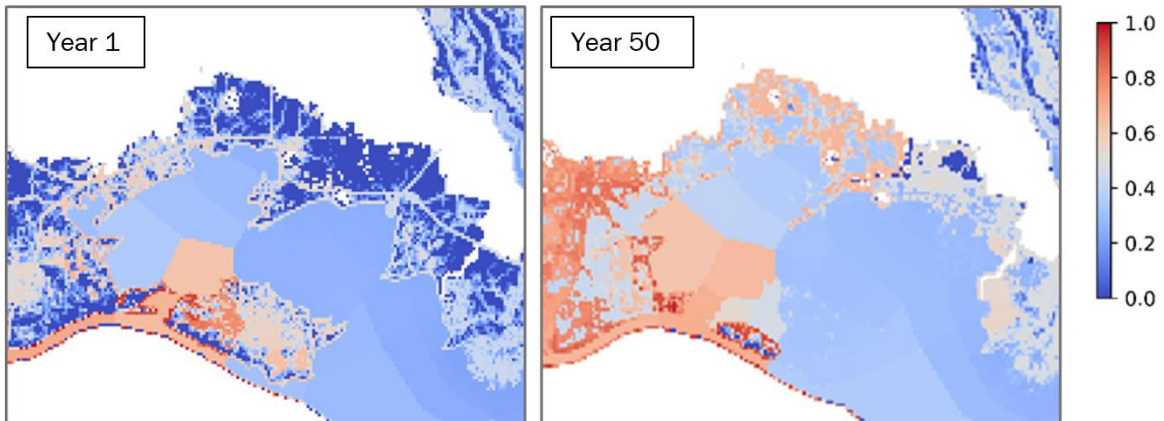


Figure 149. Small juvenile brown shrimp HSI scores across the Teche/Vermilion/Bays ecoregion for Year 1 and Year 50 of the S08 environmental scenario. Scores range from 0.0, completely unsuitable habitat, to 1.0, optimal habitat.

## 5.10 DISCUSSION

Although, there is a significant effect of the scenarios on land change, vegetation composition stays very similar under both scenarios (Figure 150).

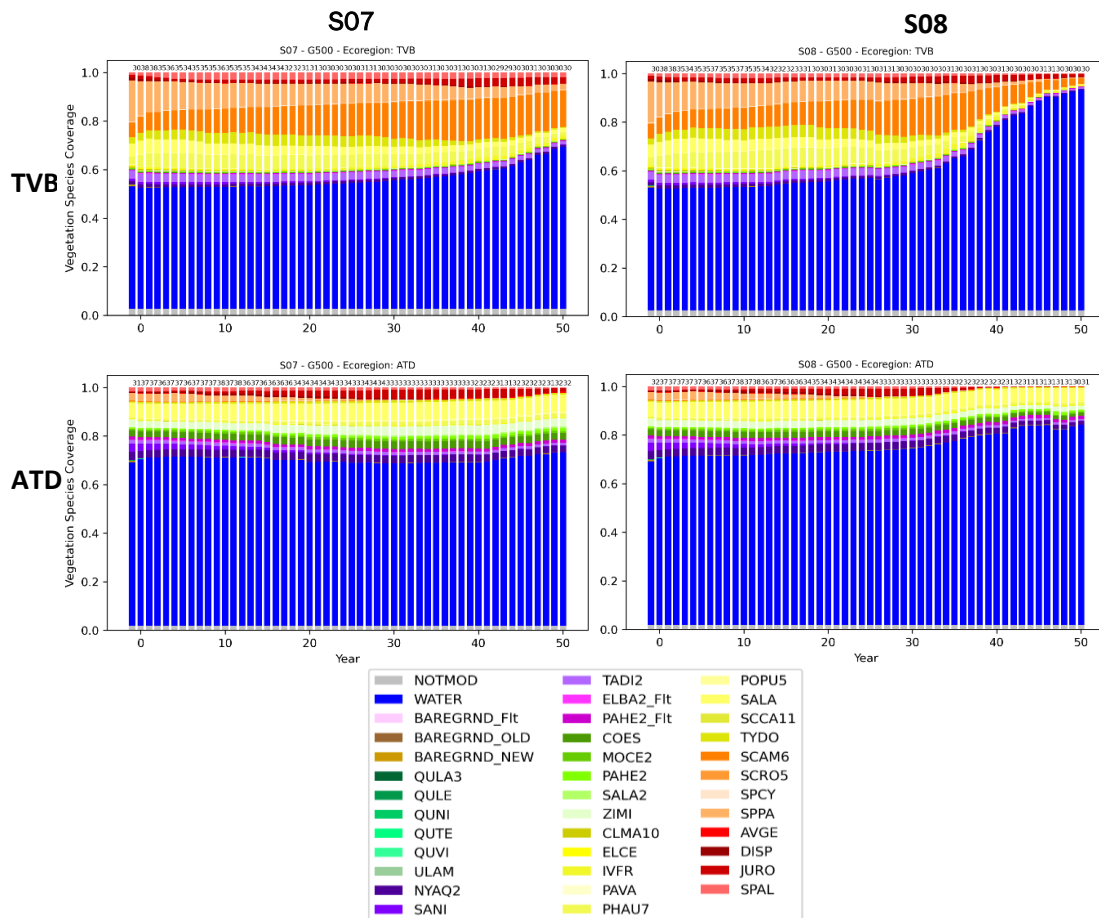


Figure 150. Comparison of vegetation cover change in the Central Coast region between the two scenarios, by ecoregion. Ecoregion vegetation coverages for the lower scenario (S07) on left, and higher scenario (S08) on the right.

There are some variations in response between the scenarios but some areas of the Wax Lake Delta maintain land throughout most of the simulation for both scenarios. CRMS0479 is located on the upper part of the Delta and despite relatively high total subsidence (8.3 mm/yr for deep and 7.2 mm/yr for shallow for S08) shows an increase in elevation over time for both scenarios (Figure 151). This is due to high organic accretion as the compartment is designated active delta for organic matter accumulation. Although mean water level rises more in S08, mean annual inundation is still below the threshold for loss until Year 49.

S07 AND S08 CRMS0479

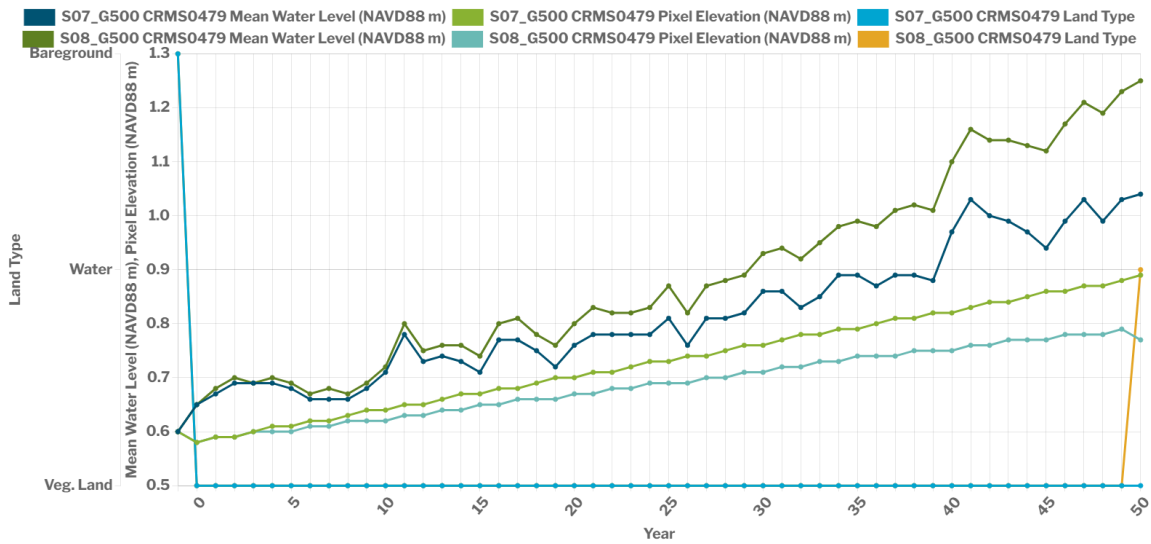


Figure 151. Comparison of conditions for S07 and S08 for CRMS0479.

Further to the northwest in marshes east of the Bayou Sale ridge, at QAQC2200 deep subsidence is slightly lower (6.6 mm/yr) and the compartment is not designated as active delta. Thus although it remains fresh (salinity <1 ppt even at the end of S08) it receives less organic accretion than the site above in the active delta. Marsh elevation is maintained in the face of subsidence in S07 but the higher shallow subsidence in S08 leads to a lowering of elevation and increased inundation results in a transition to open water in Year 36 (Figure 152). Once this transition occurs elevation decreases more rapidly due to the lack of organic accretion.

S07 AND S08 QAQC2200

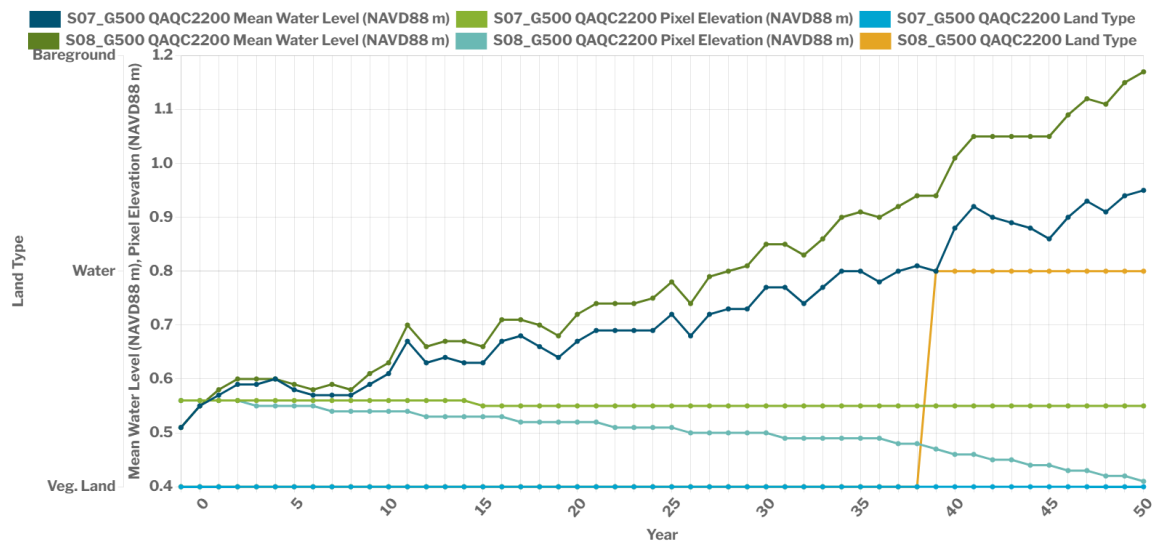


Figure 152. Comparison of conditions for S07 and S08 for QAQC2200.

Neither environmental scenario had much of an effect on habitat suitability in the Atchafalaya Basin and Atchafalaya Delta ecoregions. Wetland loss and increased water levels had somewhat greater influence on these ecoregions in the S08 environmental scenario, but their effects on habitat suitability were minor and habitat conditions were otherwise relatively stable. By comparison, there was a much larger difference between the scenarios in the Teche/Vermilion/Bays ecoregion. Wetland loss was extensive in the ecoregion during both scenarios, but in the S08 scenario most of the wetland habitat was converted into open water habitat. While these open water habitats were unsuitable for the wildlife species, they did have some value for fish and shellfish and particularly those associated with higher salinities. Regardless, the S08 scenario greatly reduced the amount of highly-suitable habitat in the Teche/Vermilion/Bays ecoregion.

# 6.0 CHENIER PLAIN

## 6.1 INTRODUCTION

The Chenier Plain spans from the Texas border to Pecan Island, Louisiana. Three main river watersheds drain through the Chenier Plain; the Sabine River on the border with Texas, the Calcasieu River, and the Mermentau River. The Chenier Plain's hydrology is highly managed. It includes major water control structures like locks and flap-gated culverts, and countless smaller ditches, culverts, and plugs. This region includes the Mermentau Basin, which is bordered on the west by Highway 27, on the south by Highway 82, and on the east by Freshwater Bayou. The major drainage outlet from the basin is via the Mermentau River where drainage is controlled by the Catfish Point Water Control Structure, which was designed to reduce saltwater intrusion to Grand Lake from the Mermentau River. High water levels in the Gulf often limit gravity drainage through this and other smaller structures, resulting in prolonged inundation of the region's intermediate to saline marshes. The Cameron Creole Watershed and large parts of the Calcasieu-Sabine Basin are extensively managed to control water levels.

Over the last century, the hydrology of the Chenier Plain has been altered dramatically through a combination of navigation channels, canals, and drainage or water control features. Major historic changes to water flow in this region resulted from dredging the Calcasieu and Sabine-Neches Ship Channels to the Gulf as well as efforts that connected the ship channels by dredging the GIWW along the northern portion of the region. Smaller, more localized changes to oilfield canals, construction of salinity and water-level control structures and levees, and impoundment of large areas of the marsh for wildlife management have also impacted the area's hydrology. At the current sea level, opportunities for drainage from the managed marsh ecosystem into coastal lakes are already highly limited – all but the tidally connected marshes are flooded too deeply and for too long to continue to support healthy marsh vegetation. With continued sea level rise in the future, drainage is expected to become more challenging in the region. More information about these issues can be found in CPRA's 2019 Basin Summary Report for the Calcasieu-Sabine Basin (McGinnis et al., 2019).

## 6.2 FWOA STAGE

### LOWER PROJECT SELECTION SCENARIO (S07)

As in other regions, water levels in the Chenier Plain generally follow the trend of the sea level rise rates that are assumed as the boundary condition under S07. While large portions of the Chenier Plain are hydraulically managed, in the model, this management is assumed to be largely gravity-drained. So, even while many structures may be flapgated and would prevent flood tides from entering, they will only be able to drain once a positive hydraulic head is present. Therefore, without forced drainage,

the impounded areas throughout the Chenier Plain are projected to remain impounded and track the overarching sea level rise of the region. Therefore, areas that are on the interior of drainage structures, such as the interior of Grand Lake (Figure 153), trend in the same upward manner as tidally connected areas, such as West Cove of Calcasieu Lake (Figure 154). While the impounded areas are not protected from high water levels due to sea level rise, the interior locations do see a slightly dampened effect, as compared to the purely tidal locations directly connected to the Gulf.

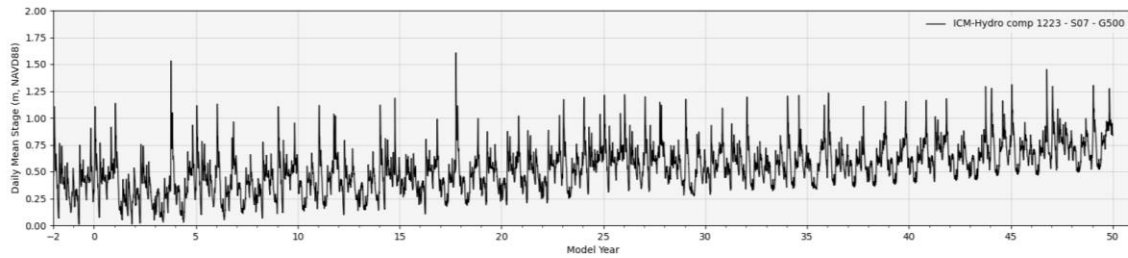


Figure 153. Stage, under S07, in Grand Lake on the interior of the Mermentau system of locks (compartment 1223).

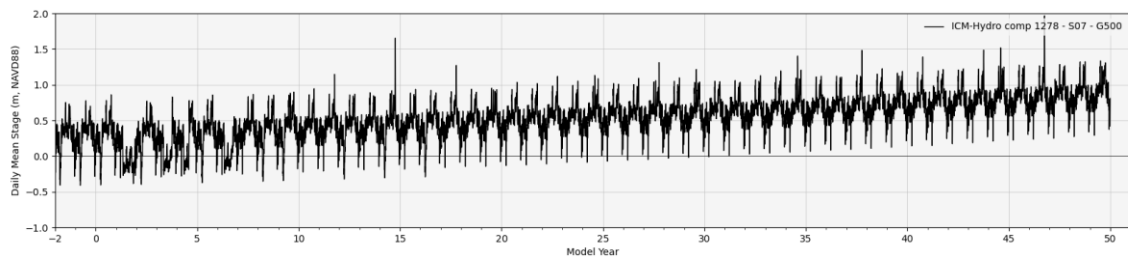


Figure 154. Stage, under S07, in West Cove of Calcasieu Lake – directly connected to the Gulf (compartment 1278).

## HIGHER PROJECT SELECTION SCENARIO (S08)

The higher rate of sea level rise in S08, as compared to S07, results in a more dramatic long-term increase in water levels across the Chenier Plain, particularly areas that are tidally connected. Again, even areas on the interior of control structures still saw a marked increase in water levels due to the higher levels in the downstream boundary conditions of any drainage structure (Figure 155). However, even though the impounded areas will see a large increase in water levels under S08, it appears that they do not rise quite as much as a more tidally-connected region, such as West Cove (Figure 156). Such a situation could rely in much longer periods of no drainage due to high downstream boundary conditions – at this point the local net precipitation/water balance could potentially become a more significant driver of water levels.

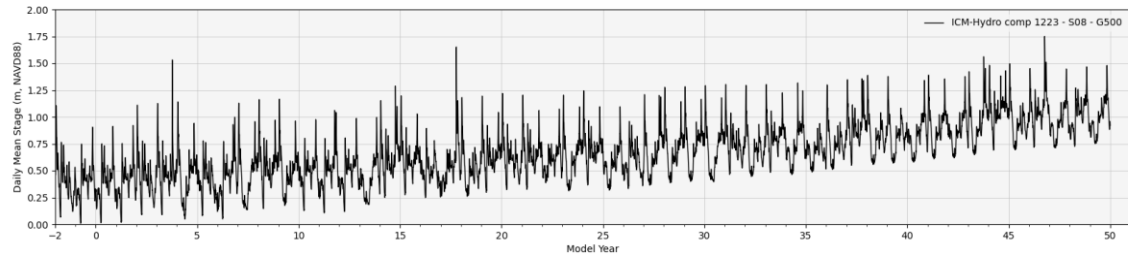


Figure 155. Stage, under S08, in Grand Lake on the interior of the Mermentau system of locks (compartment 1223).

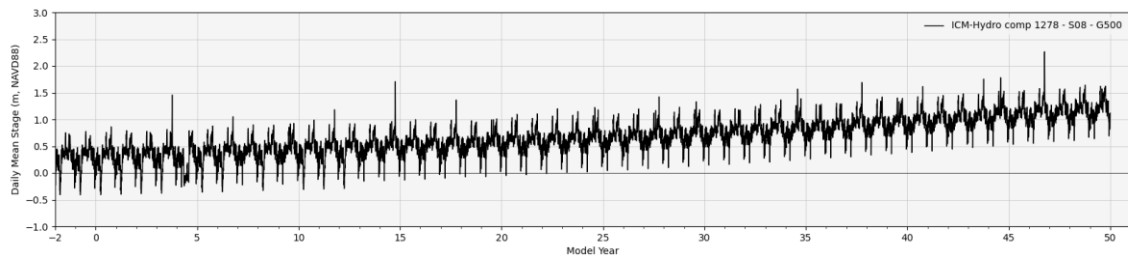


Figure 156. Stage, under S08, in West Cove of Calcasieu Lake – directly connected to the Gulf (compartment 1278).

## 6.3 FWOA TIDAL RANGE

### LOWER PROJECT SELECTION SCENARIO (S07)

Throughout the Chenier Plain, there is a distinct pattern of tidal range variability; resulting from the numerous hydraulic control structures throughout the region. This pattern is best seen in the Mermentau River system. In all areas of the Chenier Plain that are tidally connected, such as the outlet of the Mermentau (Figure 157), there is a tidal range that mimics the Gulf tidal range, albeit dampened here due to the tidal signal traveling upstream through the Mermentau River. The further from the tidal source, the greater the dampening of the tidal range, as seen partway up the Mermentau River towards Grand Lake (Figure 158). However, once the tidal signal interacts with one of the many control structures, the tidal range is essentially negligible on the interior of the structure. This can be seen in the interior of Grand Lake (Figure 159), which is bounded on all sides from tidal signals due to the numerous locks surrounding the Mermentau system.

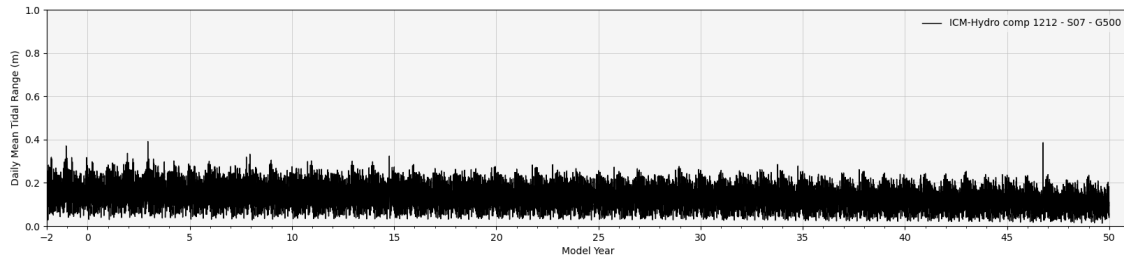


Figure 157. Tidal range, under S07, in the Mermentau River, immediately upstream of the outlet at the Gulf (compartment 1212).

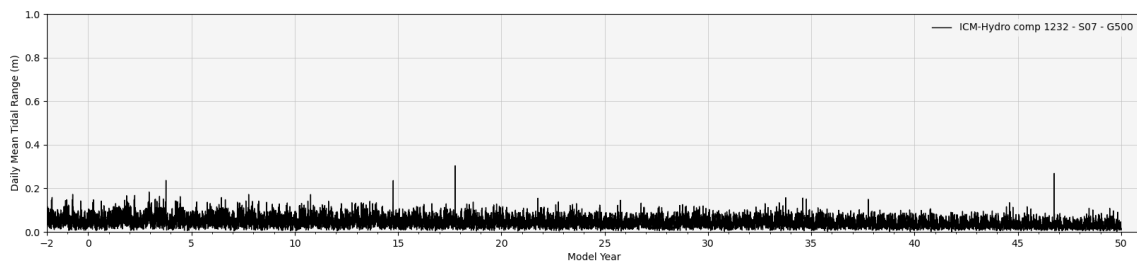


Figure 158. Tidal range, under S07, in the Mermentau River, between the Gulf outlet and the Catfish Point structure at Grand Lake (compartment 1232).

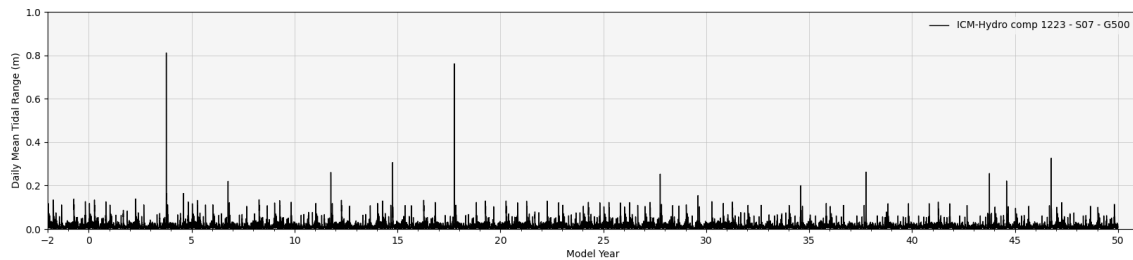


Figure 159. Tidal range, under S07, in Grand Lake on the interior of the Mermentau system of locks (compartment 1223).

## HIGHER PROJECT SELECTION SCENARIO (S08)

The tidal range dynamics under S08 in the Chenier Plain are quite similar to that of S07. Another example of the tidal-to-impounded gradient in tidal range is evident in the most southwestern portion of the Sabine Basin. Sabine Lake has a tidal range of 0.2 to 0.4 m with very little change over the long-term, even under the higher rates of sea level rise assumed in S08; it remains essentially open to the Gulf tidal dynamics (Figure 160).

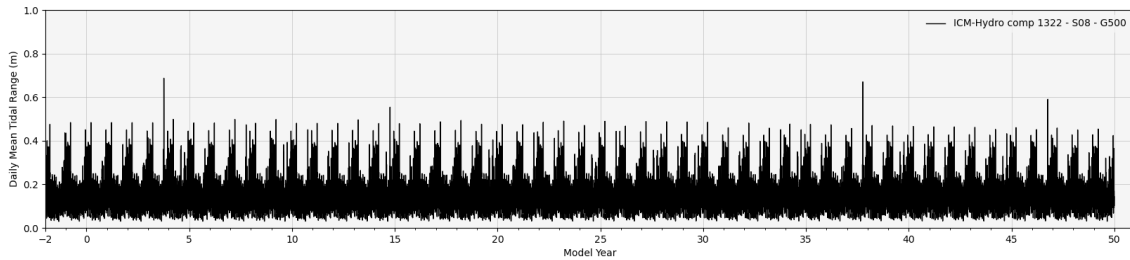


Figure 160. Tidal range, under S08, in southwestern Sabine Lake (compartment 1322).

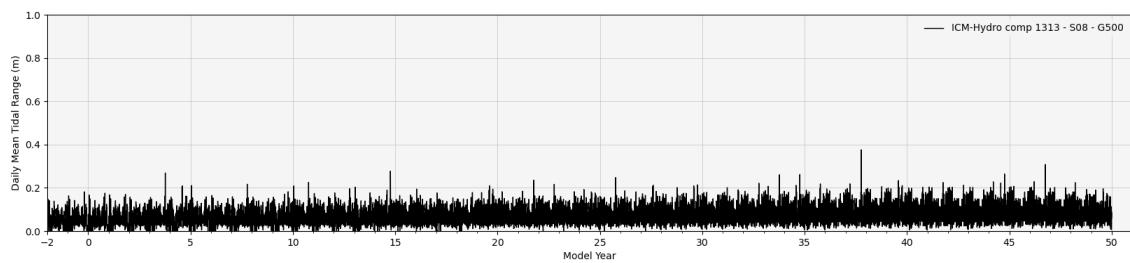


Figure 161. Tidal range, under S08, in Johnson Bayou – adjacent to Sabine Lake (compartment 1313).

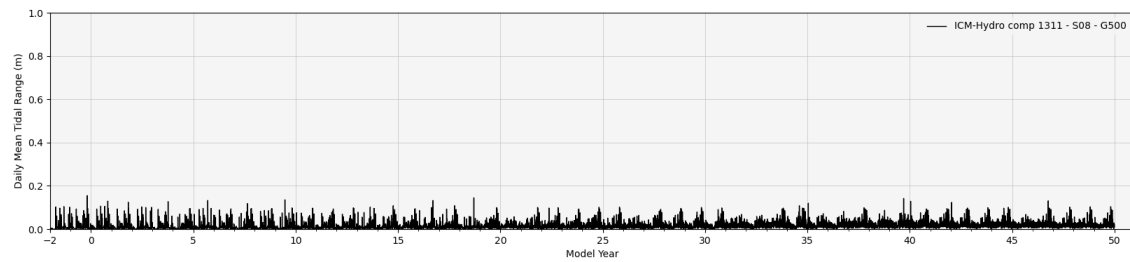


Figure 162. Tidal range, under S08, in the interior of southern Sabine Basin, north of Hamilton Lake and south of Starks South Canal (compartment 1311).

Moving towards the interior along Johnson Bayou, this tidally connected meandering waterway has a dampened tidal range, as compared to the lake, but it still sees a strong tidal signal (Figure 161). Moving further towards the interior, now behind drainage structures in the impoundments bounded by the Starks South Canal on the north, Johnson and Deep bayous on the west, and a chenier ridge on the south, the tidal range is almost completely dampened, resulting in nearly still water within this impoundment (Figure 162). This dynamic, like the Mermentau River example above, does not experience much change in future decades; even though water levels have risen substantially under S08, the tidal fluctuations (or lack thereof) are remarkably consistent; assuming, of course, that the hydraulic control structures are maintained and operated in the same manner as they are currently.

## 6.4 FWOA SALINITY

### LOWER PROJECT SELECTION SCENARIO (S07)

The many structures that impact tidal range throughout the Chenier Plain were largely put in place as means to control and minimize salinity intrusion throughout the region. To that end, the dynamics seen in the tidal range are largely mimicked in salinity dynamics under S07; the closer to a tidal connection, the greater the salinity; with reduced salinity areas on the interior of hydraulic control structures (Figure 163, Figure 164, & Figure 165).

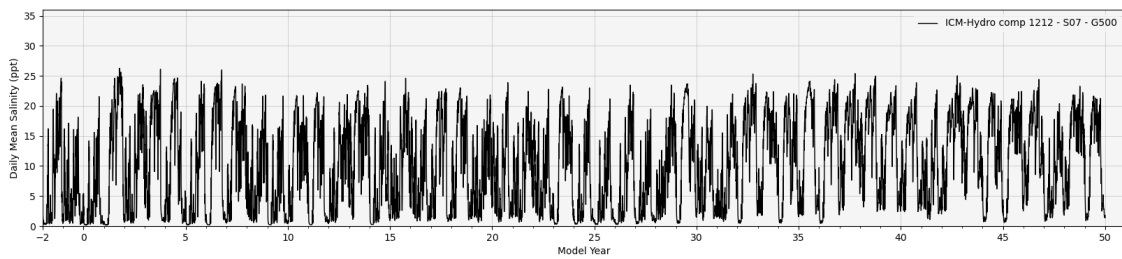


Figure 163. Salinity, under S07, in the Mermentau River, immediately upstream of the outlet at the Gulf (compartment 1212).

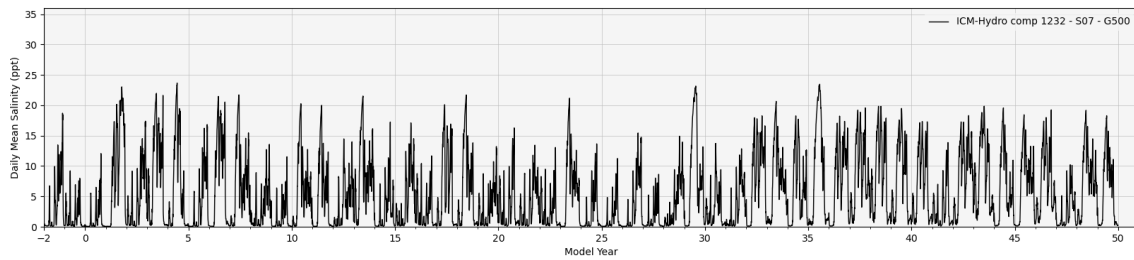


Figure 164. Salinity, under S07, in the Mermentau River, between the Gulf outlet and the Catfish Point structure at Grand Lake (compartment 1232).

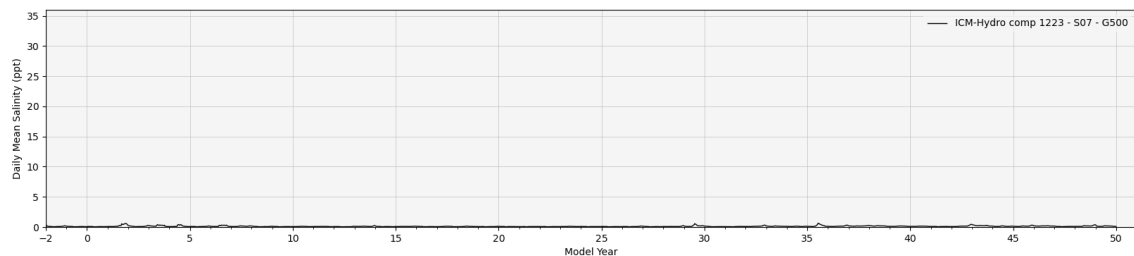


Figure 165. Salinity, under S07, in Grand Lake on the interior of the Mermentau system of locks (compartment 1223).

However, while water levels will never increase on the interior of the drainage structures from a flood tide due to the required positive hydraulic head to open a flap gate, the salinity levels on the interior can still increase via chemical diffusion. While the primary transport of salinity is due to mass convection (e.g., salinity particles move with the flowing water they are dissolved into), there is also the possibility for chemical diffusion of salinity due not to flow, but instead concentration gradients. The larger the gradient (e.g., very salty water coming into contact with very fresh water) the greater the potential for chemical diffusion. Therefore due to this transport mechanism, there can still be increasing salinity increases on the interior of the controlled system.

## HIGHER PROJECT SELECTION SCENARIO (S08)

It should be noted that both water levels and salinity concentrations at observation locations were used during model calibration and validation. While there are calibration parameters available to adjust the chemical diffusion of salinity, there is no way to measure what components of salinity in the observations can be partitioned between convective versus diffusive transport. Therefore, the diffusive behavior of salinity in future years are being modeled from calibrated values set under present-day observations, which likely have much different salinity gradients than may be experienced in future decades, particularly under the S08 sea level rise case.

## 6.5 FWOA TOTAL SUSPENDED SOLIDS (TSS)

### LOWER PROJECT SELECTION SCENARIO (S07)

In many portions of the Chenier Plain, there is very little access to suspended sediments, particularly when compared to wetlands in the active delta of other regions to the east. While there are acute periods of higher suspension during hurricane periods, the background suspended sediment concentrations in some portions of the Chenier Plain are quite low, essentially negligible. This is evident in the marshes immediately south of White Lake (Figure 166), in areas that are generally disconnected from any riverine or tidal flows.

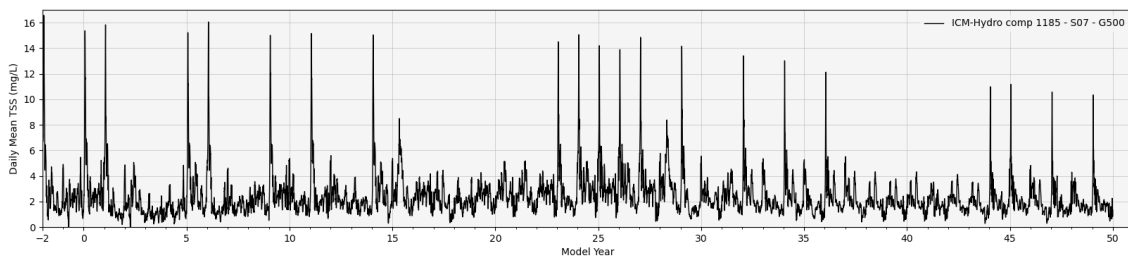


Figure 166. TSS, under S07, in largely disconnected marsh south of White Lake (compartment 1185).

## HIGHER PROJECT SELECTION SCENARIO (S08)

The low sediment supply to many areas of the Chenier Plain is consistent under S08. As seen in S07, areas with little connection to tidal or riverine flows see very little sediment entering or leaving the local system. Most of the sediment being resuspended is likely local to the wetland where it is repeatedly resuspended and deposited primarily in the same water bodies without much transport out, or into, the local system. This phenomenon would explain the decreasing concentration of TSS in later decades under S08 (Figure 167). As this area loses land under the higher scenario, the available volume of water in which the same mass of sediment can be resuspended into gets larger. Therefore, if the sediment mass remains roughly constant, but the storage volume increases, then the concentration could decrease.

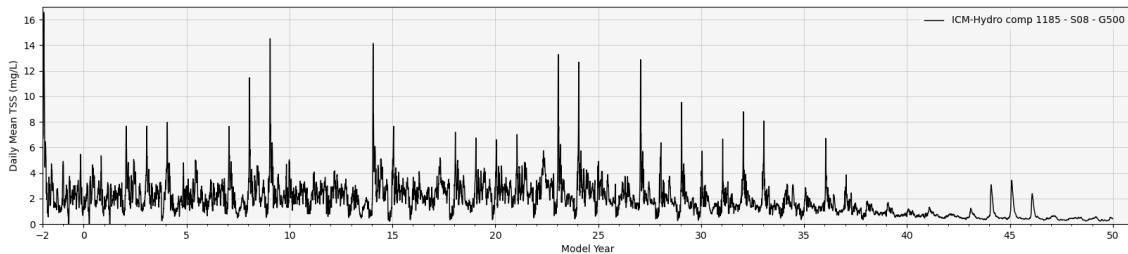


Figure 167. TSS, under S08, in largely disconnected marsh south of White Lake (compartment 1185).

## 6.6 FWOA WATER TEMPERATURE

### LOWER PROJECT SELECTION SCENARIO (S07)

Similar to the TSS signal as a result of a lack of riverine sediment availability, water temperatures in the Chenier Plain are also impacted by a lack of connectivity to the cold springtime waters of the Mississippi (and Atchafalaya) River flows. Therefore, under S07, disconnected marshes of the Chenier Plain (Figure 168) have much warmer low temperatures than that of wetlands connected to the Mississippi River in other coastal regions in the active delta plain.

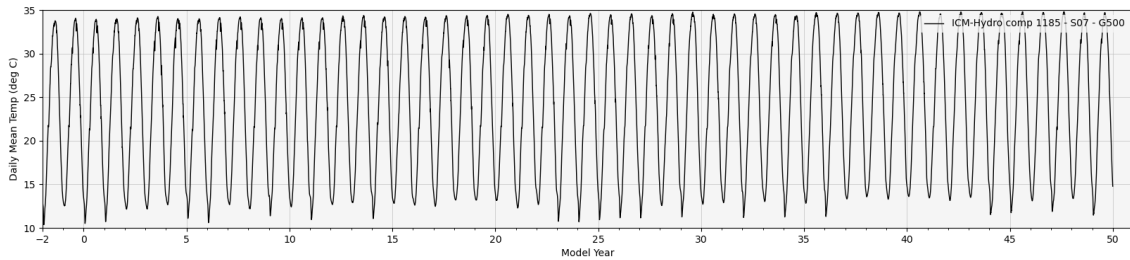


Figure 168. Temperature, under S07, in largely disconnected marsh south of White Lake (compartment 1185).

## HIGHER PROJECT SELECTION SCENARIO (S08)

The same trend in water temperatures can be seen under S08 as it was under S07. The Chenier Plain does not have access to the colder waters of the Mississippi River flows, and the minimum temperatures in the winter are indicative of warmer estuarine waters (Figure 169). In the ICM there is only one estuarine water temperature boundary condition defined for the entire offshore domain – and that is from an observation station located in Barataria Bay. Some of the impounded and disconnected marshes in the Chenier Plain are much shallower and are likely most sensitive to the atmospheric air temperature boundary conditions. The atmospheric impact of air temperature, particularly on shallower waters that would also be influenced by solar radiative forcings is not a well validated component of the model (nor is there much observational data available to help with such a validation effort). It is beyond the scope of the ICM to assess such nuances on water temperature, and would likely also require a much more robust treatment of temperature with regards to wetland vegetation growth before it would be a worthwhile candidate for detailed model improvements in ICM-Hydro. However, as climate change continues, the system will be warmer, with more shallow open water than in the past; perhaps resulting in greater sensitivities to such dynamics in future warmer decades.

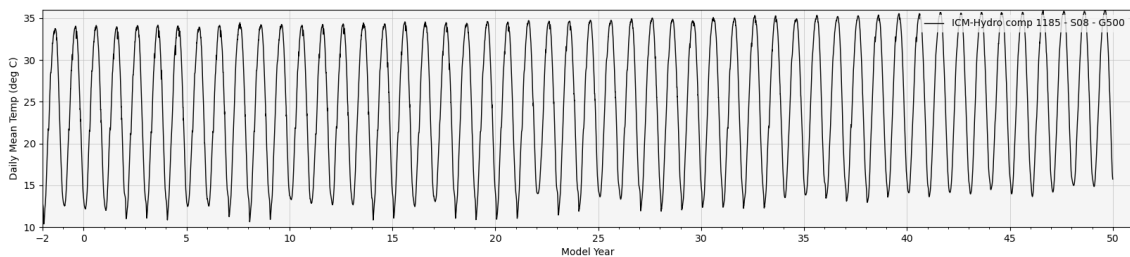
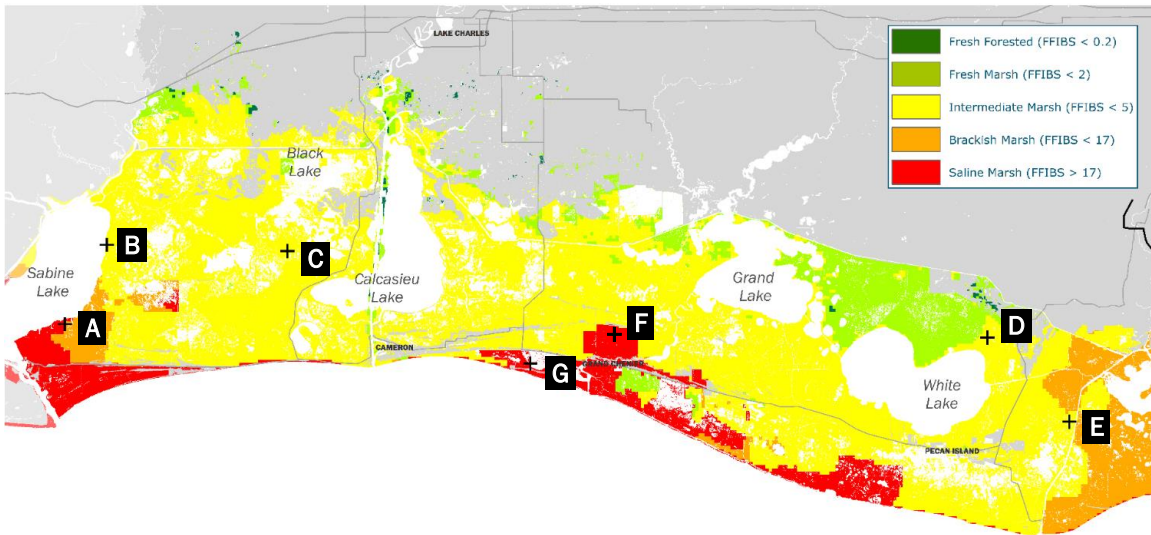


Figure 169. Temperature, under S08, in largely disconnected marsh south of White Lake (compartment 1185).

## 6.7 FWOA VEGETATION

### LOWER PROJECT SELECTION SCENARIO (S07)

Under scenario S07 there is very little change in wetland types over the first 45 years of FWOA. In the Calcasieu and Sabine basins, there is a gradual reduction of brackish marsh as it converts to intermediate marsh in the first 25 years. This is mostly due to the expansion of TYDO and a loss of SPPA. The intermediate marsh is dominated by cattails throughout the Chenier Plain. In the SAB PHAU7 and PAVA also occupy large areas, while in CAL PAVA is important in the first decade. In the MEL there is an expansion of brackish marsh west of the Freshwater Bayou Canal that is mostly due to the expansion of SCAM6. This expansion also coincides with an increase of ELCE, and a decrease in TYDO. An example is CRMS0619 (Figure 172, Point E in Figure 170 & Figure 171), which switches from SALA to SCAM6. In the CHR, there is a gradual loss of all marsh types in the first 25 years. After Year 25, loss continues with an acceleration in the last decade, while brackish marsh dominated by SCAM6 expands. During the last decade, the loss acceleration is primarily due to the loss of SPAL and DISP. The example of salt marsh loss in this region is QAQC2058 (Point G in Figure 170 & Figure 171), this site is dominated by SPAL and does not significantly change in species composition over time. There are also examples of loss in the intermediate marsh (e.g., CRMS0581), which has increasing areas occupied by PAVA which reflects decreasing water fluctuation as the impounded area has fewer opportunities for water drainage.



**2023 COASTAL MASTER PLAN  
FUTURE WITHOUT ACTION**

VEGETATED HABITAT CLASSIFICATION - YEAR 25  
LOWER PROJECT SELECTION SCENARIO - S07

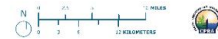
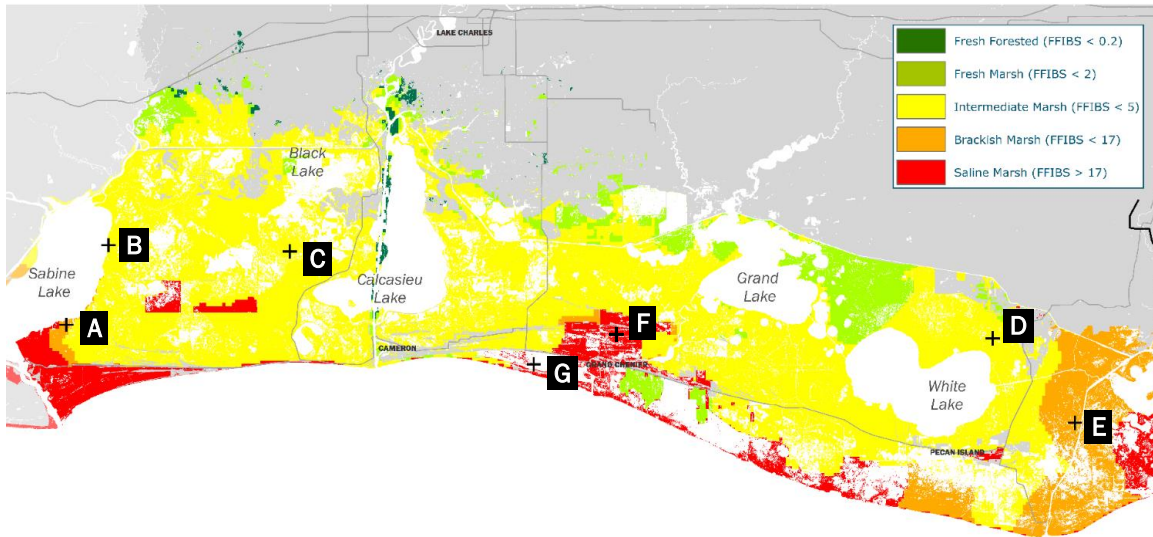


Figure 170. Wetland type (FFIBS score) distribution of the Chenier Plain region under scenario S07 in Year 25.



**2023 COASTAL MASTER PLAN  
FUTURE WITHOUT ACTION**

VEGETATED HABITAT CLASSIFICATION - YEAR 50  
LOWER PROJECT SELECTION SCENARIO - S07



Figure 171. Wetland type (FFIBS score) distribution of the Chenier Plain region under scenario S07 in Year 50.

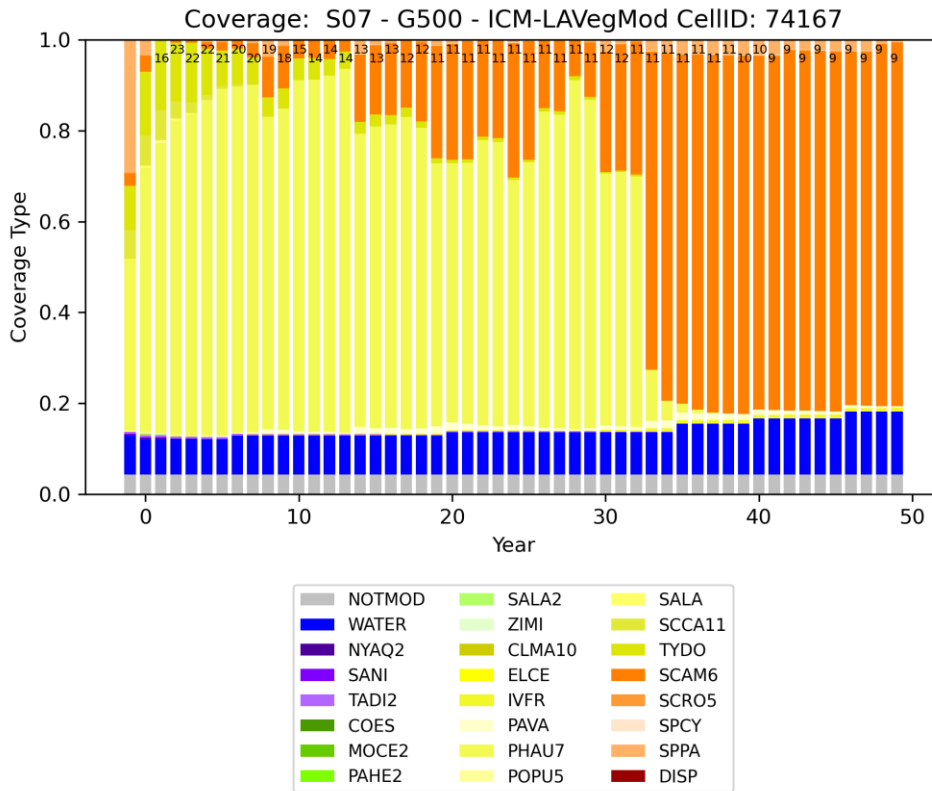


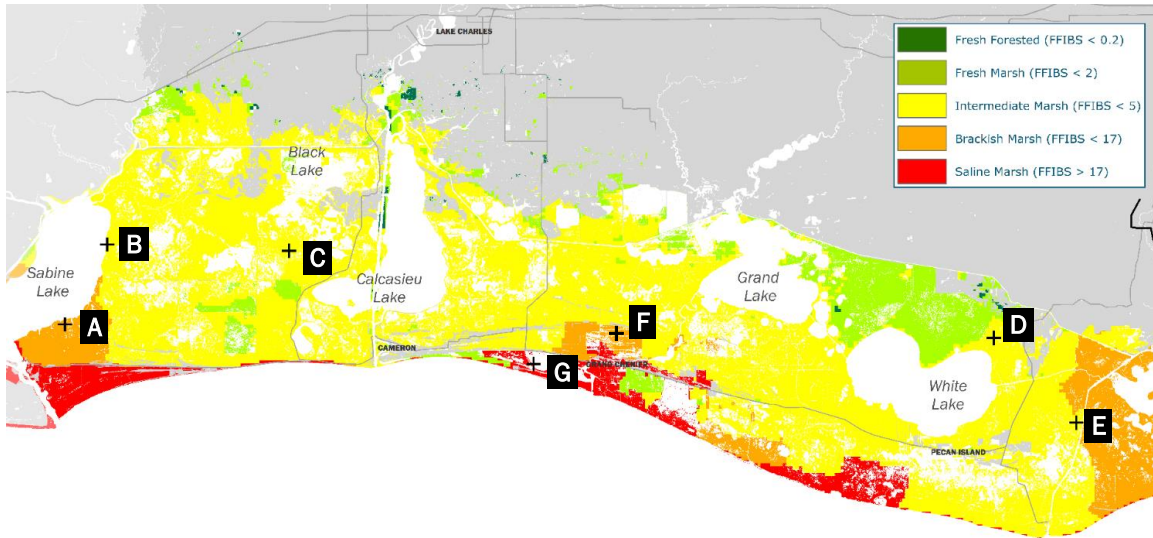
Figure 172. Change in vegetation cover under S07 is shown at CRMS0619, a representative point in the Chenier Plain region. Point location is Point E shown in previous Chenier Plain region map figures.

## HIGHER PROJECT SELECTION SCENARIO (S08)

Under the S08 future there is land loss throughout the Chenier Plain; however, loss rates are highest in the MEL and CHR ecoregions. The SAB region shows the lowest land loss and may be associated with a gradual conversion of brackish marsh to intermediate marsh along the edge of Sabine Lake over the 50-year simulation. These changes are illustrated by CRMS2189 (Point B in Figure 175) on the northern edge of Sabine Lake, where vegetation changes from SPPA to SCAM6 in the first 15 years. Then a three-year period dominated by PHAU7 with PAVA and TYDO and a 15-year period dominated by PAVA. The final 17 years are dominated by Roseau cane (PHAU7), which coincides with land loss in this area. Along the southern edge at CRMS0684 (Point A in Figure 175), SPPA remains the first decade and the increase in SCAM6 occurs over the next two decades. But the conversion to PHAU7 occurs near Year 34 and leads to increase land loss.

Most of the Chenier Plain land loss occurs in the intermediate marsh areas. In some areas there is no change in species composition. For example, CRMS0635 (Point C in Figure 175) remains a mixture of TYDO and ELCE as land loss occurs and QAQC2058 (Point G in Figure 175) remains SPAL as land loss

occurs. However in other areas, there are changes in species composition before land loss occurs. At CRMS0570 (Point D in Figure 175), there is a switch from TYDO to PHAU7 before land loss starts. At CRMS0619 (Point E in Figure 175), land loss is associated with SCAM6 replacing PHAU7, while at CRMS0622 (Point F in Figure 175) land loss starts when the site is dominated by SPAL.

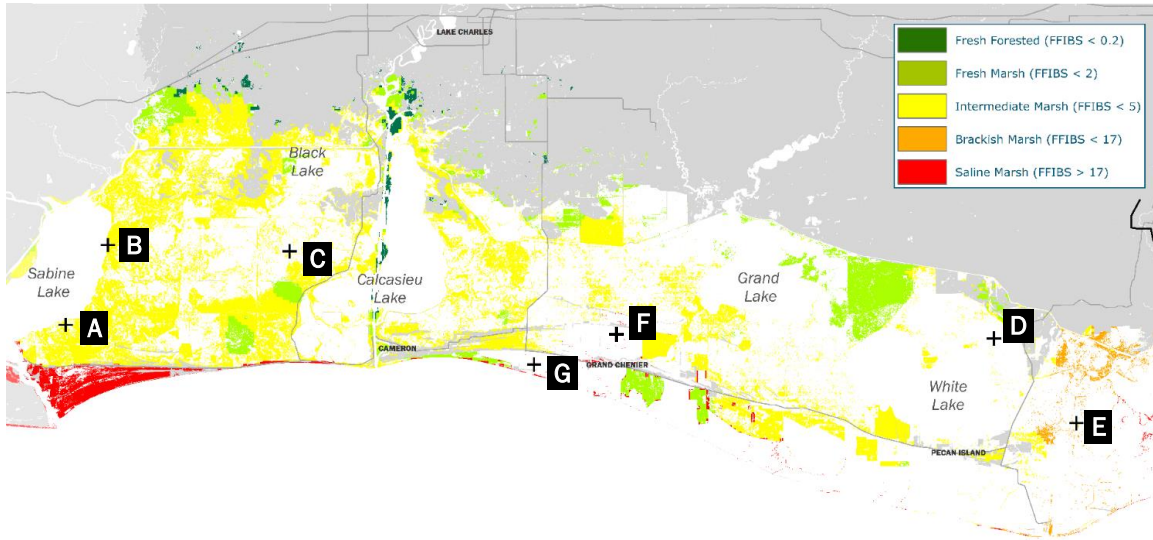


**2023 COASTAL MASTER PLAN  
FUTURE WITHOUT ACTION**

VEGETATED HABITAT CLASSIFICATION - YEAR 25  
HIGHER PROJECT SELECTION SCENARIO - S08



Figure 173. Wetland type (FFIBS score) distribution of the Chenier Plain region under scenario S08 in Year 25.



**2023 COASTAL MASTER PLAN  
FUTURE WITHOUT ACTION**

VEGETATED HABITAT CLASSIFICATION - YEAR 50  
HIGHER PROJECT SELECTION SCENARIO - S08



Figure 174. Wetland type (FFIBS score) distribution of the Chenier Plain region under scenario S08 in Year 50.

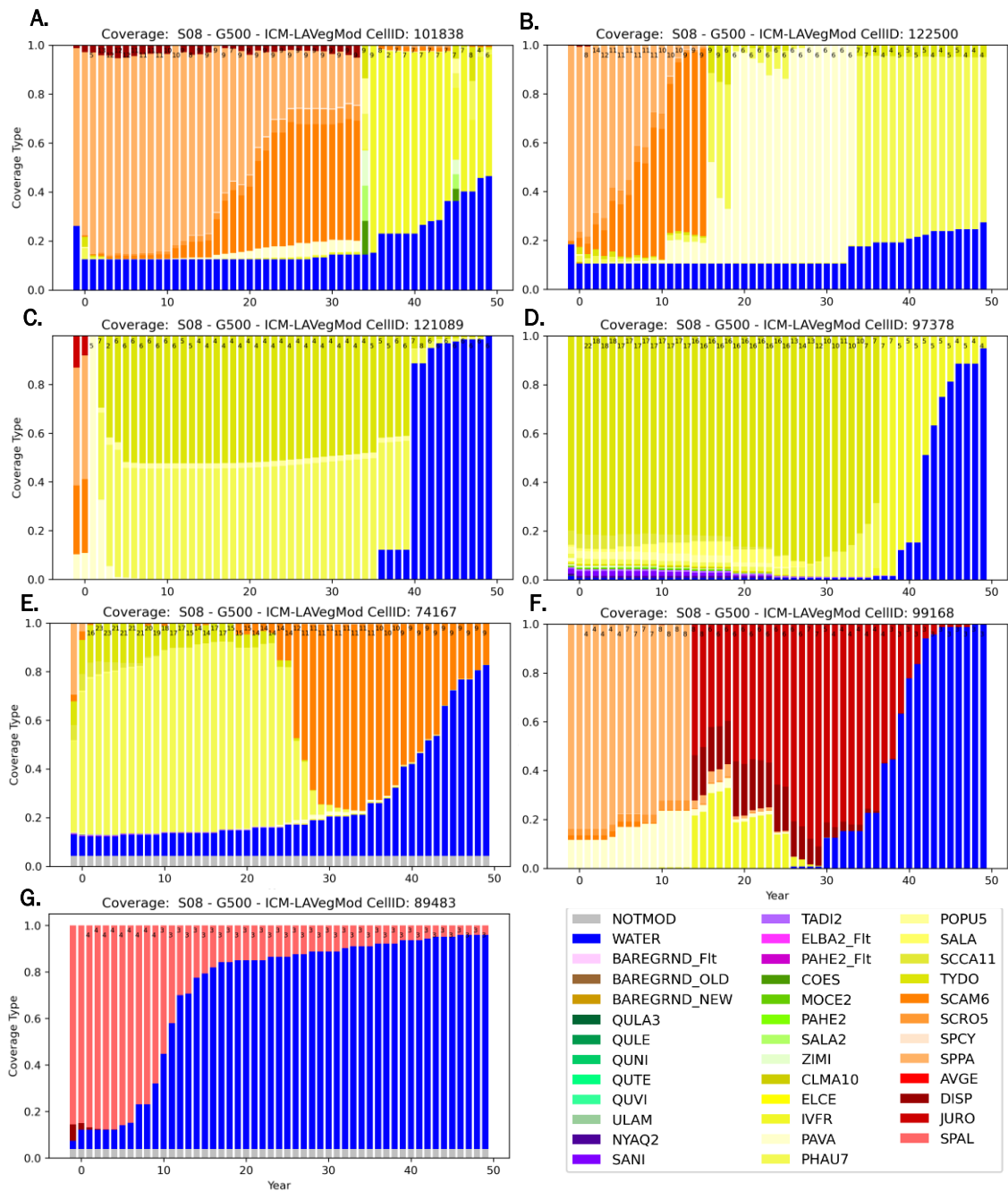


Figure 175. Change in vegetation cover under S08 is shown at representative points in the Chenier Plain region. Point locations are shown in previous Chenier Plain region map figures.

## 6.8 FWOA WETLAND MORPHOLOGY

### LOWER PROJECT SELECTION SCENARIO (S07)

Due to the managed nature of this region, land loss and gain tends to be confined to individual ICM-Hydro compartments, and the timing and amount of changes are more closely tied to the dynamics in an individual compartment than region wide trends.

The Sabine ecoregion does not experience much change until the last decade. During the first forty years, there is a narrow strip of land loss along the edge of Sabine Lake, and small amounts of both land loss and gain occurs throughout the region. A large land loss event occurs in Year 46, after the mean water level increases from 0.52 m and 0.78 m in Years 43 and 44, respectively, to 1.55 m and 1.04 m in Years 45 and 46. These high water levels cause all land to be lost in ICM-Hydro compartments 1318, 1314, and 1320 and partial loss in ICM-Hydro compartments to the west (e.g., 1327, 1331, 1316, & 1307). It also increases the salinity, causing intermediate vegetation to die and creating bareground in the area bordering the now open water (ICM-Hydro compartment 1308). That bareground is lowered each year but remains land until it is re-vegetated (CRMS0677, Figure 176). A portion of the open water converts back to land in Year 48 and remains through Year 50. In the last year of the simulation, a large area of vegetated land converts to bareground south of Sabine Lake (ICM-Hydro compartment 1312).

S07 CRMS0677 SAB

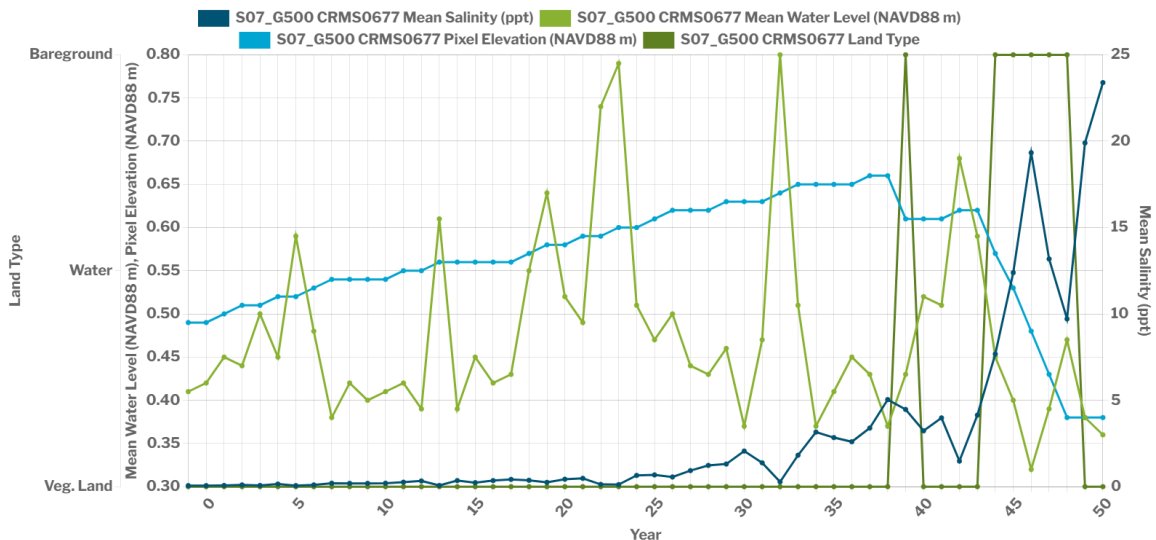


Figure 176. Salinity and inundation dynamics at CRMS0677 under S07.

Little change occurs in the Calcasieu ecoregion. Minor amounts of land loss and gain occur along marsh edges over the 50-year period. Some areas of land gain are concentrated in the northern part of the Cameron Creole watershed (ICM-Hydro compartment 1043) and along the edges of the

Calcasieu Ship Channel. The Rabbit Island restoration remains land in Year 50.

Similarly, in the Mermentau/Lakes ecoregion change is concentrated in the southwest area (north of Highway 82 between the Creole Canal and the Mermentau River) and south of Grand Lake, but overall this ecoregion remains intact. There are isolated pockets of land loss (ICM-Hydro compartments 1416 & 1198) starting in the first decade that are regained by the fourth decade. Flotant is lost in the area north of White Lake (ICM-Hydro compartment 1162) in the last two decades.

The greatest land loss occurs in the Chenier Ridges ecoregion. The area experiences minor land loss in the first two decades that is concentrated west of Mud Lake in the Rockefeller Refuge (ICM-Hydro compartment 1063) and along the coastal edge. In the third decade, the loss is more substantial but remains generally confined to those areas. Land loss expands to the area along the coast in the fourth and fifth decades. The Rockefeller shoreline stabilization project is about 50% intact in Year 50.

QAQC2072 in the Chenier Ridge ecoregion (ICM-Hydro compartment 1080) follows the typical land loss pattern in the area. While vegetated, the elevation is maintained but does not increase (Figure 177). Once the inundation threshold is crossed and it becomes open water in Year 26, the elevation decreases steadily from 0.1 to 0.07 m NAVD88.

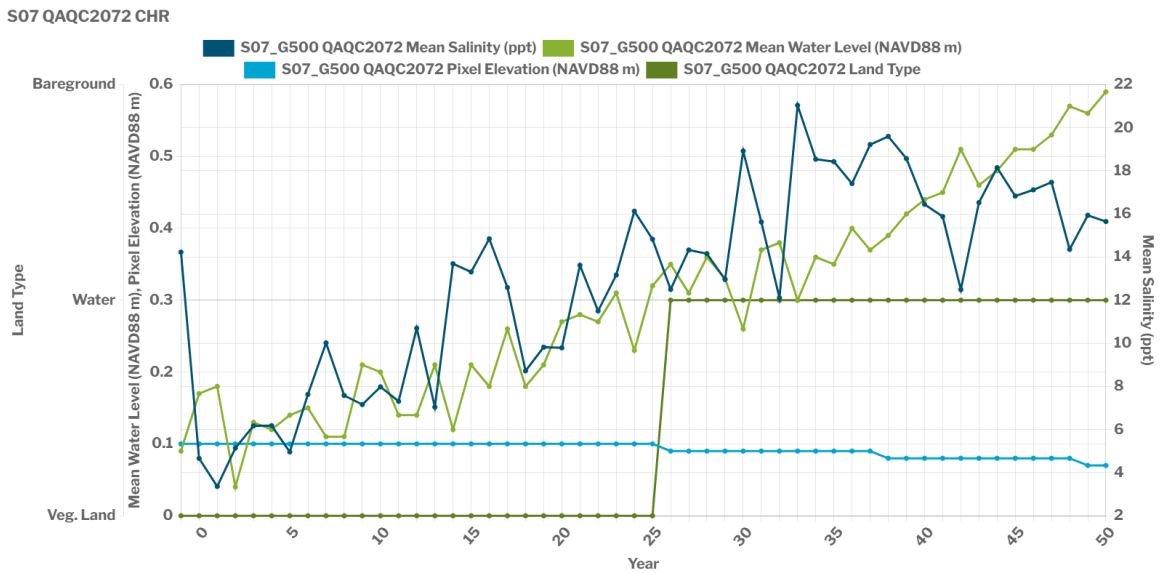


Figure 177. Salinity and inundation dynamics at QAQC2072 under S07.

## HIGHER PROJECT SELECTION SCENARIO (S08)

Most of the Chenier Plain is under managed hydrology of some type and so patterns of land loss often reflect areas bounded by features such as roads and levees that may be directly managed or are semi-impounded. This is reflected in the first two decades of land loss in the region. Loss occurs where compartments experience high water levels, e.g., compartment 1416 north of the GIWW in Year 11, or compartments 1294 and 1308 in Year 17 where stage appears to increase for several years in a row before draining. A similar dynamic occurs in compartment 1061 and 1062, east of Cameron and south of the chenier ridge, where water levels progressively increase through Year 18, rising over 1 m, and the marsh is lost to open water by Year 14. That area is fresh and a different dynamic results in land loss just to the east in Year 11 in compartment 1063 which is open to the tide. At QAQC2058 (Figure 178) loss occurs in Year 10. FFIBS scores are high (24) and although subsidence is relatively low (~7.5 mm/yr) organic accretion is only 0.5 cm/yr resulting in a slight decrease in elevation in the first decade. Along with the rising stage this means that the inundation threshold for higher salinity (salinity is 11-15 ppt in the first decade) is crossed. Once the site transitions to open water mineral sediment deposition increases and is sufficient to counter deep subsidence of only ~1 mm/yr (shallow subsidence only applies while the area is land), and so elevation increases. However, the rise in stage is faster and the site does not vegetate again.

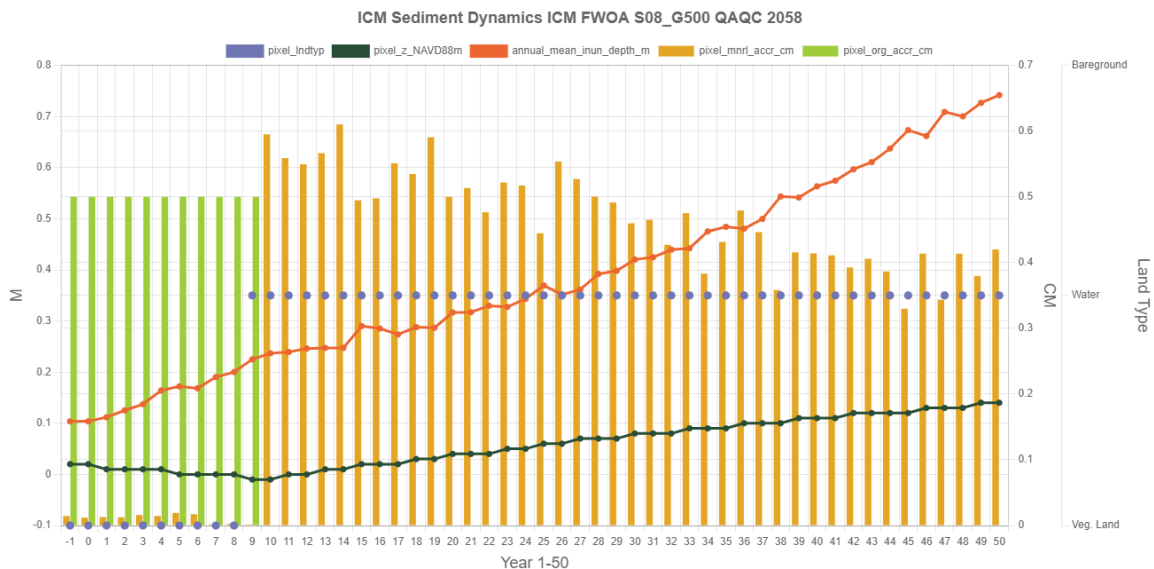


Figure 178. Sediment dynamics at QAQC2058 under S08.

More extensive land loss occurs in the region by Year 20 including areas south of Grand Lake, within the Rockefeller Refuge and in the Sabine ecoregion between Five Lakes and Highway 82. In compartment 1308 water levels peak in Year 18 at approximately 1 m higher than at the start of the

simulation. Once water levels begin to decline and reach similar levels to the start of the simulation in Year 21-22 the area turns to bareground and is once again vegetated by Year 25. Continued loss occurs by Year 30 in the areas noted above, including in the more saline areas south of Highway 82 near the Rockefeller Refuge. Areas with saline FFIBS scores in the Chenier Plain have less organic accretion than brackish areas. However, saline parts of the Sabine ecoregion, south of Highway 82 and southwest of Johnson’s Bayou, remain intact due to lower shallow subsidence rates in this ecoregion. The low subsidence rates in Sabine seem to be resulting in less land loss in the fourth decade of the simulation, when loss is more extensive in the Mermentau ecoregion, including areas south of Grand Lake and north of Mermentau Lake (an area with increasing FFIBS scores). By Year 40, loss of land south of Highway 82 to the east is extensive and by Year 50 only a few areas remain. Figure 179 shows the elevation and inundation trends for CRMS0581 in the Rockefeller Refuge.

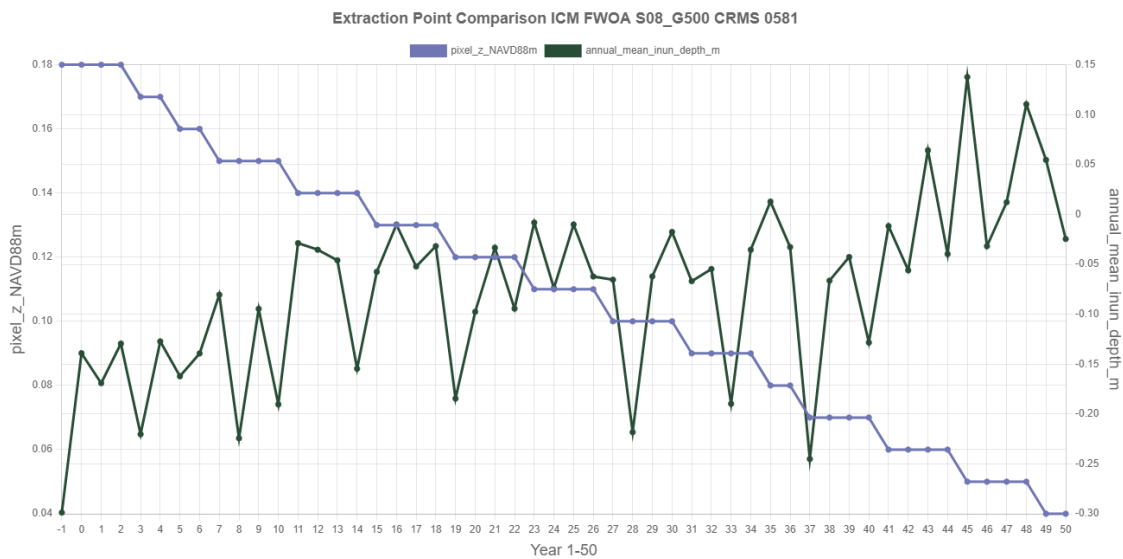


Figure 179. Inundation dynamics at CRSM0581 under S08.

There is some decrease in elevation over time as there is a deficit of about 3 mm/yr between organic accretion and total subsidence. This leads to an increase in inundation (there is no trend in stage for this compartment due to water level management) but mean annual inundation is mostly negative until the last decade, and as the site stays fresh for the entire 50 years is well below the threshold for inundation loss.

CRMS1738 in the Cameron-Creole Watershed area also is maintained for the entire 50 years (Figure 180). Total subsidence here is much less than further east, only ~2 mm/yr. However, as the elevation of the marsh is so high, it does not get inundated early in the simulation so there is no organic accretion (or mineral sediment deposition) resulting in a slight decrease in elevation. However, as

water levels rise, inundation increases and after Year 12 organic accretion is more frequent. FFIBS scores are about 2.5 leading to organic accretion of over 5 mm/yr which results in a gradual increase in elevation. Even though inundation of the marsh surface increases in the last two decades, salinities are less than 0.5, it does not become high enough to reach the inundation loss threshold and the marsh is maintained for the entire 50 years.

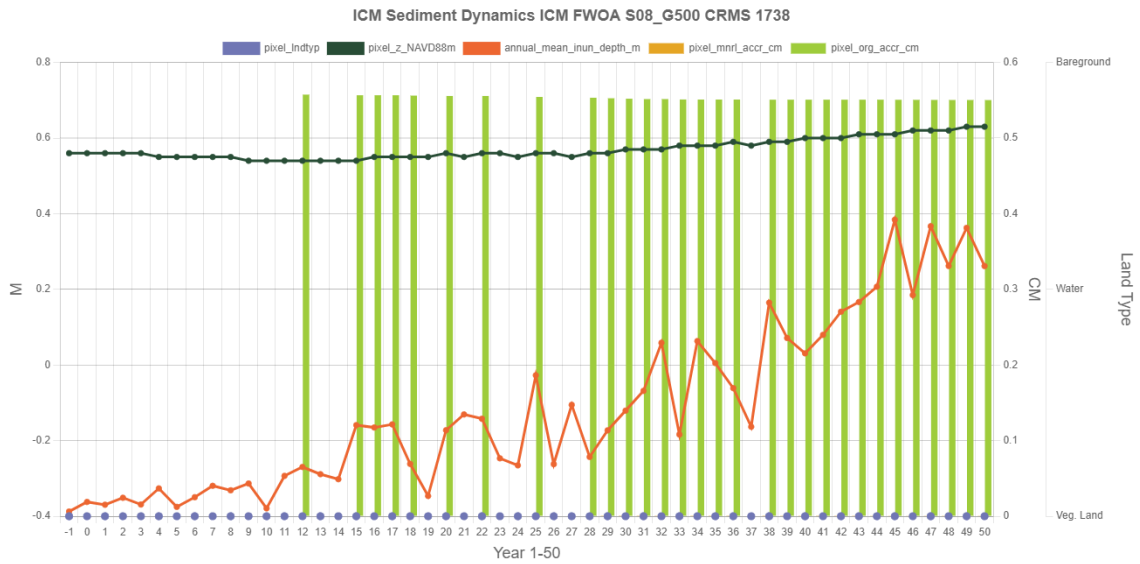


Figure 180. Sediment dynamics at CRSM1738 under S08.

Land loss in the Sabine and Calcasieu ecoregions and north of White Lake increases markedly between Year 40 and 45. Previously this latter area had been quite stable except for the conversion of floatant marsh to open water in Year 37. Conversion of marsh to open water begins in the years following and by Year 45 large areas are lost. CRMS0570, northeast of White Lake, illustrates the dynamics (Figure 181). FFIBS scores are between 2 and 3 and so organic accretion of just over 5 mm/yr is only slightly less than total subsidence. Marsh elevation is maintained but inundation increases over time, as does salinity, and the marsh converts to open water in Year 40. Note the increase in salinity in Year 37 associated with the loss of floatant in this area.

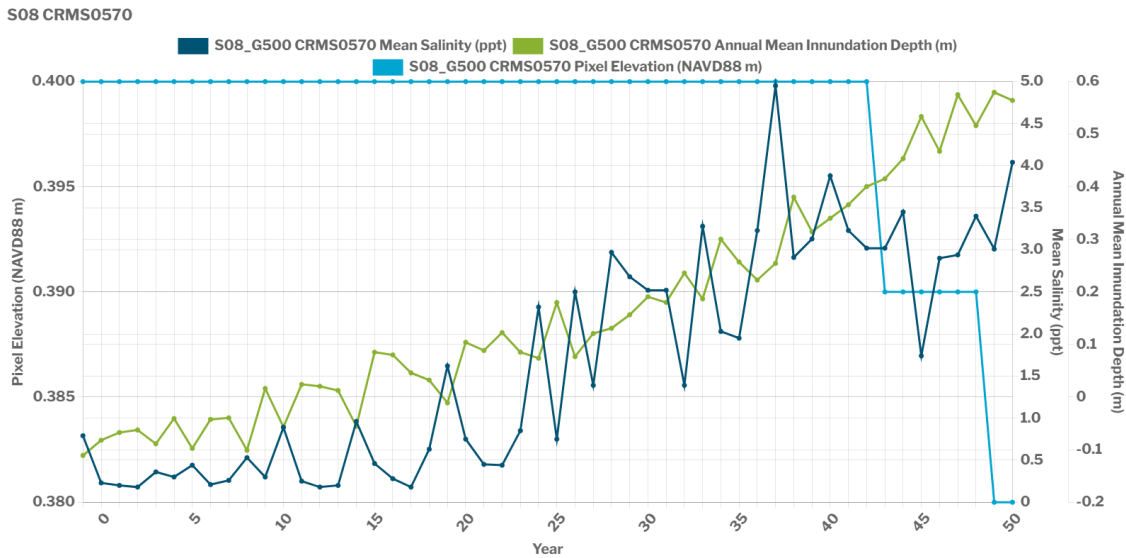
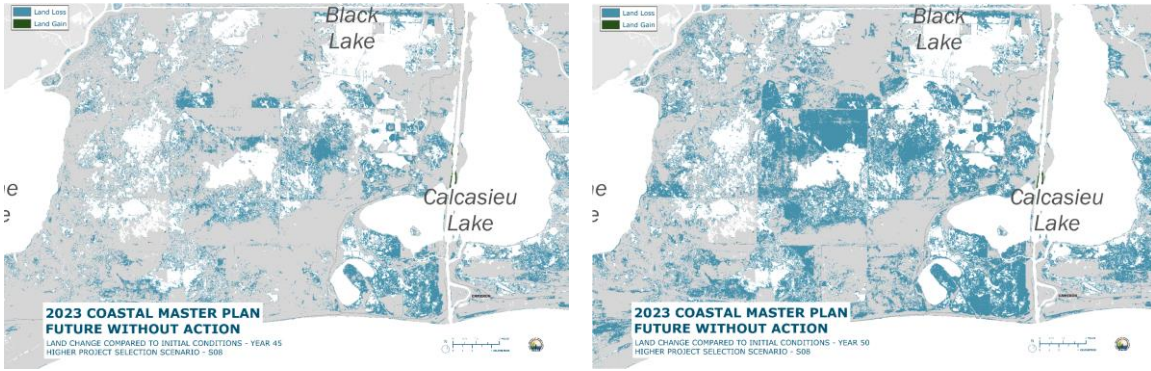


Figure 181. Salinity, elevation, and inundation dynamics at CRMS0570 under S08.

An area northwest of White Lake remains fresh through the simulation and is maintained as marsh. Data from TRNS0200 and compartment 1163 shows that this area is similar to CRMS0581 shown above, where water management means there is no progressive increase in stage, and inundation increases as elevations are gradually decreased by subsidence. However, the area stays fresh and the inundation threshold is not crossed.

Apart from areas of water management where stage increases are reduced, several of which are noted above, much of the land in the Mermentau ecoregion is lost by Year 50. Less loss occurs in the Sabine and Calcasieu ecoregions. This appears to be due to lower subsidence rates. Most of the remaining marsh has intermediate FFIBS scores by Year 50 except for isolated areas that remain fresh and the saline marshes in the southwest of the Sabine ecoregion. In Sabine, much of the loss occurs in the last five years of the simulation. Figure 182 shows this change (Year 45 left, Year 50 right) and data from two CRMS stations.



S08 CRMS0693 AND CRMS0635

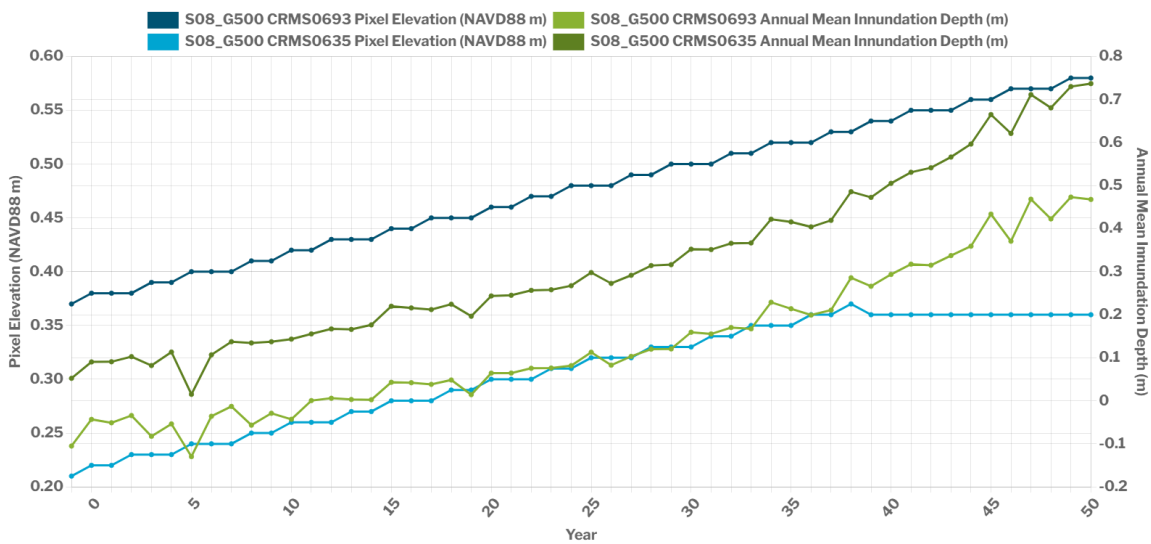


Figure 182. Land change and dynamics for parts of the Sabine ecoregion under S08: cumulative land change by Year 45 (top left) and by Year 50 (top right). Bottom figure shows elevation and inundation for CRMS0693 and CRMS0635.

CRMS0693 converts to open water at Year 50. It starts with a relatively high elevation and intermediate FFIBS scores and low subsidence lead to substantial increase in elevation overtime. Rise in stage is rapid in the last decade and finally reached the inundation threshold despite the increase in elevation. CRMS0635 also has intermediate FFIBS scores which increase elevation over time. However, the starting elevation is much lower and the inundation threshold is crossed at Year 39. Inspection of the initial DEM for the simulation and the Year 50 land loss map for the Sabine ecoregion shows that many of the areas which do not convert to water have relatively high starting elevations (Figure 183).

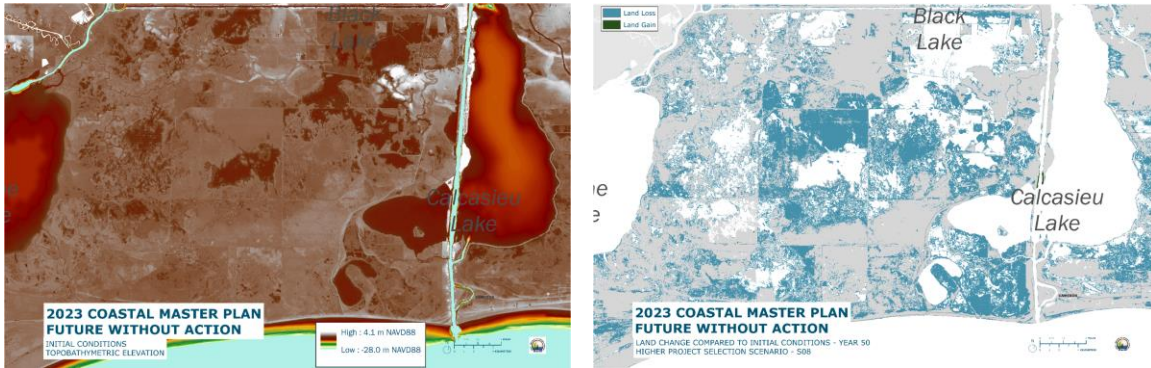


Figure 183. Existing conditions elevation (left) – darker brown shows higher marsh elevation; and areas of wetland loss at Year 50 under S08 (right).

There are several FWOA restoration projects included in this region. Two of these are on the Rockefeller Refuge in the Chenier Ridges ecoregion which has relatively high shallow subsidence rates (6.6 mm/yr). The CIAP Rockefeller Shoreline Protection Demonstration converts to open water between Year 14 and 25, and the larger Rockefeller Refuge Gulf Shoreline Stabilization with a higher starting elevation has almost completely converted to open water by Year 40. There are also several projects in the Sabine ecoregion. Rabbit Island restoration remains land throughout the 50-year simulation due to a high starting elevation (0.9-1 m NAVD88). In contrast the Oyster Bayou Marsh Creation project has an initial elevation of 0.47 m and it converts to open water around Year 48. The Cameron Meadows Marsh Creation project has a higher starting elevation (~0.6 m at Year 1) and survives throughout the 50-year period.

## 6.9 FWOA HABITAT SUITABILITY INDICES

### LOWER PROJECT SELECTION SCENARIO (S07)

Habitat suitability for fish and shellfish did not change much over time across the Sabine, Calcasieu, and most of the Mermentau/Lakes ecoregions in the S07 environmental scenario simulation. This was likely due to water management practices in these ecoregions, which resulted in relatively consistent habitat conditions during the simulation. However, there were some areas where conditions fluctuated over time due to varying riverine freshwater inflow, particularly in the marshes of the western Sabine ecoregion and along the Mermentau River in the Mermentau/Lakes ecoregion. Salinities in these areas varied in response to the inflow, and this resulted in fluctuations in habitat suitability for higher-salinity species (i.e., species whose optimal salinities were >5 ppt). For example, suitability scores for adult spotted seatrout fluctuated between 0.2 and 0.6 over the first 20 years of the simulation as a result of varying Mermentau River inflow and resulting salinities (Figure 184).

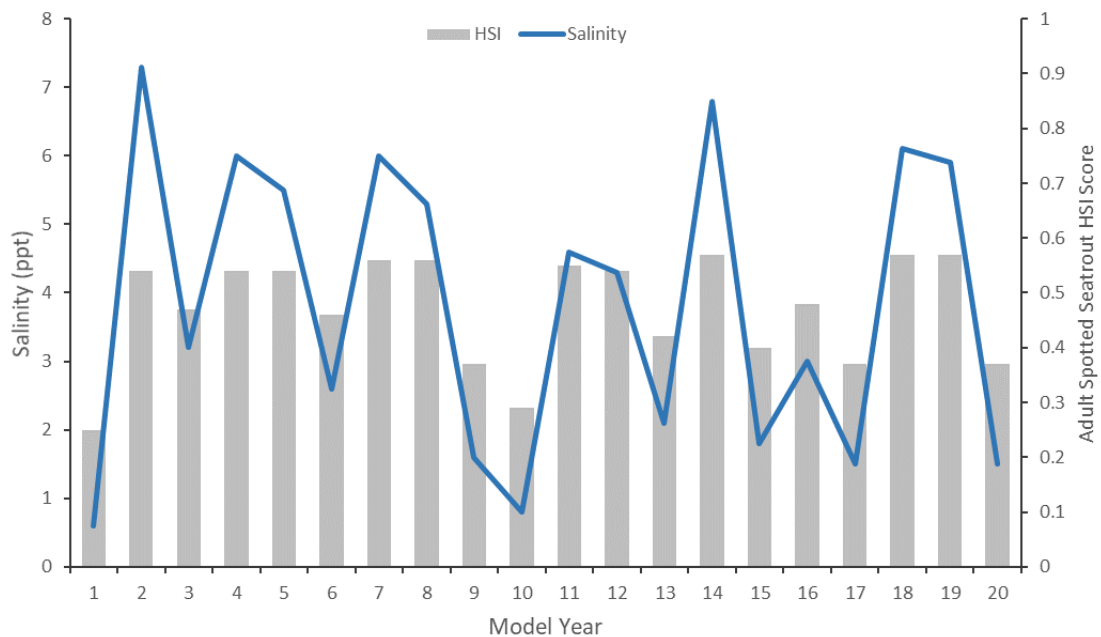


Figure 184. Adult spotted seatrout HSI scores compared to salinity simulated for the marshes along the lower Mermentau River over the first 20 years of the S07 environmental scenario simulation. Scores range from 0.0, completely unsuitable habitat, to 1.0, optimal habitat.

Notable increases in habitat suitability for fish and shellfish occurred in the Chenier Ridges ecoregion, and in parts of the Mermentau/Lakes ecoregion near the lower Mermentau River and Freshwater Bayou. For the most part, this increased suitability was due to wetland loss in these areas, which resulted in a more suitable fragmented marsh landscape for the fish and shellfish. However, salinities also increased somewhat over time in these areas, and this contributed to the increased suitability observed for the higher-salinity species, such as oysters, brown shrimp, white shrimp, and spotted seatrout (Figure 185).

Compared to the fish and shellfish, much more change in habitat suitability was observed for the wildlife species in the Chenier Plain region. In some cases, these changes were attributed to increased salinities or changes in marsh habitat type. For example, habitat suitability for alligator decreased near Freshwater Bayou because salinities were near its upper tolerance threshold by the end of the simulation, and marsh converted from intermediate marsh to less suitable brackish marsh (Figure 186). However, most of the changes were attributed to increased water levels as a result of sea level rise. Increased water levels resulted in increased marsh inundation, which had a negative effect on habitat suitability for alligator and seaside sparrow across the region. However, areas where water level management continued throughout the simulation, such as the impoundment northwest of White Lake (Figure 186), remained highly suitable habitat for these species, and in the case of seaside sparrow represented the only habitat remaining in the region. In contrast, the increased water levels generally resulted in increased habitat suitability for mottled duck and gadwall (Figure 187). This was

because, as water levels increased, marsh habitats were inundated such that the amount of suitable shallow water habitat increased over time for these species.

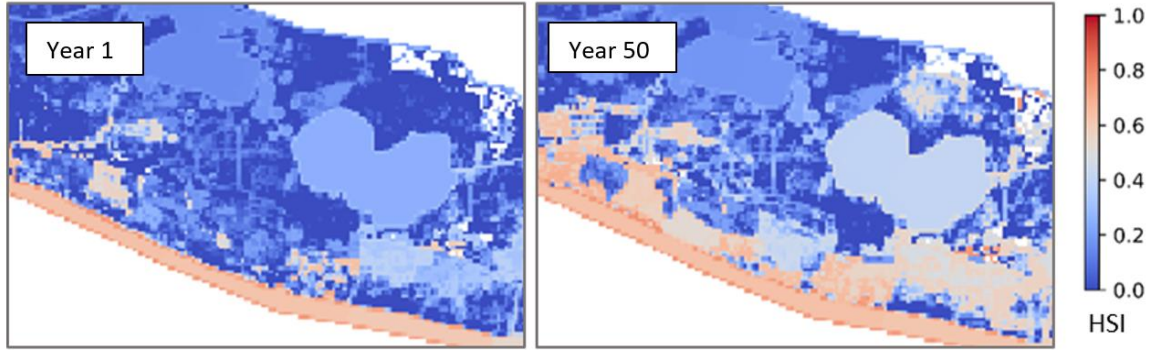


Figure 185. Adult spotted seatrout HSI scores across the Mermentau/Lakes and Chenier Ridges ecoregions for Year 1 (left) and Year 50 (right) of the S07 environmental scenario. Scores range from 0.0, completely unsuitable habitat, to 1.0, optimal habitat.

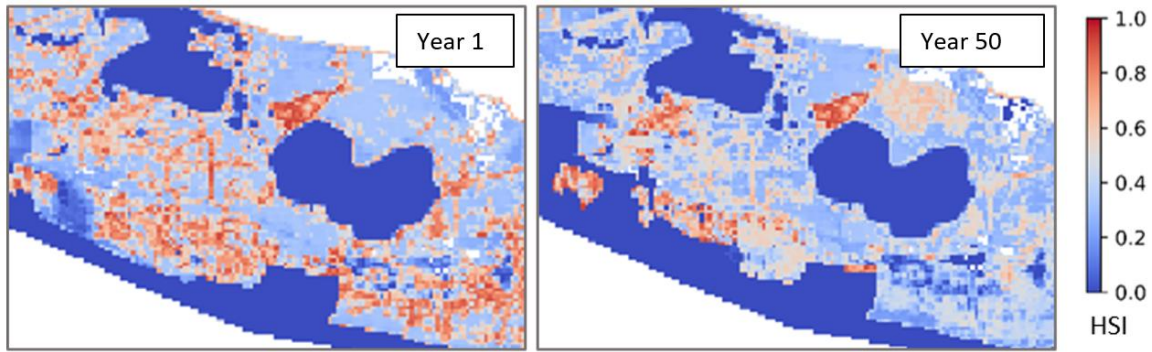


Figure 186. Alligator HSI scores across the Mermentau/Lakes and Chenier Ridges ecoregions for Year 1 (left) and Year 50 (right) of the S07 environmental scenario. Scores range from 0.0, completely unsuitable habitat, to 1.0, optimal habitat.

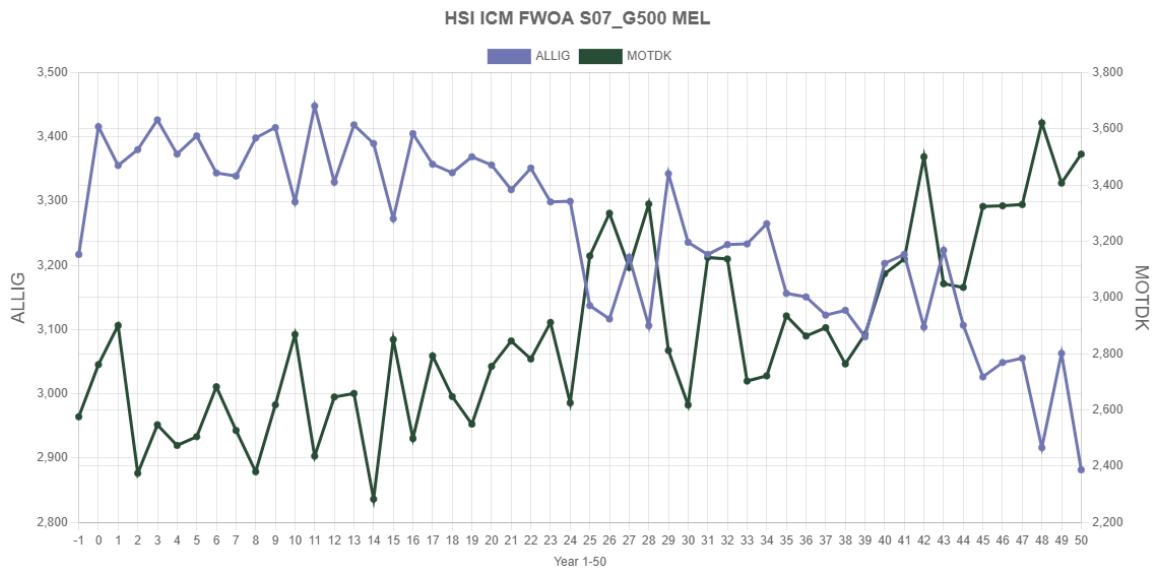


Figure 187. Total HSI score for alligator and mottled duck in the Mermentau/Lakes ecoregion over the 50-year S07 environmental scenario simulation. The total HSI score was calculated by summing the individual scores for each model cell within the ecoregion.

## HIGHER PROJECT SELECTION SCENARIO (S08)

Changes to fish and shellfish habitat suitability over the S08 environmental scenario simulation were primarily driven by high rates of wetland loss. Wetland loss converted the relatively solid marshes across the region into highly-suitable fragmented marshes, and as a result habitat suitability for fish and shellfish steadily increased over much of the simulation. During the last decade, however, most of the wetlands in the Chenier Ridges and Mermentau/Lakes ecoregion were converted into less-suitable open water habitats. Consequently, habitat suitability stopped increasing in these ecoregions, and for many species there was a decrease in suitability over the last decade (Figure 188). This was not seen in the Sabine and Calcasieu ecoregions, because wetland loss was not as great in these ecoregions and a large amount of fragmented marsh remained at the end of the simulation.

Though not as influential as wetland loss, increased salinities contributed to the changes in habitat suitability for fish and shellfish in parts of the Chenier Plain region. In the Chenier Ridges ecoregion, salinities increased to >10 ppt by the end of the simulation in unmanaged areas. As a result, the decline in habitat suitability that occurred over the last decade was somewhat greater for low-salinity species, such as juvenile gulf menhaden, as compared to higher-salinity species, such as brown shrimp (Figure 188). Meanwhile, extensive wetland loss in the eastern Mermentau/Lakes ecoregion allowed brackish waters from Freshwater Bayou to extend farther into the ecoregion. This resulted in large decreases in habitat suitability for low-salinity species, such as alligator, and large increases in suitability for higher-salinity species, such as spotted seatrout, in the ecoregion (Figure 189).

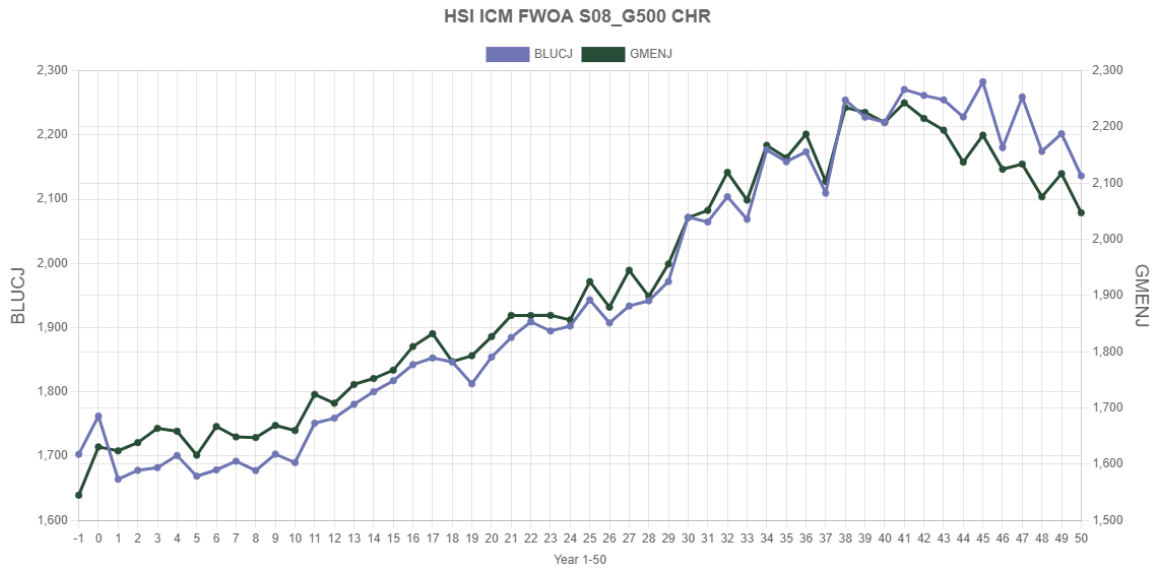


Figure 188. Total HSI score for juvenile blue crab and juvenile gulf menhaden in the Chenier Ridges ecoregion over the 50-year S08 environmental scenario simulation. The total HSI score was calculated by summing the individual scores for each model cell within the ecoregion.

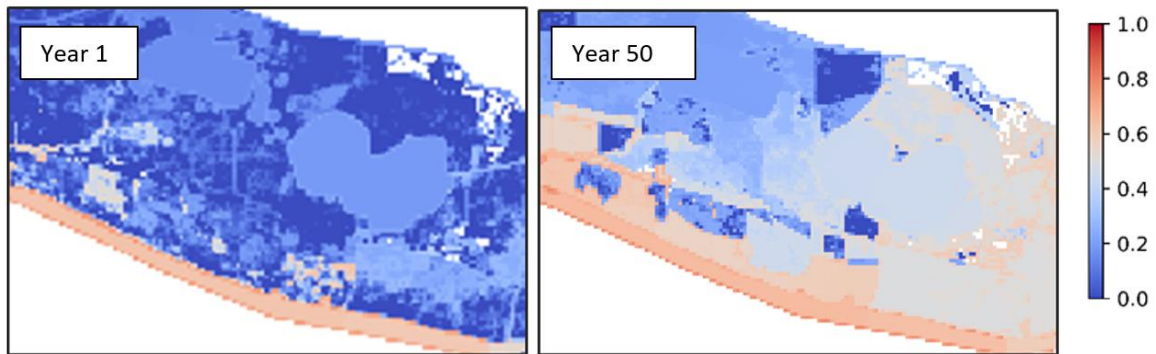


Figure 189. Adult spotted seatrout HSI scores across the Mermentau/Lakes and Chenier Ridges ecoregions for Year 1 and Year 50 of the S08 environmental scenario. Scores range from 0.0, completely unsuitable habitat, to 1.0, optimal habitat.

Increased water levels had a large effect on habitat suitability for wildlife species in the Chenier Plain region. As water levels increased over time in the simulation there was a commensurate increase in marsh inundation rates across the region. This resulted in large decreases in habitat suitability for alligator and seaside sparrow because increased inundation would greatly affect the nesting success for these species. In contrast, habitat suitability increased over much of the simulation for gadwall and mottled duck because there was an increase in the amount of shallow water habitat. However, as water levels continued to increase, the amount of shallow water habitat decreased and thus habitat suitability decreased for these species over the last decade. This pattern was not observed in the

Sabine ecoregion, though, as habitat suitability continued to increase over the simulation in this ecoregion. This was likely due to the lower marsh inundation rates simulated for the Sabine ecoregion, which resulted in a greater amount of marsh and shallow water habitat available at the end of the simulation, compared to the rest of the Chenier Plain region.

## 6.10 DISCUSSION

Overall there is much more extensive land loss in S08 in the Chenier Plain than in S07. This is especially the case in the Mermentau Basin. QAQC0989, shown in Figure 190, between the Creole Canal and the Mermentau River north of Highway 82, demonstrates how both the subsidence and inundation are greater in S08, which combine to produce a greater rate of relative sea level rise. Surface elevation increases by 2 cm in S08 before the conversion to open water as accretion slightly exceeds subsidence, while in S07 for the same period surface elevation increases by 15 cm illustrating the effects of shallow subsidence variation across the scenarios. This compounds the greater sea level rise in S08 to increase inundation. This area remains vegetated in S07 and is converted to open water in S08 in Year 39.

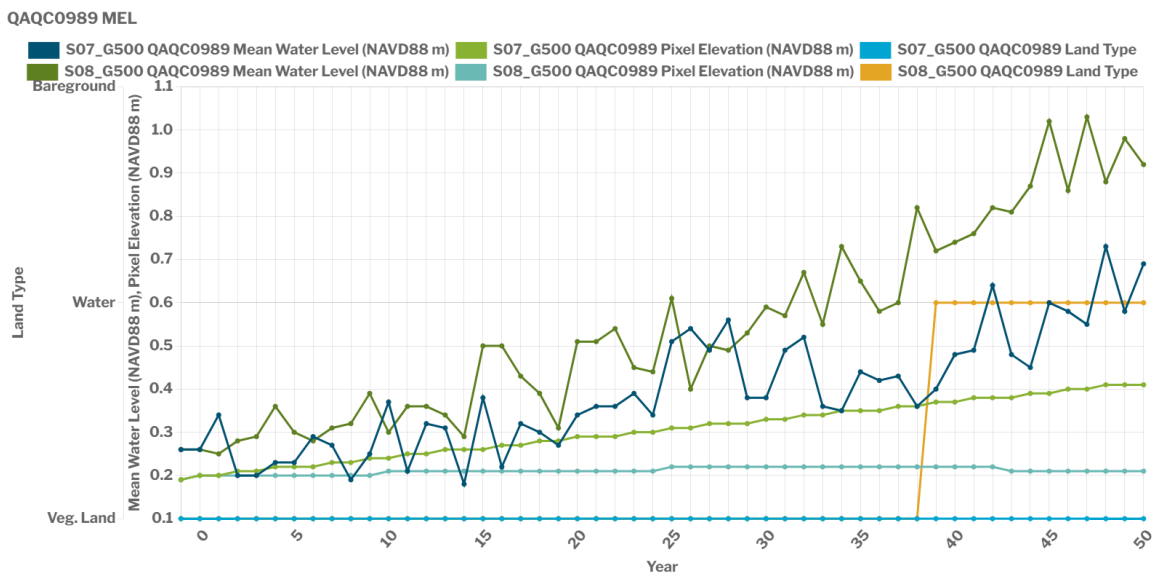


Figure 190. Comparison of S07 and S08 conditions for QAQC0989 in MEL.

QAQC2023 (Figure 191), in the Rockefeller Refuge area within the Chenier Ridge ecoregion, is open water throughout the simulations in both scenarios thus has the same subsidence. There are very minor differences in mineral accretion, leading to essentially the same surface elevation. The mean water level is greater in S08 starting in about project Year 28 due to the effects of greater sea level rise.

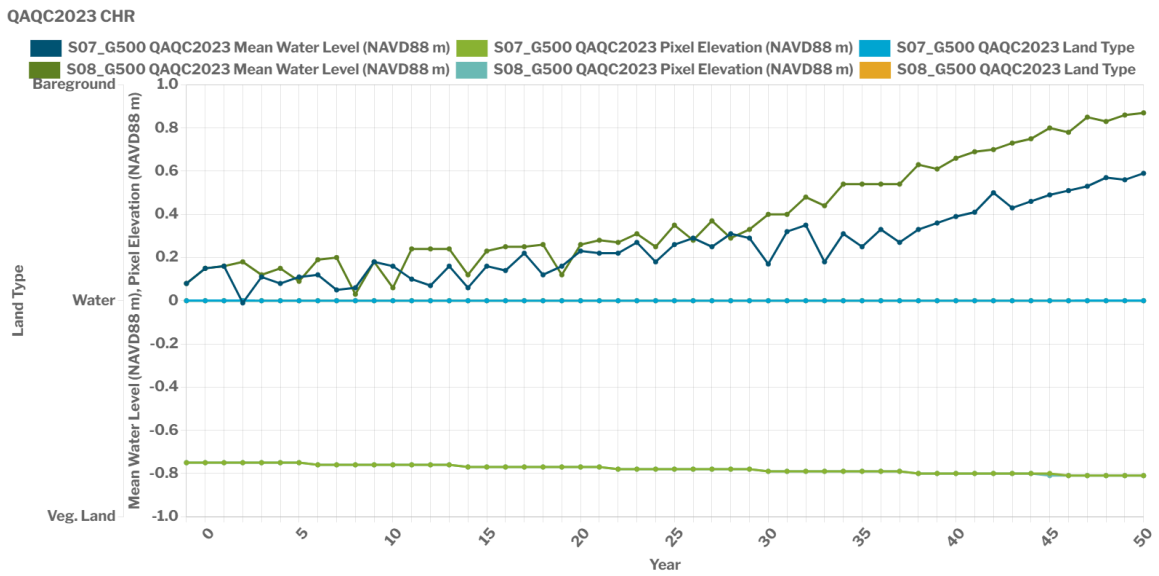


Figure 191. Comparison of S07 and S08 conditions for QAQC2023 in CHR.

Spatial and temporal patterns of habitat suitability in the Chenier Plain region were generally similar between the S07 and S08 environmental scenario simulations. For the most part, the fragmentation of marshes in the region and increases in water levels with sea level rise caused an increase in the suitability of habitats for most fish, shellfish, and wildlife over both simulations. The biggest difference between the scenarios occurred during the last 10 to 15 years of the simulations when rates of wetland loss and water level increase were considerably higher in the S08 scenario. As a result of this, habitat suitability for fish, shellfish, and wildlife generally began to decline over the last decade across most of the region. The only exception to this pattern was in the Sabine ecoregion, where the effects of sea level rise were less pronounced and marsh loss was mitigated somewhat by regular freshwater inflow. As a result, habitat conditions in the Sabine ecoregion remained favorable for most species up until the end of the S08 scenario.

## 7.0 REFERENCES

McGinnis, T. et al., 2019. 2019 Basin Summary Report for the Calcasieu-Sabine Basin. CPRA.  
<https://cims.coastal.la.gov/RecordDetail.aspx?Root=0&sid=23810>